Investigation on the V Protein Mediated Host Pathogen Interaction in *Peste des petits ruminants* Infection

Thesis

Submitted to the
DEEMED UNIVERSITY
ICAR-Indian Veterinary Research Institute
Izatnagar - 243 122 (U.P.), India

Dr. P. Kirthika
Roll No. 1720

IN PARTIAL FULFILMENT OF THE REQUIREMENTS FOR THE DEGREE OF

Doctor of Philosophy
(Animal Biochemistry)

2018

For

My Grandfather

भा.कृ.अनु.प.–भारतीय पशु चिकित्सा अनुसंधान संस्थान
(सम विश्वविद्यालय)
इज्जतनगर –243122, (उ.प्र.), भारत

DIVISION OF ANIMAL BIOCHEMISTRY
ICAR-INDIAN VETERINARY RESEARCH INSTITUTE
(Deemed University)
IZATNAGAR - 243 122, U.P., INDIA

Dr. Praveen Singh,
Ph.D.
Principal Scientist

Dated: 19/01/ **2018**

Certificate

This is to be certified that the research work embodied in this thesis entitled **"Investigation on the V protein mediated host pathogen interaction in *Peste des petits ruminants* infection"** *submitted by* **Dr. P. Kirthika, Roll No. P-1720,** *for the award of* **Doctor of Philosophy** *Degree in* **Animal Biochemistry** *at Indian Veterinary Research Institute, Izatnagar, is the original work carried out by the candidate herself under my supervision and guidance.*

It is further certified that **Dr. P. Kirthika, Roll No. P-1720,** *has worked for more than 30 months in the Institute and has put in more than 300 days attendance under me from the date of registration for the Doctor of Philosophy Degree in this Deemed University, as required under the relevant ordinance.*

Praveen Singh

(PRAVEEN SINGH)
Chairman
Advisory Committee

Certificate

We the undersigned members of Advisory Committee of **Dr. P. Kirthika, Roll No. P-1720,** *a candidate for the degree of* **Doctor of Philosophy** *with the major discipline* **Animal Biochemistry,** *agree that the thesis entitled* **"Investigation on the V protein mediated host pathogen interaction in *Peste des petits ruminants* infection"** *may be submitted in partial fulfillment of the requirement for the degree.*

We have gone through the contents of the thesis and are fully satisfied with the work carried out by the candidate, which is being presented for the award of **Doctor of Philosophy** *Degree of this Institute.*

It is further certified that the candidate has completed all the prescribed requirements governing the award of **Doctor of Philosophy** *Degree of the Deemed University, Indian Veterinary Research Institute, Izatnagar.*

Signature
Name
External Examiner

21.02.2018

Date : 21.02.2018

(Praveen Singh)
Chairman
Advisory Committee

Date : 19/02/2018

MEMBERS OF STUDENT'S ADVISORY COMMITTEE

Dr. Paritosh Joshi, Principal Scientist
Division of Animal Biochemistry, ICAR-IVRI, Izatnagar

Dr. Manish Mahawar, Senior Scientist
Division of Animal Biochemistry, ICAR-IVRI, Izatnagar

Dr. Deepak Kumar, Scientist (Sr. Scale)
Division of Veterinary Biotechnology, ICAR-IVRI, Izatnagar

Dr. Mihir Sarkar, Principal Scientist
Division of Physiology and Climatology, ICAR-IVRI, Izatnagar

Dr. R.P. Singh, Principal Scientist & Head
Division of Biological Products, ICAR-IVRI, Izatnagar

Dr. P.K. Gupta, Principal Scientist
Division of Veterinary Biotechnology, ICAR-IVRI, Izatnagar

ACKNOWLEDGEMENTS

Foremost, I owe my deepest gratitude and greatest appreciation to my guide, Dr. Praveen Singh. None, of this work would have been possible without his patience, dedication and encouragement.

I would like to thank Dr. Paritosh Joshi for his intellectual support, encouragement and guidance. His dedication to research and his working ethics inspired me beyond scientific field.

I would like to express my sincere gratitude to Dr. Kaushal Kishor Rajak and Dr.Deepak Kumar, for the enormous amount of knowledge with which they were always ready to help with upon request.

I also would like to take this opportunity to thank Dr. Mihir Sarkar for his untiring support and guidance during my entire curriculum.

Also, I would like to express my gratitude to Dr. Ajay Kumar for his priceless support and encouragement and for providing all the facilities required to conduct the present study.

I also would like to take this opportunity to thank the members of the advisory committee, Dr. Manish Mahawar, Dr. R.P.Singh and Dr.Praveen K Gupta for their timely guidance during my entire curriculum.

At the Division of Animal Biochemistry, I would especially like to thank Dr. Meena Katariya, Dr.Mohini Saini, Dr. Sanjeev K Bhure and Dr.Mukesh for organizing and keeping in touch with me all the time to help my research work progress very well.

I would like to express my appreciation to Dr.Shikha Saxena, Dr. K. S. Priya, Dr.Santhamani, Dr.Sophia and Dr. Madhura Reddy for their scientific support and friendship.

I appreciate the generous assistance and help of Dr. Anil Gattani and Dr. Aditya Agrawal during the entire period of my research.

I am particularly grateful for Vijay, Madhu, and Apoorva's friendship and enthusiastic support. I would like to thank Parvathy Spi, Soya, Indhu, Shafiya, and Reena for their excellent friendship and extended support.

I truly appreciate their moral support that makes this dissertation possible: Mam Meeta, Mam Barkha, All the members of Kannada Balaga, seniors, juniors and Colleagues at the Division of Biochemistry.

I would like to express my appreciation to the non-teaching staff of CIF (Bio-Engineering): Mr.Surendranath, Subhashji, Hari Bhaiya, and Babla Bhaiya.

I would like to express my appreciation to the non-teaching staff of the Division of Biochemistry.

Mr. Dharmendar (Chachu), Pradeep (D.P) and Kuldeep deserve my sincere appreciation for the artistic and exquisite typing of the manuscript.

Finally, I couldn't be more thankful to my devoted parents, who provide me with unconditional love and support. Mostly, I am very grateful to my brothers, Raj Balaji and Abhimanyu, whose love and patience helped me throughout the years.

Date: 19|01|2018
Place: *ICAR-IVRI, Izatnagar*

Kirthika
(Kirthika)

ABBREVIATIONS

$	:	Dollars
%	:	Percentage
@	:	at the rate of
°C	:	Degree Celsius
Ago	:	Argonaut
APAF1	:	Apoptotic protease activating factor 1
ATP	:	Adenosine Triphosphate
BH3	:	BCL-2 homology domain 3
BID	:	BH3-interacting death domain agonist
BLAST	:	Basic Local Alignment Search Tool
bp	:	Basepair
BTV	:	Blue tongue Virus
CD46	:	Cluster of Differentiation 46
CDV	:	Canine distemper Virus
CNS	:	Central nervous system
CPE	:	Cytopathogenic effect
C-terminus	:	Carboxyl terminus
DEPC	:	Diethyl pyrocarbonate
DISC	:	Death-inducing signaling complex
DNA	:	Deoxyribonucleic acid
dsRNA	:	Double stranded RNA
EBV	:	Epstein–Barr Virus
ER	:	Endoplasmic reticulum
FADD	:	FAS-associated death domain protein
FAS	:	First apoptosis signal
FBS	:	Fetal bovine serum
FMIL motif	:	Phenylalanine, Methionine, Isoleucine, Leucine motif
g	:	Grams
G residues	:	Guanine residues
GAPDH	:	Glyceraldehyde 3-phosphate dehydrogenase
GFP	:	Green fluorescent protein
GM-CSF	:	Granulocyte-macrophage colony-stimulating factor
hpi	:	Hours post infection
hPIV	:	Human parainfluenza Virus
hr	:	Hours
IFN	:	Interferon
IL	:	Interleukin

ISRE	:	Interferon-sensitive response element
IVRI	:	Indian Veterinary Research Institute
Kb	:	Kilo Basepair
kDa	:	Kilo Dalton
LC3	:	Light chain
MCL1	:	Myeloid cell leukaemia
min	:	Minutes
ml	:	Milli liter
moi	:	Multiplicity of infection
MOMP	:	Mitochondrial outer membrane permeabilization
mRNA	:	Messenger Ribonucleic acid
MTT	:	3-(4,5-Dimethylthiazol-2-yl)-2,5-Diphenyltetrazolium Bromide
MV	:	Measles Virus
NCBI	:	National Center for Biotechnology Information
NDV	:	New castle disease
NFW	:	Nuclease free water
ng	:	Nanograms
nm	:	Nano meter
NS	:	Non structural
NSG	:	Next generation sequence
NTC	:	Non template control
N-terminal	:	Amino terminal
OD	:	Optical Density
OIE	:	*Office International des Epizooties*
ORF	:	Open Reading Frame
PBMC	:	Peripheral blood mononuclear cell
PKR	:	Protein Kinase R
PPRV	:	Peste Des Petits Ruminants Virus
RB1CC1	:	RB1 Inducible Coiled Coil Protein 1
RE	:	Restriction enzyme
RISC	:	RNA-induced silencing complex
RNA	:	Ribonucleic acid
RNAi	:	RNA interference
RNAP	:	RNA polymerase
RPMI-1640	:	Roswell Park Memorial Institute
RPV	:	Rinderpest Virus
SDS-PAGE	:	Sodium dodecyl sulfate polyacrylamide gel electrophoresis
sec	:	Seconds
SeV	:	Sendai Virus

shRNAs	:	Short hairpin RNAs
siRNAs	:	Small interfering RNAs
SLAM	:	Signaling lymphocytic activation molecule
SMAC	:	Second mitochondria-derived activator of caspases
STAT	:	Signal Transducer and Activator of Transcription
SV	:	Simian Virus
TAE	:	Tris-acetate-EDTA
tBID	:	truncated BID
$TCID_{50}$	:	50% Tissue culture infectious dose
TNF	:	Tumor necrosis factor
TOR	:	Target of rapamycin
TRAILR	:	(TNF)-related apoptosis-inducing ligand (TRAIL) receptor
U residues	:	Uridine residues
UTRs	:	Untranslated regions
UV	:	Ultra-violet
V	:	Volts
VP	:	Viral protein
Vps34	:	Vesicular protein sorting
XIAP	:	X-linked inhibitor of apoptosis protein
µl	:	Micro liter
µm	:	Micrometer

LIST OF TABLES

Table No.	Title	Page No.
Table 3.1	Primers sequence of cytokine genes for qRT-PCR	28
Table 3.2	siRNA inserts sequences	28
Table 3.3	Primers for qRT-PCR for time course studies of V protein coding region of the P gene expression	28
Table 3.4	Ligation of siRNA insert into psiRNA h7SKGFPzeo vector	40
Table 3.5	Time course studies of V protein encoding region of P gene at various time intervals	43
Table 4.1	Kinetics of V gene and S1 construct/V gene mRNA in B95a transfected and co-transfected cells respectively. Data are presented as the fold increases in mRNA levels.	52
Table 4.2	Kinetics of V gene and S1 construct/Virus mRNA in B95a transfected and co-transfected cells respectively. Data are presented as the fold increases in mRNA levels.	52
Table 4.3	Kinetics of V gene and S2 construct/V gene mRNA in B95a transfected and co-transfected cells respectively. Data are presented as the fold increases in mRNA levels.	52
Table 4.4	Kinetics of V gene and S2 construct/Virus mRNA in B95a transfected and co-transfected cells respectively. Data are presented as the fold increases in mRNA levels.	52
Table 4.5	Kinetics of V gene and S3 construct/V gene mRNA in B95a transfected and co-transfected cells respectively. Data are presented as the fold increases in mRNA levels.	52
Table 4.6	Kinetics of V gene and S3 construct/Virus mRNA in B95a transfected and co-transfected cells respectively. Data are presented as the fold increases in mRNA levels.	52
Table 4.7	Kinetics of V gene and Virus mRNA in B95a transfected and co-transfected cells respectively. Data are presented as the fold increases in mRNA levels.	52

Table No.	Title	Page No.
Table 4.8	Kinetics of Virus & S1 construct/V gene mRNA in B95a transfected and co-transfected cells respectively. Data are presented as the fold increases in mRNA levels	52
Table 4.9	Kinetics of Virus and S1 construct/Virus mRNA in B95a transfected and co-transfected cells respectively. Data are presented as the fold increases in mRNA levels.	52
Table 4.10	Kinetics of Virus and S2 construct/V gene mRNA in B95a transfected and co-transfected cells respectively. Data are presented as the fold increases in mRNA levels.	52
Table 4.11	Kinetics of Virus and S2 construct/Virus mRNA in B95a transfected and co-transfected cells respectively. Data are presented as the fold increases in mRNA levels.	52
Table 4.12	Kinetics of Virus and S3 construct/V gene mRNA in B95a transfected and co-transfected cells respectively. Data are presented as the fold increases in mRNA levels.	52
Table 4.13	Kinetics of Virus and S3 construct/Virus mRNA in B95a transfected and co-transfected cells respectively. Data are presented as the fold increases in mRNA levels.	52
Table 4.14	Kinetics of S1 Construct/V gene and S2 Construct /V gene mRNA in B95a transfected and co-transfected cells respectively. Data are presented as the fold increases in mRNA levels.	52
Table 4.15	Kinetics of S3 Construct/V gene and S1 Construct /V gene mRNA in B95a transfected and co-transfected cells respectively. Data are presented as the fold increases in mRNA levels.	52
Table 4.16	Kinetics of S3 Construct/V gene and S2 Construct /V gene mRNA in B95a transfected and co-transfected cells respectively. Data are presented as the fold increases in mRNA levels.	52
Table 4.17	Kinetics of S1 Construct/Virus and S2 Construct /Virus mRNA in B95a transfected and co-transfected cells respectively. Data are presented as the fold increases in mRNA levels.	52
Table 4.18	Kinetics of S3 Construct/Virus and S1 Construct /Virus mRNA in B95a transfected and co-transfected cells respectively. Data are presented as the fold increases in mRNA levels.	52

Table No.	Title	Page No.
Table 4.19	Kinetics of S3 Construct/Virus & S2 Construct /Virus mRNA in B95a transfected and co-transfected cells respectively. Data are presented as the fold increases in mRNA levels.	52
Table 4.20	Percentage silencing after siRNA construct(s) transfection in B95a cells. The expression was monitored at various time intervals (24, 48, 72 and 96 hpi)	52
Table 4.21	Caspase-Glo 3/7 assay analyses for caspase-3 expression in positive and negative controls. The RLUs were recorded for different time intervals post treatment	55
Table 4.22	Caspase-Glo 3/7 assay analyses for caspase-3 expression in B95a cells transfected with S2 construct and positive control. The RLUs were recorded for different time intervals	55
Table 4.23	Caspase-Glo 3/7 assay analyses for caspase-3 expression in B95a cells transfected with S2 construct and negative control. The RLUs were recorded for different time intervals	55
Table 4.24	Caspase-Glo 3/7 assay analyses for caspase-3 expression in B95a cells transfected with S2 construct and B95a cells transfected with V gene construct. The RLUs were recorded for different time intervals	55
Table 4.25	Caspase-Glo 3/7 assay analyses for caspase-3 expression in B95a cells transfected with S2 construct and B95a cells co-transfected with S2/V gene construct. The RLUs were recorded for different time intervals	55
Table 4.26	Caspase-Glo 3/7 assay analyses for caspase-3 expression in B95a cells transfected with S2 construct and B95a cells co-transfected with S2/Virus construct. The RLUs were recorded for different time intervals	55
Table 4.27	Caspase-Glo 3/7 assay analyses for caspase-3 expression in B95a cells transfected with S2 construct and B95a cells infected with virus. The RLUs were recorded for different time intervals	55
Table 4.28	Caspase-Glo 3/7 assay analyses for caspase-3 expression in B95a cells transfected with V gene construct and positive control. The RLUs were recorded for different time intervals	55

Table No.	Title	Page No.
Table 4.29	Caspase-Glo 3/7 assay analyses for caspase-3 expression in B95a cells transfected with V gene construct and negative control. The RLUs were recorded for different time intervals	55
Table 4.30	Caspase-Glo 3/7 assay analyses for caspase-3 expression in B95a cells transfected with V gene construct and B95a cells co-transfected with S2/V gene construct. The RLUs were recorded for different time intervals	55
Table 4.31	Caspase-Glo 3/7 assay analyses for caspase-3 expression in B95a cells transfected with V gene construct and B95a cells co-transfected with S2/Virus construct. The RLUs were recorded for different time interval	55
Table 4.32	Caspase-Glo 3/7 assay analyses for caspase-3 expression in B95a cells transfected with V gene construct and B95a cells infected with virus. The RLUs were recorded for different time intervals	55
Table 4.33	Caspase-Glo 3/7assay analyses for caspase-3 expression in B95a cells co-transfected with S2/V gene construct and positive control. The RLUs were recorded for different time intervals	55
Table 4.34	Caspase-Glo 3/7 assay analyses for caspase-3 expression in B95a cells co-transfected with S2/V gene construct and negative control. The RLUs were recorded for different time intervals	55
Table 4.35	Caspase-Glo 3/7assay analyses for caspase-3 expression in B95a cells co-transfected with S2/V gene construct and B95a cells co-transfected with S2/Virus. The RLUs were recorded for different time intervals	55
Table 4.36	Caspase-Glo 3/7 assay analyses for caspase-3 expression in B95a cells co-transfected with S2/V gene construct and B95a cells infected with Virus. The RLUs were recorded for different time intervals	55
Table 4.37	Caspase-Glo 3/7 assay analyses for caspase-3 expression in B95a cells co-transfected with S2/Virus and Positive control. The RLUs were recorded for different time intervals	55
Table 4.38	Caspase-Glo 3/7 assay analyses for caspase-3 expression in B95a cells co-transfected with S2/Virus and negative control. The RLUs were recorded for different time intervals	55

Table No.	Title	Page No.
Table 4.39	Caspase-Glo 3/7 assay analyses for caspase-3 expression in B95a cells co-transfected with S2/Virus and B95a cells infected with Virus. The RLUs were recorded for different time intervals	55
Table 4.40	Caspase-Glo 3/7 assay analyses for caspase-3 expression in B95a cells infected with Virus and positive control. The RLUs were recorded for different time intervals	55
Table 4.41	Caspase-Glo 3/7 assay analyses for caspase-3 expression in B95a cells infected with Virus and negative control. The RLUs were recorded for different time intervals	55
Table 4.42	Caspase-Glo 8 assay analyses for caspase-8 expression in positive and negative controls. The RLUs were recorded for different time intervals post treatment	55
Table 4.43	Caspase-Glo 8 assay analyses for caspase-8 expression in B95a cells transfected with S2 construct and positive control. The RLUs were recorded for different time intervals	55
Table 4.44	Caspase-Glo 8 assay analyses for caspase-8 expression in B95a cells transfected with S2 construct and negative control. The RLUs were recorded for different time intervals	55
Table 4.45	Caspase-Glo 8 assay analyses for caspase-8 expression in B95a cells transfected with S2 construct and B95a cells transfected with V gene construct. The RLUs were recorded for different time intervals	55
Table 4.46	Caspase-Glo 8 assay analyses for caspase-8 expression in B95a cells transfected with S2 construct and B95a cells co-transfected with S2/V gene construct. The RLUs were recorded for different time intervals	55
Table 4.47	Caspase-Glo 8 assay analyses for caspase-8 expression in B95a cells transfected with S2 construct and B95a cells co-transfected with S2/Virus construct. The RLUs were recorded for different time intervals	55

Table No.	Title	Page No.
Table 4.48	Caspase-Glo 8 assay analyses for caspase-8 expression in B95a cells transfected with S2 construct and B95a cells infected with virus. The RLUs were recorded for different time intervals	55
Table 4.49	Caspase-Glo 8 assay analyses for caspase-8 expression in B95a cells transfected with V gene construct and positive control. The RLUs were recorded for different time intervals	55
Table 4.50	Caspase-Glo 8 assay analyses for caspase-8 expression in B95a cells transfected with V gene construct and negative control. The RLUs were recorded for different time intervals	55
Table 4.51	Caspase-Glo 8 assay analyses for caspase-8 expression in B95a cells transfected with V gene construct and B95a cells co-transfected with S2/V gene construct. The RLUs were recorded for different time intervals	55
Table 4.52	Caspase-Glo 8 assay analyses for caspase-8 expression in B95a cells transfected with V gene construct and B95a cells co-transfected with S2/Virus construct. The RLUs were recorded for different time interval	55
Table 4.53	Caspase-Glo 8 assay analyses for caspase-8 expression in B95a cells transfected with V gene construct and B95a cells infected with virus. The RLUs were recorded for different time intervals	55
Table 4.54	Caspase-Glo 8 assay analyses for caspase-8 expression in B95a cells co-transfected with S2/V gene construct and positive control. The RLUs were recorded for different time intervals	55
Table 4.55	Caspase-Glo 8 assay analyses for caspase-8 expression in B95a cells co-transfected with S2/V gene construct and negative control. The RLUs were recorded for different time intervals	55
Table 4.56	Caspase-Glo 8 assay analyses for caspase-8 expression in B95a cells co-transfected with S2/V gene construct and B95a cells co-transfected with S2/Virus. The RLUs were recorded for different time intervals	55
Table 4.57	Caspase-Glo 8 assay analyses for caspase-8 expression in B95a cells co-transfected with S2/V gene construct and B95a cells infected with Virus. The RLUs were recorded for different time intervals	55

Table No.	Title	Page No.
Table 4.58	Caspase-Glo 8 assay analyses for caspase-8 expression in B95a cells co-transfected with S2/Virus and Positive. The RLUs were recorded for different time intervals	55
Table 4.59	Caspase-Glo 8 assay analyses for caspase-8 expression in B95a cells co-transfected with S2/Virus and negative control. The RLUs were recorded for different time intervals	55
Table 4.60	Caspase-Glo 8 assay analyses for caspase-8 expression in B95a cells co-transfected with S2/Virus and B95a cells infected with Virus. The RLUs were recorded for different time intervals	55
Table 4.61	Caspase-Glo 8 assay analyses for caspase-8 expression in B95a cells infected with Virus and positive control. The RLUs were recorded for different time intervals	55
Table 4.62	Caspase-Glo 8 assay analyses for caspase-8 expression in B95a cells infected with Virus and negative control. The RLUs were recorded for different time intervals	55
Table 4.63	Caspase-Glo 9 assay analyses for caspase-9 expression in positive and negative controls. The RLUs were recorded for different time intervals post treatment	55
Table 4.64	Caspase-Glo 9 assay analyses for caspase-9 expression in B95a cells transfected with S2 construct and positive control. The RLUs were recorded for different time intervals	55
Table 4.65	Caspase-Glo 9 assay analyses for caspase-9 expression in B95a cells transfected with S2 construct and negative control. The RLUs were recorded for different time intervals	55
Table 4.66	Caspase-Glo 9 assay analyses for caspase-9 expression in B95a cells transfected with S2 construct and B95a cells transfected with V gene construct. The RLUs were recorded for different time intervals	55
Table 4.67	Caspase-Glo 9 assay analyses for caspase-9 expression in B95a cells transfected with S2 construct and B95a cells co-transfected with S2/V gene construct. The RLUs were recorded for different time intervals	55

Table No.	Title	Page No.
Table 4.68	Caspase-Glo 9 assay analyses for caspase-9 expression in B95a cells transfected with S2 construct and B95a cells co-transfected with S2/Virus construct. The RLUs were recorded for different time intervals	55
Table 4.69	Caspase-Glo 9 assay analyses for caspase-9 expression in B95a cells transfected with S2 construct and B95a cells infected with virus. The RLUs were recorded for different time intervals	55
Table 4.70	Caspase-Glo 9 assay analyses for caspase-9 expression in B95a cells transfected with V gene construct and positive control. The RLUs were recorded for different time intervals	55
Table 4.71	Caspase-Glo 9 assay analyses for caspase-9 expression in B95a cells transfected with V gene construct and negative control. The RLUs were recorded for different time intervals	55
Table 4.72	Caspase-Glo 9 assay analyses for caspase-9 expression in B95a cells transfected with V gene construct and B95a cells co-transfected with S2/V gene construct. The RLUs were recorded for different time intervals	55
Table 4.73	Caspase-Glo 9 assay analyses for caspase-9 expression in B95a cells transfected with V gene construct and B95a cells co-transfected with S2/Virus construct. The RLUs were recorded for different time interval	55
Table 4.74	Caspase-Glo 9 assay analyses for caspase-9 expression in B95a cells transfected with V gene construct and B95a cells infected with virus. The RLUs were recorded for different time intervals	55
Table 4.75	Caspase-Glo 9 assay analyses for caspase-9 expression in B95a cells co-transfected with S2/V gene construct and positive control. The RLUs were recorded for different time intervals	55
Table 4.76	Caspase-Glo 9 assay analyses for caspase-9 expression in B95a cells co-transfected with S2/V gene construct and negative control. The RLUs were recorded for different time intervals	55
Table 4.77	Caspase-Glo 9 assay analyses for caspase-9 expression in B95a cells co-transfected with S2/V7 gene construct and B95a cells co-transfected with S2/Virus. The RLUs were recorded for different time intervals	55

Table No.	Title	Page No.
Table 4.78	Caspase-Glo 9 assay analyses for caspase-9 expression in B95a cells co-transfected with S2/V gene construct and B95a cells infected with Virus. The RLUs were recorded for different time intervals	55
Table 4.79	Caspase-Glo 9 assay analyses for caspase-9 expression in B95a cells co-transfected with S2/Virus and Positive. The RLUs were recorded for different time intervals	55
Table 4.80	Caspase-Glo 9 assay analyses for caspase-9 expression in B95a cells co-transfected with S2/Virus and negative control. The RLUs were recorded for different time intervals	55
Table 4.81	Caspase-Glo 9 assay analyses for caspase-9 expression in B95a cells co-transfected with S2/Virus and B95a cells infected with Virus. The RLUs were recorded for different time intervals	55
Table 4.82	Caspase-Glo 9 assay analyses for caspase-9 expression in B95a cells infected with Virus and positive control. The RLUs were recorded for different time intervals	55
Table 4.83	Caspase-Glo 9 assay analyses for caspase-9 expression in B95a cells infected with Virus and negative control. The RLUs were recorded for different time intervals	55

LIST OF FIGURES

Fig. No.	Title	After Page No.
Fig. 1.1	Geographical distribution of the phylogenetic lineages of PPRV	5
Fig. 1.2	Schematic diagram of the peste des petits ruminants' virus (PPRV) virion and genome	6
Fig. 1.3	Realignment possibilities at the paramyxovirus mRNA editing sites	14
Fig. 1.4	Wild-type and vaccine strains of measles virus (MeV) use distinct receptors to gain entry into a host	16
Fig. 1.5	Extrinsic and intrinsic apoptotic signalling pathways	21
Fig. 1.6	Molecular circuitry and signalling pathways regulating autophagy	23
Fig. 1.7	The RNA interference (RNAi) pathway	25
Fig. 4.1	B95a cells were infected with the PPRV Sungri/96 strain with MOI of 0.1 TCID50/cell. Cytopathic effects (CPE) were observed under microscope (Magnification "10X, 20X and 40X) at different time points post infection.	48
Fig. 4.2	PCR amplification of V protein coding region of the P gene	48
Fig. 4.3	Characterization of the amplicon and vector by RE digestion	48
Fig. 4.4	Cloning of V protein coding region of the P gene in pDsRed-Express-N1 Vector	48
Fig. 4.5	Colony PCR of recombinant pDsRed-Express-N1 clone in *E.coli* DH5α cells	50
Fig. 4.6	Restriction enzyme digestion of recombinant pDsRed-Express-N1 with *Bgl II* and *EcoR I* enzymes	50
Fig. 4.7	Homology studies with the nucleotide sequence among the V protein of PPRV	50
Fig. 4.8	Phylogenic tree analysis of V protein of PPRV	50
Fig. 4.9	Restriction enzyme digestion of recombinant psiRNA h7SK-GFPzeo with Hind III and Acc I enzymes	50

Fig. No.	Title	After Page No.
Fig. 4.10	Ligation of annealed siRNA inserts with the double digested psiRNA vector	50
Fig. 4.11	Colony PCR of recombinant psiRNA h7SKGFPzeo clones in *E.coli* GT116 cells	50
Fig. 4.12	Fluorscent imaging microscopy of B95a cells during transfection with green fluorescent protein (GFP)-encoding plasmid and Lipofectamine 2000 over a time period 24 hpi, 48 hpi, 72 hpi, and 96 hpi.	50
Fig. 4.13	Fluorscent microscopy of B95a cells during transfection with red fluorescent protein (pDsRED)-encoding plasmid and Lipofectamine 2000 over a time period 24 hpi, 48 hpi, 72 hpi, and 96 hpi.	50
Fig. 4.14 (a)	Fluorscent microscopy of B95a cells during co-transfection with green fluorescent protein (GFP)-siRNA construct(s) and red fluorescent protein (pDsRED)-Vgene and Lipofectamine 2000 after 24 hpi.	52
Fig. 4.14 (b)	Fluorscent microscopy of B95a cells during co-transfection with green fluorescent protein (GFP)-siRNA construct(s) and red fluorescent protein (pDsRED)-Vgene and Lipofectamine 2000 after 48 hpi.	52
Fig. 4.14 (c)	Fluorscent microscopy of B95a cells during co-transfection with green fluorescent protein (GFP)-siRNA construct(s) and red fluorescent protein (pDsRED)-Vgene and Lipofectamine 2000 after 72 hpi.	52
Fig. 4.14 (d)	Fluorscent microscopy of B95a cells during co-transfection with green fluorescent protein (GFP)-siRNA construct(s) and red fluorescent protein (pDsRED)-Vgene and Lipofectamine 2000 after 96 hpi.	52
Fig. 4.15	Kinetics of Vgene and S1 construct/V gene mRNA in B95a transfected & co-transfected cells respectively	52
Fig. 4.16	Kinetics of Vgene and S1 construct/Virus mRNA in B95a transfected and co-transfected cells respectively	52

Fig. No.	Title	After Page No.
Fig. 4.17	Kinetics of Vgene and S2 construct/ Vgene mRNA in B95a transfected and co-transfected cells respectively	52
Fig, 4.18	Kinetics of Vgene and S2 construct/ Virus mRNA in B95a transfected and co-transfected cells respectively	52
Fig. 4.19	Kinetics of Vgene and S3 construct/ Vgene mRNA in B95a transfected and co-transfected cells respectively	52
Fig. 4.20	Kinetics of Vgene and S3 construct/ Virus mRNA in B95a transfected and co-transfected cells respectively	52
Fig. 4.21	Kinetics of Vgene and Virus mRNA in B95a transfected & co-transfected cells respectively	52
Fig. 4.22	Kinetics of Virus and S1 construct/V gene mRNA in B95a transfected and co-transfected cells respectively	52
Fig. 4.23	Kinetics of Virus and S1 construct/Virus mRNA in B95a transfected and co-transfected cells respectively	52
Fig. 4.24	Kinetics of Virus and S2 construct/V gene mRNA in B95a transfected and co-transfected cells respectively	52
Fig. 4.25	Kinetics of Virus and S2 construct/Virus mRNA in B95a transfected and co-transfected cells respectively	52
Fig. 4.26	Kinetics of Virus and S3 construct/V gene mRNA in B95a transfected and co-transfected cells respectively	52
Fig. 4.27	Kinetics of Virus and S3 construct/Virus mRNA in B95a transfected and co-transfected cells respectively	52
Fig. 4.28	Kinetics of S1 construct/V gene and S2 construct/Vgene mRNA in B95a transfected and co-transfected cells respectively	52
Fig. 4.29	Kinetics of S3 construct/V gene and S1 construct/Vgene mRNA in B95a transfected and co-transfected cells respectively	52
Fig. 4.30	Kinetics of S3 construct/V gene and S2 construct/Vgene mRNA in B95a transfected and co-transfected cells respectively	52
Fig. 4.31	Kinetics of S1 construct/Virus and S2 construct/Virus mRNA in B95a transfected and co-transfected cells respectively	52

Fig. No.	Title	After Page No.
Fig. 4.32	Kinetics of S3 construct/Virus and S1 construct/Virus mRNA in B95a transfected and co-transfected cells respectively	52
Fig. 4.33	Kinetics of S3 construct/Virus and S2 construct/Virus mRNA in B95a transfected and co-transfected cells respectively	52
Fig. 4.34	The percentage gene silencing (% Knockdown) compared with B95a cells co-transfected with plasmid-S1/plasmid-S2 construct with plasmid- V protein coding region of the P gene and with infection with PPRV @0.01 moi.	52
Fig. 4.35	Non-specific amplification of each primer set of cytokine gene transcripts	54
Fig. 4.36	Specific amplification of primer set of GAPDH gene transcripts	54
Fig. 4.37	Caspase-3 expression in positive and negative controls. The RLUs were recorded for different time intervals post treatment	55
Fig. 4.38	Caspase-3 expression in B95a cells transfected with S2 construct and positive control. The RLUs were recorded for different time intervals post treatment	55
Fig. 4.39	Caspase-3 expression in B95a cells transfected with S2 construct and negative control. The RLUs were recorded for different time intervals post treatment	55
Fig. 4.40	Caspase-3 expression in B95a cells transfected with S2 construct and V gene construct. The RLUs were recorded for different time intervals post treatment	55
Fig. 4.41	Caspase-3 expression in B95a cells transfected with S2 construct and B95a cells co-transfected with S2/V gene construct. The RLUs were recorded for different time intervals post treatment	55
Fig. 4.42	Caspase-3 expression in B95a cells transfected with S2 construct and B95a cells co-transfected with S2/Virus. The RLUs were recorded for different time intervals post treatment	55
Fig. 4.43	Caspase-3 expression in B95a cells transfected with S2 construct and B95a cells infected with virus. The RLUs were recorded for different time intervals post treatment	55

Fig. No.	Title	After Page No.
Fig. 4.44	Caspase-3 expression in B95a cells transfected with V gene construct and positive control. The RLUs were recorded for different time intervals post treatment	55
Fig. 4.45	Caspase-3 expression in B95a cells transfected with V gene construct and negative control. The RLUs were recorded for different time intervals post treatment	55
Fig. 4.46	Caspase-3 expression in B95a cells transfected with transfected with V gene construct and B95a cells co-transfected with S2/V gene construct. The RLUs were recorded for different time intervals post treatment	55
Fig. 4.47	Caspase-3 expression in B95a cells transfected with V gene construct and B95a cells co-transfected with S2/Virus construct. The RLUs were recorded for different time intervals post treatment	55
Fig. 4.48	Caspase-3 expression in B95a cells transfected with V gene construct and B95a cells infected with virus. The RLUs were recorded for different time intervals post treatment	55
Fig. 4.49	Caspase-3 expression in B95a cells with co-transfected with S2/V gene construct and positive control. The RLUs were recorded for different time intervals post treatment	55
Fig. 4.50	Caspase-3 expression in B95a cells co-transfected with S2/V gene construct and negative control.. The RLUs were recorded for different time intervals post treatment	55
Fig. 4.51	Caspase-3 expression in B95a cells co-transfected with S2/V gene construct and B95a cells co-transfected with S2/Virus. The RLUs were recorded for different time intervals post treatment	55
Fig. 4.52	Caspase-3 expression in B95a cells co-transfected with S2/V gene construct and B95a cells infected with Virus. The RLUs were recorded for different time intervals post treatment	55
Fig. 4.53	Caspase-3 expression in B95a cells co-transfected with S2/V gene construct and Positive control. The RLUs were recorded for different time intervals post treatment	55

Fig. No.	Title	After Page No.
Fig. 4.54	Caspase-3 expression in B95a cells co-transfected with S2/V gene construct and Negative control. The RLUs were recorded for different time intervals post treatment	55
Fig. 4.55	Caspase-3 expression in B95a cells co-transfected with S2/Virus and B95a cells infected with Virus. The RLUs were recorded for different time intervals post treatment	55
Fig. 4.56	Caspase-3 expression in B95a cells infected with Virus and positive control. The RLUs were recorded for different time intervals post treatment	55
Fig. 4.57	Caspase-3 expression in B95a cells infected with Virus and negative control. The RLUs were recorded for different time intervals post treatment	55
Fig. 4.58	Caspase-8 expression in B95a cells positive and negative control. The RLUs were recorded for different time intervals post treatment	55
Fig. 4.59	Caspase-8 expression in B95a cells transfected with S2 construct and positive control. The RLUs were recorded for different time intervals post treatment	55
Fig. 4.60	Caspase-8 expression in B95a cells transfected with S2 construct and negative control. The RLUs were recorded for different time intervals post treatment	55
Fig. 4.61	Caspase-8 expression in B95a cells transfected with S2 construct and B95a cells transfected with V gene construct. The RLUs were recorded for different time intervals post treatment	55
Fig. 4.62	Caspase-8 expression in B95a cells transfected with S2 construct and B95a cells co-transfected with S2/V gene construct. The RLUs were recorded for different time intervals post treatment	55
Fig. 4.63	Caspase-8 expression in B95a cells transfected with S2 construct and B95a cells co-transfected with S2/Virus construct. The RLUs were recorded for different time intervals post treatment	55
Fig. 4.64	Caspase-8 expression in B95a cells transfected with S2 construct and B95a cells infected with Virus. The RLUs were recorded for different time intervals post treatment	55

Fig. No.	Title	After Page No.
Fig. 4.65	Caspase-8 expression in B95a cells transfected with V gene and positive control. The RLUs were recorded for different time intervals post treatment	55
Fig. 4.66	Caspase-8 expression in B95a cells transfected with V gene and negative control. The RLUs were recorded for different time intervals post treatment	55
Fig. 4.67	Caspase-8 expression in B95a cells transfected with V gene construct and B95a cells co-transfected with S2/V gene construct. The RLUs were recorded for different time intervals post treatment	55
Fig. 4.68	Caspase-8 expression in B95a cells transfected with V gene construct and B95a cells co-transfected with S2/Virus construct. The RLUs were recorded for different time intervals post treatment	55
Fig. 4.69	Caspase-8 expression in B95a cells transfected with V gene construct and B95a cells infected with virus. The RLUs were recorded for different time intervals post treatment	55
Fig. 4.70	Caspase-8 expression in B95a cells co-transfected with S2/V gene construct and positive control. The RLUs were recorded for different time intervals post treatment	55
Fig. 4.71	Caspase-8 expression in B95a cells co-transfected with S2/V gene construct and negative control. The RLUs were recorded for different time intervals post treatment	55
Fig. 4.72	Caspase-8 expression in B95a cells co-transfected with S2/V gene construct and B95a cells co-transfected with S2/Virus. The RLUs were recorded for different time intervals post treatment	55
Fig. 4.73	Caspase-8 expression in B95a cells co-transfected with S2/V gene construct and B95a cells infected with Virus. The RLUs were recorded for different time intervals post treatment	55
Fig. 4.74	Caspase-8 expression in B95a cells co-transfected with S2/Virus construct and positive control. The RLUs were recorded for different time intervals post treatment	55

Fig. No.	Title	After Page No.
Fig. 4.75	Caspase-8 expression in B95a cells co-transfected with S2/Virus construct and negative control. The RLUs were recorded for different time intervals post treatment	55
Fig. 4.76	Caspase-8 expression in B95a cells co-transfected with S2/Virus construct and B95a cells infected with Virus. The RLUs were recorded for different time intervals post treatment	55
Fig. 4.77	Caspase-8 expression in B95a cells infected with Virus and positive control. The RLUs were recorded for different time intervals post treatment	55
Fig. 4.78	Caspase-8 expression in B95a cells infected with Virus and negative control. The RLUs were recorded for different time intervals post treatment	55
Fig. 4.79	Caspase-9 expression in B95a cells positive and negative control. The RLUs were recorded for different time intervals post treatment	55
Fig. 4.80	Caspase-9 expression in B95a cells transfected with S2 construct and positive control. The RLUs were recorded for different time intervals post treatment	55
Fig. 4.81	Caspase-9 expression in B95a cells transfected with S2 construct and negative control. The RLUs were recorded for different time intervals post treatment	55
Fig. 4.82	Caspase-9 expression in B95a cells transfected with S2 construct and B95a cells transfected with V gene construct. The RLUs were recorded for different time intervals post treatment	55
Fig. 4.83	Caspase-9 expression in B95a cells transfected with S2 construct and B95a cells co-transfected with S2/V gene construct. The RLUs were recorded for different time intervals post treatment	55
Fig. 4.84	Caspase-9 expression in B95a cells transfected with S2 construct and B95a cells co-transfected with S2/Virus construct. The RLUs were recorded for different time intervals post treatment	55

Fig. No.	Title	After Page No.
Fig. 4.85	Caspase-9 expression in B95a cells transfected with S2 construct and B95a cells infected with virus. The RLUs were recorded for different time intervals post treatment	55
Fig. 4.86	Caspase-9 expression in B95a cells transfected with V gene construct and positive control. The RLUs were recorded for different time intervals post treatment	55
Fig. 4.87	Caspase-9 expression in B95a cells transfected with V gene construct and negative control. The RLUs were recorded for different time intervals post treatment	55
Fig. 4.88	Caspase-9 expression in B95a cells transfected with V gene construct and B95a cells co-transfected with S2/V gene construct. The RLUs were recorded for different time intervals post treatment	55
Fig. 4.89	Caspase-9 expression in B95a cells transfected with V gene construct and B95a cells co-transfected with S2/Virus construct. The RLUs were recorded for different time intervals post treatment	55
Fig. 4.90	Caspase-9 expression in B95a cells transfected with V gene construct and B95a cells infected with Virus. The RLUs were recorded for different time intervals post treatment	55
Fig. 4.91	Figure 4.91: Caspase-9 expression in B95a cells co-transfected with S2/V gene construct and positive control. The RLUs were recorded for different time intervals post treatment	55
Fig. 4.92	Caspase-9 expression in B95a cells co-transfected with S2/V gene construct and negative control. The RLUs were recorded for different time intervals post treatment	55
Fig. 4.93	Caspase-9 expression in B95a cells co-transfected with S2/V gene construct and B95a cells co-transfected with S2/Virus. The RLUs were recorded for different time intervals post treatment	55
Fig. 4.94	Caspase-9 expression in B95a cells co-transfected with S2/V gene construct and B95a cells infected with Virus. The RLUs were recorded for different time intervals post treatment	55

Fig. No.	Title	After Page No.
Fig. 4.95	Caspase-9 expression in B95a cells co-transfected with S2/Virus and Positive control. The RLUs were recorded for different time intervals post treatment	55
Fig. 4.96	Caspase-9 expression in B95a cells co-transfected with S2/Virus and negative control. The RLUs were recorded for different time intervals post treatment	55
Fig. 4.97	Caspase-9 expression in B95a cells co-transfected with S2/Virus and B95a cells infected with Virus. The RLUs were recorded for different time intervals post treatment	55
Fig. 4.98	Caspase-9 expression in B95a cells infected with Virus and positive control. The RLUs were recorded for different time intervals post treatment	55
Fig. 4.99	Caspase-9 expression in B95a cells infected with Virus and negative control. The RLUs were recorded for different time intervals post treatment	55

CONTENTS

Sl. No.	CHAPTER	PAGE NO.
1.	INTRODUCTION	01-02
2.	REVIEW OF LITERATURE	03-26
3.	MATERIALS AND METHOD	27-46
4.	RESULTS	47-55
5.	DISCUSSION	56-65
6.	SUMMARY AND CONCLUSIONS	66-68
7.	MINI ABSTRACT	69
8.	HINDI ABSTRACT	70
9.	REFERENCES	71-87
10.	APPENDIX	

Introduction

1 INTRODUCTION

Livestock have been for very long, an integral part of Indian farming system. Livestock contribute in several ways towards socio-economic development of the mankind and play a major role in providing food and nutritional security of a country. More than 18 million people primarily derive their livelihood from animal husbandry sector. Animal husbandry practices are greatly influenced not only by the agro-climatic condition of a region but also by the socio-economic status and traditions of the people there. The small ruminant rearing has been integral part of the animal husbandry practices providing livelihood to the marginal and small farmers in particular. This sector fulfills multi-dimensional needs like milk, meat, skin etc. However, more than 90% of goat and sheep that are found in the developing countries including India remains the primary commodity for meat, skin and carpet wool. Small ruminants especially goat being a considerably hardy animal and can survive on multiple unwanted shrubs and trees in a griming environment and barren lands where no other food crop can be grown. The goat population in our country has declined by 3.82% over the 18th census of livestock and the total Goat and sheep population in the country is 135.17 and 65.06 million in 2012, respectively. Among the many possible causes, health constraints can be targeted and controlled. One of the major disease to wreak havoc in the small ruminant farming is PPR *(peste des petits ruminants)* resulting in a net loss of $2500millions/year(Balamurugan *et al.*, 2012; Balamurugan *et al.*, 2014).

To work out an effective approach for vaccination and treatment of PPR there is a need to assess the host-pathogen interactions. Virus proteins interact with the host's cellular machinery, and bring about various outcomes that effect both virus and the host physiology. It

is important to identify and annotate virus host interactions for the discovery of new drug targets as well as for assessing the efficiency of antiviral drug therapies on host subpopulations (Brander and Walker, 2000).Furthermore, virus-host interactions can be used to suggest roles for virus proteins, and investigate common viral strategies for interacting with their hosts (Dampier and Tozeren, 2007).Various studies have been carried out and the data has been gathered for virus-host interactions to determine host factors necessary for the virus life cycle. These interactions take the form of virus-host protein interactions, host gene expression responses to infection, and genetic screens for host genes that are necessary for virus survival and pathogenesis (Navratil *et al.,* 2010). As far as PPR virus is concerned the particulars regarding the host-virus interactions and the role of proteins specially the non-structural ones are scarce. Virus-host interaction data can be primarily collected from small interfering RNA (siRNA) screens as this phenomenon of RNA interference (RNAi) has been successfully used against many viruses *in vitro*, both through chemical and viral vectors. These siRNA molecules help us study the virus-host protein interactions by silencing the gene sequence that codes for that protein. The investigation on the V protein mediated host pathogen interaction in PPR infection using siRNA can be an initial lead in this direction and for further *in vivo* studies to finally help develop better antiviral therapeutics.

Keeping in view the above facts the present study was designed with the following objectives:

1. **To study the role of V protein in virus-host interaction in PPR infection using siRNA.**
2. **Elucidating the role of V protein in triggering cytokine expressing genes and the apoptotic cascade in PPR infection**

Review of Literature

2 REVIEW OF LITERATURE

The myriad world of animal cells is instrumental for the survival of viruses that have evolved in an assorted manner (Shatkin, 1974). With the ability to make a living at the expense of animal well being, viruses have made important contribution to the better understanding of their replication, evolution, underlying molecular biology and interaction with the host. The diverse legion of viruses can be classified into seven groups according to the relationships between virion, nucleic acid and mRNA transcription (Baltimore, 1971; Adams *et al*., 2012). The RNA viruses can be classified according to the sense or polarity of their RNA into negative-sense, positive-sense, or ambisense RNA viruses (Koonin, 1991; Kondo *et al.,* 2012). The RNA found in a negative-sense virus is not infectious by itself, as it needs to be transcribed into positive-sense RNA. The complementary plus-sense mRNA must be made before proteins can be translated from the viral genome. This RNA negative-strand to positive-strand copying is carried out by an RNA-dependent RNA-polymerase. Each virion that has one negative-strand copy can be transcribed to several positive-sense RNAs (Steinhauer and Holland, 1987).A number of viral diseases in livestock and companion animals have devastating consequences.

***Peste des petits ruminants* (PPR): The goat plague**

PPR is one of the most devastating, acute viral diseases of small ruminant caused by PPR virus (PPRV), a single stranded negative sense *Morbillivirus* that belongs to the *Paramyxoviridae* family (Gibbs *et al.,* 1979). This disease is highly contagious in goats whereas

sheep and other related wild animals seem to suffer a comparatively lesser insult. For a very long time this disease was thought to be caused by a variant of rinderpest virus, adapted to small ruminants as PPR clinically mimics cattle plague (Rinderpest), characterized by fever, erosive stomatitis, enteritis, pneumonia, and death (Gibbs *et al.,* 1979). The high prevalence of RP and the scarcity of diagnostic tests to differentiate PPR from RP only added to the woes (Singh *et al.,* 2009). Due to cross-neutralization between PPRV and RPV, small ruminants infected with RPV would have developed protective antibodies suppressing the clinical outcome of PPRV infection(Baron *et al.*,2011).This disease gained momentum when a severe case of RP like ailment was recorded in the herds of sheep and goat which failed to cause any clinical signs in the cattle that were reared in the close vicinity (Taylor and Abegunde,1979; Taylor *et al.*,1990). The disease was reported in 1942 for the first time in the Côte d' Ivoire (Gargadennec and Lalanne,1942; Kumar *et al*., 2014) and was designated as a separate member of the genus Morbillivirus in 1979(Gibbs *et al.,* 1979). After its designation, the prevalence of PPRV has been reported from to sub Saharan Africa, the Middle East, Turkey and the Indian subcontinent. Recently, outbreaks have been reported for the first time in China, Kenya, Uganda, Tanzania, Morocco and Tunisia (Munir *et al*., 2013). The disease exists in one serotype separated into four lineages (I–IV); these lineages are based on the genetic comparison of a fragment of the fusion protein or the nucleoprotein (Banyard *et al.*, 2010). The four lineages follow a geographic distribution where lineages I and II are found in Western and Central Africa where the disease was first identified, Lineage III is restricted to the Middle East and East Africa. Although, lineage IV is predominantly considered an Asian lineage, it is now overwhelming the other lineages in African countries, while still being predominant in Asia (Banyard *et al.*, 2010; Kwiatek *et al*., 2011). Recent reports of PPRV from the previously PPRV-free countries belong to lineage IV, which implies that lineage IV is a novel group of PPRV and may replace the other lineages in the near future. It's not clear whether the differences between lineages solely reflect geographical speciation or if they are also correlated with variability in pathogenicity between isolates (Banyard *et al*., 2010).

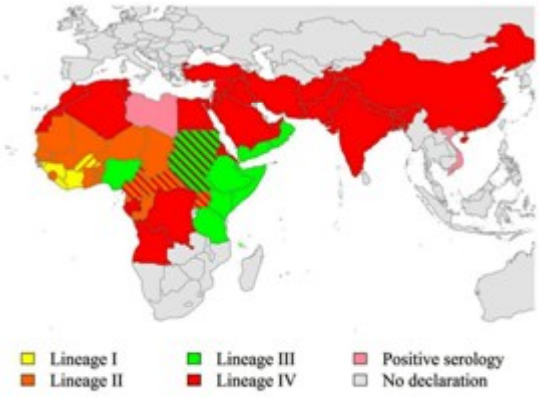

Fig 1.1: Geographical distribution of the phylogenetic lineages of PPRV

Indian platform and the economic impact

The small ruminant rearing has been integral part of the animal husbandry practices providing livelihood to the marginal and small farmers in particular. This sector fulfills multi-dimensional needs like milk, meat, skin etc. India is home to 65.06 million sheep and 135.17 million goats (19th Livestock census, 2012). The goat population in our country has declined by 3.82% over the 18th census of livestock and one of the major reasons for this drastic decline in the goat population is PPR outbreaks (Balamurugan *et al*., 2012). In India, PPR is enzootic belongs to Lineage IV and the outbreaks are reported around the year (Singh *et al.*,2002). Although, the disease was reported for the first time in 1989 in Tamilnadu (Shaila *et al*., 1989), during 1993-1994 various veterinary laboratories across the nation reported outbreaks of pasteurellosis which were typical PPR cases (Srinivas and Gopal,1996). No further cases of rinderpest in small ruminants was reported after the recognition of the disease in India. The economic importance of PPR is mainly due to its contagious nature, with a case fatality rate as high as 100%. In India, PPR causes a net loss of $2500millions/year (Balamurugan *et al.,* 2012).

The viral agenda

This havoc wrecking disease is caused by the member of the *Morbillivirus* genus in the family *Paramyxoviridae*. (sub family *Paramyxoviridae*) under the order *Mononegavirales*. This genus also includes Rinderpest virus, Canine distemper virus, human Measles virus and viruses of marine mammals, Phocine distemper virus of seals and the certain Cetacean Morbillivirus isolated from clinical samples (Gibbs *et al*., 1979; Barrett *et al*., 1993;

Abubakar *et al*., 2009). This RNA enveloped virus is a pleomorphic particle with a lipoprotein membrane that cases a ribo-nucleoprotein core, which contains RNA genome (Balamurugan *et al.,* 2014). An approximately 16 kilo bases long negative sense single stranded RNA with negative polarity forms the genome (Chard *et al*.,2008). The genome is structured into six transcriptional units and arranged in the sequential order of 3' N–P/C/V–M–F–H–L 5'. Each of these units encodes for a minimum of one non overlapping protein: the nucleocapsid (N) which encapsidates the RNA and protects it from the catastrophic nuclease attack (Andzhaparidze *et al.,*1986), two surface glycoproteins, the hemagglutinin (H) protein and the fusion (F) protein, which plays a vital role in the attachment and fusion of the virus with the host cell membrane, are embedded in the virus envelope and give it a fringed appearance, the matrix (M) protein acts as a link, which associates with the nucleocapsid and the two external viral proteins, the fusion (F) protein and the HN protein,the polymerase or large (L) which along with the phosphoprotein (P) forms the viral RNA-dependent RNA polymerase (Diallo, 1990; Dhar *et al*., 2002). The P gene also codes for two non structural proteins; V and C which are a result of a co-transcriptional editing strategy (Muthuchelvan *et al*., 2006a).

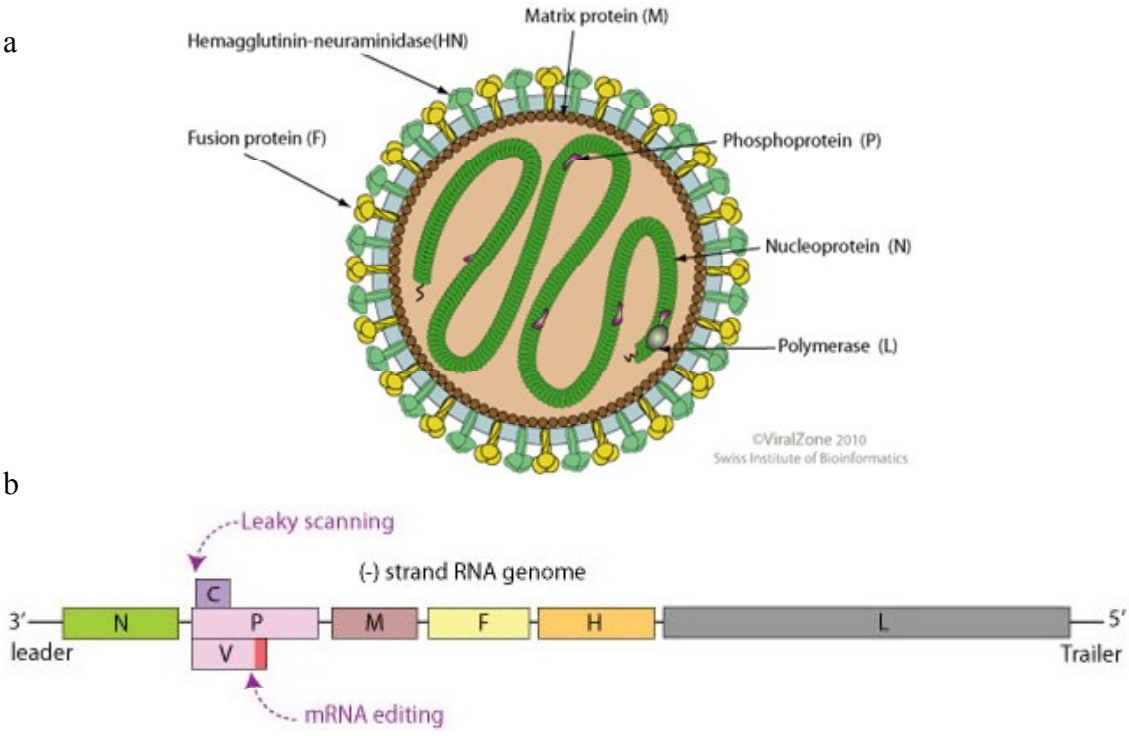

Fig. 1.2: Schematic diagram of the peste des petits ruminants' virus (PPRV) virion and genome. (a) A virion contains a single or multiple RNA genome(s) and six viral proteins (H, F, M, N, P and L). The V and C proteins are nonstructural. Although the H and F proteins are drawn separately in

the figure, they are associated closely with each other in the envelope. (b) A ~16 kb, non-segmented RNA genome of MV contains six genes. The P gene encodes the P, V and C proteins. The P and C proteins are translated from overlapping reading frames on a functionally bicistronic mRNA and the V protein is translated from V mRNA, which is formed after insertion of a single nucleotide G by RNA editing. The terminator region of each gene is followed by a three nucleotide-long conserved (GAA) region called intergenic region (IG). IG region is also found at the junction of leader sequences and the N gene (first gene) and between the L gene (last gene) and the trailer region. Each transcription unit (to produce individual viral protein) is composed of the coding sequence(s), IG region and the conserved start and stop signals that flank the coding sequence(s).

The structural proteins

Nucleocapsid (N) protein

With sequence similarities between the N proteins within the family ranging from 67% to 74% (Barrett *et al.,* 2006) it is produced in the highest amount in Morbilliviruses (Diallo *et al.,* 1987). The molecular weight of the PPRV N protein is about 58 kDa and it encapsidates the viral genome into ribonucleoprotein (RNP) complex (Ismail *et al.,* 1995). The region responsible for self assembly of the N protein is conserved and called Ncore; only the wild-type but not mutated N protein can encapsidate the viral RNA (Bankamp *et al*., 1996). The N protein of the Arabian strain and African strain have a single glycosylation site and two glycosylation sites respectively. This difference could contribute to the difference in the mobility of respective strains on SDS-PAGE. Moreover, it is conceivable that N protein is highly susceptible to proteolysis and degradation products may vary between the two viruses and hence differ in molecular weight. However, such prediction requires future explicit experiments (Munir *et al*., 2013).Like its other counterparts, the N protein of PPRV is likely to interact with other N proteins (N–N interaction), with the P protein (N–P interaction) and with polymerase units (P–L interaction) to take part in the replication complex. The N protein plays a pivotal role in the replication of PPRV (Servan de Almeida *et al.,* 2007). The silencing of N mRNA can block the production of N transcripts and the expression of N protein. It has been demonstrated that the shutting down of the N protein indirectly inhibits the production of M protein. The shutdown of both the proteins results in the inhibition of PPRV progeny by 10,000-fold (Singh *et al.,* 2004; Keita *et al*., 2008). Being most abundant, N is a highly immunogenic protein. Its antigenic stability and plentiful in the virus, the N protein is widely targeted for diagnostic assays. Given its intra-viral location the immune response against N protein are non-protective (Munir *et al.,* 2013).

Phosphoprotein (P)

The P protein of the PPRV is the longest among the structural proteins. Owing to richness in serine and threonine, the acidic P protein undergoes intensive post-translational phosphorylation (Diallo *et al.,* 1987). P protein is one of the least conserved proteins within the family which can be substantiated from studies that show that PPRV and RPV share only 51.4% amino acid identity of the P protein (Mahapatra *et al*., 2003). The C-terminus of the P protein is more conserved than the N-terminus and is involved in the N-P interaction. This influences various biological processes such as cell cycle, transcription and translation regulation (Johansson *et al.,* 2003). This protein has an integral role triggering an immune response and replication (Munir *et al*., 2013). This protein is a part of the viral L–polymerase complex, and considered to direct the pathogenicity of Morbillivirus cross-species (Yoneda *et al*., 2004).

Matrix (M) protein

With a predicted molecular weight of about 37.8 kDa the M protein is considered the smallest proteins among all the structural proteins of morbilliviruses. A calculated identity and similarity of about 85.0% and 92.5% has reported between PPRV and RPV, respectively. Being highly conserved within the family the M protein seems to be important in progeny formation and interaction with the surface glycoprotein of the cell membrane. This opinion of high degree of conservation was further strengthened when the replacement of M protein of RPV with that of PPRV, it did not affect the growth of RPV in cell culture (Mahapatra *et al.,* 2006). Three ATG repeats (^{956}tctATGATGATGtca^{970}) have been identified in the gene for the M protein of PPRV, RPV and MV, whereas the M gene of CDV, PDV, and DMV are deprived of this domain (Muthuchelvan *et al*., 2005). M protein lines the inner coat of the viral envelop and acts as a link between the surface glycoprotein (F and HN) and the ribonucleoprotein core (genome, N, P and L). Studies in Nipah virus, a member of the same family which shares the identity with that in the M protein of PPRV shows the importance of the motif (FMYL) at amino acid position 50–53 required for the localization of the M protein in the cell membrane to facilitate the budding process (Ciancanelli and Basler, 2006).

Fusion (F) protein

The F protein is embedded in the viral lipid bilayer envelope and protrudes as spikes on the viral surface. The cleavage of the F protein is vital for paramyxovirus virulence. This protein is highly conserved among all the members of morbilliviruses and this reflects the cross-protection between PPRV and RPV (Taylor and Abegunde, 1979). With a molecular weight of 59.137 kDa, the naive form of the F protein (F0) undergoes post-translational proteolytic cleavage and forms two active subunits, F1 and F2. Although the mechanism is not well understood for PPRV, the presence of RRTRR at position 104–108 is thought to be cleaved by a trans-Golgi associated furin endopeptidase (Chard *et al*., 2008). F protein of all the morbilliviruses contain a leucine zipper motif that facilitates the oligomerization and fusion function of the F protein through a mechanism yet to be elucidated (Plemper *et al*., 2001). In PPRV, this motif is located at position 459–480 and is conserved among all PPRV strains characterized so far.

Haemagglutinin-neuraminidase (HN) protein

With a molecular weight of 67 kDa HN protein is the least conserved. The HN protein of PPRV and RPV share only a 50% amino acid identity. This plays a role in viral specificity for cell tropism and therefore determines the host range. The H protein of the PPRV has both hemagglutinin and neuraminidase activities (Seth and Shaila, 2001). The HN protein is responsible for virus attachment to host cell as well as cleavage of the sialic acid residue at the carbohydrate moiety in the glycoprotein of the host (Langedijk *et al*., 1997). The HN protein is under ever increasing immunological pressure as most of the viral neutralizing antibodies are mainly directed against it (Renukaradhya *et al*., 2002). Studies have shown that the HN protein of PPRV required a homologous F protein for proper functioning in virus replication (Das *et al*., 2000). H protein is the fundamental antigenic determinant of the morbilliviruses as it is the major determinant of cell tropism in MV and plays a vital role in cross-species pathogenesis in lapinized RPV (Yoneda *et al*., 2002). This protein down regulates CD46, a cell membrane protein involved in the complement regulation on host cells (Galbraith *et al*., 1998).

Large (L) protein

The largest protein in PPR virions is 2183 amino acids long (Yunus and Shaila, 2012). The mRNA encoding for the L protein is the least abundant (Flanagan *et al*., 2000). L protein is conserved among morbilliviruses: PPRV has an identity with RPV and CDV of 70.7 and 57.0%, respectively (Bailey *et al*., 2005). The L protein acts as RNA-dependent RNA polymerase and performs transcription and replication of the viral genomic RNA. Apart from these functions, the L protein carries out capping, methylation and polyadenylation of viral mRNA. All these steps are essential for efficient replication of the viruses. Three motifs in the L protein have been identified, which are directly linked to the functions of this protein (Munir *et al*., 2013). The first domain has conserved sequence KEXXRLXXKMXXKM from residues 1 to 606 and is believed to be an RNA binding motif. The second domain contains the conserved sequence GDDD flanked by hydrophobic regions (from residues 650 to 1694) and is believed to be the functional site for RdRp. The third domain from residues 1717 to 2183 has kinase activity (Barrett *et al*., 2006). The sequence (ILYPEVHLDSPIV at positions 9–21) act as a binding site for P and L proteins and is conserved in paramyxoviruses: in PPRV it is totally conserved except the first amino acid, which is valine instead (Chard *et al*., 2008).

The non structural proteins

The P cistron of the PPRV encodes two more proteins, C and V. Whether these non structural proteins serve a specialized or accessory function during virus replication, pathogenicity and interaction during host-virus cascade is yet to be elucidated. The C and V proteins are synthesized through alternative open reading frame and RNA editing, respectively (Mahapatra *et al*., 2003; Barrett *et al*., 2006). The C protein weighs about 20 kDa. This protein is translated from a second open reading frame (ORF) (11 relative to P ORF) initiated from the second AUG located19 nucleotides (nt) downstream of the P AUG, thus giving rise to an unique amino acid (aa) sequence (Bellini *et al*., 1985). The C proteins are found in all Paramyxoviruses and related amongst the Morbilliviruses; but the amino acid sequences are not conserved within this group. The C protein of Sendai virus (SeV) is thought to participate in the down regulation of viral transcription by a promoter-specific mechanism (Tapparel *et al*., 1997). Studies done in recombinant SeV devoid of all C ORFs nullified the importance of C protein for replication (Kurotani *et al*., 1998). On the other hand the silenced C protein of

Measles virus (MV) didn't seem to affect viral growth in cell culture (Radecke and Billeter, 1996).

The P protein seems to be phosphorylated and can bind both N and L proteins and hence is believed to regulate RNA synthesis (Sweetman *et al*., 2001). The predicted molecular mass and iso-electric point of the V protein of PPRV is 32.28 kDa and 4.68, respectively. The length of the V protein is highly variable among morbilliviruses (Munir *et al*., 2013). Both C and V proteins are associated with IFN regulations at ISRE level in an *in vitro* reporter system. However, the molecular mechanism of inhibition needs to be studied. The process by which the virus synthesis this protein is rather an interesting mechanism.

A stuttered synthesis

The wide spread notion that the DNA-encoded exonic sequence information in the genome directly predicts the amino acid composition of the final gene product(s) needed to be revisited with the discovery of RNA editing. The programmed post-transcriptional alteration of a DNA encoding sequence (Maas and Rich, 2000; Gray, 2003) is termed as RNA editing. This term was coined in 1986 after the sequence determination of the *cox II* transcripts revealed four extra reading frame-restoring nucleotides at the frameshift position that are not encoded in the DNA (Benne *et al.*, 1986).The term RNA editing is now used to describe a large number of different processes that produce RNA transcripts whose sequence and information differs from that encoded by the corresponding exonic region of the DNA. An array of RNA editing by various other mechanisms including nucleotide insertion, deletion, and base substitution, were subsequently elucidated. These observed changes in the nucleotide identity differ from the classical 'RNA modification' *viz*., addition of a methyl group or 5'- and 3'-end formation or splicing or the creation of hypermodified bases (Mass and Rich, 2000; Gray, 2003).The process of editing can occur co-transcriptionally by nucleotide insertion, wherein the modification of the RNA from its synthesis occurs concurrently. The classical examples of co-transcription are the mitochondrial RNA of *Physarum polycephalum* (a eukaryotic microbe, slime) and the P genes of paramyxovirus (Jacques and Kolakofsky, 1991). Although the insertion of cytidylates or uridylates, and certain dinucleotides is closely coupled with the synthesis of the RNA, the editing is relatively complex in *Physarum* species. The editing of *Physarum* RNAs

usually involvs single, widely spaced insertions rather than intensive editing "blocks" or repeated copying of a templated base(s) (Cattaneo, 1991; Visomirski-Robic and Gott, 1997). In contrast, the editing of paramyxovirus P gene mRNAs is relatively simple and only guanylates are added (Haussmann *et al*., 1999) by pseudotemplated transcription. The transcriptional frameshifting due to the programmed insertion of different numbers of guanylates is analogous to the ribosomal frameshifting that occurs in retroviruses and coronaviruses to synthesis gag-pol polyprotein (Jacks and Varmus, 1985; Manktelow *et al*., 2005) except that the paramyxovirus mRNA editing occurs during mRNA synthesis. The Paramyxovirinae consists of three genera: Rubulaviruses (which includes simian virus 5 [SV5] and mumps virus among others); Respiroviruses (Sendai virus (SeV) and human and bovine parainfluenza virus type 3 [h- and bPIV3]); and Morbilliviruses which include measles virus, distemper viruses and Peste des petits ruminants (PPR) (Amarasinghe *et al*., 2017). These viruses contain a single-stranded RNA with a genome size of 15 948 bp (Bailey *et al*., 2005; Mahapatra *et al*., 2006). The genome is helical nucleocapsid and each nucleocapsid protein (N) subunit is associated with precisely six nucleotides. This pleomorphic genome follows the rule of six *i.e*., the viral genome found in nature are always in multiples of six nucleotides (Calain and Roux,1993; Kolakofsky *et al*.,1998). The genome encodes for 6 proteins, including a nucleoprotein (N), a Large protein (L), a matrix protein (M), a fusion protein (F), a hemagglutinin protein (H) and an RNA-polymerase and a multifaceted phosphoprotein co-factor (P) (Couacy-Hymann *et al*., 2007). The large (L) protein works as an RNA-dependent-RNA polymerase (RdRp) and initiates the transcription of the six messenger RNAs (mRNAs) in the order N, P, M, F, HN, and L (Egleman *et al*., 1989). All these mRNAs are the lone primary product from a single open reading frame (ORF) except for P gene mRNA. The P gene is the second proximal to the 3'-terminus and mRNA usually contains one or two alternate ORFs that overlap with mid region of the P protein ORF and are expressed as fusion protein with the N-terminal half of P (Bellini *et al*.,1985; Cattaneo *et al*.,1989). The ability of P gene mRNA to give rise to multiple protein sequences by means of overlapping frames is possible because of a noteworthy process called co-transcriptional mRNA editing (Vidal and Kolakofsky, 1990) also known as pseudotemplated addition of nucleotides (Kato *et al*.,1997; Muthuchelvan *et al*., 2006b). Reports in paramyxovirus P gene mRNAs elucidates that only a single site per 15 kb viral

genome is modified owing to the editing process and only guanylates are added within a short run of guanylates. Although the RNA editing to insert pseudotemplated G residues is found for all the three paramyxovirus genera, the programmed insertion of numbers of guanylates at their editing sites is a virus-specific event (Wardrop and Briedis, 1991; Kolakofsky *et al*., 1993). Most paramyxoviral P genes contain a 52 A_nG_n purine run at the start of the internal, overlapping V ORF. Along with the faithful copies of their templates the mRNAs with expanded G runs are transcribed from these genes, and the number of G insertions which occur for each virus group depends on their requirements to switch between the *in*-frame and *trans*-frame downstream ORFs. In Sendai virus (SeV) and measles virus/Rinderpest virus (*Morbillivirus*), the unedited mRNA of the P gene encodes the P (phospho) protein, while a single nucleotide insertion to frameshift to the V ORF from the genome-encoded P ORF *i.e.,* addition of one G residue produces an mRNA that encodes the V protein (Vidal *et al.*, 1990; Park and Krystal, 1992; Galinski *et al.*, 1992). On the contrary with insertion of one or two G residues encodes the P protein and the unedited version encodes V protein for the genus Rubulavirus including SV5 (Thomas *et al.*, 1988) mumps virus (Paterson and Lamb, 1990). In bovine parainfluenza virus type 3 (genus *Paramyxovirus*), both V and another ORF (called D) overlap the middle of the genome-encoded P ORF, one to six Gs are added at roughly equal frequency so that mRNAs encoding all three overlapping ORFs are expressed. In all the above cases, the P and V proteins are amino-co-terminal, while the frameshift is used to generate the carboxy terminal half from the edited mRNA (Kato *et al.,* 1997).This cotranscriptional mRNA editing is possible because of what is known as the 'stuttering model'. This model is analogous to the elongation-termination decision of *Escherichia coli* RNA polymerase (RNAP) (von Hippel and Yager, 1992). The ability of the negative-strand virus RNAPs to polyadenylate their mRNAs by stuttering on a short run of template U residues (4 to 7 nucleotides [nt] long) at the end of each gene strongly suggested that the G insertions would occur in the similar manner by pseudotemplated transcription (Thomas *et al.*, 1988;Vidal *et al.*, 1990). According to the model the viral RNAP reiteratively copies a short stretch of C residue at a specific region in the genome during mRNA synthesis, and the polymerase pauses at this site and, when the pause is sufficiently long, slippage of the nascent mRNA occurs by one or two nucleotides, thereby reiteratively inserting one or two Gs. These insertions alter the reading frame in the middle of the gene and allow ribosomes to translate the alternate ORF downstream. At any

given template position the elongation complex of the paramyxovirus RNAP can either extend the nascent chain by a single nucleotide, or it can be induced by template or nascent chain sequence to pause. The process of polymerase stuttering is similar to the polyadenylation that occurs at end of each gene that leads to formation of poly (A)-tail. The site of stutter and the poly (A)-termination sites are related mechanistically and the former seem to be evolved from the later. During polyadenylation the pause is seemingly much stronger, and can only be relieved by chain termination and not continued elongation. On the other hand no such chain terminations are found

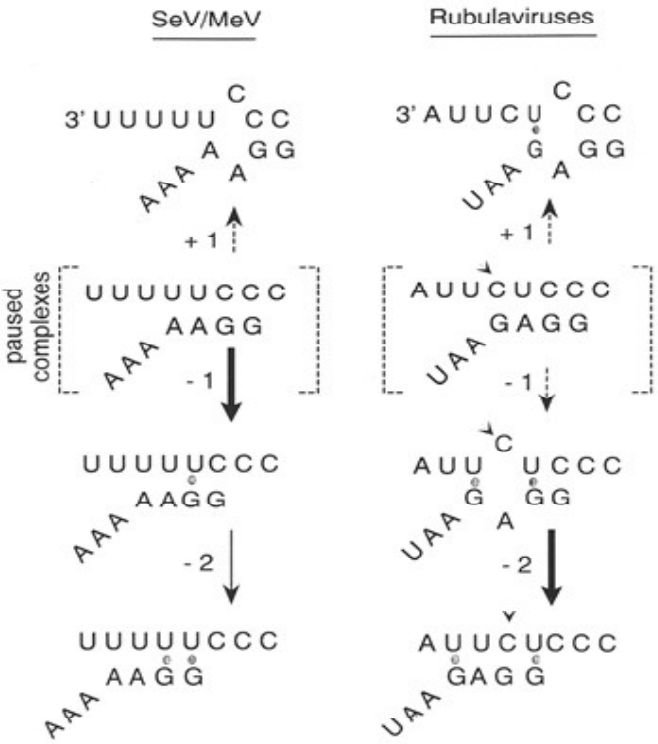

Fig. 1.3: Realignment possibilities at the paramyxovirus mRNA editing sites.RNA synthesis complexes of the template(top strand, written 3' to 5')and nascent chain (bottom strand, 5' to 3')containing four base pairs are shown, for the SeV group and morbilliviruses(left side) and rubulaviruses(right side).The polymerase whose catalytic site contains the 3' end of the nascent chain is proposed to pause after incorporation opposite the middle template C residue(second level, in dotted brackets),and the nascent chain to realign on the template, allowing for U:G pairs (highlighted with a shaded circle in between),but not A:C (which are shown looping out). The frequencies of the realignments that occur during natural virus infection are indicated by the strengths of the arrows. Numbers indicate the realignment of the nascent chain; minus as upstream and plus as downstream *i.e.,* the opposite of the subsequent insertions. For, rubulaviruses,the -1 realignment is prevented by the marked (arrowhead) template C residue (which is a U in the SeV/MV group). Once bypassed by a -2 shift(bottom panel),this template C aligns only with Gs in further shifts.

Kicking the infection: Host–Pathogen Interactions and Anti-Viral Immunity

Role of cell surface receptors in infection

The PPRV requires 6–8 h in cultured cells to complete its life cycle (Kumar *et al*., 2013). The initial step of infection, *i.e.,* the binding of virus to the host cell and delivery of the nucleocapsid into host cell cytoplasm,plays an important role in the pathogenesis of the virus and susceptibility to the host. The primary receptors for PPRV are the signalling lymphocyte activation molecule (SLAM) or CD150 protein and Nectin-4 (poliovirus receptor-like protein 4 ,PVRL4). SLAM is a costimulatory glycoprotein belonging to the CD2 subset of the immunoglobulin super family and is expressed on the activated cells of immune system *i.e*., surface of a proportion of primary B cells, Epstein-Barr virus (EBV) transformed B cells (B95a cells), activated T cells, memory T cells, T cell clones, immature thymocytes, mature dendritic cells, and activated monocytes.This is seldom present on epithelial cells.SLAM expression in peripheral blood mononuclear cells (PBMCs) is positively correlated with the magnitude of virus replication(Pawar *et al*., 2008). It's cytoplasmic domain has an immunoreceptor tyrosine-based switch motif that binds small SH-2 domain adaptor proteins which plays a pivotal role in cell signaling (Yanagi *et al*., 2002; Ohno *et al*., 2003). On the other hand,Nectin-4 an adherent junction protein of the immunoglobulin superfamily is expressed on epithelial cells, but is not expressed in lymphocytes and dendritic cells (Adombi *et al.,*2011). The presence of two types of receptors can be attributed to the fact that Morbilliviruses are both lymphotropic as well as epitheliotropic.Apart from the above mentioned receptors,the laboratory adapted,vaccine strains are thought to use CD46 (membrane cofactor protein, MCP), a complement regulatory protein which is expressed on nearly all nucleated cells (Liszewski *et al*.,1991). Nectin-4, has been found to play an important role for dissemination of MeV throughout the body by facilitating amplification and subsequent release of the virus via different secretions (exit receptor) (Noyce *et al*.,2011; Noyce and Richardson, 2012). Studies in MV has shown that both vaccine and wild-type strains can use SLAM as a receptor, but wild-type strains do not use CD46 efficiently (Yanagi *et al*., 2002). As PPRV and MV belong to the same family and postulated to follow the same mechanism to attach to the cell surface receptor and thus represented diagramatically.

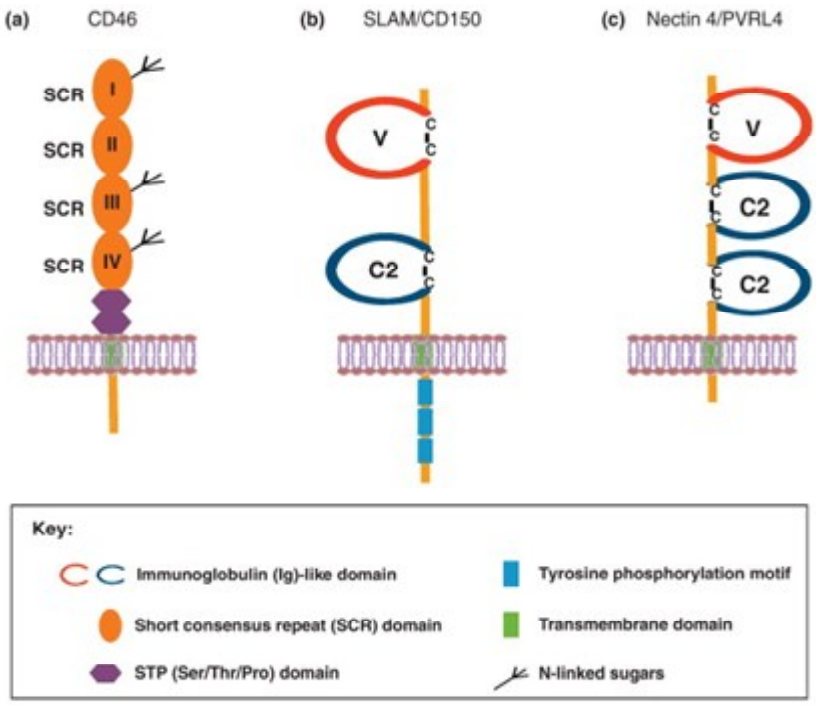

Fig. 1.4: Wild-type and vaccine strains of measles virus (MV) use distinct receptors to gain entry into a host. Vaccine and laboratory-adapted strains of MV (Edmonston) were previously shown to use (a) CD46/MCP, a receptor that is expressed on nucleated cells. It is a complement regulatory protein that contains 4 sushi/short consensus repeat (SCR) domains, a serine-threonine-proline (STP) rich domain, a transmembrane domain, and a cytoplasmic region. (b) However, clinical isolates of MV use CD150/SLAM, a receptor that is expressed on immune cells, including activated lymphocytes, dendritic cells and macrophages. It is a signaling molecule found on immune cells that contains cytoplasmic tyrosine phosphorylation sites. It is a member of the immunoglobulin (Ig) superfamily and contains a variable (V) region and one type 2 constant region (C2). (c) Wild-type MeV isolates can also enter the basolateral side of epithelia in the respiratory tract through Nectin 4/PVRL4. Vaccine strains of MeV can also use this receptor in cultured cells. Nectin 4/PVRL4 is found in the adherens junctions and is also a member of the Ig superfamily. It contains a V region and two C2s (Noyce *et al*., 2012)

How the proteins contribute to pathogenesis

The first interaction of the host and pathogen (attachment) is mediated by the tetrameric H protein *via* interaction with cell surface receptors, which triggers the conformational change of the trimeric F protein and then,the membrane fusion and the delivery of the viral RNP core into the cytoplasm (Brindley *et al*., 2012; El Najjar *et al*., 2014). Unlike other members of the Paramyxovirus, H protein solely interacts with the virus receptor for attachment instead of HN. All the receptor binding regions on the H protein are found on the lateral surface of the head structure and are usually overlapping (Santiago *et al.,* 2002; Santiago *et al.,* 2010;

Biebask *et al*., 2002; Masse *et al*., 2004; Vongpunsawad *et al*., 2004; Colf *et al.,* 2007; Hashiguchi *et al*., 2007; Hashiguchi *et al*., 2011).

H and F protein

H and F cooperate to induce fusion of the viral envelope and cellular plasma membrane for entry. Infected cells expressing the viral glycoproteins at the cell surface can also fuse with uninfected cells to produce multinucleated giant cells followed by cell death. However, not all types of infected cells fuse to form syncytia. *In vivo*, giant cells are observed in the lung, skin, and lymphatic tissue, but not the central nervous system (CNS). Cellular protein synthesis is relatively unaffected by MV infection, but specific cellular proteins (e.g. cell surface receptors) and functional responses (e.g. signal transduction and expression of transcription factors) may be altered in a cell-type-specific manner (Bazarsky *et al*., 1997).

The role of viral non structural proteins in countering the immune system

Studies in various viral NS proteins have illustrated their critical roles in virus replication, and elucidation of their mechanisms of action is one of the central themes in virus research today. An increasing body of evidence based on works in viruses shows that these NS proteins control many of the key replication and assembly processes within the infected target cell and therefore may serve as suitable targets for antiviral intervention strategies. *Bluetongue virus* (BTV) a dsRNA non enveloped *Arbovirus* encodes four NS proteins, NS1, NS2, and NS3 and the related NS3A (Owens *et al*.,2004). Although, not much is known about the functions of these protein in the viral life cycle but the functional mechanisms of NS3 has been illustrated. Being the only viral-encoded cell surface glycoprotein it interacts with the p11 subunit of the heterotetrameric calpactin II complex as well as with the VP2 outer capsid protein thereby provide a mechanism by which newly assembled virions exploit the exocytic pathway for nonlytic virus release (Beaton *et al*., 2002). Whereas the NS1 protein is shown to specifically bind to the single-chain antibody (scFv-NS1).This antibody is responsible for the observable changes in the viral life cycle due to interference with NS1 function or tubule formation(Owens *et al*., 2004). The NS 1 protein of the influenza A virus also contributes to viral pathogenesis, mainly by enabling the virus to disarm the host cell type interferon defense system (Geiss *et al*.,

2002). The interferon (IFN) system is the first line of host defense against virus infection. Interferons induce an antiviral state that may inhibit virus replication and control virus spread. The effectiveness of IFN responses has prompted many viruses to adopt strategies to evade the IFN-induced antiviral responses (Huang *et al*., 2003). Studies in the New Castle Disease virus (NDV) that belongs to family Paramyxoviridae have shown how its NS protein V played a role in STAT1 protein degradation during infections.And this degradation was evident only in cells infected with parental virus but not with the mutant viruses. The carboxyl-terminal domain of V protein in NDV that is cysteine rich and binds to zinc and possess a high level of amino acid sequence conservation (Steward *et al*., 1993; Steward *et al*., 1995). This region plays a critical role in paramyxovirus replication and pathogenesis. IFN-antagonist activity of the NDV V protein is located in the carboxyl-terminal domain.A similar effect was reported in mumps and human parainfluenza virus (hPIV2) (Kubota *et al*., 2001; Nishio *et al*., 2001). Therefore, carboxyl-terminal domain of the V protein is thought to be sufficient for IFN-antagonist activity.To be more specific C terminus of the NDV V protein targets the STAT1 and degrades it thereby blocking both IFN-α/β and IFN-γ signaling., but the cascade followed to do so is yet to be elucidated. There are certain viral species wherein the N coterminal has shown to have IFN-antagonist activity.One such classic example is that of Nipah virus. The N-terminal but not the C-terminal domain of the Nipah virus V protein is involved in antagonizing IFN activity.Another noteworthy feature of the Nipah virus P protein is that it does not induce STAT degradation but instead efficiently prevents STAT1 and STAT2 activation and nuclear translocation in response to IFN, thus inhibiting cellular responses to both IFN-α and IFN-γ (Rodriguez *et al*., 2002). The same result was recorded in Simian virus(SV) wherein a single amino acid substitution (N to D) in the N terminus of the V protein was responsible for the difference in its ability to block IFN signaling in human and murine cells (Young *et al*., 2001). The N coterminal doesn't inhibit activation of the IFN-α/β-responsive promoter.This further strengthens the fact that the cysteine-rich C terminus of the V protein is essential for targeting STAT1 for proteasome-mediated degradation (Young *et al*., 2001; Wansley and Parks, 2001). Although, both STAT1 and STAT2 are in the host cells to establish a degradation-permissive environment, there has been a species dependent preference. The V protein of SV and NDV

evade host IFN response by specifically targeting the STAT1 protein for proteolytic degradation whereas the V protein of hPIV2 was found to block IFN signaling by preferentially inducing degradation of STAT2, but not STAT1(Prisien *et al*., 2001; Didcock *et al*., 1999). The V protein of Sendai virus (SeV) has shown to inhibit the IFN-β activity by blocking interferon regulatory factor (IRF)-3 and NF-κB activation (Komatsu *et al*., 2004). Similar antagonizing activity was illustrated by V protein of SV5 (Poole *et al*., 2002). In SeV, the IFN signaling blocking using STAT1 and STAT2 are carried out by yet another NS protein, C protein (Gotoh *et al.*, 1999). The V protein of paramyxoviruses are thought to play essential roles for evading host innate immunity, especially the IFN system, upon virus infection. However, it is still unclear how the inhibitory capacity of V protein revealed *in vitro* is actually involved in *in vivo* viral replication and pathogenesis.

A comparison between various members of the sub-family Paramyxovirinae viruses have demonstrated how these viruses have adopted effective ways to antagonize the host immune system.Three different routes seem to be plausible: (a) They inhibit the function of IFN-induced host antivirus proteins by viral protein; (b)The members of the sub-family may antagonize the production of type I IFN. This effect was illustrated in RPV, MV, CDV and PPRV. Further studies demonstrate that PPRV can specifically block the IFN-β production that is induced by SeV; (c) they interact with the components of IFN signal transduction pathway and either inhibit or elicit the cascade. They also can induce ubiquitination of proteins within IFN pathway. Ma *et al.* (2015), elucidated that V proteins of the Paramyxovirinae sub-family can directly combine with the cellular STAT protein that is responsible for IFN transduction inhibition.

Programmed cell death in *Peste des petits ruminants virus* infection

Two distinct self-destructive processes that determine the turnover of cytoplasmic organelles and entire cells are: apoptosis ('self-killing') and autophagy('self-eating'). Both the processes,autophagy or apoptosis influence numerous pathological processes, and these phenomena affect each other (Maiuri *et al*., 2007). Apoptosis, or programmed cell death, is a naturally occurring process that has an essential role in development and the maintenance of

homeostasis in multicellular organisms. Cells undergoing apoptosis show highly characteristic morphological changes, including shrinkage, blebbing of the plasma membrane, chromatin condensation and DNA fragmentation (Kerr *et al*. 1972). In health, apoptotic cell death is tightly linked to cell multiplication and leads to the regulated turnover of cells crucial to the preservation and function of adult organisms. Defects in cell death pathways, or uncoupling of cell death and proliferation, can lead to developmental abnormalities and are a major part of the pathogenesis of a wide range of degenerative and neoplastic diseases. Apoptosis is mediated by the sequential activation of caspases, a family of cysteine proteases. Caspases have proteolytic activity and are able to cleave proteins at aspartic acid residues, although different caspases have different specificities involving recognition of neighboring amino acids. Once caspases are initially activated, there seems to be an irreversible commitment towards cell death. Ten major caspases have been identified and broadly categorized into initiators (caspase-2,-8,-9,-10), effectors or executioners (caspase-3,-6,-7) and inflammatory caspases (caspase-1,-4,-5) (Cohen,1997). The other caspases that have been identified include caspase-11, which is reported to regulate apoptosis and cytokine maturation during septic shock, caspase-12, which mediates endoplasmic-specific apoptosis and cytotoxicity by amyloid-β, caspase-13, which is suggested to be a bovine gene, and caspase-14, which is highly expressed in embryonic tissues but not in adult tissues (Hu *et al*., 1998). Caspases are constitutively present in most cells as inactive single chain proenzymes and are activated by specific proteolytic cleavage and assembly into tetramers (Green, 2000). Caspases have the capacity to activate each other and co-operate in an intracellular 'cascade' leading to the activation of downstream 'effector' caspases-3, –6 and –7. Engagement of effector caspases is a key event that commits the cell to the cleavage of essential substrates and results in the morphological changes of apoptosis and the degradation of chromosomal DNA (Enari *et al*. 1998). At least two kinds of pathways converge on the activation of caspase-3. These pathways were previously thought to be independent, but are now known to interact in a cell specific manner (Li *et al*. 1998). The first one called intrinsic pathway is regulated by mitochondria, which are now recognized to play a central and rate-limiting role in cell death (Green and Reed 1998; Kroemer and Reed 2000). The second pathway called extrinsic pathway begins with the activation of caspases-8

and –10 by members of the death receptor family. Activated caspase-8 then acts directly on caspase-3 to initiate apoptosis (Ashkenazi and Dixit 1998).

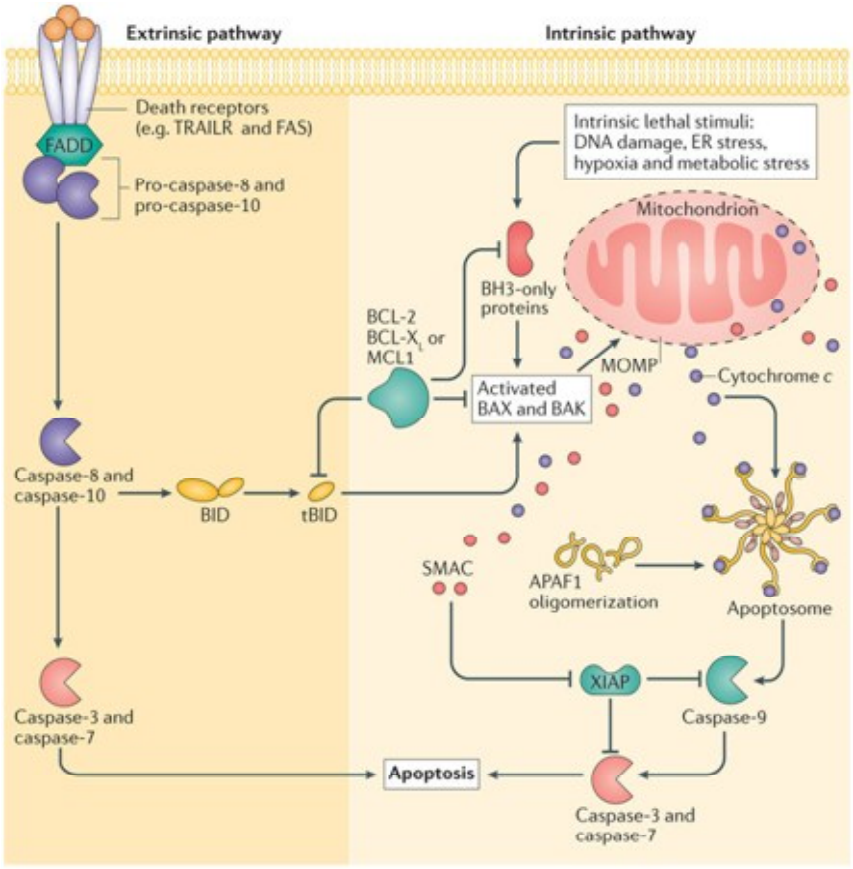

Fig. 1.5: Extrinsic and intrinsic apoptotic signalling pathways:- In the extrinsic apoptotic pathway, upon binding to their cognate ligand, death receptors such as tumour necrosis factor (TNF)-related apoptosis-inducing ligand (TRAIL) receptor (TRAILR) and FAS can activate initiator caspases (caspase-8 and caspase-10) through dimerization mediated by adaptor proteins such as FAS-associated death domain protein (FADD). Active caspase-8 and caspase-10 then cleave and activate the effector caspase-3 and caspase-7, leading to apoptosis. The intrinsic (or mitochondrial) pathway of apoptosis requires mitochondrial outer membrane permeabilization (MOMP). Cell stresses engage BCL-2 homology domain 3 (BH3)-only protein activation, leading to BAX and BAK activity that triggers MOMP. Anti-apoptotic BCL-2 family proteins counteract this. Following MOMP, mitochondrial intermembrane space proteins such as second mitochondria-derived activator of caspases (SMAC) and cytochrome c are released into the cytosol. Cytochrome c interacts with apoptotic protease activating factor 1 (APAF1), triggering apoptosome assembly, which activates caspase-9. Active caspase-9, in turn, activates caspase-3 and caspase-7, leading to apoptosis. Mitochondrial release of SMAC facilitates apoptosis by blocking the caspase inhibitor X-linked inhibitor of apoptosis protein (XIAP). Caspase-8 cleavage of the BH3-only protein BH3-interacting death domain agonist (BID) enables crosstalk between the extrinsic and intrinsic apoptotic pathways. ER, endoplasmic reticulum; MCL1, myeloid cell leukaemia 1; tBID, truncated BID (Ichim and Tait,2016)

Apoptosis is genetically controlled and several viral gene products affect apoptosis by interacting directly with components of the highly conserved biochemical pathway which regulates cell death. Viruses may perform two functions. One is that viruses have evolved mechanisms to block the premature apoptosis of infected cells facilitating either the establishment and maintenance of persistent infection or prolonging the survival of lytically infected cells such that the production of progeny virus is maximized. The other function is that increasing number of viruses actively promote apoptosis, which is the culmination of a lytic infection and serving to spread virus progeny to neighbouring cells while evading the host inflammatory responses. Viral induction of apoptosis occurs when one or several cells in a living organism is infected with a virus leading to cell death. Cell death in organisms is necessary for normal development of cells and cell cycle maturation. It is also critical in maintaining the regular functions and activities of cells (Fan *et al*., 2014).

Autophagy(previously called macro-autophagy), also known as type II programmed cell death. It begins with an isolation membrane, also known as a phagophore that is likely derived from lipid bilayer contributed by the endoplasmic reticulum (ER) and/or the trans-Golgi and endosomes (Axe *et al*., 2008). This phagophore expands to engulf intra-cellular cargo, such as protein aggregates, organelles and ribosomes, thereby sequestering the cargo in a double-membraned autophagosome (Mizushima, 2007). The loaded autophagosome matures through fusion with the lysosome, promoting the degradation of autophagosomal contents by lysosomal acid proteases. Lysosomal permeases and transporters export amino acids and other by-products of degradation back out to the cytoplasm, where they can be re-used for building macromolecules and for metabolism (Glick *et al*.,2010). Thus, autophagy may be thought of as a cellular 'recycling factory' that also promotes energy efficiency through ATP generation and mediates damage control by removing non-functional proteins and organelles. How is this complex process orchestrated at the molecular level? There are five key stages (Figure 6): (a) phagophore formation or nucleation; (b) Atg5–Atg12 conjugation, interaction with Atg16L and multi-merization at the phagophore; (c) LC3 processing and insertion into the extending phagophore membrane; (d) capture of random or selective targets for degradation; and (e) fusion of the autophagosome with the lysosome, followed by proteolytic degradation by lysosomal proteases of engulfed molecules.

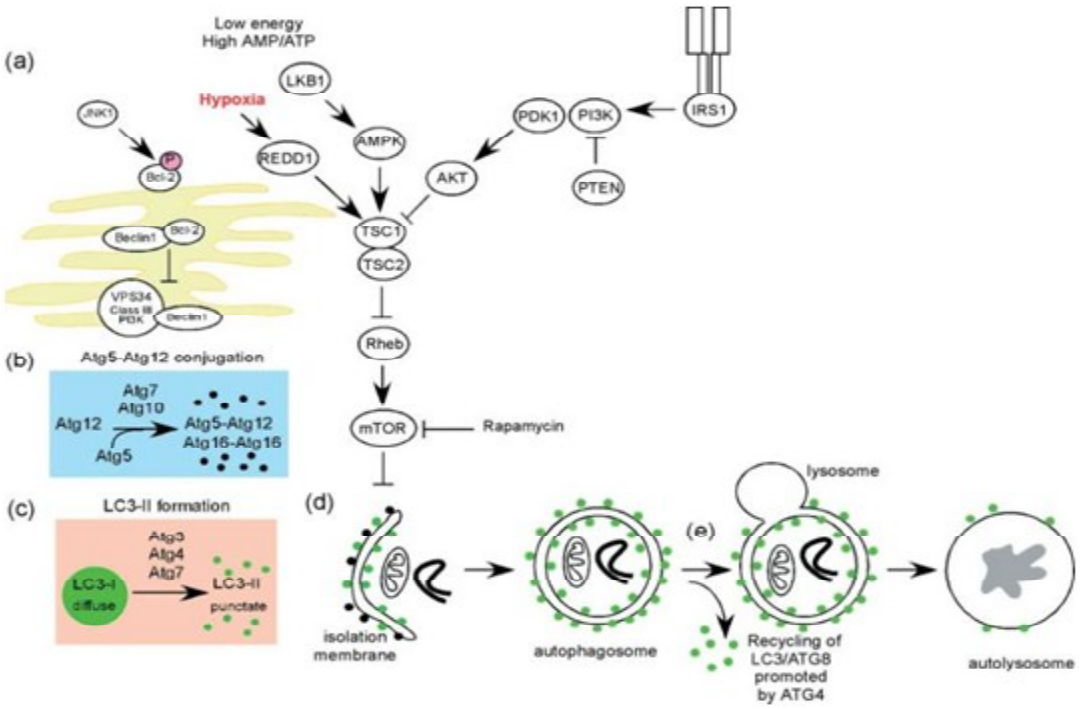

Fig. 1.6: Molecular circuitry and signalling pathways regulating autophagy (Glick *et al.*,2010). Autophagy is a complex self-degradative process that involves the following key steps: (a) control of phagophore formation by Beclin-1/VPS34 at the ER and other membranes in response to stress signalling pathways; (b) Atg5–Atg12 conjugation, interaction with Atg16L and multimerization at the phagophore; (c) LC3 processing and insertion into the extending phagophore membrane; (d) capture of random or selective targets for degradation, completion of the autophagosome accompanied by recycling of some LC3-II/ATG8 by ATG4, followed by; (e) fusion of the autophagosome with the lysosome and proteolytic degradation by lysosomal proteases of engulfed molecules. Autophagy is regulated by important signalling pathways in the cell, including stress-signalling kinases such as JNK-1, which promotes autophagy by phosphorylating Bcl-2, thereby promoting the interaction of Beclin-1 with VPS34 (Wei *et al.*,2008). Perhaps the central signalling molecule in determining the levels of autophagy in cells is the mTOR kinase that likely mediates its effects on autophagy through inhibition of ATG1/Ulk-1/-2 complexes at the earliest stages in phagophore formation from lipid bilayers (Xie and Klionsky, 2007). mTOR is key to integrating metabolic, growth factor and energy signalling into levels of both autophagy, on the one hand, which is inhibited by mTOR when nutrients are plentiful and, on the other hand, to growth-promoting activities, including protein translation, that are stimulated by mTOR signalling (Díaz-Troya *et al.*, 2008). Autophagy is induced by hypoxia and low cytosolic ATP levels that feed through REDD1 and AMP-kinase to inhibit mTOR activity through reduced Rheb GTPase activity. Conversely, autophagy is inhibited by increased growth factor signalling through the insulin receptor and its adaptor, IRS1, as well as other growth factor receptors that activate the Class I group of PI3-kinases and Akt, to promote mTOR activity through inhibition of TSC1/TSC2 and increased Rheb GTPase activity (Díaz-Troya *et al.*, 2008; Sabatini,2006). Vps34,vesicular protein sorting 34; LC3,light chain 3; TOR,target of rapamycin;BID,BH3-interacting domain death agonist.

Another form of cell death is necrosis. Necrosis is a form of traumatic cell death that results from acute cellular injury, such as poison, a bodily injury, an infection or getting cut off from the blood supply.The central processes of apoptosis are remarkably conserved.Although these changes in apoptotic cell death are distinct from those seen in death caused by necrosis,it is now clear that the pathways that lead to necrosis and apoptosis are not entirely separate (Thomson, 2001).

Zhang *et al.* (2013) showed that PPRV infection triggers autophagy and enhances autophagic flux in Vero cells. Their work illustrated the appearance of abundant double- and single-membrane vesicles, the accumulation of LC3 fluorescent puncta, the enhancement of LC3-I/-II conversion, and autophagic flux.Studies using rapamycin for induction of autophagy showed a significant increase in PPRV progeny yield and nucleocapsid (N) protein expression.It is also demonstrated that the replication of PPRV leads to autophagy and vice versa (Zhang *et al*., 2013). Computational studies in PPRV have demonstrated their ability to express RB1 Inducible Coiled Coil Protein 1 (RB1CC1) gene an apoptosis and autophagy regulator.This gene along with another five expressed genes are illustrated to have important roles in immune regulation and are involved in viral entry (Manjunath *et al*., 2015).

RNA interference (RNAi)

Fire *et al.* (1998) described the phenomenon of RNAi for the first time.The researchers' illustrated that the presence of a double-stranded RNA (dsRNA) in the nematode, *Caenorhabditis elegans,* resulted in potent sequence-specific gene silencing at the post-transcriptional level. The RNAi can follow one of the two known cascades (Fig.7). In the first step, the dsRNA that triggers the silencing response is cleaved into small interfering RNAs (siRNAs) (Dykxhoorn and Lieberman, 2006;) of 21–23 nucleotides. This is accomplished by Dicer, an RNase-III-family nuclease (Cullen,2014). In the second step, siRNAs are incorporated into a targeting complex, known as RISC (RNA-induced silencing complex), which destroys mRNAs that are homologous to the integral siRNA (Cullen, 2014). In both the cases the net result is suppression of gene expression. A process comparable to RNAi had been previously identified in plants, where it was referred to as posttranscriptional gene silencing, and in some fungi, where it was termed quelling.

It has been suggested that the RNAi response might be an evolutionarily conserved mechanism for combating viruses or parasitic endogenous genetic elements. However, mammals, with their adaptive immune systems, have clearly evolved alternative, or perhaps additional, defense mechanisms. Nevertheless, it is clear that RNAi pathways, which are conserved in mammalian cells, might be exploited therapeutically as an antiviral defense to augment the adaptive immune system. However, the use of RNAi as an experimental or therapeutic tool in mammalian systems was initially problematic owing, ironically, to the presence of an endogenous antiviral response. In most mammalian somatic cells, dsRNA of >30 bp activates a set of pathways that ultimately induce cell death. These mechanisms are enhanced by the presence of interferons, but even in the absence of these immune modulators, dsRNA activates Protein Kinase R (PKR) and RNase L pathways, leading to a generalized suppression of gene expression followed by apoptosis.

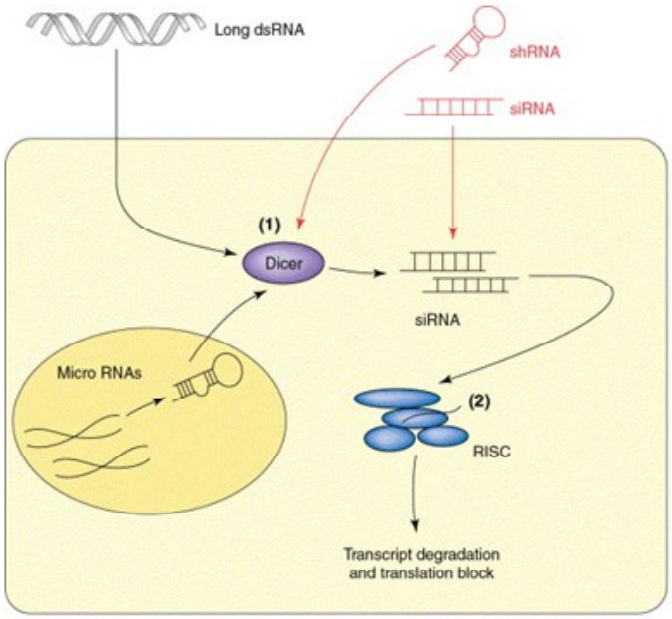

Fig. 1.7: The RNA interference (RNAi) pathway. Short hairpin RNAs (shRNAs) transcribed in vivo from expression constructs or chemically synthesized siRNAs (both red) can be used to artificially stimulate this pathway. RNAi is a two-step process that results in the degradation of targeted mRNA. (1) The exogenous dsRNAs are processed by the cytoplasmic RNase III enzyme Dicer into <"22-bp dsRNA duplexes, called small interfering RNAs (siRNAs). (2) One strand of the siRNA duplex is then essentially randomly loaded into the RNA-induced silencing complex RISC, where it serves as a guide RNA to direct RISC to complementary mRNA targets. Once bound, the Argonaut (Ago) component of RISC induces endonucleolytic cleavage of the mRNA, leading to mRNA degradation.

RNA interference (RNAi) in PPRV infections

- *In vitro* screening using siRNA and NGS have largely been used for global PPRV gene expression profiling (Kumar *et al*., 2014).

- A small interfering RNA (siRNA)-mediated study confirmed that SLAM could be a putative co-receptor for PPRV (Pawar *et al*., 2008). The group elucidated that under silenced SLAM receptor in B95a cells (a marmoset lymphoblastoid cell line), PPRV replication was observed to be reduced by 12- to 143-fold, while the virus titre ranged from $\log_{10}$1.09 to 2.28 (12–190 times).

- Five sets of chemically synthesized siRNAs targeting the nucleocapsid (N) genes of PPRV and RPV for the specific inhibition of virus replication were used to study ruminant morbillivirus replication.As indicators of siRNA functionality,the reduction in viral RNAand protein expression, reduction in virus particle production and the cytopathic effects induced in infected cell were studied (de Almeida *et al*., 2007). It was shown that synthetic siRNAs directed against one gene region (position 480–498) selectively inhibited the N genes of PPRV and RPV (de Almeida *et al*., 2007).

- Vero cells transfected with ATG7-targeting siRNA exhibited a significantly reduced expression level of endogenous Atg7 protein, indicating that autophagy was successfully inhibited in Vero cells. The decline in the level of autophagy was also reflected in a slight decrease in the amount of LC3-II. The reduction in autophagic capacity ultimately led to a significant decrease in the expression of PPRV N protein (Zhang *et al*., 2013).

Materials and Methods

3 MATERIALS AND METHODS

3.1 Materials

3.1.1 PPR virus and Cell line

PPR vaccine virus (PPRV/Sungri 96) passage 35 in Vero cells (Sreenivasa *et al*., 2000) were procured from Biological Products Division, Izatnagar.

3.1.2 Culture media and antibiotics

RPMI-1640,Antibiotic-antimycotic solution, Fetal Bovine Serum(Hyclone);Luria Bertani broth, Luria Bertani agar(Amresco); *E. coli* Fast-Media® XGal, Zeocin, kanamycin (Invivogen).

Composition of media,buffers and solutions used in this study are given in the Appendix or at appropriate places.

3.1.3 Primers and siRNA constructs

The desalted oligonucleotide primers obtained in lyophilized from from Integrated DNA technologies, Inc. (Imperial Life Science,India) were reconstituted in Nuclease-free water(NFW).Ten picomole μ^{-1} was used as working concentration from 100 picomole μ^{-1} of stock.

Table 3.1. Primers sequence of cytokine genes for qRT-PCR

Housekeeping gene (GAPDH) for	5'GTGGTCTCCTCTGACTTCAAC3'
Housekeeping gene (GAPDH) rev	5' CCTGTTGCTGTAGCCAAATTC3'
Interleukin 2 for	5'TCCCAAACTCACAAGGATGC 3'
Interleukin 2 rev	5'TCCCTGGTGTCTCTTAAGTGA 3'
Interleukin 4 for	5'GCAAAAGACTCTGTGCACCA 3'
Interleukin 4 rev	5'GATCGGATCAGCTGCTTGTG 3'
Interleukin 10 for	5'AAACAAGAGCAAGGCAGTGG 3'
Interleukin 10 rev	5' CGCCCGGATGTTTCAGTTTT 3'
Interleukin 1 alpha for	5'TCTAGTACTTGCGAGCCCTG 3'
Interleukin 1 alpha rev	5' CAGTGGTCTCATGGTCCTCA 3'
Interferon gamma for	5'CTTTTCAGCTCTGCGTCGTT 3'
Interferon gamma rev	5'TGTCACCCTCCTCTCTCCAA 3'

3.1.3.3 siRNA inserts

The oligonucleotides (forward and reverse) obtained in lyophilized from GeneX, India were reconstituted in Nuclease-free water (NFW). 25 µM was used as working concentration from 100 µM of stock.

Table 3.2 siRNA inserts sequences

SiRNA insert 1 (S1)	CAGCGUUACUAUGUUUAUAdTdT
SiRNA insert 2 (S2)	CUUGUCUCCUGAAGAUAAUdTdT
SiRNA insert (S3)	GAGUCAAGAUGGAAGUCAUdTdT

Table 3.3. Primers for qRT-PCR for time course studies of V protein coding region of the P gene expression

Forward primer	5'GTGGTCTCCTCTGACTTCAAC 3'
Reverse primer	5' CCTGTTGCTGTAGCCAAATTC3'

3.1.4 Reagents for DNA and RNA

Trizol reagent, Chloroform, Isopropanol and Nuclease free water (Sigma Chemicals Company St. Louis, MO, USA);Taq DNA polymerase enzyme(Invitrogen);*pfu* DNA polymerase, MuMLV reverse transcriptase,Diethyl pirocarbonate (DEPC),Oligo dT

primer,10mM dNTPs,T4 ligase,100bp plus DNA ladder, λDNA *EcoRI*/*BglIII* digest, λDNA *HindIII*/*AccI* digest, RNase A, Proteinase K,6X gel loading dye and other chemicals were purchased from MBI Fermentas.Other chemicals/reagents used in the study were ethanol molecular grade (Merck);Calcium chloride,Sodium chloride,Chloroform,Agrose (Amresco); Ethidium Bromide (Hi Media), Lipofectamine™ 2000 Reagent (Life technologies, Carlsbad, USA)

3.1.5 Commercial kits

Viral RNA/DNA mini kit (Invitrogen, USA); MiniElute Gel extraction kit, PCR purification kit, Miniprep plasmid extraction kit (Thermo scientific, Lithuania, EU); QuantiTech SYBR Green PCR kit (QIAGEN GmbH, Hilden, Germany); pDsRed-Express-N1 Vector system (Clontech,USA); Expresso Rhamnose SUMO Vector system (Lucigen,USA), psiRNA-h7SK G1 GFPzeo Vector system (Invivogen,USA), Caspase-Glo® 3/7 Assay Systems (Promega, India); Caspase-Glo® 8 Assay Systems (Promega,India); Caspase-Glo® 9 Assay Systems (Promega, India)

3.1.6 Host

$DH_5\alpha$ and GT116 strains of *E. coli* were used for the propagation of transformed recombinant clones. For PPR virus propagation B95a (an Epstein Barr virus-transformed marmoset B cell line) cell line was used.

3.1.7 Software used

Laser gene software 6.0 DNASTAR inc., (Madison,USA);Genetool Lite 1.0,SPSS (SPSS for windows); DeepView/Swiss-Pdb viewer (http://www.expasy.org/spdbv); Primer3 output, Primer 3 (primer3_www.results.cgi); siRNA Wizard (www.sirnawizard.com); Basic local alignment search tool (BLAST,NCBI) were used.

3.1.8 Glasswares and Plasticwares

All glasswares and plasticwares used for the study were purchased from Borosil,Schott Duran, Axygen, Tarson, Nalgene, Nunc, Corning, and Eppendroff. The cell culture flasks and tissue culture plates were procured from Nunc and Eppendroff. The white plates used in luminometry were from Nunc.

3.1.9 Equipments

The below given instruments were used: Universal 32R centrifuge (Hettich, Zentrifugen); Refrigerated microcentrifuge-Biofuge (Heraeus Instruments, Hanau, Germany); Microcentrifuge Minispin (eppendroff, AG, Hamburg,Germany);Water bath (Jouan, France); Orbital shaker CLASSIC C24 (New Brunswick scientific Co. Inc, Edison, USA); Thermal cycler-Model 9600 Perkin Elmer Cetus (USA); Master gradient (Eppendroff AG, Humburg, Germany); Real time PCR system (model Mx3000p) (Stratagene, La Jolla, CA, USA), SYNGENE Gel Documentation system (UK) ; Eclipse Ti-U Inverted Microscopes (Nikon, Japan); Class II Biological Safety Cabinet (Telstar Bio IIA), New Brunswick CO_2 incubator (Galaxy 170 R) (Eppendroff); Horizontal Laminar flow (Klenzaids, India); SPINWIN microfuge spin apparatus, Horizontal agrose gel electrophoresis with power pack (Biotech India Ltd.); Semi dry transfer cell (Pharmacia Biotech); Millipore syringe filters (0.2m pore size); Micropipette (Eppendroff); Spectramax M5 (Molecular devices)

3.2 Methods

3.2.1 Virus propagation and titration

PPR vaccine virus (PPRV/Sungri 96) passage 35 in Vero cells were subsequently subcultured in B95a cells in a RPMI-1640 medium containing 2% Fetal Bovine Serum(FBS) in a CO_2 atmosphere to obtain B95a adapted PPR virus. After 6^{th} passage the virus was seen to adapt to the new host.Once adapted virus propagation and titration was carried out in the B95a cells. Briefly, the virus was propagated by infecting B95a cells, cultured in 75 cm2 cell culture flasks RPMI-1640 medium containing 5% FBS at multiplicity of infection (MOI) of 0.1 $CCID_{50}$/ml. When viral cytopathic effect (CPE) is almost complete (~80%), the cells were freeze-thawed 3 times and aliquots will be stored at -80°C. To study the infectivity titer of PPRV, virus titration was performed (Mariner *et al*., 1990). Briefly, B95a cells were subcultured and 100 ml of the cell suspension was added to each well (0.5×10^6 cells/ml) in 96 well tissue culture plates. Plates were incubated at 37°C in a 5% CO_2 incubator. The next day, virus was diluted 10-fold in RPMI-1640 containing 2% FBS in deep well plate. An aliquot of 100 µl of virus suspension was added to each well keeping four replicates per dilution. One

well was kept as control (without virus) per replicate. The plates were incubated at 37°C in the presence of 5% CO_2. Media were replaced each alternate day with RPMI-1640 containing 2% FBS.Reading was taken on the sixth day of titration. End points were calculated using Reed and Muench method (1938).

3.2.2 Viral RNA isolation

A 25 cm^2 flask with viral cytopathic effect (CPE) almost complete (~80%), was freeze-thawed 3 times.2ml of the supernatant was transferred to a 2ml Eppendrof tube for viral RNA isolation using Pure Link® Viral RNA/DNA Mini Kit as per the manufacturer's instructions. Briefly,25 µL Proteinase K was dispersed into a sterile microcentrifuge tube. To this 200 µL of cell-free sample (equilibrated to room temperature) was added. A 200 µL Lysis Buffer (containing 5.6 µg Carrier RNA) was added and the tube was vortexed for 15 seconds. This was followed by incubation at 56°C for 15 min. 250 µL 96–100% ethanol was added to the lysate tube and mixed thoroughly by vortexing for 15 seconds followed by incubation for 5 minutes at room temperature. The lysate with ethanol (~675 µL) was transferred into the Viral Spin Column and centrifuged at ~6800 × g for 1 minute. The collection tube with the flow through was discarded.The spin column was placed in a clean Wash Tube (2 mL) and a500 µL Wash Buffer (WII) with ethanol was added to the spin column. The column was centrifuged at ~6800 × g for 1 minute. The flow-through was discarded and the spin column was placed back into the Wash Tube and centrifuged at ~6800 × g for 1 minute. The spin column was placed in another clean, Wash Tube (2 mL) and centrifuged at maximum speed in a microcentrifuge for 1 minute to dry the membrane completely. The Wash Tube was discarded with the flow through. The Viral Spin Column was placed in a clean 1.5-mL Recovery Tube supplied.10–50 µL of Sterile; RNase-free water was added to the center of the column. The tube is incubate at room temperature for 1 minute and centrifuged at maximum speed for 1 minute. The Recovery Tube containing the purified viral RNA was stored at –80°C until further use. RNA concentration was determined using a nanodrop (Eppendrof, Hamburg, Germany). The quality of RNA was tested by evaluation on 1.8% TAE-agarose gel before being used for cDNA production. To exclude genomic DNA contamination, viral RNA was treated with RNase free DNase.

3.2.3 Reverse transcription of Viral RNA (First strand cDNA synthesis)

Total RNA was reverse transcribed into cDNA in a 20 µl reaction mixture using revert aid first strand cDNA synthesis kit (Thermo scientific, Lithuania, EU) according to the manufacturer's instructions. cDNA was synthesized using viral RNA as template and oligo dT primers. A mixture without the reverse transcriptase enzyme was run in parallel to those with the enzyme included to ensure that there was no disturbance from genomic DNA.

3.2.4 Amplification of V protein coding region of the P gene from cDNA

3.2.4.1 Polymerase Chain Reaction (PCR)

The PCR reaction was carried out in standard 25µl reaction volume for V protein coding region of the P gene target using the designed primer pair following standard protocol. A typical PCR reaction contained the following reagents (Bioline Gmbh) was performed in a 0.2 ml (Axygen, USA) PCR tube.

Nuclease free water (NFW)	18.3 µl
10X *Taq* polymerase Buffer	2.5 µl
10mM dNTPs	0.5 µl (200 µM)
50mM $MgCl_2$	0.5 µl (1 mM)
For. primer (10 pmoles/µl)	1 µl (10 pmoles)
Rev primer (10 pmoles/µl)	1 µl (10 pmoles)
cDNA	1 µl
Taq DNA polymerase (5 U/µl)	0.2 µl (1U)
Total reaction volume	25 µl

The cycling conditions used for amplifying the V protein coding region of the P gene were as follows:

Step 1: Denaturation	94°C for 5 min
Step 2: Denaturation	94°C for 50 sec
Step 3: Annealing	56°C for 50 sec
Step 4: Elongation	72°C for 50 sec
From step 2 – step 4 was repeated for 30 cycles.	
Step 5: Final elongation	72°C for 10 min

3.2.4.2 Agarose gel electrophoresis of amplicon

1.2% molten agarose (Amresco, USA) was prepared in TAE buffer (Appendix) in microwave oven. It was then allowed to cool to about 50°C and ethidium bromide (10 µg /ml) was added to a final concentration of 0.5 µg/ml. About 50 ml of molten gel was poured into horizontal electrophoresis apparatus (Bangalore Genei) and then the comb was inserted. Gel was allowed to solidify at RT for 20 min. Electrophoresis tank was filled with TAE buffer and the gel was immersed in buffer and the combs were removed. Samples were prepared by mixing 5 µl of PCR product and 1 µl of 6X loading buffer (MBI Fermentas) containing 0.25% w/v bromophenol blue, 0.25% W/V, xylene cyanol FF and 40% W/V sucrose in water. Samples were loaded in parallel with 100 bp DNA ladder plus molecular weight marker (MBI Fermentas). The electrophoresis was carried out for 45 min at 70 V. Then the gel was visualized in a transilluminator (SYNGENE Gel documentation system, UK) and documented.

3.2.4.3 Purification of PCR product

PCR product was purified using Qiagen Mini elute gel extraction kit: QIAGEN [QIAGEN GmbH, Hilden, Germany] following manufacturer's protocol. The procedure used was as follows:

The PCR product was run in 1.2% low melting point (LMP) agarose (Sigma-Aldrich, St. Louis, USA) gel in TAE buffer along with molecular weight DNA ladder. With a clean, sharp scalpel or razor blade; the gel slice containing the desired DNA fragment was excised on a UV transilluminator with minimum UV exposure. The slice was then cut into small pieces and was placed into a sterile 1.5 ml microcentrifuge tube. 0.6 ml QG buffer (supplied with the kit) was added to it and incubated at 50°C in a heated water bath for 10 min until the gel was completely dissolved. The tube was inverted at every 1-2 min during incubation. A mini elute column (supplied with the kit) was placed onto a 2 ml collection tube provided in the kit and 0.7 ml of dissolved gel mixture was added into the column. The column was centrifuged at 12,000 x g for 30-60 sec and the flow-through was discarded. The column was washed with 0.7 ml PE buffer (supplied with the kit) by centrifuging for 30-60 sec at 12,000 x g and the flow-through was discarded. The column was then centrifuged at full speed for another 3 min

to remove residual ethanol present in column. The column was placed onto a new 1.5 ml microcentrifuge tube and 12 µl of pre-heated elution buffer (provided with the kit) or nuclease free water was added onto the centre of the resin column. The column was left to stand at 37°C for 1-2 min and then centrifuged at 13000 rpm for 1-2 min to elute the DNA. The eluted DNA was stored at -20°C for further use.

3.2.4.4 Characterization of the PCR product and pDsRed-Express-N1 Vector by restriction endonuclease (RE) digestion

Isolated putative amplicon was characterized by digestion with 2 different restriction endonucleases (RE*) viz., Bgl I* and *EcoR I*. For a single digestion the following reagents were used in the RE analysis.

For PCR product	
NFW	11 µl
10X Buffer	2.0 µl
Bgl II (10 U/µl)	1.0 µl
EcoR I (10 U/µl)	1.0 µl
Purified PCR product	5.0 µl
Total reaction volume	20 µl
For pDsRed-Express-N1 Vector	
NFW	11 µl
10X Buffer	2.0 µl
Bgl II (10 U/µl)	1.0 µl
EcoR I (10 U/µl)	1.0 µl
Purified Plasmid	5.0 µl
Total reaction volume	20 µl

The reaction mix was prepared in a 0.5 ml microcentrifuge tube. The contents were mixed thoroughly followed by a brief spin. The tube was then incubated overnight at 37°C. The RE digested product was then run in a 1.2% agarose gel with molecular weight DNA marker to check the restriction fragment pattern for the V protein coding region of the P gene.

3.2.5 Cloning of the PCR product

The purified PCR products were cloned into pDsRed-Express-N1 Vector (Promega, WI, USA). The PCR products were quantified in 1.2% agarose gel by densitometric comparison with Molecular mass ladder (MBI Fermentas) using Genetool software in Gel documentation system (SynGene, UK). The appropriate amount (ng/µl) of the PCR product was subsequently cloned into the plasmid vector keeping the insert: vector molar ratio to 3:1 as per the following formula:

$$\text{ng of insert (PCR product)} = \frac{50\text{ng of vector} \times \text{kb size of insert}}{\text{kb size of vector}} \times \frac{3}{1}$$

$$\text{ng of insert (PCR product)} = \frac{50 \times 1 \times 3}{5} = 30\,\text{ng}$$

3.2.5.1 Ligation of the PCR products into the plasmid vector

The PCR product was ligated with pDsRed-Express-N1 vector as detailed below

Purified PCR product	2 µl (30 ng)
PDsRed-Express-N1 Vector	1 µl (50 ng)
10X T4 DNA Ligase buffer	1.0 µl
T4 DNA Ligase	1.0 µl (1 Weiss unit)

Volume made up to 10 µl by NFW. The ligation was performed at 4°C for 16 hrs.

3.2.5.2 Preparation of *E. coli* $DH_5\alpha$ competent cells

Two LB agar plates were prepared, one with kanamycin and another without kanamycin. The *E. coli* DH5 cells, from frozen stock (grown in LB media), were streaked on both the plates and incubated overnight at 37°C. Bacterial colonies which appeared on LB agar (without kanamycin) but not on LB agar with kanamycin were picked and grown into 5 ml of LB broth without kanamycin. The culture was then incubated overnight at 200 rpm at 37°C in a shaker-cum- incubator. About 2.0 ml ($1/100^{th}$ volume) of the overnight-grown culture was inoculated in 200 ml of LB broth and further incubated at 220 rpm until the culture

reached an O.D. of 0.3-0.4 at A_{600} nm (usually for 3-4 hrs.). The culture was chilled on ice and the cells were harvested by centrifuging at 6000 x g for 15 min at 4°C. The cell pellet was resuspended in 20 ml ($1/10^{th}$ volume) ice-cold solution of sterile 100 mM $CaCl_2$ and was on ice for 30 min. The cells were again pelleted by centrifuging at 6000 x g for 15 min at 4°C. Finally, the pellet was resuspended in 1.75 ml of ice-cold 100 mM $CaCl_2$ solution with 0.75 ml of sterile glycerol. The suspension was gently mixed, aliquoted @ 100-200µl/tube in 1.5ml microcentrifuge tubes and stored at –80°C for further use.

3.2.5.3 Transformation of $DH_5\alpha$ competent cells

The stored competent cells were thawed on ice (usually for 5-10 min). 5 µl of ligated product was added to it; the tube was flicked gently for homogenous mixing and was kept in ice for 20 min. The cells were then heat-shocked at 42°C for 45-50 sec in a water bath and then immediately transferred on ice and kept for 2 min. 850 µl of LB (Appendix) medium was added to it and incubated at 37°C for 90 min at 200 rpm in a shaker-cum-incubator. 200 µl of the transformant culture was spread over the freshly prepared LB/kanamycin/X-gal/IPTG (Appendix) plates, which were then incubated for 16-18 hrs at 37°C.

3.2.5.4 Colony screening for identification of positive clones

PDsRed-Express-N1 vector allows easy screening of the recombinant clones among the transformants. For PCR confirmation of the clones, a direct colony PCR was performed. Recombinant clones represented as white colonies (half of a single colony) were picked up with a sterile loop and transferred to a microfuge tube containing 50 ml of NFW. Then, it was boiled for 10 min and immediately placed on ice for 5 min. After spinning at 13,000 rpm for 1 min to pellet the cell debris, 5 ml of the clear supernatant was used as template for the PCR reaction using the gene specific forward and reverse primers

NFW	14.3 µl
10X *Taq* polymerase buffer	2.5 µl
10mM dNTPs	0.5 µl (200 µM)
50mM $MgCl_2$	0.5 µl (1 mM)
For primer (10 pmoles/µl)	1 µl (10 pmoles)

Rev primer (10 pmoles/µl)	1 µl (10 pmoles)
Template DNA	5 µl
Taq DNA polymerase (5 U/µl)	0.2 µl (1 U)
Total reaction volume	25 µl

The cycling conditions used for amplifying the V protein coding region of the P gene were as follows:

Step 1: Denaturation	94°C for 5 min
Step 2: Denaturation	94°C for 50 sec
Step 3: Annealing	56°C for 50 sec
Step 4: Elongation	72°C for 50 sec
From step 2 – step 4 was repeated for 30 cycles.	
Step 5: Final elongation	72°C for 10 min

Recombinant clones represented as white colonies as well as colony PCR positive were picked up and inoculated into 5 ml of LB broth containing kanamycin (100µg/µl) and grown overnight at 37°C in a shaker incubator for plasmid isolation and characterization.

3.2.5.5 Isolation of plasmid

Plasmid was extracted with AuPrep SPIN Miniprep Kit [Life Technologies India (Pvt.) Ltd, New Delhi, India] following manufacturer's protocol.

Five millilitres of overnight culture was taken in a 2.0 ml microcentrifuge tube and centrifuged at 8,000 x g for 2 min. Supernatant was discarded and the pellet was resuspended with 250 µl of MX1 (supplied by manufacturer) by vortexing. About 250 µl of MX2 (supplied by manufacturer) was added to it and was mixed gently by inverting until lysate becomes clear. The mixture was kept for 1- 5 min at RT. About 350 l of MX3 (supplied by manufacturer) was added to it, inverted upside down to mix gently. The mix was then centrifuged at 13000 x g for 5 min and the supernatant was transferred to a SPIN™ Column onto a collection tube. The spin column was centrifuged for 60 sec at 8000 x g. The flow-through was discarded; the column was washed once with 0.5 ml WF (supplied by manufacturer) buffer by centrifuging for 60 sec. The flow-through was discarded. The column was washed once with 0.7 ml WS (supplied

by manufacturer) Buffer by centrifuging for 60 sec and the flow-through was discarded. The column was centrifuged at full speed for another 3 min to remove residual ethanol. The column was placed onto a fresh 1.5 ml microcentrifuge tube; 50 µl of NFW was added onto the column which was then left to stand for 1-2 min and centrifuged for 1-2 min to elute DNA. The eluted DNA was preserved at -20°C for future use.

3.2.5.6 Characterization of putative recombinant plasmid

Isolated putative recombinant plasmids were further characterized by digestion with appropriate restriction enzymes and sequencing to check the presence of desired insert.

NFW	11 µl
10X Buffer	2.0 µl
Bgl II (10 U/µl)	1.0 µl
EcoR I (10 U/µl)	1.0 µl
Isolated Plasmid DNA	5.0 µl
Total reaction volume	20 µl

The reaction mix was prepared in a 0.5 ml microcentrifuge tube. The contents were mixed thoroughly followed by a brief spin. The tube was then incubated overnight at 37°C. The RE digested product was then run in a 1.0% agarose gel with molecular weight DNA marker to check the release of the insert of desired size from recombinant plasmid DNA. The clones, releasing the exact size of insert, were selected as positive clones for further sequencing purpose. About 850 µl of the positive bacterial culture was mixed with 150 µl of sterile glycerol and stored at -80C, while extracted plasmid DNAs was stored at -20°C until further use.

3.2.5.7 Sequencing of the cloned target

The putative recombinant vector plasmid were sent to Sanger Seq Bioserve, Hyderabad for nucleotide sequencing using automated sequencer ABIPRISM®3100 (AME Bioscience, Toroed, Norway).

3.2.5.8 Sequence analysis of the amplicon

The sequences were initially analyzed using NCBI online BLAST Server (Altschul *et al.,* 1997) to identify the sequence identity. Based on the BLAST results of BLAST server,

sequences were further compared with nucleotide sequences of other members of V protein coding region of the P gene available in the GenBank database. Sequence identities among all the V protein coding region of the P gene were determined using the programmes MegAlign of the Lasergene 6.0 software (DNASTAR Inc., Madison, USA) and GeneTool Lite 1.0.

3.2.6 Cloning of siRNA inserts into psiRNA h7SKGFPzeo vector

3.2.6.1 Annealing of siRNA inserts

The siRNA inserts were annealed as detailed below:

Components of annealing solution	siRNA insert (S1)	siRNA insert (S2)	siRNA insert (S3)
Nuclease free water(NFW)	20 µl	20 µl	20 µl
Forward oligonucleotide (25 µM)	2 µl	2 µl	2 µl
Reverse oligonucleotide (25 µM)	2 µl	2 µl	2 µl
0.5 M NaCl	6 µl	6 µl	6 µl
Total reaction volume	30 µl	30 µl	30 µl

The annealing mixture was incubated for 2 minutes at 80 °C and maintained in water bath until the temperature reached 35 °C. The annealed siRNA insert was used for ligation or stored at -20 °C for further use.

3.2.6.2 Characterization of the psiRNA vector by restriction endonucleases (RE) digestion

The psiRNA h7SKGFPzeo vector was characterized by digestion using two different FastDigest® enzymes *viz.*, *HindIII* and *AccI*

NFW	6µl
10X FastDigest®Green buffer	2 µl
HindIII (10 U μl^{-1})	1µl
AccI (10 U μl^{-1})	1 µl
psiRNA h7SKGFPzeo vector	5 µl
Total reaction volume	15 µl

The reaction mixture was incubated at 37°C for 45 mins.

3.2.6.3 Ligation of siRNA insert into psiRNA

Table 3.4. Ligation of siRNA insert into psiRNA h7SKGFPzeo vector: The siRNA inserts were ligated with the psiRNA h7SKGFPzeo vector as detailed below:

Components of annealing solution	Annealed siRNA insert (S1)	Annealed siRNA insert (S2)	Annealed siRNA insert (S3)
Nuclease free water(NFW)	15 µl	15 µl	15 µl
Digested psiRNA (100 ng)	1 µl	1 µl	1 µl
Respective annealed siRNA insert(s)	1 µl	1 µl	1 µl
T4 DNA Ligase (1 unit)	1 µl	1 µl	1 µl
10X ligation buffer	2 µl	2 µl	2 µl
Total reaction volume	20 µl	20 µl	20 µl

3.2.6.4 Reconstitution of *E. coli* GT116 strain

E. coli GT116 was reconstituted according to the manufacture's protocol. Briefly, 1 ml of LB medium was added in the tube containing the paper disk and was allowed to sit for 5 minutes. The suspension was mixed gently by vortexing for 1-2 minutes. Bacteria was taken from this suspension and streaked on a LB agar plate. The plate was incubated at 37 °C overnight. A single colony was picked and grown in LB medium. The competent cells were prepared utilizing the protocol mentioned in section 3.2.5.2.

3.2.6.5 Transformation of *E. coli* GT116 competent cells

The transformation of the construct was carried out in the similar fashion as in case of DH5α. Recombinant clones represented as white colonies were picked up and inoculated into 5 ml of low salt LB broth containing Zeocin™ (100 µg/µl) as high salt inhibits activity of Zeocin™ and grown overnight at 37°C in a shaker incubator for plasmid isolation and characterization.

3.2.6.5 Plasmid extraction and sequencing of the siRNA insert

Plasmid was extracted with AuPrep SPIN Miniprep Kit [Life Technologies India (Pvt.) Ltd, New Delhi, India] as mentioned in section 3.2.5.5. The sequencing was carried as

mentioned in section 3.2.5.7 using the sequencing primers provided by the manufacturer: OL559 (forward primer) and OL408 (reverse primer).

3.2.7 The kill curve analysis

B95a cells @ 2.0×10^5 cells/ml were plated in 0.5 ml complete growth medium per well in a 24-well tissue culture plate one day prior to introducing antibiotic selection. The cells reached the high confluence (~60-80%) prior to adding the selection antibiotic. The next day the complete growth Medium was replaced with Selection Medium supplemented with a range of antibiotic concentrations, including untreated control cells with Growth Medium only (no selective antibiotic added). Typical antibiotic working concentration range for mammalian cells was used in this experiment *i.e.,* 0.5-10 µg/µL for Kanamycin and 1-20 µg/µL for Zeocin. The spent media was replaced with media containing selection antibiotic every 2-3 days for up to 15 days. Visual toxicity was assessed for upto 2 weeks to determine low, optimal and high doses for antibiotic selection.

3.2.8 Transfection of B95a cells

B95a cells were grown in RPMI-1640 supplemented with 10% FBS, antibiotic concentration depending on the kill curve analysis and maintained at all times in temperature controlled incubators at 37°C, in a humidified environment enriched with 5% CO_2. The cells were plated in a 48 well plate 12hrs prior to transfection to achieve a 40-80% confluence at the time of transfection. The transfection was carried out in triplicates. Briefly, two 1.5ml screw cap microfuge tubes were prepared for each reaction with 100µl of plain medium (*i.e.,* RPMI-1640 without FBS) per transfection. In the first microfuge of each reaction, 1µg of respective plasmid was added and mixed well. In the second well, lipofectamine was added at the rate of 5 µl/µg DNA and mixed well. The DNA mix was dripped into the lipid mix and allowed to sit the hood for 20-30 minutes while preparing the cells. Meanwhile, the medium was removed from each well, and the cells were washed gently with 0.5-1.0ml of plain RPMI 1640 medium. 250µl of 2% RPMI-1640 was added to each well and plates were returned to the incubator for 5-10 min. The respective Lipo/DNA mix was added to each well, rocked gently and returned the plate to the incubator. After 3-6 hrs, the medium was removed and replaced with 500µl of complete media.

The Lipo/DNA mix was added in the below given order:

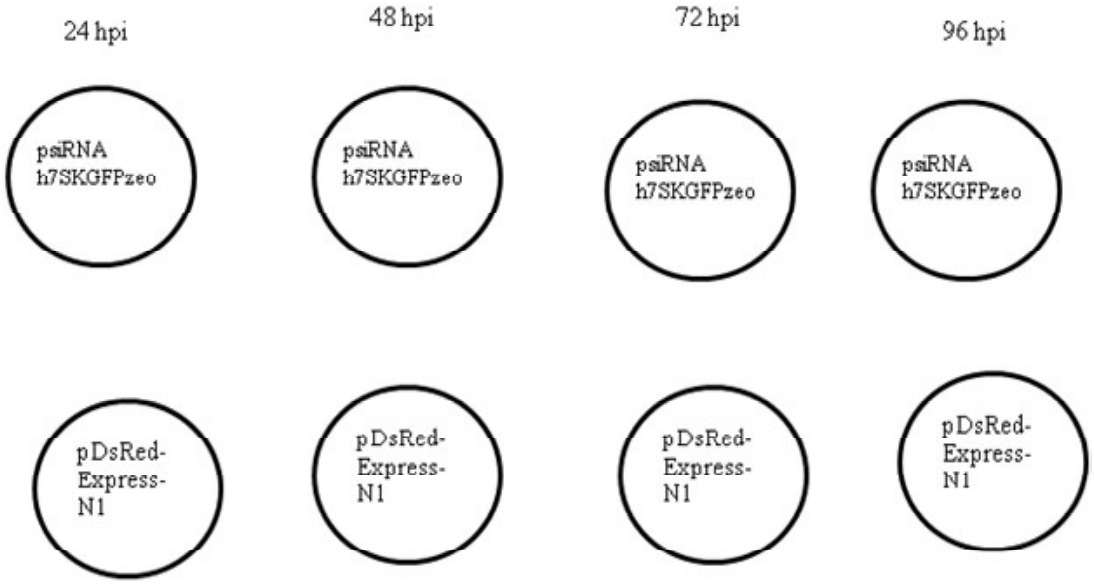

3.2.9 Time course studies of transfection efficiency

The number or percent of cells transfected and the intensity of GFP expression and pDsRED expression was determined using microscopy (Eclipse Ti-U Inverted Microscope).

3.2.9.1 Fluorscent microscopy

After 24hr, 48hr, 72hr and 96hr posttransfection, the 48-well tissue culture plates were removed from the CO_2 incubator. The transfection efficiency was analyzed by direct fluorescence, using an Inverted Microscope (Eclipse Ti-U, Nikon Instruments, Tokyo). Images were taken with a Nikon digital sight USB(H) Ext.1/0 camera and edited with NIS-Elements Imaging Software (Nikon Instruments, Tokyo).

3.2.10 Time course studies of gene silencing

In order to define and compare the kinetics of V protein coding region of the P gene expression in the B95a cells following *in vitro* transfection/co-transfection at optimum plasmid concentration, time course experiments were carried out. For time course studies of V protein coding region of the Pgene expression, the cells were cultured and transfected/co-transfected

as mentioned in section 3.2.8. The gene silencing was analysed by Fluorscent microscopy (as mentioned in 3.2.9.1) and real time PCR measurements. Once the cells are viewed under microscope, they are collected into individual 1.5 ml centrifuge tubes for different time period

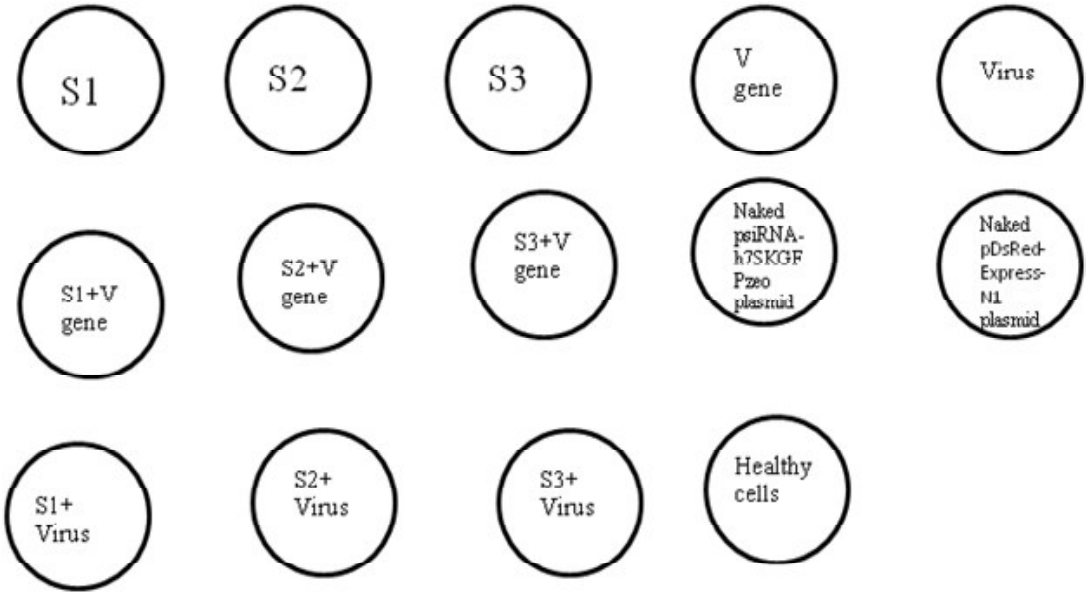

and different treatment. Then, cells were centrifuged at 100g for 10 min and total RNAs were extracted for quantitative RT-PCR measurements.

Table 3.5 Time course studies of V protein encoding region of P gene at various time intervals

Plasmid(s) containing respective gene construct	Time course of transfection/Co-transfection			
	24hr	48hr	72hr	96hr
Plasmid(s) containing respective gene construct @ optimum concentration	√	√	√	√

3.2.10.1 RNA isolation and quantification

The total RNA was extracted from B95a cells after transfection/co-transfection with Plasmid(s) containing respective gene construct for different time periods by TRIzol method mentioned in section 3.2.2.

3.2.10.2 First strand cDNA synthesis

Total RNA from each treatment group was reverse transcribed into cDNA in a 20 µl reaction mixture using revert aid first strand cDNA synthesis kit as mentioned in section 3.2.3. cDNA was synthesized using 125 ng of sample RNA as template and random hexamer primers. A mixture without the reverse transcriptase enzyme was run in parallel to those with the enzyme included to ensure that there was no disturbance from genomic DNA.

3.2.10.3 Real time quantitative PCR analysis

Expression levels of transcripts of V protein coding region of the P gene and GAPDH (Housekeeping gene) were measured by Lightcycler 480 real time PCR instrument with software version 1.5. Each sample was tested in triplicate in Lightcycler®Multiwell plate 96 (Roche Diagnostics, Mannheim, Germany). The oligonucleotides for qPCR were designed on the basis of prior sequence information from and BLAST analysis against the PPRV genome. The reaction mixture (10 µl total volume) comprised of 2 µl cDNA, 5 µl 2× SYBR green master mix (Thermo scientific, Lithuania, EU), 0.5 µM primer pairs and 2 µl PCR-grade water (Sigma-Aldrich, St. Louis, MO, USA). A no template control reaction (NTC) was included in each assay. The thermocycling conditions employed for all the genes were: pre incubation at 95°C for 10 min followed by 45 cycles of 25 sec at 95°C, 25 sec at 60°C, and 25 sec at 72°C. After the amplification, a melting peak analysis with a temperature gradient of 0.1°Csec-1 from 65°C to 97°C was performed to confirm the PCR amplification specificity, contamination and absence of primer-dimers. Relative quantification of a target gene was done by comparing expression level of reference gene GAPDH, as per the method of Livak and Schmittgen (2001). For each set of primers, the PCR efficiency was between 90 and 95%.

3.2.11 Time course studies of cytokine gene expression

In order to define and compare the kinetics of different cytokine genes expression in the B95a cells following *in vitro* transfection at optimum plasmid concentration, time course experiments were carried out. For time course studies of cytokine gene expression, the cells were cultured and transfected/co-transfected in the same way as for the gene expression experiment(s). Cultures were centrifuged after various stimulation times, and cells were collected for RNA isolation.

3.2.11.1 RNA isolation and quantification

The total RNA was extracted from B95a cells after transfection/co-transfection with Plasmid(s) containing respective gene construct for different time periods by TRIzol method mentioned in section 3.2.2.

3.2.11.2 First strand cDNA synthesis

Total RNA from each treatment group was reverse transcribed into cDNA in a 20 µl reaction mixture using revert aid first strand cDNA synthesis kit as mentioned in section 3.2.3. cDNA was synthesized using 125 ng of sample RNA as template and random hexamer primers. A mixture without the reverse transcriptase enzyme was run in parallel to those with the enzyme included to ensure that there was no disturbance from genomic DNA.

3.2.11.3 Real time quantitative PCR analysis

Expression levels of transcripts of cytokine genes IL-1α, IL-2, IFN-γ, IL-4, IL-10 and GAPDH (housekeeping gene) were measured by Lightcycler 480 real time PCR instrument with software version 1.5. The experiment was carried out as mentioned in section 3.2.10.3.

3.2.12 Apoptosis cascade

The cell seeding and transfection were performed following the protocol mentioned in a white walled 96-well as mentioned in the above mentioned section. Following transfection/ co-transfection cells were subjected to Caspase 3/7, 8, 9 activities measurement with Caspase-Glo assay kit (Promega, Madison USA). Briefly, the plates containing cells were removed from the incubator and allowed to equilibrate to room temperature for 30 minutes. 100 µl of Caspase-Glo reagent was added to each well, the content of well was gently mixed with a plate shaker at 300–500 rpm for 30 seconds. The plate was then incubated at room temperature for 2 hours. The luminescence of each sample was measured in a plate-reading luminometer ((M5, Spectrmax plate reader) with parameters of 1 minute lag time and 0.5 second/well read time. The experiments were performed in triplicate and repeated on two separately-initiated cultures.

Statistical analysis

All the experiments were replicated three times. Results were expressed as the means ± SEM. A difference with value $p<0.05$ was considered statistically significant. Data were analysed by ANOVA and statistical differences between the various treatment group means were determined by least square difference (LSD) using the statistical Product and Service Solutions, Version 17.0.1 software (SPSS Inc., Chicago, IL, USA).

Results

4 RESULTS

4.1 Virus propagation and titration

B95a cells were propagated in RPMI 1640 medium supplemented with 10% fetal bovine serum under a 5% CO_2 atmosphere. These cells were maintained in the same medium supplemented with 2% fetal bovine serum. The PPR virus isolate, PPR Sungri/96, originally isolated in B95a cells and held at 5th passage level were used in this study. This isolate belongs to isolates belong to genetic lineage 4 (Dhar *et al*., 2002). For the multistep growth curve of the virus, confluent monolayer of B95a cells in a 24-well tissue culture plate was infected with PPRV at an MOI of 0.1 $TCID_{50}$/cell in 1 ml maintenance medium. Culture supernatant from infected wells was harvested initially at 6-hourly intervals upto 24 hr and subsequently after an interval of 24 hr up to 5 days (Sreenavasa *et al.,* 2006). CPE was recorded during the entire experimental period. The characteristic CPE in the form of rounding, ballooning and large syncytia was observed 48hr days post infection. Extensive CPE was observed between 72hr and 96 hr (Fig.4.1), followed by degeneration of infected cells by the 120 hr onwards. The infected cells were dislodged in 1 ml of fresh medium and cell extract was prepared after two freeze-thaw cycles. The culture fluids and cell extracts were collected from duplicate wells and pooled. The infectivity of the culture fluids and cell extracts was determined on a preformed monolayer of B95a cells using a 96-well microtitre plate. The virus titre was calculated according to the method of Reed and Muench (1938).

4.2 Extraction of total RNA and synthesis of First strand cDNA from virus

Isolation of total RNA (~12µg from $5x10^6$ cells) was achieved by homogenization through pipetting with Trizol, a monophasic solution of phenol and guanidium isothiocynate,

followed by phase separation with chloroform and isopropyl alcohol precipitation and washing with 75% alcohol.RNA pellet was suspended in 0.01% DEPC treated nuclease free water (NFW) and stored at -70°C for further use.

Synthesis of cDNA was carried out using the pelleted RNA using random hexamer primer and MuMLV-RT in a typical 20µl reaction mix. After the reaction it was stored at -20°C for further use.

4.3 Amplification of V protein coding region of the P gene from cDNA

V protein coding region of the P gene was amplified using gene-specific primer sets (Forward and Reverse primers). In 1.2% agarose gel, a single band of 917bp amplified product (Fig.4.2) was observed. Two such 25µl of PCR reaction were set and the products were purified by using commercially available mini elute gel extraction kit (Qiagen). The PCR products were quantified on a 1.2% agarose gel by densitometric comparison with molecular mass ladder (MBI Fermentas) using GeneTool software in Gel documentation system (SynGene,UK). The concentration of the purified amplicon was around 40ng μl^{-1}.

4.4 Characterization of the amplicon and vector by RE digestion

The purified putative PCR product and vector were digested with two different restriction endonucleases separately *viz.*, *Bgl II* and *EcoR I* (Fig.4.3). The digested products were run on a 1.2% agarose gel.

4.5 Cloning of V protein coding region of the P gene in pDsRed-Express-N1 Vector

Purified V protein coding region of the P gene was cloned in pDsRed-Express-N1 Vector keeping the insert: vector ratio to 3: 1 (Fig.4.4).

$$\text{ng of insert (PCR product)} = \frac{50\text{ng of vector} \times \text{kb size of insert}}{\text{kb size of vector}} \times \frac{3}{1}$$

$$\text{ng of insert (PCR product)} = \frac{50 \times 1 \times 3}{5} = 30\,\text{ng}$$

By using the formulae, about 30 ng of purified amplicon was ligated to 50 ng of vector. The competent E.coli $DH_5\alpha$ cells were successfully transformed. The recombinant clones

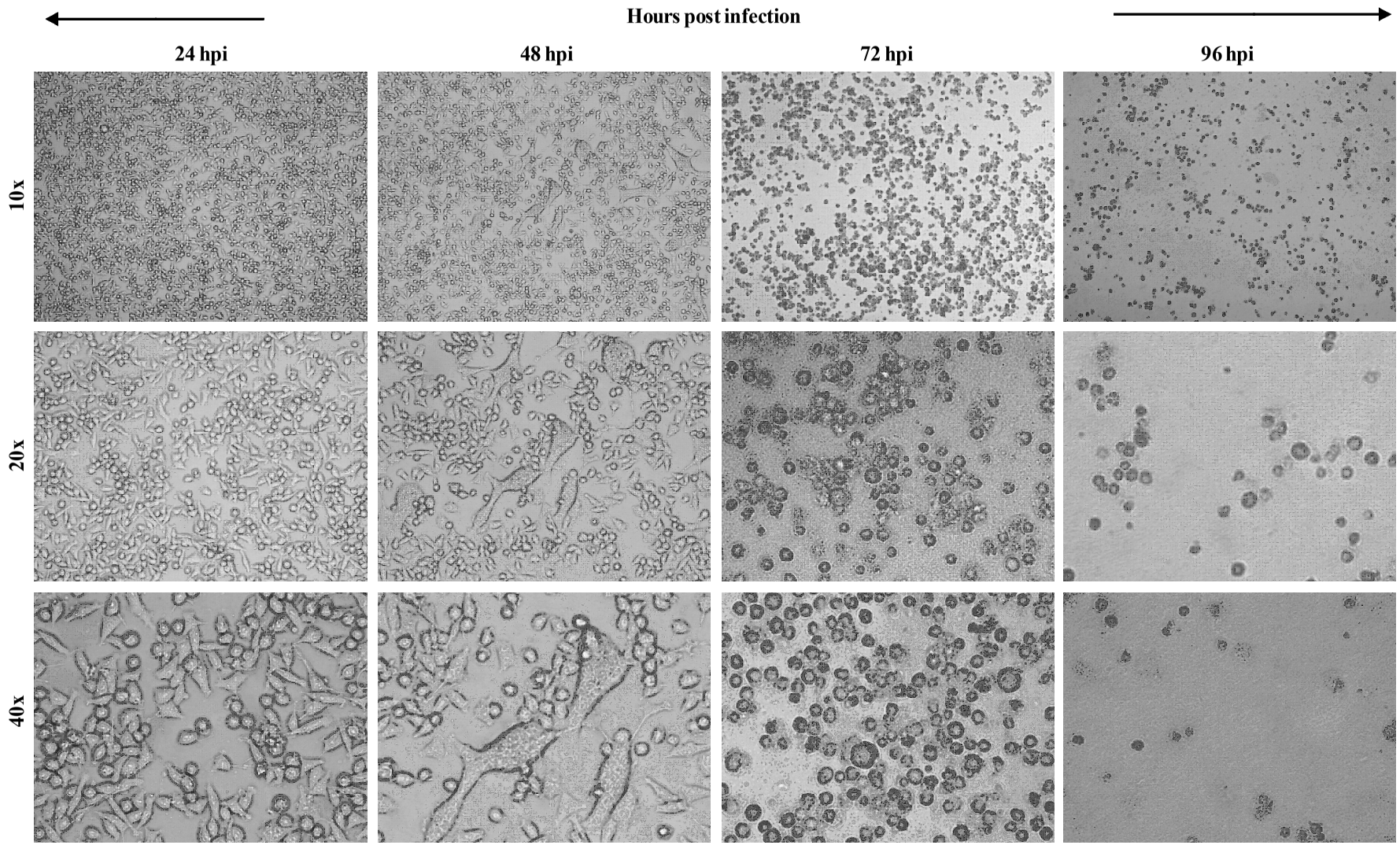

Fig. 4.1: B95a cells were infected with the PPRV Sungri/96 strain with MOI of 0.1 $TCID_{50}$/cell. Cytopathic effects (CPE) were observed under microscope (Magnification -10X, 20X and 40X) at different time points post infection.

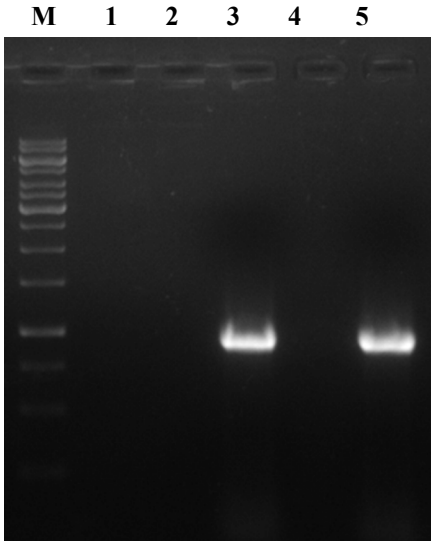

Fig. 4.2: PCR amplification of V protein coding region of the P gene
Lane M : 1Kb plus ladder
Lanes 3 and 5 : V protein coding region of the P gene (917 bp)

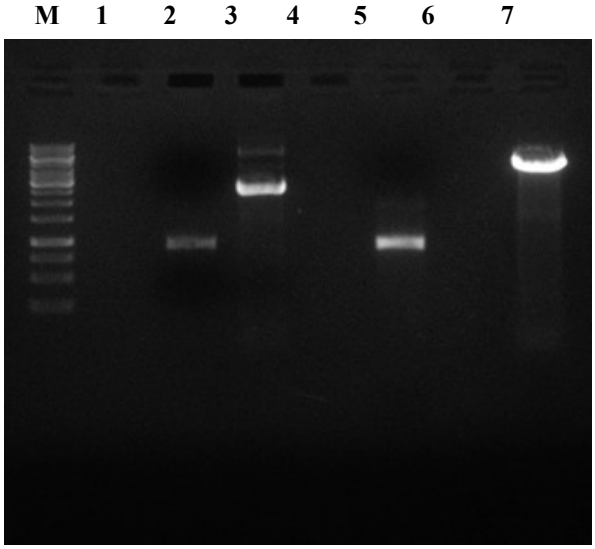

Fig. 4.3: Characterization of the amplicon and vector by RE digestion
Lane M : 1Kb plus ladder
Lanes 2, 5 : Vector digested with *Bgl II* and *EcoR I*
Lanes 3 , 7 : PCR amplicon digested with *Bgl II* and *EcoR I*

Restriction Enzyme digestion of the vector with *Bgl II* and *EcoR I*

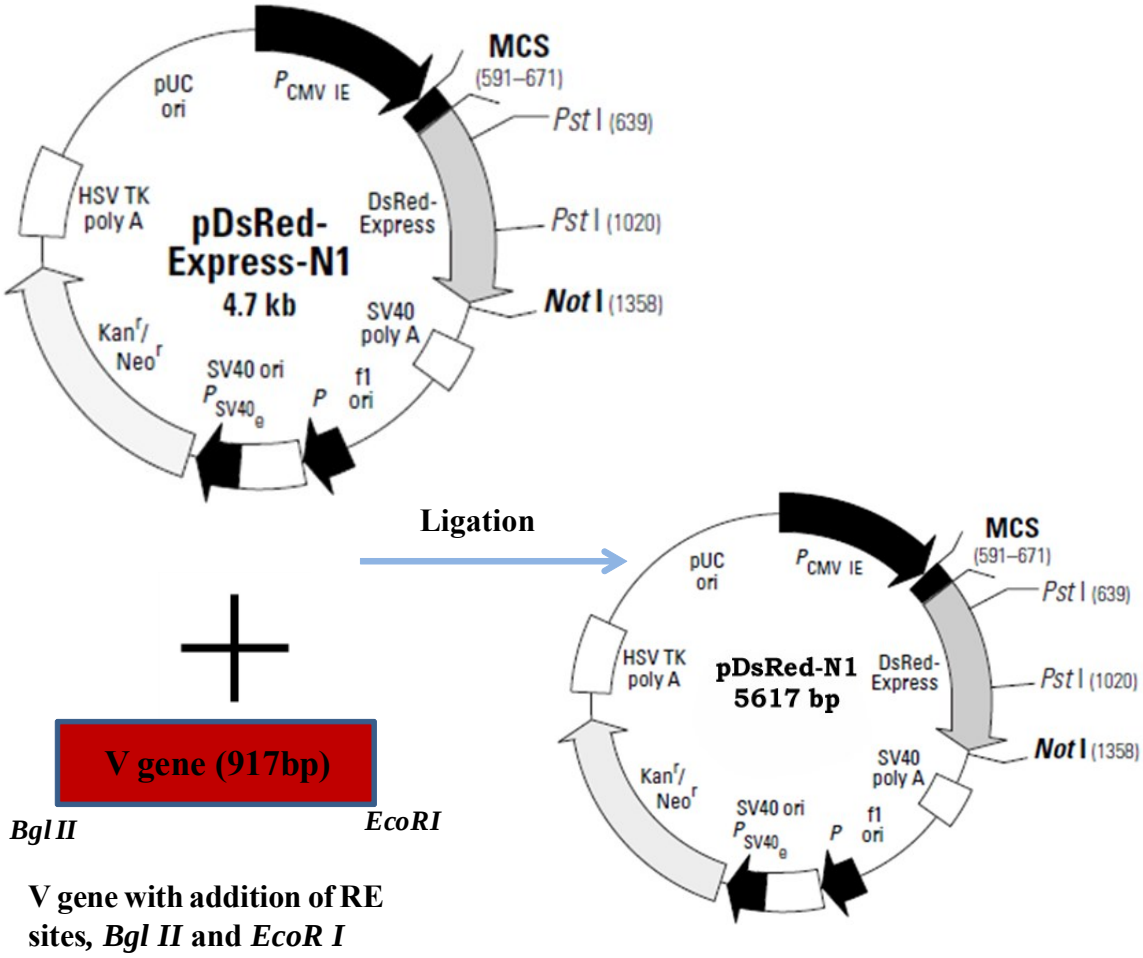

V gene with addition of RE sites, *Bgl II* and *EcoR I*

Fig. 4.4: Cloning of V protein coding region of the P gene in pDsRed-Express-N1 Vector

were screened by visualizing its blue-white colour from LB/kanamycin/X-gal/IPTG. Five such colonies were picked up for colony PCR, out of which three colonies were positive (Fig.4.5).

Plasmids were isolated from positive recombinant cells grown overnight and were subjected to restriction enzyme digestion with *Bgl II* and *EcoR I* enzymes. The digested product was checked by 1.2% agarose gel electrophoresis. Correct orientation of the insert in the vector was confirmed by restriction enzyme digestion of the plasmid, which released an insert size of 894 bp (Fig. 4.6). The clones having the correct orientation were selected and custom sequenced for nucleotides.

4.6 Sequence analysis

The transformants containing putative recombinant vector plasmid were custom sequenced .Sequence distance studies showed that V protein coding region of the P gene is similar to Peste-des-petits-ruminants virus isolate Sungri 1996 MSD (The Netherlands) (99%) and Peste-des-petits-ruminants virus strain Izatnagar/94 (99%) (Fig.4.7). Based on the sequence identity, the phylogenic tree has been represented (Fig.4.8).

4.7. Cloning of siRNA inserts into psiRNA h7SKGFPzeo vector

4.7.1. Annealing of siRNA inserts

In order to produce an annealed product of siRNA inserts, the different siRNA inserts namely siRNA, S1 (167-192); S2 (560-585) and S3 (727-752) were incubated with annealing mixture containing 0.5 M NaCl.

4.7.1. Characterization of the psiRNA vector by restriction endonucleases (RE) digestion

The psiRNA vector was digested with two different restriction endonucleases separately *viz.*, *Hind III* and *Acc I* .The digested product was run on a 1.2% agarose gel where an intense single DNA band of size 3894 bp (Fig.4.9) could be seen along with DNA molecular weight marker.

The annealed siRNA inserts were ligated with the double digested psiRNA vector. These ligation reactions were completed using DNA ligase (Fig.4.10). The recombinant products were transformed in competent GT116 strain of E. *coli*. The recombinant transformants were

screened by direct colony PCR. Out of 5 positive colonies one clone was randomly selected and plasmids were extracted. Then they were subjected to restriction enzyme digestion with *Hind III* and *Acc I* enzymes. The digested product was checked by 1.2% agarose gel electrophoresis (Fig. 4.11). The clones having the correct orientation were selected and custom sequenced for nucleotides using the forward and reverse primers.

4.8 The kill curve analysis

The optimum effectiveness of the antibiotics *i.e.*, minimum antibiotic concentration to be used in study will be the lowest concentration that kills 100% of untreated controls cells in 2-15 days from the start of antibiotic selection. The antibiotic concentration was standardized at 100 µg/ml for Zeocin and 50 µg/ml for Kanamycin.

4.9 Time course studies of transfection efficiency

For the study B95a cells were grown in RPMI-1640 supplemented with 10% FBS, 100 µg/ml of Zeocin in the medium for psiRNA vector and 50 µg/ml of Kanamycin in the medium for pDsRED vector and maintained at all times in temperature

4.9.1 Time course studies of transfection efficiency using Fluorscent microscopy

For transfection with enhanced green fluorescent protein (GFP)-encoding plasmid was carried out with Lipofectamine 2000 and followed by fluorescent imaging. The high degree of transfection is shown in Fig. 4.12. A similar protocol was followed to study the efficiency of pDsRED encoding plasmid (Fig. 4.13). After 48 hrs, a high number of cells were transfected with Lipofectamine was observed for both the plasmids. The transfection efficiency was determined microscopically by counting green cells/red cells and colorless cells.

4.10 Time course studies of gene silencing

The B95a cell were seeded in a 48-well tissue culture plate and co-transfection was carried out using Lipofectamine 2000 as explained in the previous experiment .The siRNA construct(s) were ligated into the green fluorescent protein (GFP)-encoding plasmid whereas the V gene was ligated into the pDsRED encoding plasmid. For co-transfection 1µg of each of the above mentioned plasmid per well was added. The experiments were carried out in triplicates.

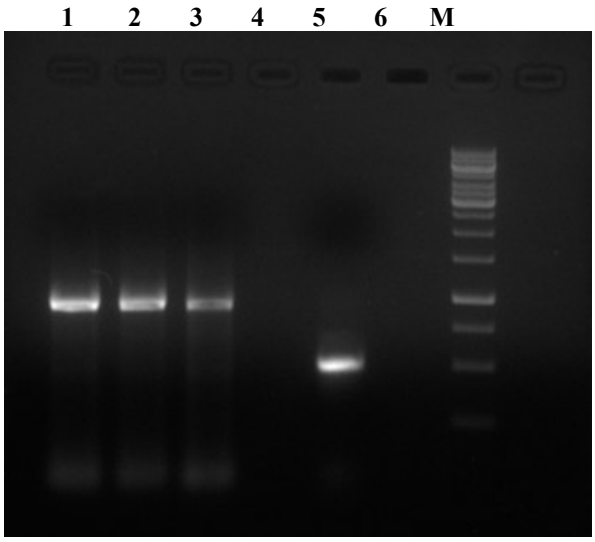

Fig. 4.5: Colony PCR of recombinant pDsRed-Express-N1 clone in *E.coli* DH5α cells

Lane M : 1Kb plus ladder

Lanes 1-3 : Positive colonies of pDsRed-Express-N1 V protein coding region of the P gene clone (917 bp)

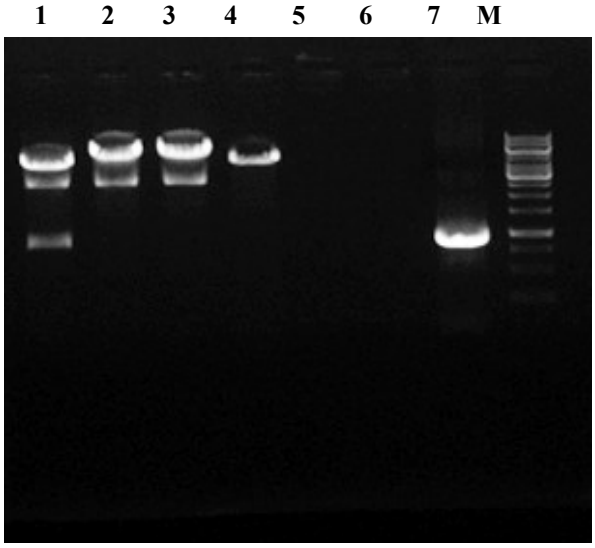

Fig. 4.6: Restriction enzyme digestion of recombinant pDsRed-Express-N1 with *Bgl II* and *EcoR I* enzymes

Lane 1 : RE digested pDsRed-Express-N1 containing V protein coding region of the P gene with *BglII &EcoRI*

Lane 2 : RE digested pDsRed-Express-N1 containing V protein coding region of the P gene with *EcoRI*

Lane 3 : RE pDsRed-Express-N1 containing V protein coding region of the P gene with *BglII*

Lane 4 : Undigested pDsRed-Express-N1 containing V protein coding region of the P gene

Lane 7 : PCR amplified V protein coding region of the P gene

Lane M : 1Kb plus ladder

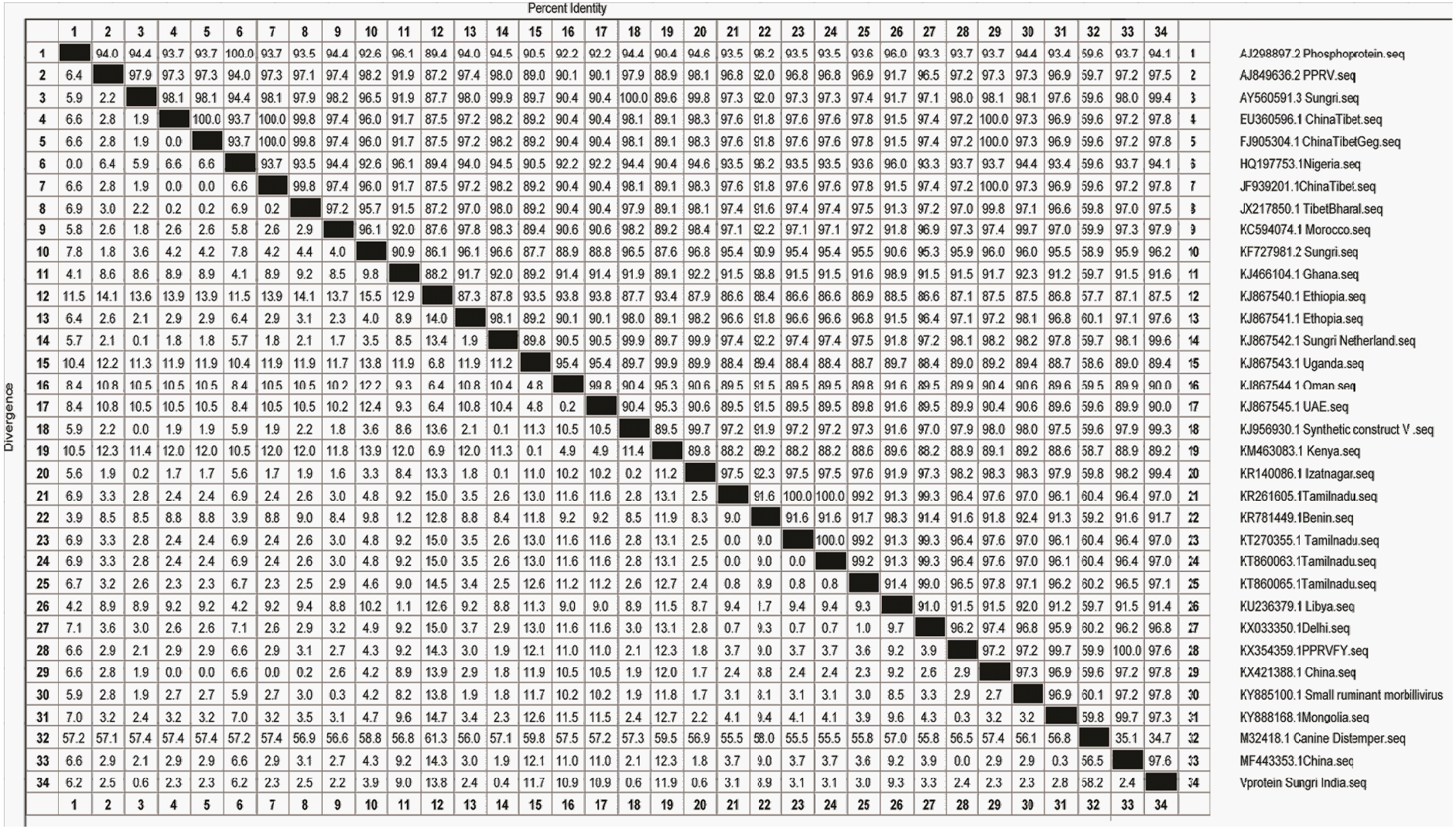

Fig. 4.7: Homology studies with the nucleotide sequence among the V protein of PPRV

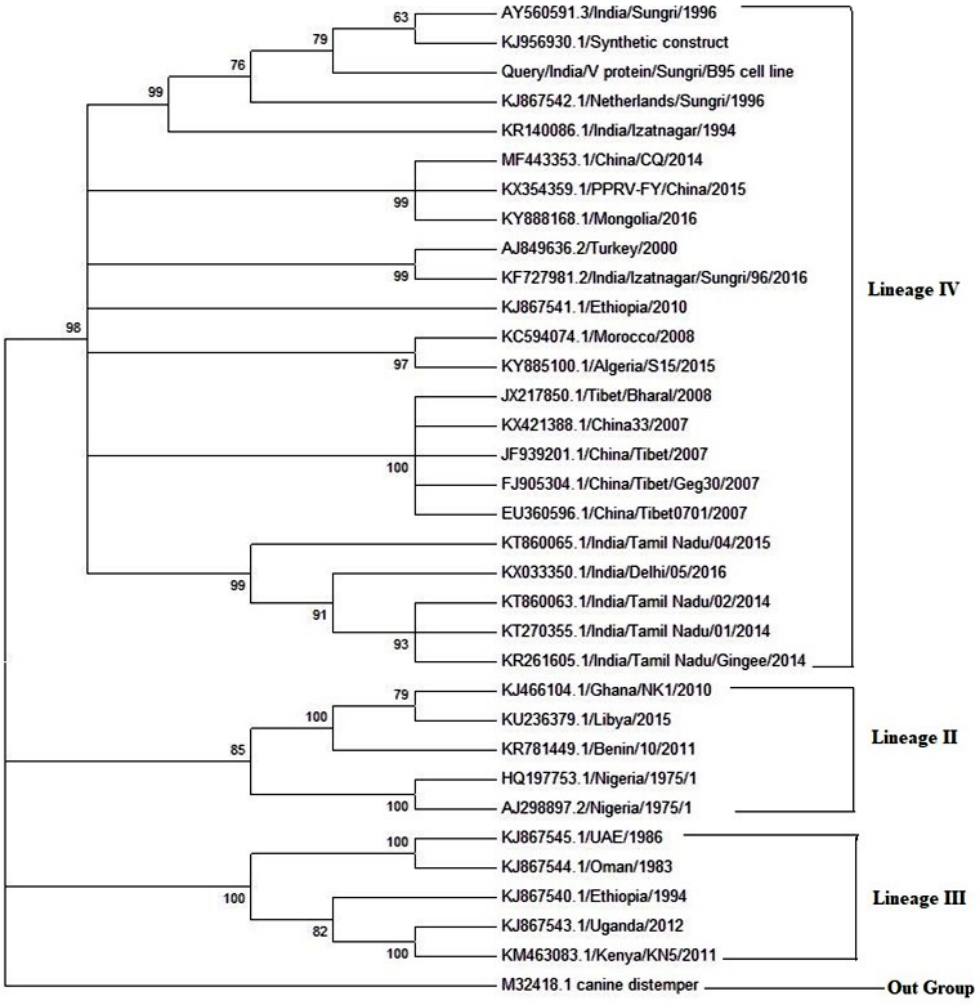

Fig. 4.8: Phylogenic tree analysis of V protein of PPRV

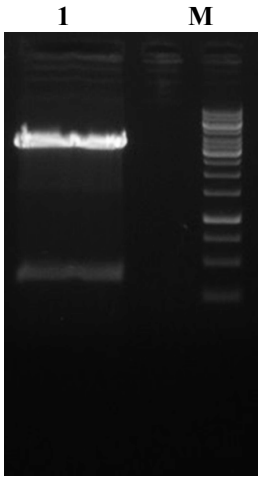

Fig. 4.9: Restriction enzyme digestion of recombinant *psiRNA* h7SK-GFPzeo with *Hind III* and *Acc I* enzymes

Lane 1 : RE digested psiRNA h7SK-GFPzeo (3894 bp)

Lane M : 1Kb plus ladder

Restriction enzyme digestion of the vector with *Acc I* & *Hind III*

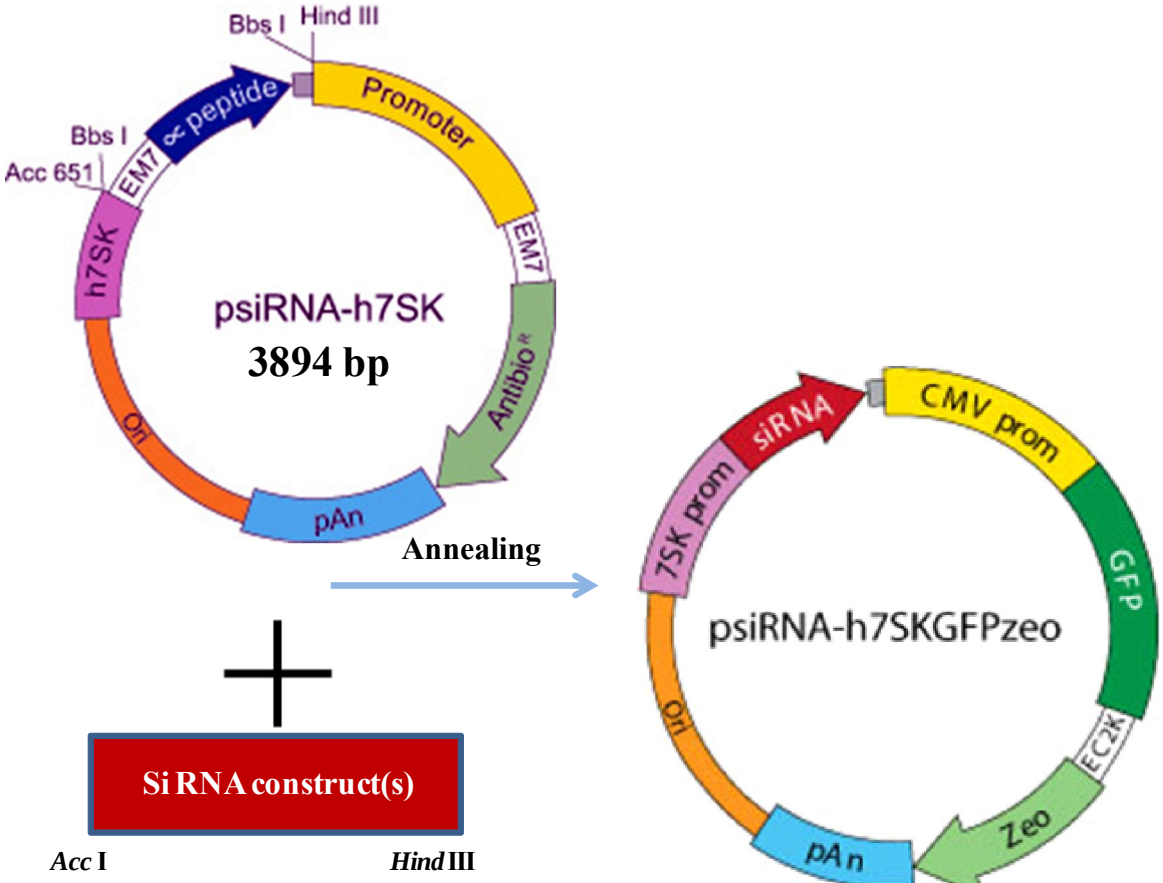

siRNA constructs with addition of RE sites, *Acc I* &*Hind III*

Fig. 4.10: Ligation of annealed siRNA inserts with the double digested psiRNA vector

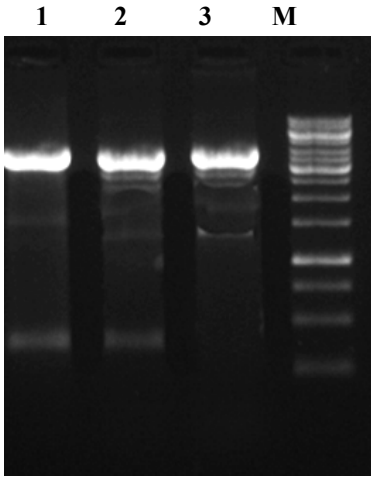

Fig. 4.11: Colony PCR of recombinant psiRNA h7SKGFPzeo clones in *E.coli* GT116 cells

Lane 1 : Positive colonies of psiRNA h7SKGFPzeo siRNA1 clone

Lane 2 : Positive colonies of psiRNA h7SKGFPzeo siRNA2 clone

Lane 3 : Positive colonies of psiRNA h7SKGFPzeo siRNA3 clone

Lane M : 1Kb plus ladder

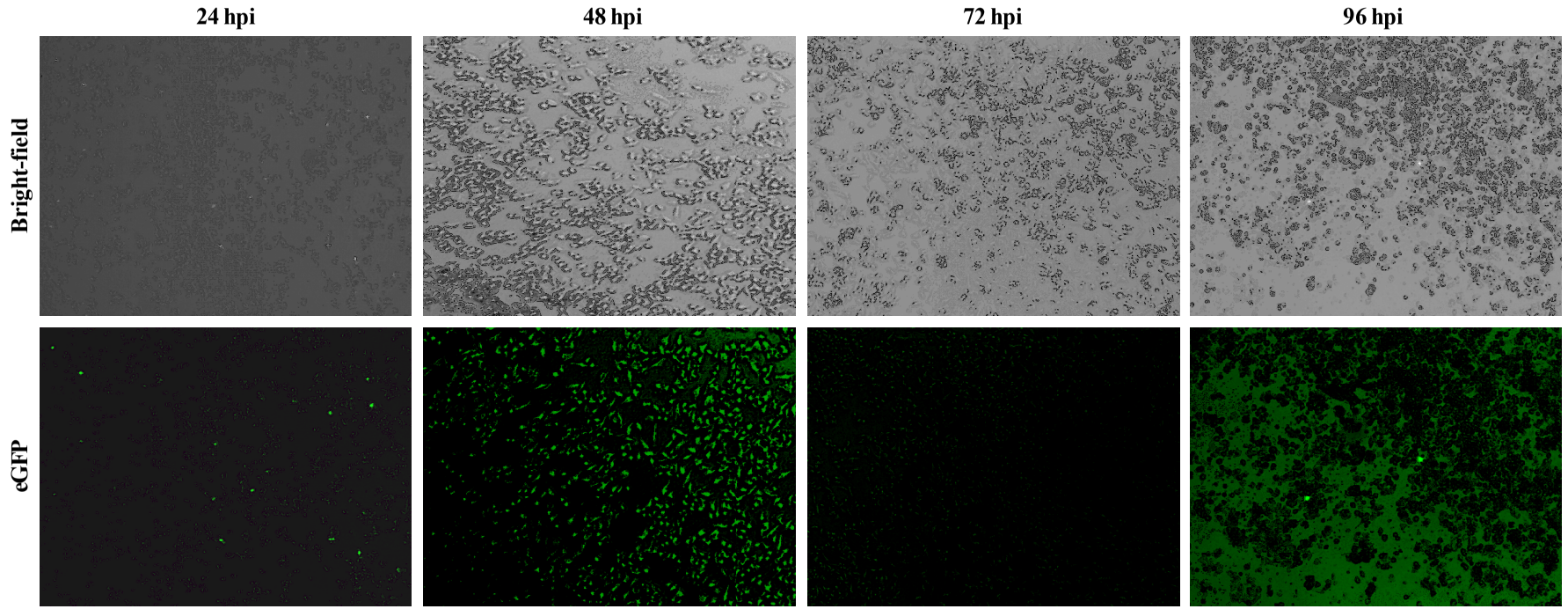

Fig. 4.12: Fluorscent imaging microscopy of B95a cells during transfection with green fluorescent protein (GFP)-encoding plasmid and Lipofectamine 2000 over a time period 24 hpi, 48 hpi, 72 hpi, and 96 hpi. The increasing number of green fluorescent cells indicates the successful transfection by Lipofectamine 2000.

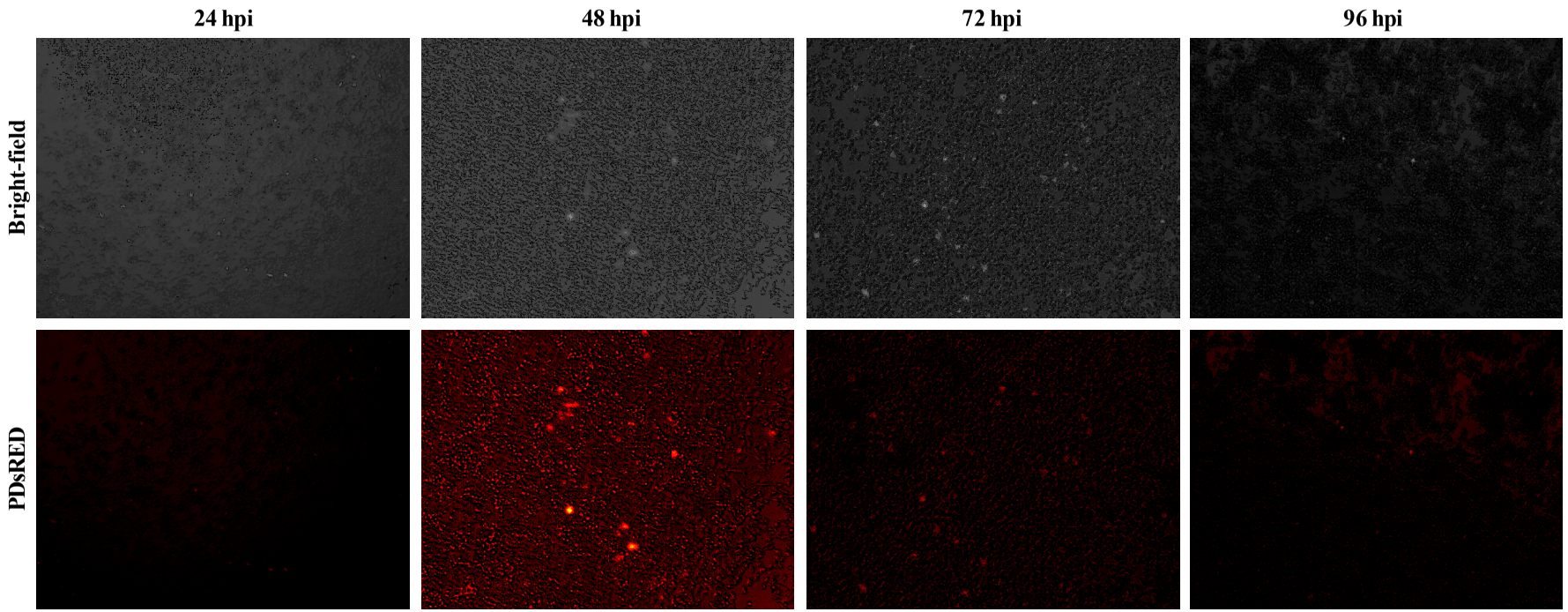

Fig. 4.13: Fluorscent microscopy of B95a cells during transfection with red fluorescent protein (pDsRED)-encoding plasmid and Lipofectamine 2000 over a time period 24 hpi, 48 hpi, 72 hpi, and 96 hpi. The increasing number of green fluorescent cells indicates the successful transfection by Lipofectamine 2000.

After every 24 hpi the plates were viewed under microscope and the results were recorded upto 96 hpi (Fig.4.14). For experiments with the whole PPRV, the cells were infected with virus @0.01 moi which was followed by transfection with plasmids containing the siRNA constructs (Fig.4.15).

4.10.1 Time course studies of gene silencing using quantitative RT-PCR

The relative expression of V protein coding region of the P gene in B95a cells were also quantified and compared by real time qPCR at each time point *i.e.* 24 hr, 48 hr, 72 hr and 96 hr after transfection/co-transfection with the respect plasmid(s) to define and compare their kinetics. The concentration of total RNA obtained from B95a cells ranged between 20 ng/µl and 33 ng/µl and purity factor was 1.98 ± 0.18. The amplification plots of V protein coding region of the P gene at different time intervals and different treatment were shown in Figs 4.15 to 4.22. The cycle threshold (Ct) or crossing point (Cp) values for all the amplification curves during the real-time PCR reaction was recorded and used for the calculation of mean fold change. Relative quantities of V protein coding region of the P gene mRNA were normalized to GAPDH and all reactions were made in triplicates using samples derived from all biological repeats. Melting curve analysis did not yield any non-specific peak from each primer set tested (Fig 4.23). Results, which are reported in terms of fold increase/decrease in gene transcripts at different time intervals were compared, are shown in Table 4.1 to 4.19 Fig. 4.15 to 4.33.

The time course expression studies revealed that the relative expression of V protein coding region of the P gene in B95a cells transfected with pDsRed-Express-N1 plasmid containing V protein coding region of the P gene decreased progressively from 24 hpi to 96 hpi and its mRNA peaked at 24 hpi (Fig 4.21; 4240-fold increase over the unstimulated B95a cells).The plasmid induced expression of V protein coding region of the P gene was significantly different($p<0.05$) between 24 and 96 hpi whereas no significant difference ($p>0.05$) was observed between 48 and 72 hpi time intervals (Table 4.7). The relative expression of V protein coding region of the P gene in B95a cells infected with PPRV@0.01 moi increased steadily up to 72 hpi (297-fold increase of V protein coding region of the P gene mRNA at 72 hpi over the unstimulated B95a cells and then began to decline at 96 hpi (Fig 4.21).The viral infection induced expression V protein coding region of the P gene was significantly different

($p<0.05$) between 24,48, and 72 hpi whereas no significant difference was observed between 24 and 96 hpi with respect to V protein coding region of the P gene expression (Table 4.7).

The relative expression of V protein coding region of the P gene in B95a cells cotransfected with plasmids containing S1 construct and V protein coding region of the P gene steadily showed a pattern of down regulation as any fold change below 1 is considered to represent down regulation of gene of interest (Fig 4.15; 0.67-fold change at 24 hpi over the unstimulated B95a cells was the peak). The down regulated gene expression was significantly different ($p<0.05$) between 24, 48, 72 and 96 hpi (Table 4.1). A similar pattern of down regulation of the gene was seen in B95a cells transfected with plasmid containing S1 construct and infected with PPRV@0.01 moi (Fig 4.16; 0.104-fold change at 96 hpi over unstimulated B95a cells was the highest). The down regulated gene expression was significantly different ($p<0.05$) between 24, 48, 72 and 96 hpi (Table 4.2).

The relative expression of V protein coding region of the P gene in B95a cells cotransfected with plasmids containing S2 construct and V protein coding region of the P gene steadily also showed a pattern of down regulation (Fig 4.17; 0.008-fold change at 72 hpi over the unstimulated B95a cells was the maximum relative expression). The down regulated gene expression was not significantly different between 24, 48, and 96 hpi whereas 72 hpi was significantly different ($p<0.05$) (Table 4.3).The gene down regulation in B95a cells transfected with plasmid containing S2 construct and infected with PPRV@0.01 moi(Fig4.18) was not significantly different between 24, 48, and 96 hpi (Table 4.4)

The relative expression of V protein coding region of the P gene in B95a cells cotransfected with plasmids containing S3 construct and V protein coding region of the P gene steadily showed a pattern of up regulation and peaked at 24 hpi (Fig 4.19; 21-fold change over the unstimulated B95a cells). No significant difference was observed between 24, 48, 72, and 96 hpi with respect to V protein coding region of the P gene expression (Table 4.5).A similar up regulation was noted in B95a cells transfected with plasmid containing S3 construct and infected with PPRV@0.01 moi and expression levels peaked at 72 hpi (Fig 4.20; 22- fold change over the unstimulated B95a cells). No significant difference was observed between

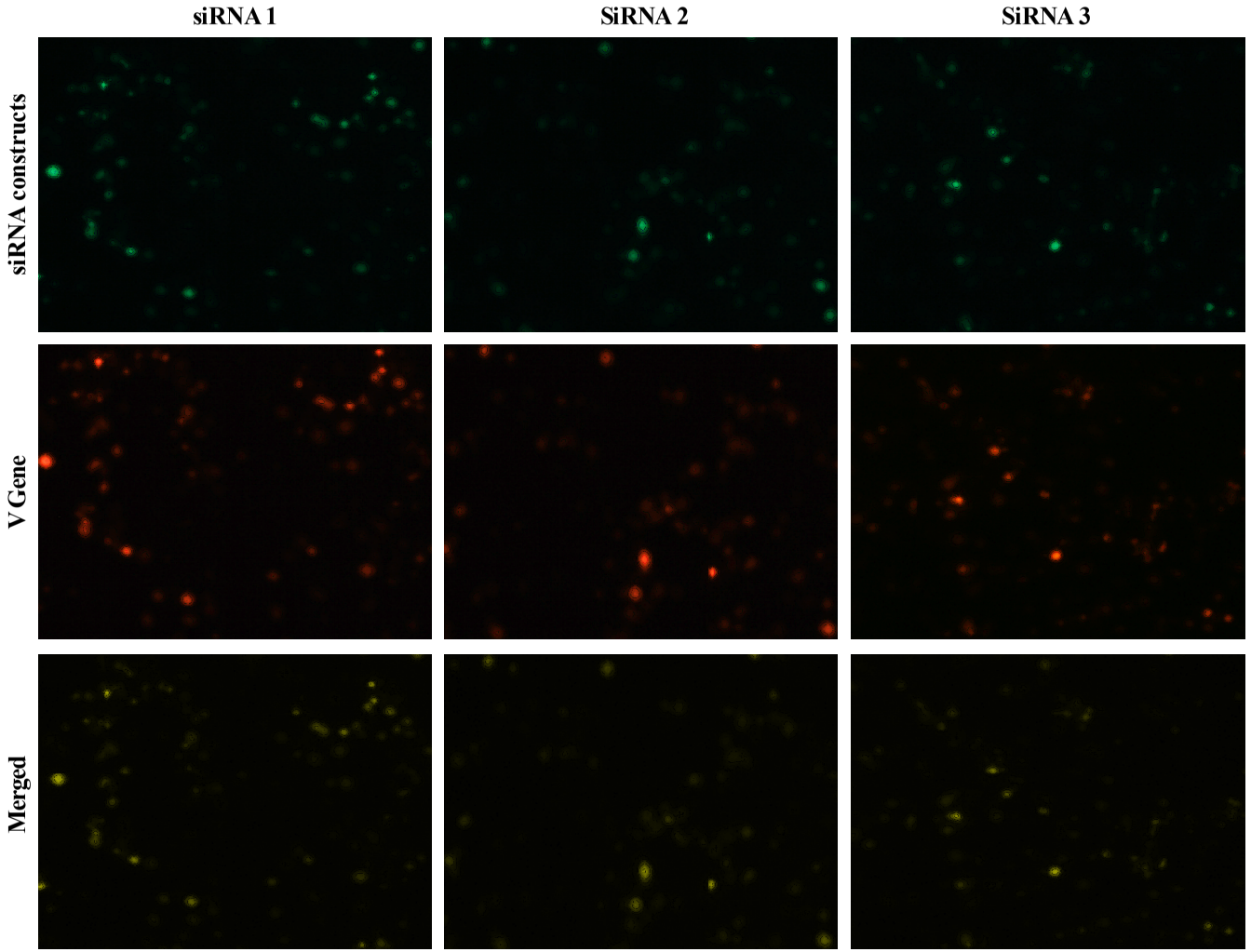

Fig. 4.14a: Fluorscent microscopy of B95a cells during co-transfection with green fluorescent protein (GFP)-siRNA construct (s) and red fluorescent protein (pDsRED)-Vgene and Lipofectamine 2000 after 24 hpi.

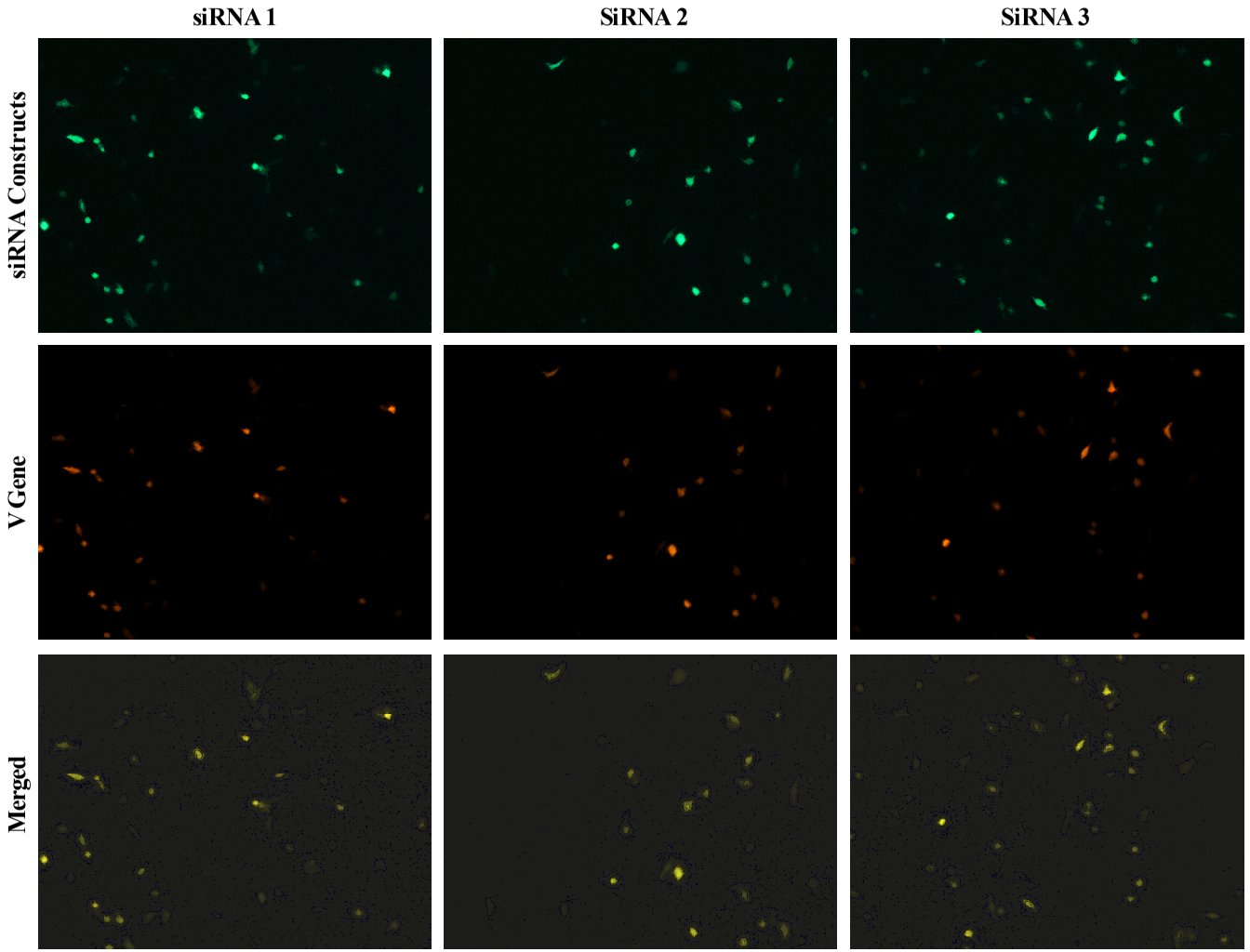

Fig. 4.14b: Fluorscent microscopy of B95a cells during co-transfection with green fluorescent protein (GFP)-siRNA construct (s) and red fluorescent protein (pDsRED)-Vgene and Lipofectamine 2000 after 24 hpi.

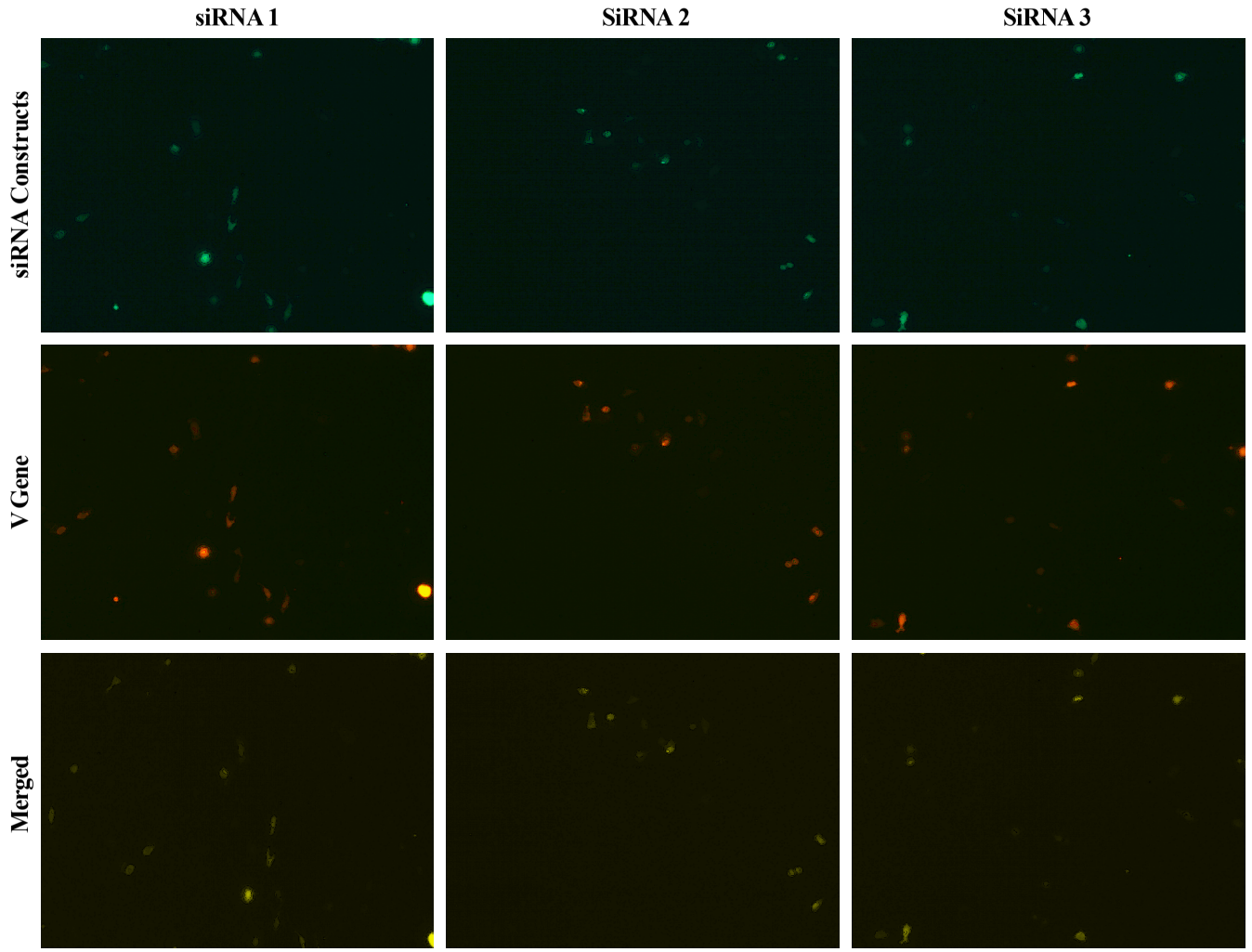

Fig. 4.14c: Fluorscent microscopy of B95a cells during co-transfection with green fluorescent protein (GFP)-siRNA construct(s) and red fluorescent protein (pDsRED)-Vgene and Lipofectamine 2000 after 72 hpi.

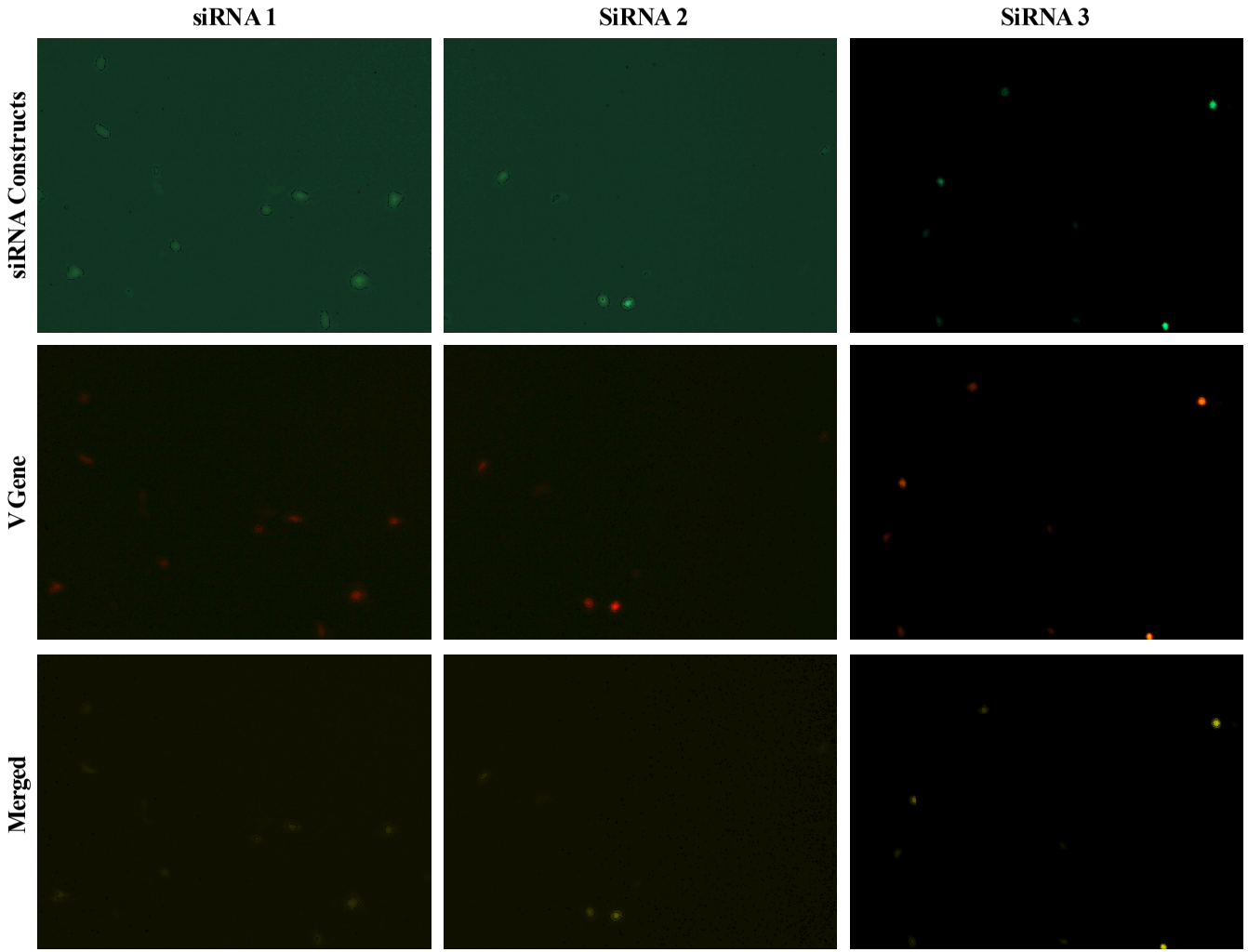

Fig. 4.14d: Fluorscent microscopy of B95a cells during co-transfection with green fluorescent protein (GFP)-siRNA construct(s) and red fluorescent protein (pDsRED)-Vgene and Lipofectamine 2000 after 96 hpi.

Table 4.1: Kinetics of V gene & S1 construct/V gene mRNA in B95a transfected and co-transfected cells respectively. Data are presented as the fold increases in mRNA levels

Construct \ Time	24 hr	48 hr	72 hr	96 hr	F- value
V gene	4240.6273[a] ±57.57633	2401.9650[b] ±57.73503	2335.5637[b] ± 88.19171	1351.1761[c] ±57.73503	327.27**
S1 construct/ V gene	0.6790[a] ±0.00058	0.4897[b] ±0.00088	0.4700[c] ±0.00058	0.3150[d] ±0.00058	303617.000**
t- value	73.640*	41.585*	26.477*	23.398*	

a, b, c, d- within V gene and S1 construct/V gene, between different time periods means differ significantly ($p<0.05$)
**Overall significant difference within V gene and S1 construct/V gene ($p<0.01$)
* Significant difference between V gene and S1 construct/V gene at the same time period ($p<0.01$)

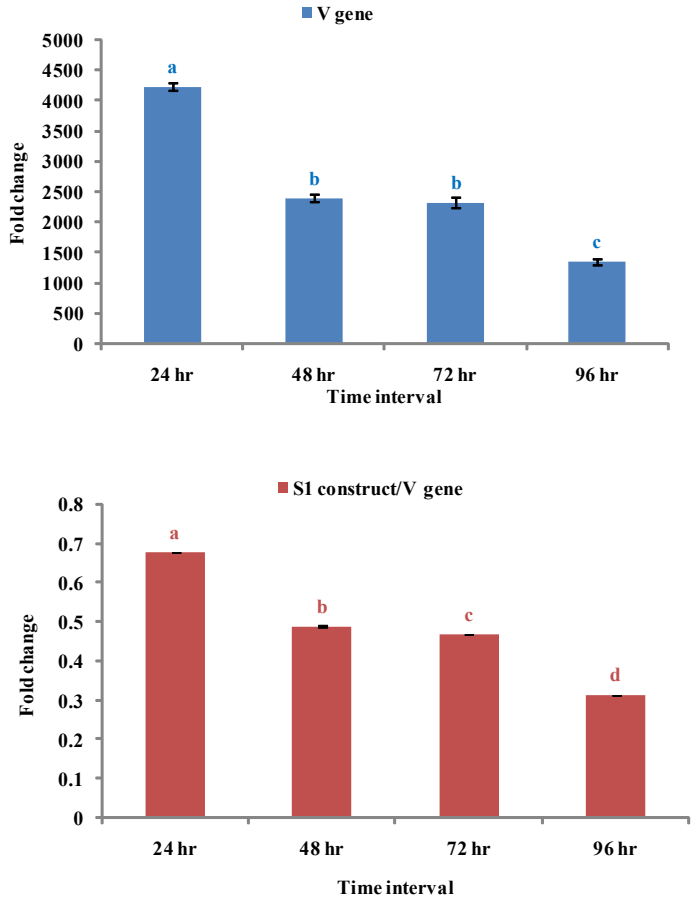

Fig. 4.15: Kinetics of Vgene and S1 construct/V gene mRNA in B95a transfected and co-transfected cells respectively

Table 4.2: Kinetics of V gene and S1 construct/Virus mRNA in B95a transfected and co-transfected cells respectively. Data are presented as the fold increases in mRNA levels.

Time Construct	24 hr	48 hr	72 hr	96 hr	F-value
V gene	4240.6273[a] ±57.57633	2401.9650[b] ±57.73503	2335.5637[b] ±88.19171	1351.1761[c] ±57.73503	327.27**
S1 construct/ Virus	0.19800[a] ±0.000577	0.47000[b] ±0.000577	0.31500[c] ±0.000577	0.10400[d] ±0.000577	74752.750**
t-value	73.649*	41.595*	26.479*	23.401*	

a, b, c, d- within V gene and S1 construct/Virus, between different time periods means differ significantly ($p<0.05$)
**Overall significant difference within V gene and S1 construct/Virus ($p<0.01$)
* Significant difference between V gene and S1 construct/Virus at the same time period ($p<0.01$)

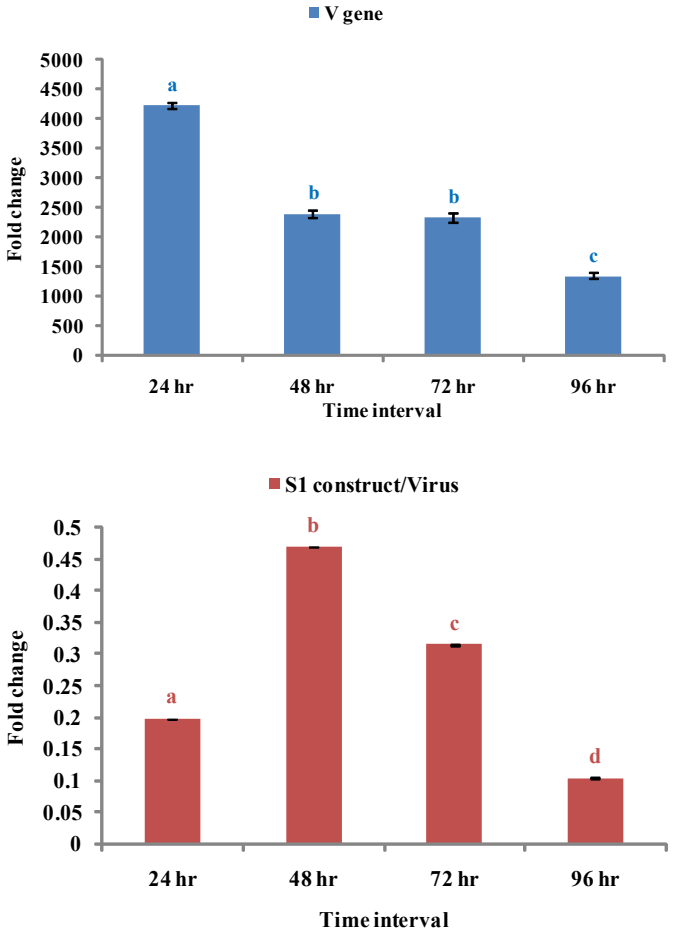

Fig. 4.16: Kinetics of Vgene and S1 construct/Virus mRNA in B95a transfected and co-transfected cells respectively

Table 4.3: Kinetics of V gene and S2 construct/V gene mRNA in B95a transfected and co-transfected cells respectively. Data are presented as the fold increases in mRNA levels.

Time Construct	24 hr	48 hr	72 hr	96 hr	F-value
V gene	4240.6273[a] ±57.57633	2401.9650[b] ±57.73503	2335.5637[b] ±88.19171	1351.1761[c] ±57.73503	327.27**
S2 Construct / V gene	0.00300[a] ±0.000577	0.00300[a] ±0.000577	0.00800[b] ±0.000577	0.00200[a] ±0.000577	22.000**
t-value	73.652*	41.603*	26.483*	23.403*	

a, b,c- within V gene and S2 construct/V gene, between different time periods means differ significantly ($p<0.05$)
**Overall significant difference within V gene and S2 construct/V gene ($p<0.01$)
* Significant difference between V gene and S2 construct/V gene at the same time period ($p<0.01$)

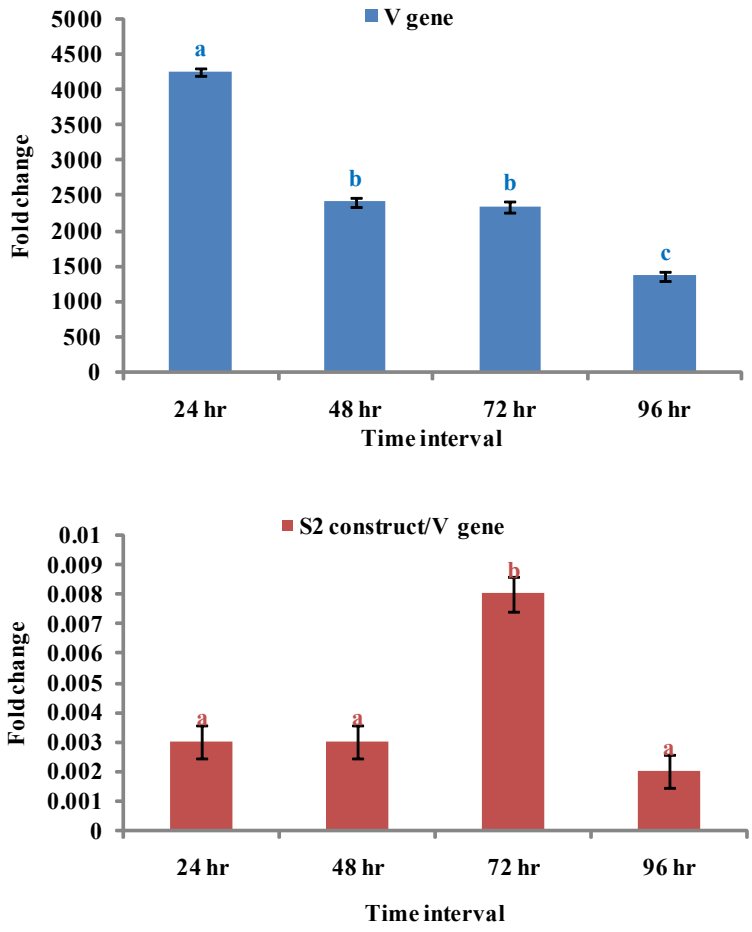

Fig. 4.17: Kinetics of Vgene and S2 construct/ Vgene mRNA in B95a transfected and co-transfected cells respectively

Table 4.4: Kinetics of V gene and S2 construct/Virus mRNA in B95a transfected and co-transfected cells respectively. Data are presented as the fold increases in mRNA levels.

Time / Construct	24 hr	48 hr	72 hr	96 hr	F-value
V gene	4240.6273[a] ±57.57633	2401.9650[b] ±57.73503	2335.5637[b] ±88.19171	1351.1761[c] ±57.73503	327.27**
S2 Construct/ Virus	0.00567[a] ±0.000882	0.00700[a] ±0.001528	0.00567[a] ±0.001764	0.00433[a] ±0.000667	0.711[NS]
t-value	73.652*	41.603*	26.483*	23.403*	

a, b, c- within V gene and S2 construct/Virus, between different time periods means differ significantly ($p<0.05$)
**Overall significant difference within V gene ($p<0.01$)
* Significant difference between V gene and S2 construct/Virus at the same time period ($p<0.01$)
NS- Overall non-significant difference within S2 construct/Virus

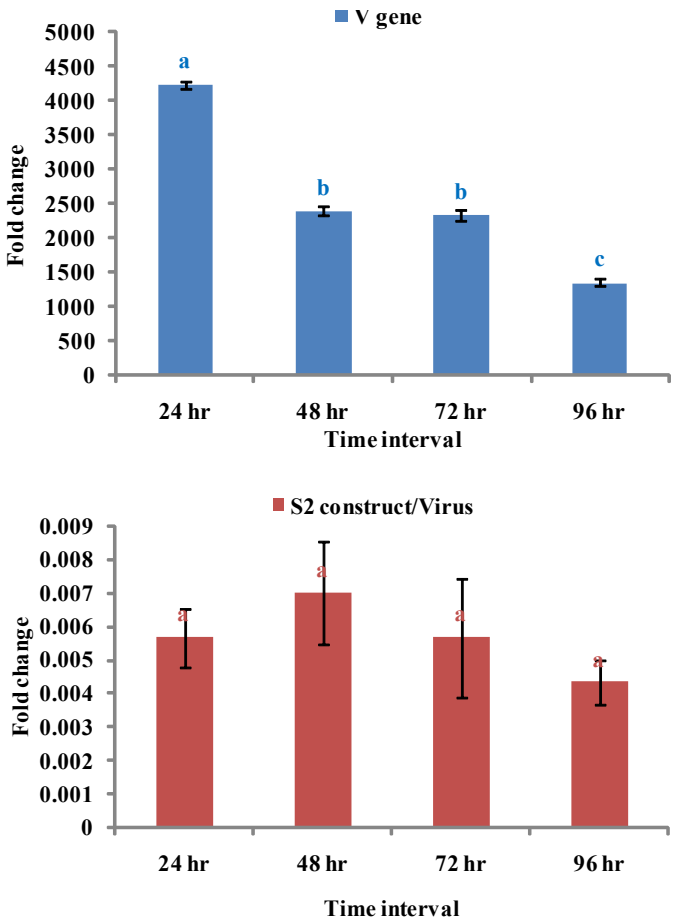

Fig. 4.18: Kinetics of Vgene and S2 construct/ Virus mRNA in B95a transfected and co-transfected cells respectively

Table 4.5: Kinetics of V gene and S3 construct/V gene mRNA in B95a transfected and co-transfected cells respectively. Data are presented as the fold increases in mRNA levels.

Time Construct	24 hr	48 hr	72 hr	96 hr	F-value
V gene	4240.6273[a] ±57.57633	2401.9650[b] ±57.73503	2335.5637[b] ± 88.19171	1351.1761[c] ±57.73503	327.27**
S3 Construct/ V gene	21.1600[a] ±0.577350	20.6090[a] ±0.577350	20.0700[a] ±0.577350	21.0120[a] ±0.577350	0.776[NS]
t- value	73.281*	41.244*	26.255*	23.053*	

a, b, c- within V gene and S3 construct/V gene, between different time periods means differ significantly ($p<0.05$)
**Overall significant difference within V gene ($p<0.01$)
* Significant difference between V gene and S3 construct/V gene at the same time period ($p<0.01$)
NS- Overall non-significant difference within S3 construct/V gene

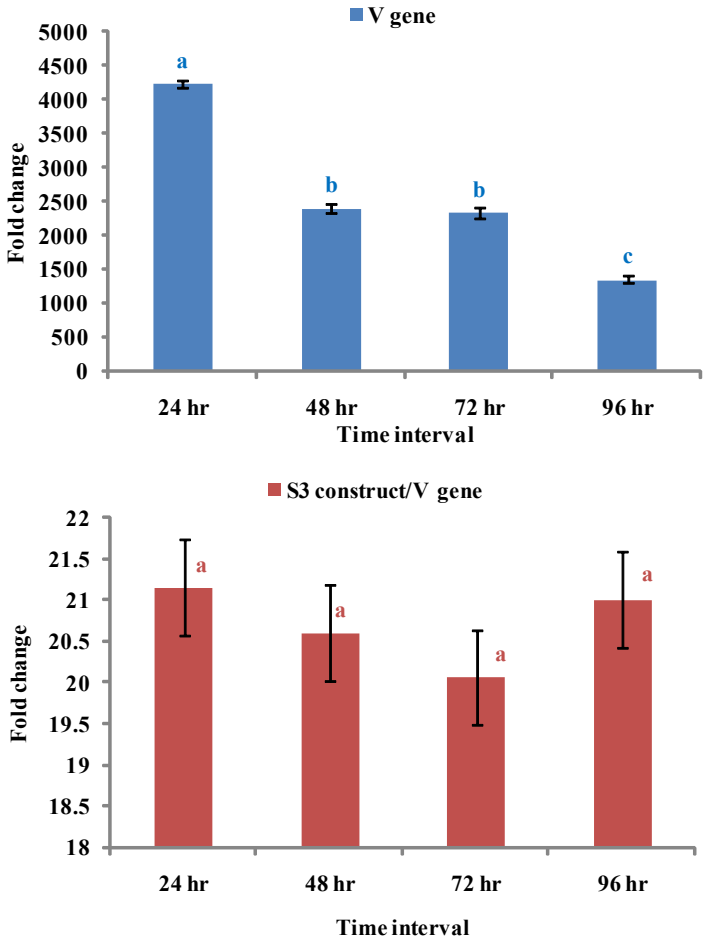

Fig. 4.19: Kinetics of Vgene and S3 construct/ Vgene mRNA in B95a transfected and co-transfected cells respectively

Table 4.6: Kinetics of V gene and S3 construct/Virus mRNA in B95a transfected and co-transfected cells respectively. Data are presented as the fold increases in mRNA levels.

Time Construct	24 hr	48 hr	72 hr	96 hr	F-value
V gene	4240.6273[a] ±57.57633	2401.9650[b] ±57.73503	2335.5637[b] ± 88.19171	1351.1761[c] ±57.73503	327.27**
S3 Construct/ Virus	20.1200[a] ±0.577350	21.0120[a] ±0.577350	22.0466[a] ±0.3333	20.7766[a] ±0.3333	2.87[NS]
t- value	73.29*	41.23*	26.23*	23.04*	

a, b, c- within V gene and S3 construct/Virus, between different time periods means differ significantly ($p<0.05$)
**Overall significant difference within V gene ($p<0.01$)
* Significant difference between V gene and S3 construct/V gene at the same time period ($p<0.01$)
NS- Overall non-significant difference within S3 construct/V gene

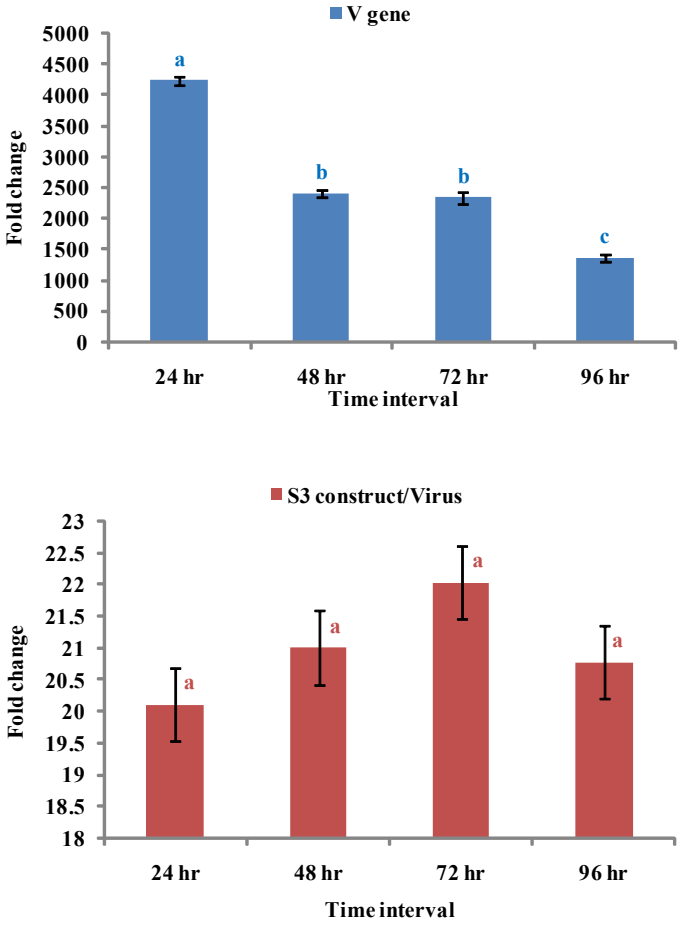

Fig. 4.20: Kinetics of Vgene and S3 construct/ Virus mRNA in B95a transfected and co-transfected cells respectively

Table 4.7: Kinetics of V gene and Virus mRNA in B95a transfected and co-transfected cells respectively. Data are presented as the fold increases in mRNA levels.

Time Construct	24 hr	48 hr	72 hr	96 hr	F-value
V gene	4240.6273[a] ±57.57633	2401.9650[b] ±57.73503	2335.5637[b] ± 88.19171	1351.1761[c] ±57.73503	327.27**
Virus	82.66±0.88[a]	107.15±0.57[b]	297.11±0.57[c]	83.13±0.57[a]	24193.58**
t- value	73.20*	39.74*	23.11*	21.96*	

a, b, c- within V gene and Virus, between different time periods means differ significantly ($p<0.05$)
**Overall significant difference within V gene and Virus ($p<0.01$)
* Significant difference between V gene & Virus at the same time period ($p<0.01$)

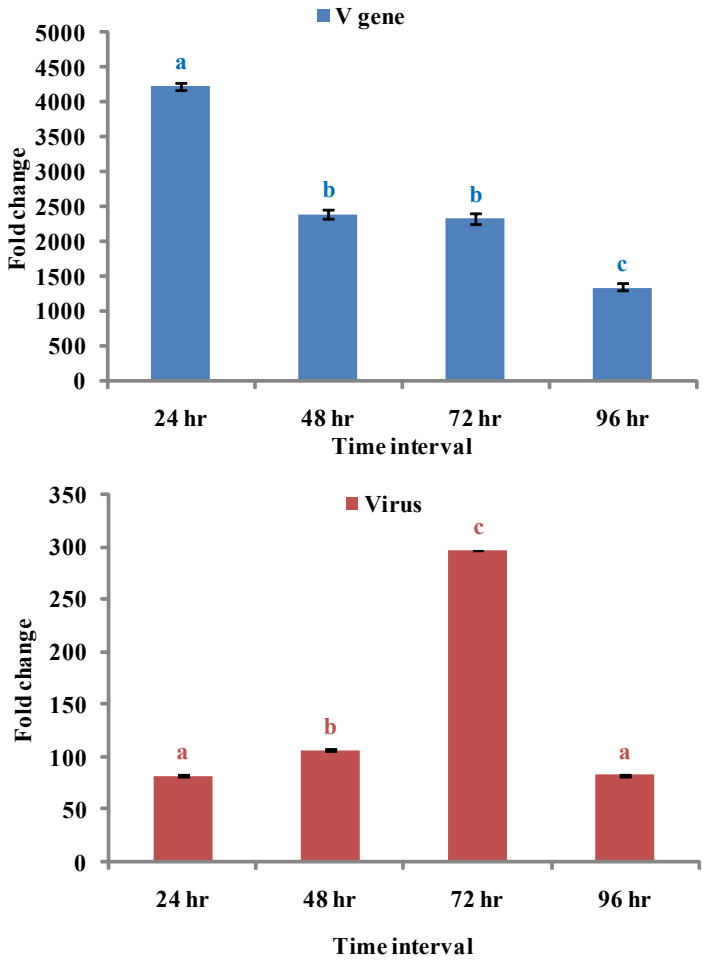

Fig. 4.21: Kinetics of Vgene and Virus mRNA in B95a transfected and co-transfected cells respectively

Table 4.8: Kinetics of Virus and S1 construct/V gene mRNA in B95a transfected and co-transfected cells respectively. Data are presented as the fold increases in mRNA levels

Time Construct	24 hr	48 hr	72 hr	96 hr	F-value
Virus	82.66[a] ±0.88	107.15[b] ±0.57	297.11[c] ±0.57	83.13[a] ±0.57	327.27**
S1 Construct/ V gene	0.6790[a] ±0.00058	0.4897[b] ±0.00088	0.4700[c] ±0.00058	0.3150[d] ±0.00058	303617.000**
t- value	92.965*	183.774 *	513.799*	143.455*	

a, b, c, d- within Virus and S1 Construct/V gene, between different time periods means differ significantly ($p<0.05$)
**Overall significant difference within Virus and S1 Construct/V gene ($p<0.01$)
* Significant difference between Virus and S1 Construct/V gene at the same time period ($p<0.01$)

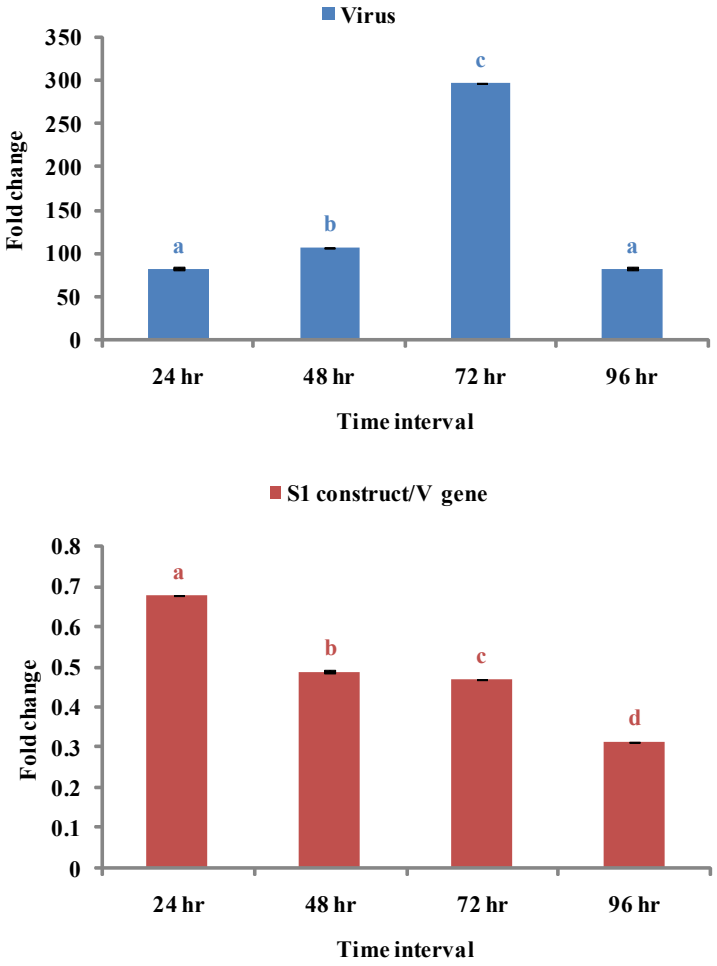

Fig. 4.22: Kinetics of Virus and S1 construct/V gene mRNA in B95a transfected and co-transfected cells respectively

Table 4.9: Kinetics of Virus and S1 construct/Virus mRNA in B95a transfected and co-transfected cells respectively. Data are presented as the fold increases in mRNA levels.

Time Construct	24 hr	48 hr	72 hr	96 hr	F-value
Virus	82.66[a] ±0.88	107.15[b] ±0.57	297.11[c] ±0.57	83.13[a] ±0.57	327.27**
S1 Construct/ Virus	0.19800[a] ±0.000577	0.47000[b] ±0.000577	0.31500[c] ±0.000577	0.10400[d] ±0.000577	74752.750**
t-value	93.51*	184.77*	514.06*	143.82*	

a, b, c, d- within Virus and S1 Construct/Virus, between different time periods means differ significantly ($p<0.05$)
**Overall significant difference within Virus and S1 Construct/Virus ($p<0.01$)
* Significant difference between Virus and S1 Construct/Virus at the same time period ($p<0.01$)

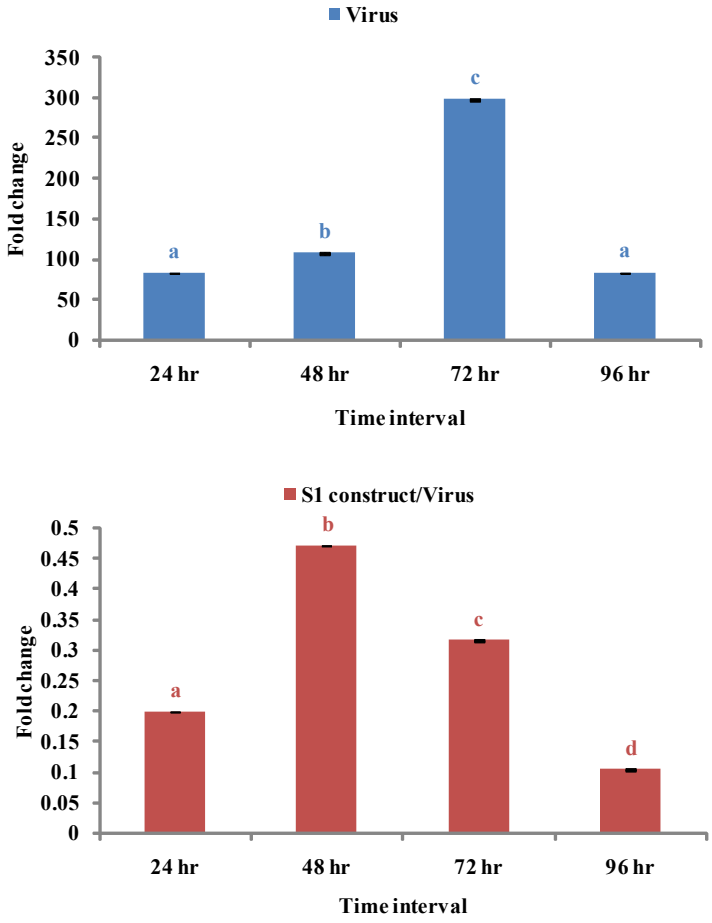

Fig. 4.23: Kinetics of Virus and S1 construct/Virus mRNA in B95a transfected and co-transfected cells respectively

Table 4.10: Kinetics of Virus and S2 construct/V gene mRNA in B95a transfected and co-transfected cells respectively. Data are presented as the fold increases in mRNA levels.

Time Construct	24 hr	48 hr	72 hr	96 hr	F-value
Virus	82.66[a] ±0.88	107.15[b] ±0.57	297.11[c] ±0.57	83.13[a] ±0.57	327.27**
S2 Construct/ V gene	0.00300[a] ±0.000577	0.00300[a] ±0.000577	0.00800[b] ±0.000577	0.00200[a] ±0.000577	22.000**
t-value	93.73*	185.58*	514.59*	143.99*	

a, b, c- within Virus and S2 Construct/V gene, between different time periods means differ significantly ($p<0.05$)
**Overall significant difference within Virus and S2 Construct/V gene ($p<0.01$)
* Significant difference between Virus and S2 Construct/V gene at the same time period ($p<0.01$)

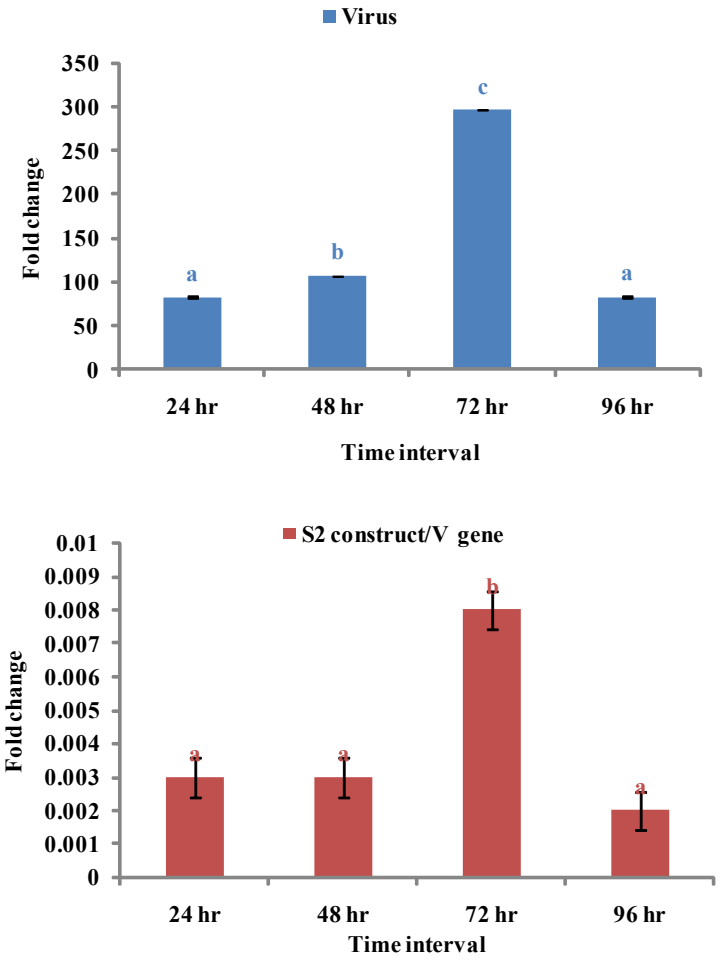

Fig. 4.24: Kinetics of Virus and S2 construct/V gene mRNA in B95a transfected and co-transfected cells respectively

Table 4.11: Kinetics of Virus and S2 construct/Virus mRNA in B95a transfected and co-transfected cells respectively. Data are presented as the fold increases in mRNA levels.

Time Construct	24 hr	48 hr	72 hr	96 hr	F-value
Virus	82.66[a] ±0.88	107.15[b] ±0.57	297.11[c] ±0.57	83.13[a] ±0.57	327.27**
S2 Construct/ Virus	0.00567[a] ±0.000882	0.00700[a] ±0.001528	0.00567[a] ±0.001764	0.00433[a] ±0.000667	0.711[NS]
t-value	93.72*	185.58*	514.60*	143.99*	

a, b, c- within Virus and S2 Construct/Virus, between different time periods means differ significantly ($p<0.05$)
**Overall significant difference within Virus ($p<0.01$)
* Significant difference between Virus and S2 Construct/Virus at the same time period ($p<0.01$)
NS- Overall non-significant difference within S2 Construct/Virus

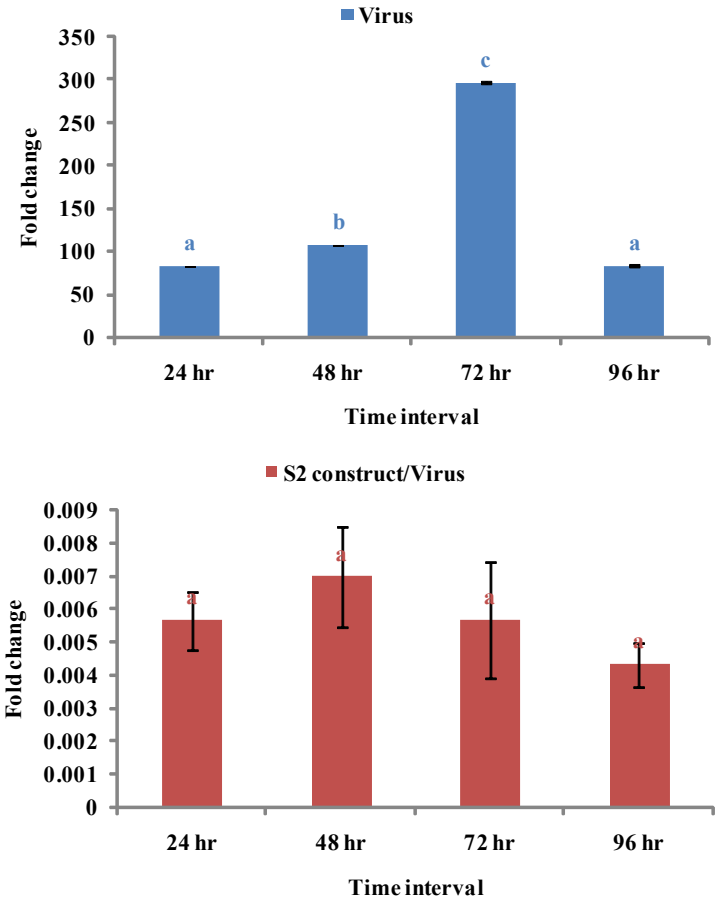

Fig. 4.25: Kinetics of Virus and S2 construct/Virus mRNA in B95a transfected and co-transfected cells respectively

Table 4.12: Kinetics of Virus and S3 construct/V gene mRNA in B95a transfected and co-transfected cells respectively. Data are presented as the fold increases in mRNA levels.

Time / Construct	24 hr	48 hr	72 hr	96 hr	F-value
Virus	82.66[a] ±0.88	107.15[b] ±0.57	297.11[c] ±0.57	83.13[a] ±0.57	327.27**
S3 construct/ V gene	21.1600[a] ±0.577350	20.6090[a] ±0.577350	20.0700[a] ±0.577350	21.0120[a] ±0.577350	0.776[NS]
t- value	58.35*	105.99*	339.30*	77.18*	

a, b, c- within Virus and S3 Construct/Vgene, between different time periods means differ significantly ($p<0.05$)
**Overall significant difference within Virus ($p<0.01$)
* Significant difference between Virus and S3 Construct/Vgene at the same time period ($p<0.01$)
NS- Overall non-significant difference within Virus and S3 Construct/Vgene

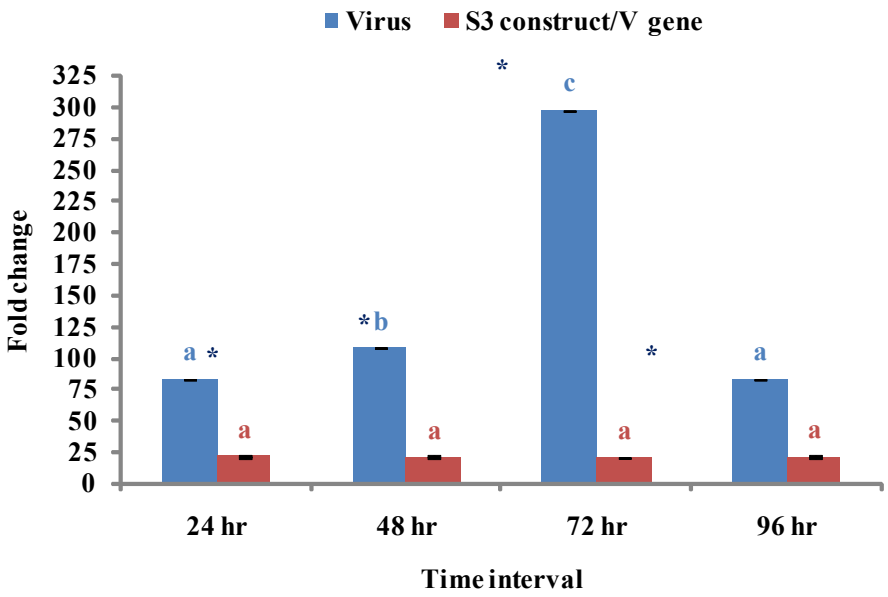

Fig. 4.26: Kinetics of Virus and S3 construct/V gene mRNA in B95a transfected and co-transfected cells respectively

Table 4.13: Kinetics of Virus and S3 construct/Virus mRNA in B95a transfected and co-transfected cells respectively. Data are presented as the fold increases in mRNA levels.

Time Construct	24 hr	48 hr	72 hr	96 hr	F-value
Virus	82.66[a] ±0.88	107.15[b] ±0.57	297.11[c] ±0.57	83.13[a] ±0.57	327.27**
S3 Construct/ Virus	20.1200[a] ±0.577350	21.0120[a] ±0.577350	22.0466[a] ±0.3333	20.7766[a] ±0.3333	2.87[NS]
t-value	59.33*	105.50*	412.59*	93.54*	

a, b, c- within Virus and S3 Construct/Virus, between different time periods means differ significantly ($p<0.05$)
**Overall significant difference within Virus ($p<0.01$)
* Significant difference between Virus and S3 Construct/Virus at the same time period ($p<0.01$)
NS- Overall non-significant difference within Virus and S3 Construct/Virus

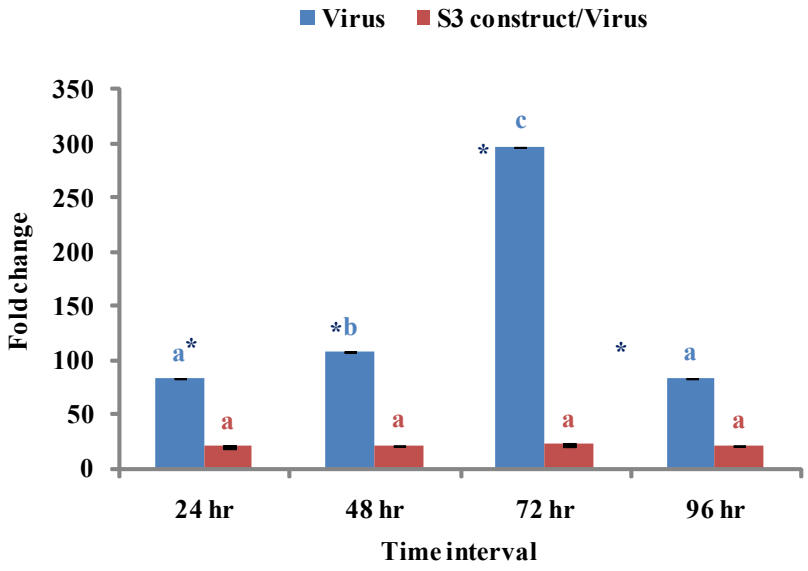

Fig. 4.27: Kinetics of Virus and S3 construct/Virus mRNA in B95a transfected and co-transfected cells respectively

Table 4.14: Kinetics of S1 Construct/V gene and S2 Construct /V gene mRNA in B95a transfected and co-transfected cells respectively. Data are presented as the fold increases in mRNA levels.

Time Construct	24 hr	48 hr	72 hr	96 hr	F- value
S1 Construct/ V gene	0.6790^{a} ±0.00058	1.0500^{b} ±0.00058	0.4700^{c} ±0.00058	0.3150^{d} ±0.00058	303617.000**
S2 Construct / V gene	0.00300^{a} ±0.000577	0.00300^{a} ±0.000577	0.00800^{b} ±0.000577	0.00200^{a} ±0.000577	22.000**
t- value	827.92*	1282.30*	565.83*	383.34*	

a, b,c- within S1 Construct/V gene and S2 Construct /V gene, between different time periods means differ significantly ($p<0.05$)
**Overall significant difference within S1 Construct/V gene and S2 Construct /V gene ($p<0.01$)
* Significant difference between S1 Construct/V gene and S2 Construct /V gene at the same time period ($p<0.01$)

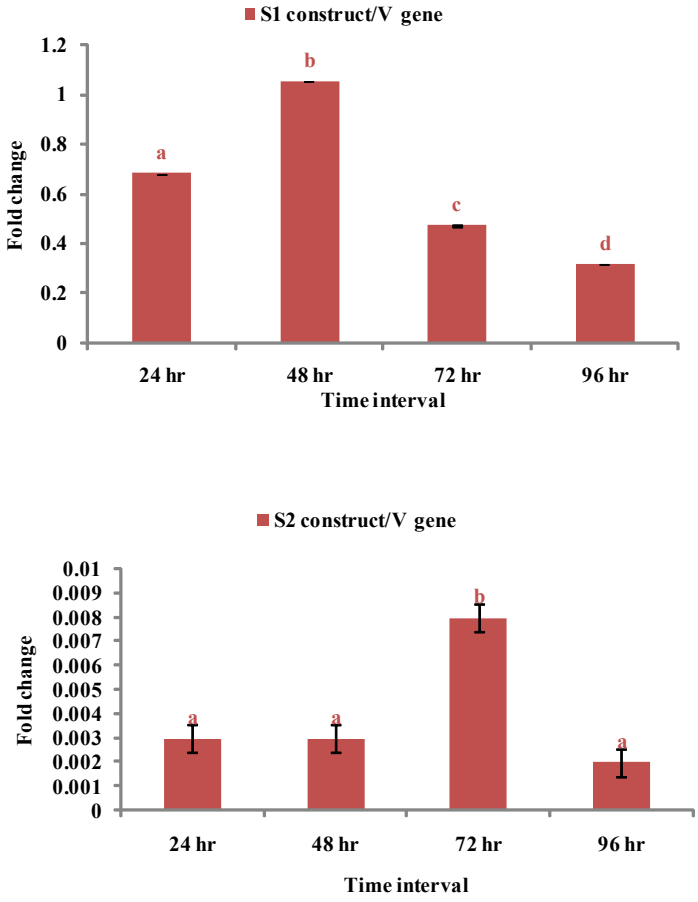

Fig. 4.28: Kinetics of S1 construct/V gene and S2 construct/Vgene mRNA in B95a transfected and co-transfected cells respectively

Table 4.15: Kinetics of S3 Construct/V gene and S1 Construct /V gene mRNA in B95a transfected and co-transfected cells respectively. Data are presented as the fold increases in mRNA levels.

Time Construct	24 hr	48 hr	72 hr	96 hr	F-value
S3 Construct/ V gene	21.1600[a] ±0.577350	20.6090[a] ±0.577350	20.0700[a] ±0.577350	21.0120[a] ±0.577350	0.776[NS]
S1 Construct/ V gene	0.6790[a] ±0.00058	1.0500[b] ±0.00058	0.4700[c] ±0.00058	0.3150[d] ±0.00058	303617.000**
t- value	35.47*	33.87*	33.94*	34.30*	

a, b, c- within S3 Construct/V gene and S1 Construct /V gene, between different time periods means differ significantly ($p<0.05$)
**Overall significant difference within S1 Construct /V gene ($p<0.01$)
* Significant difference between S3 Construct/V gene and S1 Construct /V gene at the same time period ($p<0.01$)
NS- Overall non-significant difference within S3 Construct/V gene

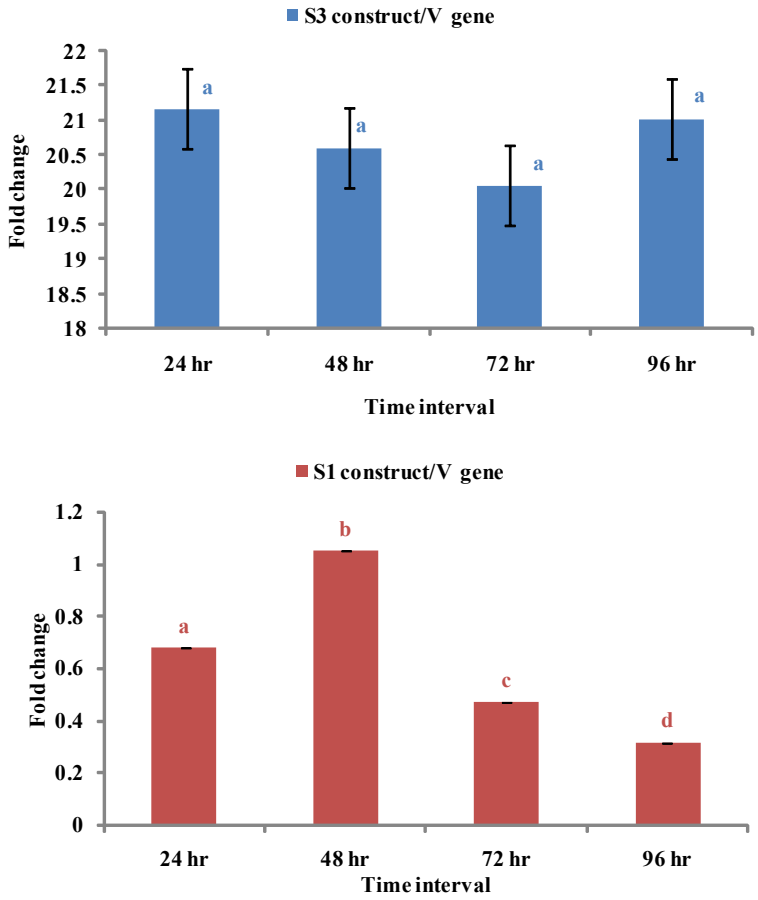

Fig. 4.29: Kinetics of S3 construct/V gene and S1 construct/Vgene mRNA in B95a transfected and co-transfected cells respectively

Table 4.16: Kinetics of S3 Construct/V gene and S2 Construct /V gene mRNA in B95a transfected and co-transfected cells respectively. Data are presented as the fold increases in mRNA levels.

Time Construct	24 hr	48 hr	72 hr	96 hr	F- value
S3 Construct/ V gene	21.1600[a] ±0.577350	20.6090[a] ±0.577350	20.0700[a] ±0.577350	21.0120[a] ±0.577350	0.776[NS]
S2 Construct/ V gene	0.00300[a] ±0.000577	0.00300[a] ±0.000577	0.00800[b] ±0.000577	0.00200[a] ±0.000577	22.000**
t- value	36.64*	35.69*	34.74*	34.84*	

a, b - within S3 Construct/V gene and S2 Construct /V gene, between different time periods means differ significantly ($p<0.05$)
**Overall significant difference within S2 Construct /V gene ($p<0.01$)
* Significant difference between S3 Construct/V gene and S2 Construct /V gene at the same time period ($p<0.01$)
NS- Overall non-significant difference within S3 Construct/V gene

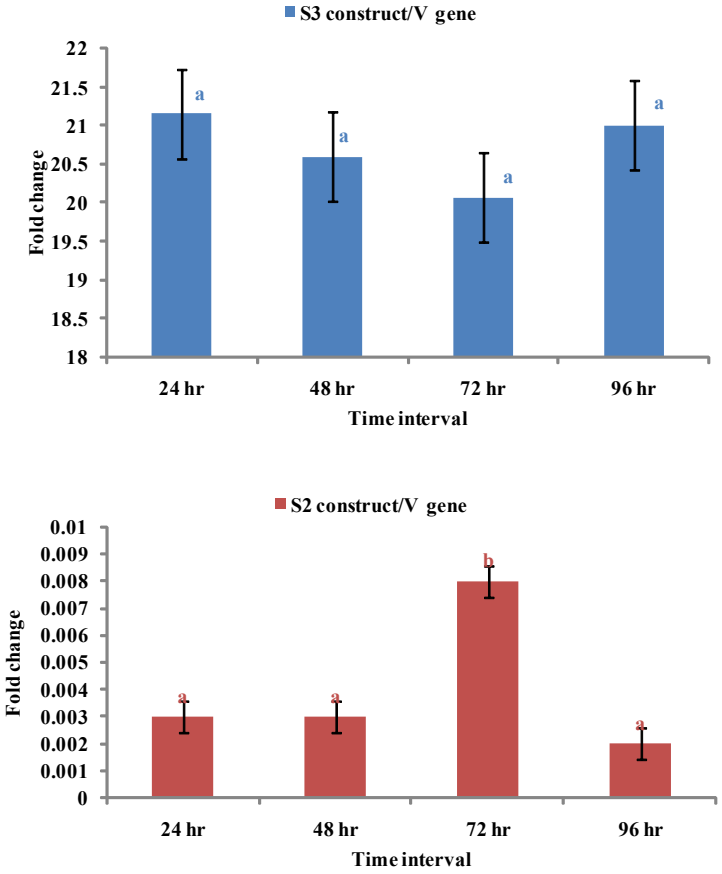

Fig. 4.30: Kinetics of S3 construct/V gene and S2 construct/Vgene mRNA in B95a transfected and co-transfected cells respectively

Table 4.17: Kinetics of S1 Construct/Virus and S2 Construct /Virus mRNA in B95a transfected and co-transfected cells respectively. Data are presented as the fold increases in mRNA levels.

Time Construct	24 hr	48 hr	72 hr	96 hr	F- value
S1 Construct/ Virus	0.19800^{a} ±0.000577	0.47000^{b} ±0.000577	0.31500^{c} ±0.000577	0.10400^{d} ±0.000577	74752.750**
S2 Construct/ Virus	0.00567^{a} ±0.000882	0.00700^{a} ±0.001528	0.00567^{a} ±0.001764	0.00433^{a} ±0.000667	0.711^{NS}
t- value	182.46*	283.52*	166.67*	113.01*	

a, b, c, d- within S1 Construct/Virus and S2 Construct /Virus, between different time periods means differ significantly ($p<0.05$)
**Overall significant difference within S1 Construct/Virus ($p<0.01$)
* Significant difference between S1 Construct/Virus and S2 Construct /Virus at the same time period ($p<0.01$)
NS- Overall non-significant difference within S2 Construct /Virus

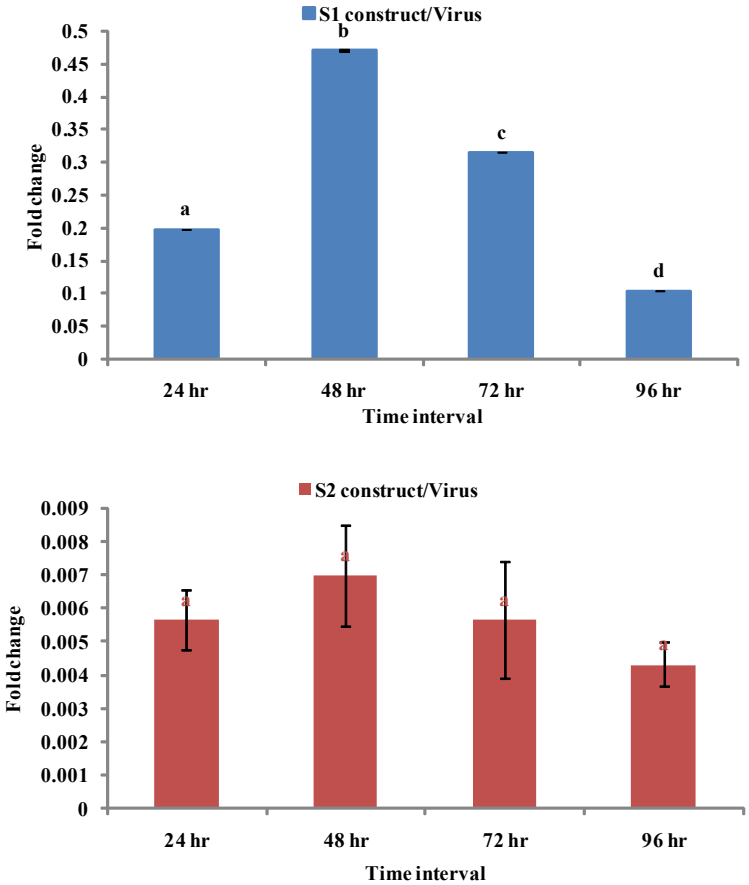

Fig. 4.31: Kinetics of S3 construct/V gene and S2 construct/Vgene mRNA in B95a transfected and co-transfected cells respectively

Table 4.18: Kinetics of S3 Construct/Virus and S1 Construct /Virus mRNA in B95a transfected and co-transfected cells respectively. Data are presented as the fold increases in mRNA levels.

Time Construct	24 hr	48 hr	72 hr	96 hr	F- value
S3 Construct/ Virus	20.1200^{a} ±0.577350	21.0120^{a} ±0.577350	22.0466^{a} ±0.3333	20.7766^{a} ±0.3333	2.87^{NS}
S1 Construct/ Virus	0.19800^{a} ±0.000577	0.47000^{b} ±0.000577	0.31500^{c} ±0.000577	0.10400^{d} ±0.000577	74752.750**
t- value	34.50*	35.58*	65.19*	62.01*	

a, b, c, d- within S3 Construct/Virus and S1 Construct /Virus, between different time periods means differ significantly ($p<0.05$)
**Overall significant difference within S3 Construct/Virus ($p<0.01$)
* Significant difference between S1 Construct/Virus and S2 Construct /Virus at the same time period ($p<0.01$)
NS- Overall non-significant difference within S1 Construct /Virus

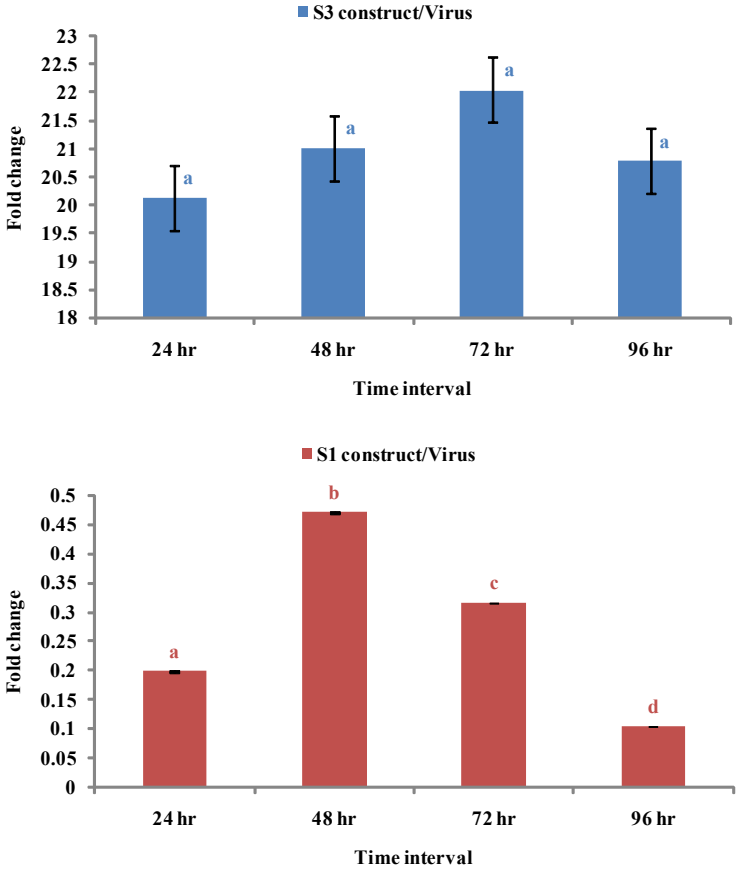

Fig. 4.32: Kinetics of S3 construct/Virus and S1 construct/Virus mRNA in B95a transfected and co-transfected cells respectively

Table 4.19: Kinetics of S3 Construct/Virus and S2 Construct /Virus mRNA in B95a transfected and co-transfected cells respectively. Data are presented as the fold increases in mRNA levels.

Time Construct	24 hr	48 hr	72 hr	96 hr	F-value
S3 Construct/ Virus	20.1200[a] ±0.577350	21.0120[a] ±0.577350	22.0466[a] ±0.3333	20.7766[a] ±0.3333	2.87[NS]
S2 Construct/ Virus	0.00567[a] ±0.000882	0.00700[a] ±0.001528	0.00567[a] ±0.001764	0.00433[a] ±0.000667	0.711[NS]
t- value	34.83*	36.38*	66.12*	62.31*	

a - within S3 Construct/Virus and S2 Construct /Virus, between different time periods means differ significantly ($p<0.05$)
**Overall significant difference within S3 Construct/Virus ($p<0.01$)
* Significant difference between S3 Construct/Virus and S2 Construct /Virus at the same time period ($p<0.01$)
NS- Overall non-significant difference within S2 Construct /Virus

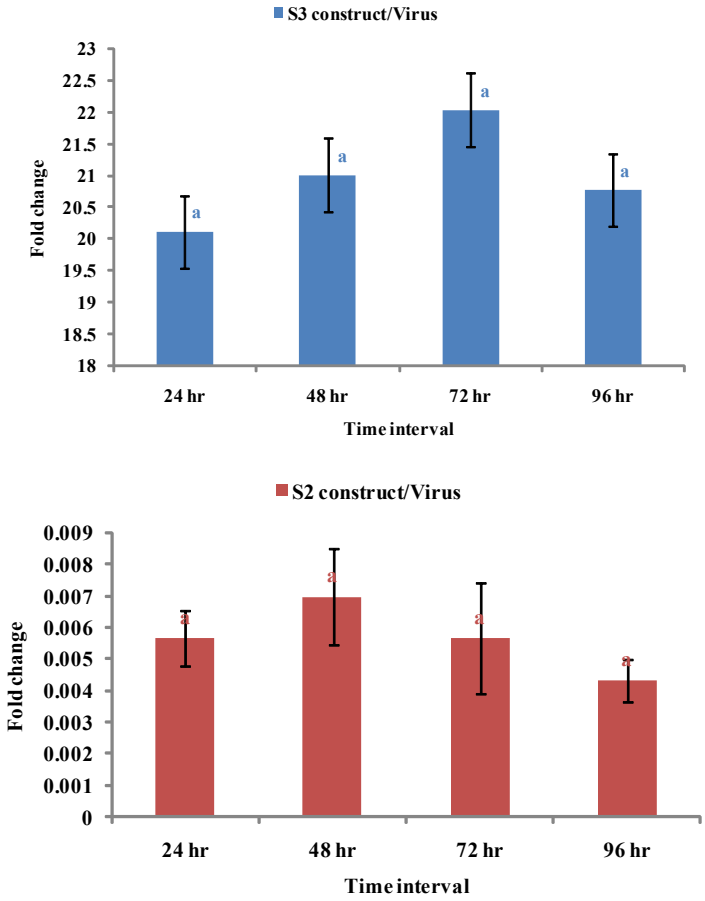

Fig. 4.32: Kinetics of S3 construct/Virus and S1 construct/Virus mRNA in B95a transfected and co-transfected cells respectively

Table 4.20: Percentage silencing after siRNA construct(s) transfection in B95a cells. The expression was monitored at various time intervals (24, 48, 72 and 96 hpi).

Construct	hpi	Gene Silencing (%)
S1construct/V gene**	24	32.1±0.057[a]
	48	50±0.088[b]
	72	53±0.057[c]
	96	68.5±0.057[d]
S1construct/Virus **	24	80.2±0.057[a]
	48	53±0.057[b]
	72	68.5±0.057[c]
	96	89.6±0.057[d]
S2 construct/V gene**	24	99.7±0.057[a]
	48	99.7±0.057[a]
	72	99.2±0.057[b]
	96	99.8±0.057[a]
S2 construct/Virus NS	24	99.4±0.088[a]
	48	99.3±0.152[a]
	72	99.4±0.176[a]
	96	99.5±0.066[a]

a,b,c,d- Within gene, between different time periods means differ significantly ($p<0.05$)
**Overall significant difference within a gene ($p<0.01$)
NS Overall no significant difference within a gene

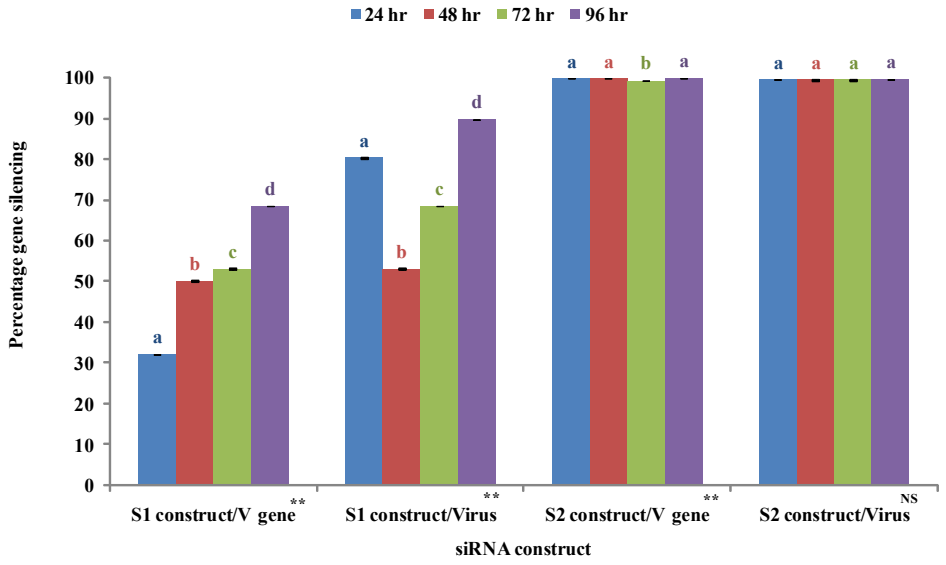

Fig. 4.34: The percentage gene silencing (% Knockdown) compared with B95a cells co-transfected with plasmid-S1/plasmid-S2 construct with plasmid- V protein coding region of the P gene and with infection with PPRV @0.01 moi.

24, 48, 72, and 96 hpi with respect to V protein coding region of the P gene expression (Table 4.6).

The % Knockdown for siRNA construct(s) was calculated using the formulae

% Knockdown =100 * (1-fold change) where fold change = $2^{-\Delta\Delta CT}$.

The % knockdown in B95a cells cotransfected with plasmid-S1 construct and plasmid-V protein coding region of the P gene steadily increased from 24 hpi through 96 hpi (Fig 4. 34) and was significantly different ($p<0.05$).A similar pattern in knockdown was seen in B95a cells transfected with plasmid-S1 construct and PPRV@0.01 moi (Table 4.20).

The % knockdown in B95a cells cotransfected with plasmid-S2 construct and plasmid-V protein coding region of the P gene steadily increased from 24 hpi through 96 hpi (Fig 4. 34).The % knockdown was significantly different ($p<0.05$) at 72 hpi whereas no significant difference was recorded at 24, 48, and 96 hpi (Table 4.20).No significant difference ($p<0.05$) was seen in B95a cells transfected with plasmid-S1 construct and PPRV@0.01 moi.

4.11 Time course studies of cytokine gene expression

In order to define and compare the kinetics, the relative expression of four cytokine genes (IL-2, IL-4, IFN-γ, and IL-10) in the B95a cells were quantified and compared by real time qPCR at each time point i.e. 0 hr (unstimulated), 24 hr, 48 hr, 72 hr and 96 hr after transfection/cotransfection/viral infection. The same protocol as in 4.10.1 was followed to report results in terms of fold increase in cytokine transcripts at different time intervals compared with the levels in unstimulated B95a cells (0 hpi). Despite, repeated attempts the B95a cells failed to secret cytokines (Fig 4.35) whereas the expression of GAPDH was well documented (Fig 4.36).

4.12 The measurement of Caspase 3/7, 8, 9 activities

The Caspase 3 activity was measured in luminescence (RLU; Relative luminescence units) (Table 4.21-4.41). The time course activity studies revealed that the Caspase 3 activity in B95a cells increased progressively from 24 to 96 hpi of transfection with plasmid-S2 construct and Caspase 3 activity peaked at 72 hpi (Fig 4.38). The Caspase 3 activity was significantly

different ($p<0.05$) between 24 and 72 hpi whereas no significant difference ($p>0.05$) was observed between 24 and 48 hpi as well as between 72 and 96 hpi (Table 4.22). The Caspase 3 activity in B95a cells increased progressively from 24 to 96 hpi of transfection with plasmid-V protein coding region of the P gene (Fig 4.40). The Caspase 3 activity was significantly different ($p<0.05$) between 24, 48 and 96 hpi whereas no significant difference ($p>0.05$) was observed between 48 and 72 hpi as well as between 72 and 96 hpi (Table 4.24).When cotransfected with plasmid-S2 and plasmid- V protein coding region of the P gene the Caspase 3 activity peaked at 48 hpi (Fig 4.41). The Caspase 3 activity was significantly different ($p<0.05$) between 24 and 48 hpi as well as 72 and 96 hpi whereas no significant difference ($p>0.05$) was observed between 24 and 96 hpi as well as between 48 and 72 hpi (Table 4.25).The Caspase 3 activity in B95a cells transfected with plasmid-S2 construct and infection with PPRV @0.01moi peaked at 48 hpi (Fig 4.42). No significant difference ($p<0.05$) was observed between 24, 48,72 and 96 hpi (Table 4.26).The cells infected with PPRV showed a steady increase in Caspase 3 activity and peaked at 72 hpi (Fig 4.43). No significant difference ($p<0.05$) was observed between 24, 48, 72 and 96 hpi (Table 4.27).

The Caspase 8 activity was measured in luminescence (RLU; Relative luminescence units) (Table 4.42-4.62). The time course activity studies revealed that the Caspase 8 activity in B95a cells increased progressively from 24 to 96 hpi of transfection with plasmid-S2 construct and Caspase 8 activity peaked at 96 hpi (Fig 4.59). The Caspase 8 activity was significantly different ($p<0.05$) between 24, 48,72 and 96 hpi (Table 4.44). The Caspase 8 activity in B95a cells increased progressively from 24 to 96 hpi of transfection with plasmid- V protein coding region of the P gene and peaked at 96 hpi (Fig 4.61). The Caspase 8 activity was significantly different ($p<0.05$) between 24, 48, 72 and 96 hpi (Table 4.46). When cotransfected with plasmid-S2 and plasmid- V protein coding region of the P gene the Caspase 8 activity peaked at 96 hpi (Fig 4.62). The Caspase 8 activity was significantly different ($p<0.05$) between 24, 48, 72 and 96 hpi (Table 4.47). The Caspase 8 activity in B95a cells transfected with plasmid-S2 construct and infection with PPRV @0.01 moi peaked at 96 hpi (Fig 4.63). The Caspase 8 activity was significantly different ($p<0.05$) between 24, 48, 72 and 96 hpi (Table 4.48).The cells infected with PPRV showed a steady increase in Caspase 8 activity and peaked

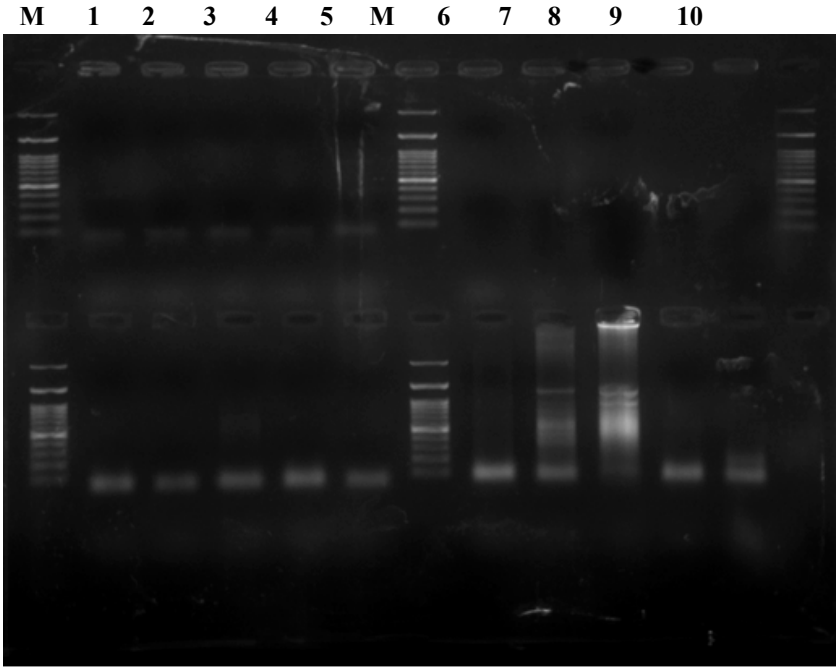

Fig. 4.35: Non-specific amplification of each primer set of cytokine gene transcripts.
Lane M : 100 Kb plus ladder
Lanes 1-5 : IL-2 (above), IL-4(below)
Lanes 6-10 : IFN-γ (above), IL-10 (below)

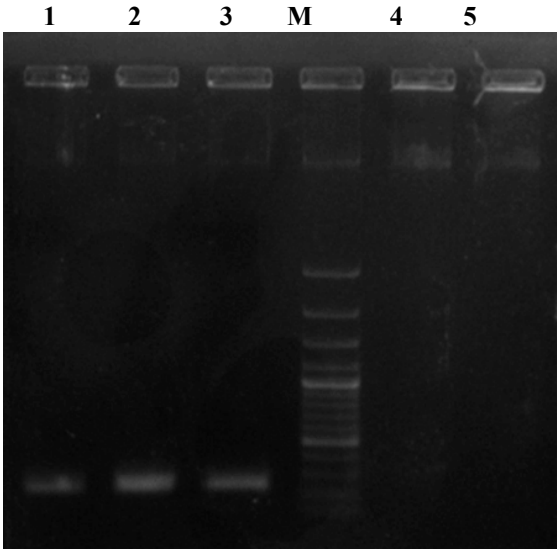

Fig. 4.36: Specific amplification of primer set of GAPDH gene transcripts.
Lane M : 100 Kb plus ladder
Lanes 1-3 : GAPDH (129 bp)

at 96 hpi (Fig 4.64). The Caspase 8 activity was significantly different ($p<0.05$) between 24, 48, 72 and 96 hpi (Table 4.49).

The Caspase 9 activity was measured in luminescence (RLU; Relative luminescence units) (Table 4.63-4.83). The time course activity studies revealed that the Caspase 9 activity in B95a cells increased progressively from 24 to 96 hpi of transfection with plasmid-S2 construct and Caspase 9 activity peaked at 96 hpi (Fig 4.77). The Caspase 9 activity was significantly different ($p<0.05$) between 24 and 72 hpi as well as 48 and 72 hpi whereas no significant difference between 24 and 48 hpi as well as 72 and 96 hpi (Table 4.64). The Caspase 9 activity in B95a cells increased progressively from 24 to 96 hpi of transfection with plasmid- V protein coding region of the P gene and peaked at 96 hpi (Fig 4.79). The Caspase 9 activity was significantly different ($p<0.05$) between 24 and 96 hpi whereas no significant difference between 24 ,48 and 72 hpi (Table 4.67). When cotransfected with plasmid-S2 and plasmid-V protein coding region of the P gene the Caspase 9 activity peaked at 72 hpi (Fig 4.85). The Caspase 9 activity was significantly different ($p<0.05$) between 24 and 48 hpi whereas no significant difference between 48, 72 and 96 hpi (Table 4.73). The Caspase 9 activity in B95a cells transfected with plasmid-S2 construct and infection with PPRV @0.01moi peaked at 96 hpi (Fig 4.86). The Caspase 9 activity was significantly different ($p<0.05$) between 24 and 72 hpi as well as 48 and 72 hpi whereas no significant difference between 24 and 48 hpi as well as 72 and 96 hpi (Table 4.74). The cells infected with PPRV showed a steady increase in Caspase 9 activity and peaked at 96 hpi (Fig 4.87). The Caspase 9 activity was significantly different ($p<0.05$) between 24, 72 and 96 hpi whereas no significant difference was seen between 24 and 48 hpi (Table 4.75)

Table 4.21: Caspase-Glo 3/7 assay analyses for caspase-3 expression in positive and negative controls. The RLUs were recorded for different time intervals post treatment

Time Construct	24 hr	48 hr	72 hr	96 hr	F-value
Positive	132427.59^{a} ±4733.76	117166.06^{ba} ±23282.15	80838.25^{b} ±3225.45	83177.82^{b} ±2951.32	4.45^{NS}
Negative	302.95^{a} ±16.56	275.30^{a} ±60.51	277.99^{a} ±11.12	266.66^{a} ±25.59	0.20^{NS}
t- value	27.91*	5.02*	24.97*	28.09*	

a, b - within positive and negative controls, between different time periods means differ significantly ($p<0.05$)
NS- Overall non-significant difference within positive and negative controls
* Significant difference between the positive and negative controls at the same time period ($p<0.05$)

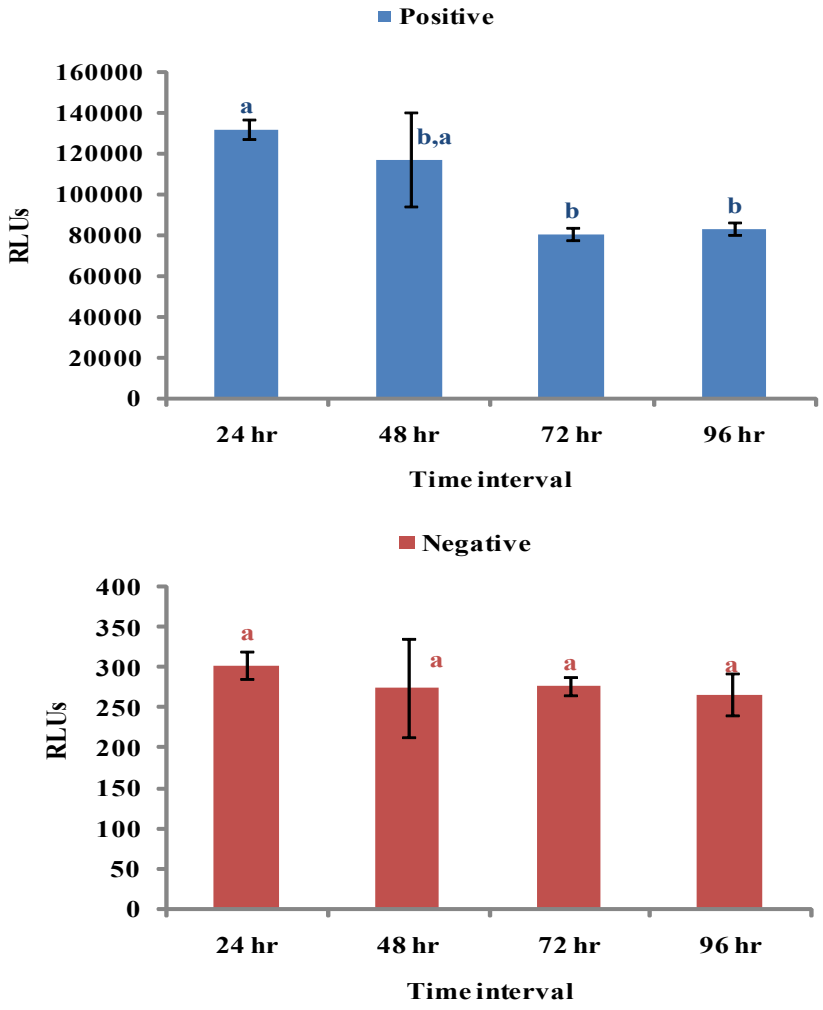

Fig. 4.37: Caspase-3 expression in positive and negative controls.
The RLUs were recorded for different time intervals post treatment

Table 4.22: Caspase-Glo 3/7 assay analyses for caspase-3 expression in B95a cells transfected with S2 construct and positive control. The RLUs were recorded for different time intervals

Time / Construct	24 hr	48 hr	72 hr	96 hr	F-value
S2	69549.42[a] ±485.99	77610.64[a,b] ±454.53	135887.74[c] ± 18289.87	116053.03[b,c] ±10466.04	8.91**
Positive	132427.59[a] ±4733.76	117166.06[b,a] ±23282.15	80838.25[b] ±3225.45	83177.82[b] ±2951.32	4.45[NS]
t- value	-13.21*	-1.69NS'	2.96NS'	3.02NS'	

a, b,c - within S2 construct and positive control, between different time periods means differ significantly ($p<0.05$)
**Overall significant difference within S2 construct ($p<0.05$)
NS- Overall non-significant difference within positive control
* Significant difference between the S2 construct and positive control at the same time period ($p<0.05$)
NS' No Significant difference between the S2 construct and positive control at the same time period

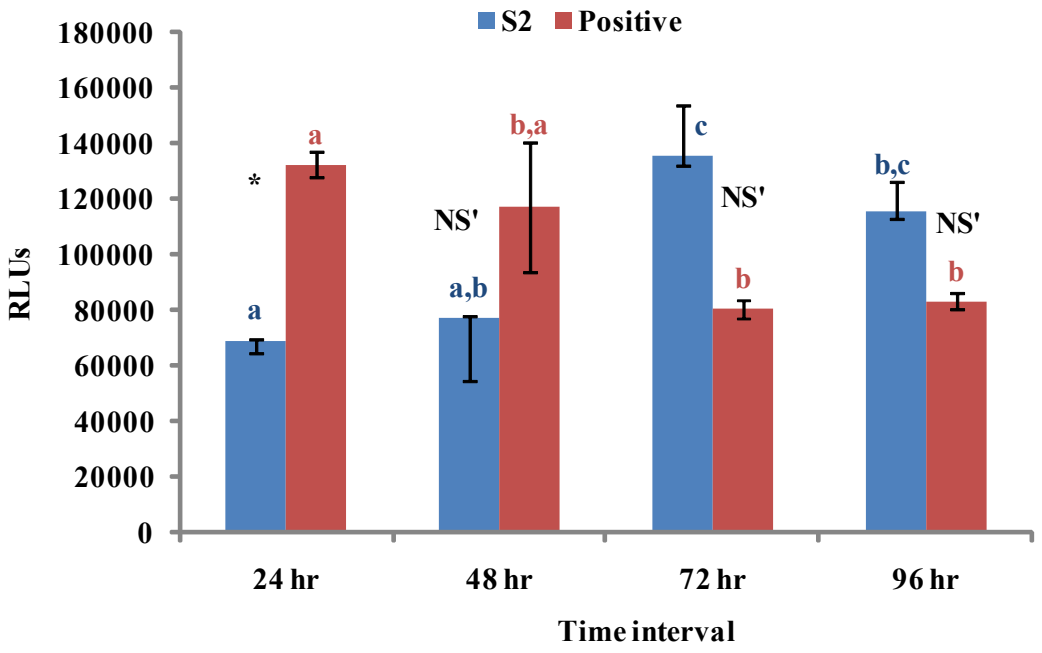

Fig. 4.38: Caspase-3 expression in B95a cells transfected with S2 construct and positive control.
The RLUs were recorded for different time intervals post treatment

Table 4.23: Caspase-Glo 3/7 assay analyses for caspase-3 expression in B95a cells transfected with S2 construct and negative control. The RLUs were recorded for different time intervals

Time / Construct	24 hr	48 hr	72 hr	96 hr	F-value
S2	69549.42[a] ±485.99	77610.64[a,b] ±454.53	135887.74[c] ± 18289.87	116053.03[b,c] ±10466.04	8.91**
Negative	302.95[a] ±16.56	275.30[a] ±60.51	277.99[a] ±11.12	266.66[a] ±25.59	0.20NS
t- value	142.40***	168.65***	7.41*	11.06***	

a, b,c - within S2 construct and negative control, between different time periods means differ significantly ($p<0.05$)
**Overall significant difference within S2 construct ($p<0.05$)
*** Significant difference between the S2 construct and negative control at the same time period ($p<0.01$)
* Significant difference between the S2 construct and negative control at the same time period ($p<0.05$)
NS- Overall non-significant difference within negative control

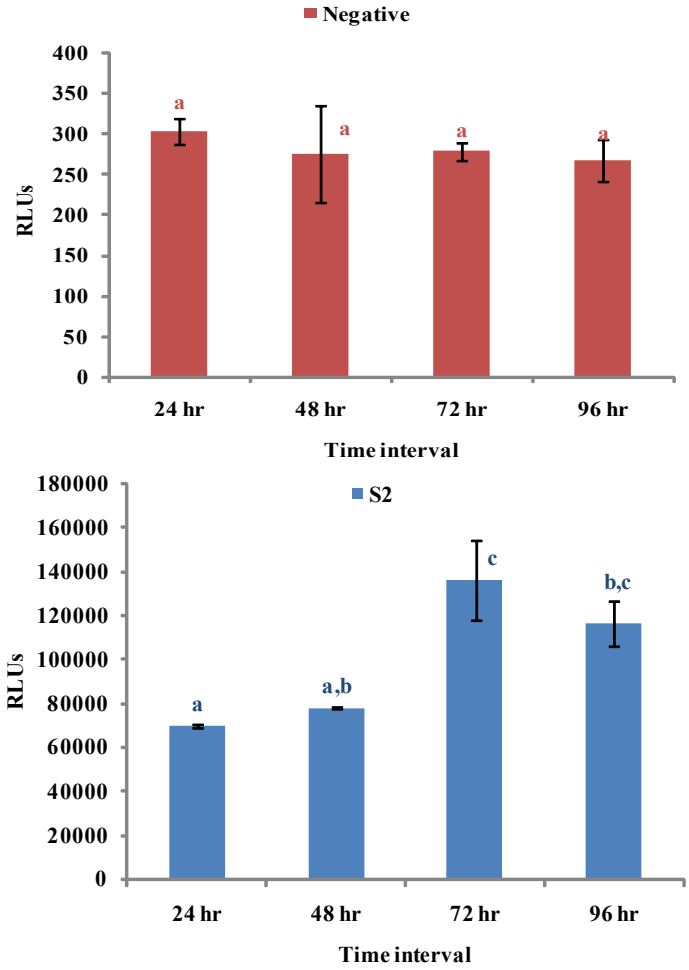

Fig. 4.39: Caspase-3 expression in B95a cells transfected with S2 construct and negative control.

The RLUs were recorded for different time intervals post treatment

Table 4.24: Caspase-Glo 3/7 assay analyses for caspase-3 expression in B95a cells transfected with S2 construct and B95a cells transfected with V gene construct. The RLUs were recorded for different time intervals

Time / Construct	24 hr	48 hr	72 hr	96 hr	F-value
S2	69549.42[a] ±485.99	77610.64[a,b] ±454.53	135887.74[c] ± 18289.87	116053.03[b,c] ±10466.04	8.91*
V gene	45831.33[a] ±60.97	69300.54[b] ±136.04	87252.11[b,c] ±8116.08	101970.06[c] ±6090.45	22.73**
t- value	48.42***	17.51***	2.43NS	1.16[NS]	

a,b,c - within S2 construct and V gene, between different time periods means differ significantly ($p<0.05$)
*Overall significant difference within S2 construct ($p<0.05$)
**significant difference within V gene ($p<0.01$)
*** Significant difference between the S2 construct and V gene at the same time period ($p<0.01$)
NS No Significant difference between the S2 construct and V gene at the same time period

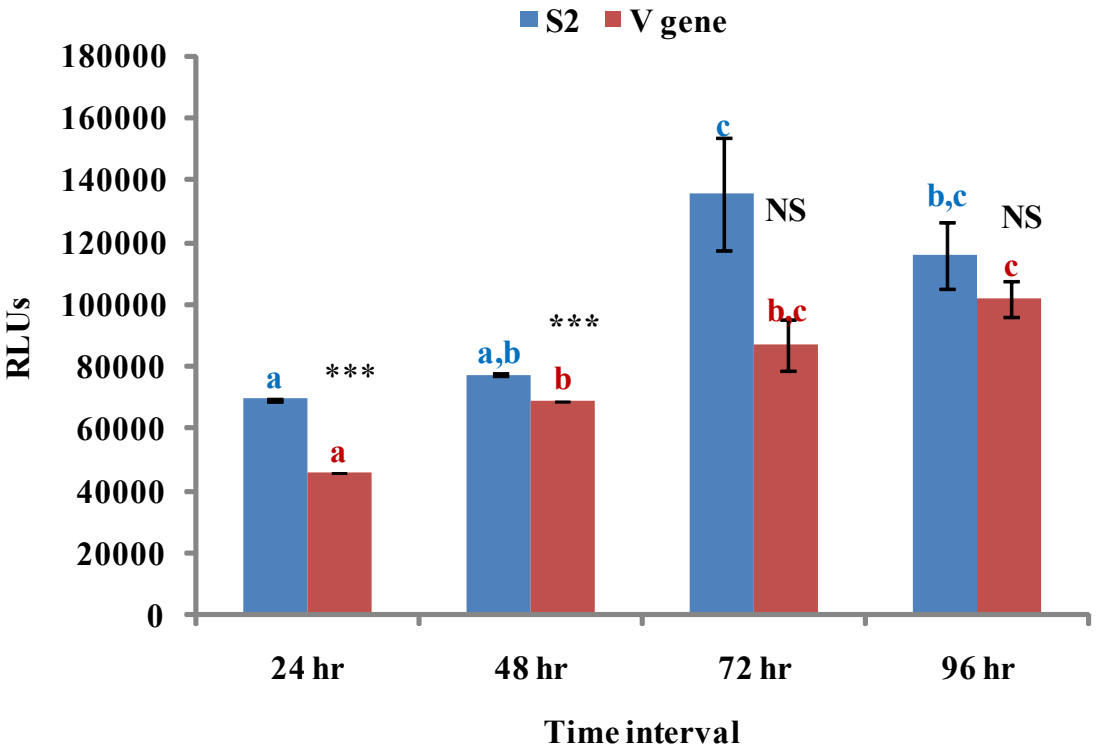

Fig. 4.40: Caspase-3 expression in B95a cells transfected with S2 construct and V gene construct.
The RLUs were recorded for different time intervals post treatment

Table 4.25: Caspase-Glo 3/7 assay analyses for caspase-3 expression in B95a cells transfected with S2 construct and B95a cells co-transfected with S2/V gene construct. The RLUs were recorded for different time intervals

Time Construct	24 hr	48 hr	72 hr	96 hr	F-value
S2	69549.42[a] ±485.99	77610.64[a,b] ±454.53	135887.74[c] ± 18289.87	116053.03[b,c] ±10466.04	8.91*
S2/V gene	72975.07[a] ±95.29	133737.34[b] ±989.00	122017.99[b] ±17584.33	46386.29[a] ±1535.62	21.64**
t-value	-6.9[A]	-51.56***	0.54[NS]	6.58[NS]	

a,b,c - within S2 construct and S2/V gene, between different time periods means differ significantly ($p<0.05$)
*Overall significant difference within S2 construct ($p<0.05$)
**significant difference within S2/V gene ($p<0.01$)
A Significant difference between the S2 construct and S2/V gene at the same time period ($p<0.05$)
*** Significant difference between the S2 construct and S2/V gene at the same time period ($p<0.01$)
NS No Significant difference between the S2 construct and S2/V gene at the same time period

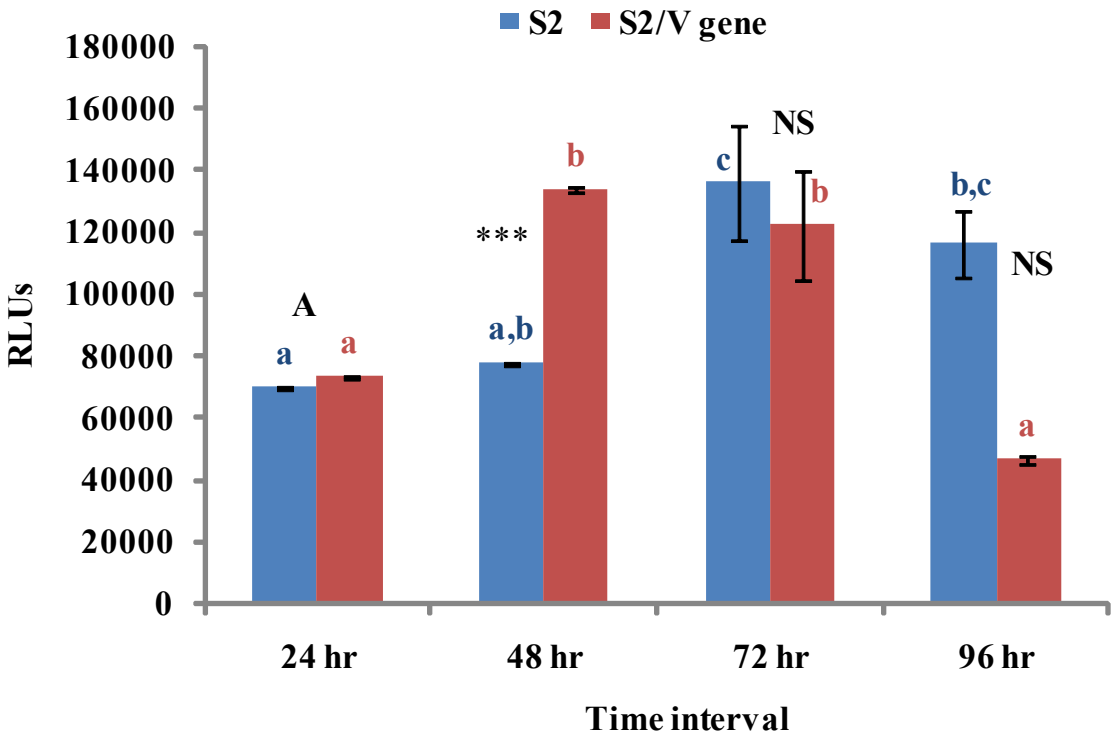

Fig. 4.41: Caspase-3 expression in B95a cells transfected with S2 construct and B95a cells co-transfected with S2/V gene construct.
The RLUs were recorded for different time intervals post treatment

Table 4.26: Caspase-Glo 3/7 assay analyses for caspase-3 expression in B95a cells transfected with S2 construct and B95a cells co-transfected with S2/Virus construct. The RLUs were recorded for different time intervals

Time Construct	24 hr	48 hr	72 hr	96 hr	F- value
S2	69549.42[a] 485.99	77610.64[a,b] ±454.53	135887.74[c] ± 18289.87	116053.03[b,c] ±10466.04	8.91*
S2/Virus	99593.82[a] ±493.03	123328.93[a] ±228.90	113753.33[a] ±18134.56	94167.35[a] ±4934.27	1.99NS
t- value	-43.39**	-89.83**	0.85[NS']	1.89[NS']	

a, b, c - within S2 construct and S2/Virus, between different time periods means differ significantly ($p<0.05$)
*Overall significant difference within S2 construct ($p<0.05$)
NS- Overall non-significant difference within S2/Virus
** Significant difference between the S2 construct and S2/Virus at the same time period ($p<0.01$)
NS' No Significant difference between the S2 construct and positive control at the same time period

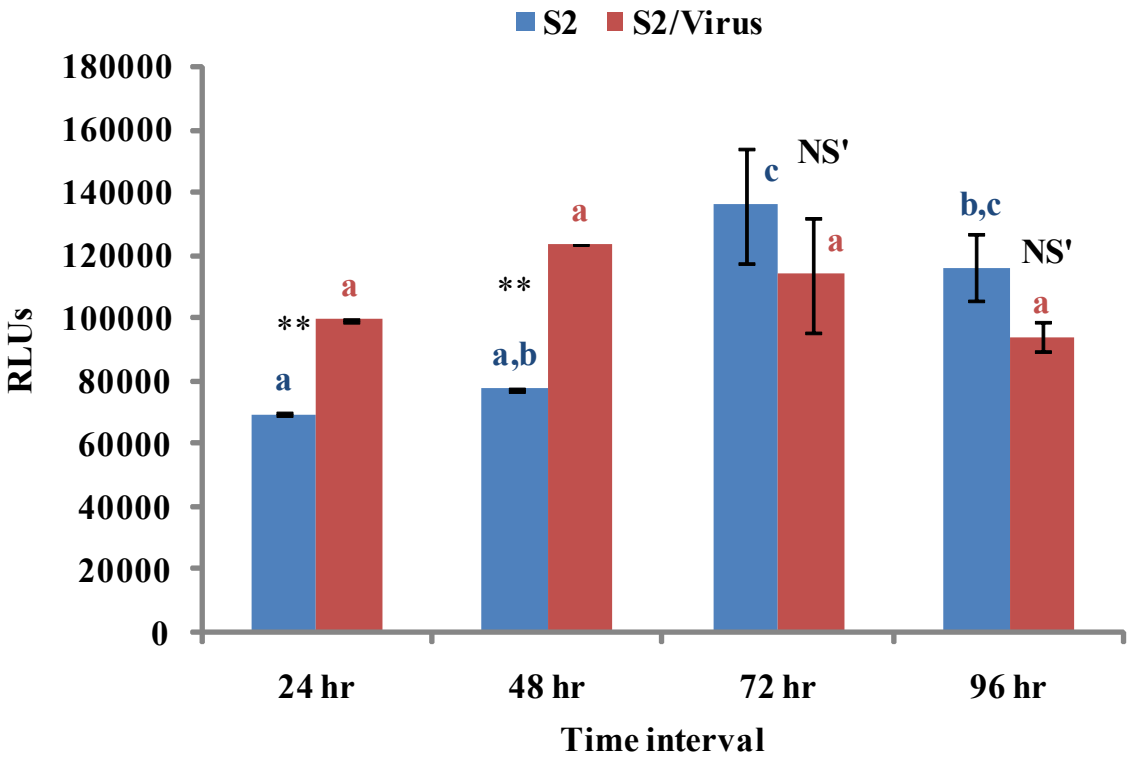

Fig. 4.42: Caspase-3 expression in B95a cells transfected with S2 construct and B95a cells co-transfected with S2/Virus.
The RLUs were recorded for different time intervals post treatment

Table 4.27: Caspase-Glo 3/7 assay analyses for caspase-3 expression in B95a cells transfected with S2 construct and B95a cells infected with virus. The RLUs were recorded for different time intervals

Time / Construct	24 hr	48 hr	72 hr	96 hr	F-value
S2	69549.42[a] ±485.99	77610.64[a,b] ±454.53	135887.74[c] ± 18289.87	116053.03[b,c] ±10466.04	8.91*
Virus	72304.30[a] ±374.81	59998.09[a] ±533.078	73321.91[a] ±3874.40	65402.92[a] ±8717.57	1.71[NS]
t-value	-4.48**	25.14***	3.34[NS']	3.71[NS']	

a, b, c - within S2 construct and Virus, between different time periods means differ significantly ($p<0.05$)
*Overall significant difference within S2 construct ($p<0.05$)
NS No significant difference within Virus
** Significant difference between the S2 construct and Virus at the same time period ($p<0.05$)
*** Significant difference between the S2 construct and Virus at the same time period ($p<0.01$)
NS' No Significant difference between the S2 construct and Virus at the same time period

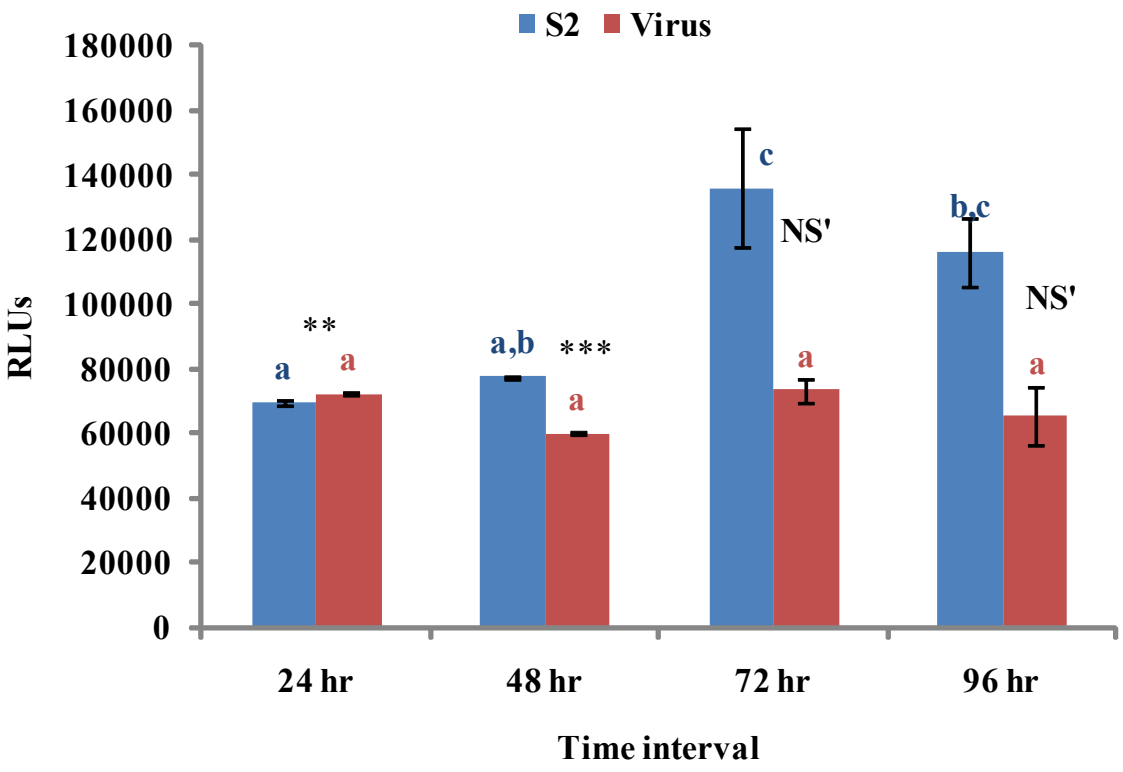

Fig. 4.43: Caspase-3 expression in B95a cells transfected with S2 construct and B95a cells infected with virus.
The RLUs were recorded for different time intervals post treatment

Table 4.28: Caspase-Glo 3/7 assay analyses for caspase-3 expression in B95a cells transfected with V gene construct and positive control. The RLUs were recorded for different time intervals

Time / Construct	24 hr	48 hr	72 hr	96 hr	F-value
V gene	45831.33[a] ±60.97	69300.54[b] ±136.04	87252.11[b,c] ±8116.08	101970.06[c] ±6090.45	22.73*
Positive	132427.59[a] ±4733.76	117166.06[b,a] ±23282.15	80838.25[b] ±3225.45	83177.82[b] ±2951.32	4.45[NS]
t-value	-18.29**	-2.05[NS']	0.073[NS']	2.77[NS']	

a, b, c - within V gene and positive control, between different time periods means differ significantly ($p<0.05$)
*Overall significant difference within V gene ($p<0.01$)
NS- Overall non-significant difference within positive control
** Significant difference between the V gene and positive control at the same time period ($p<0.01$)
NS' No Significant difference between the V gene and positive control at the same time period

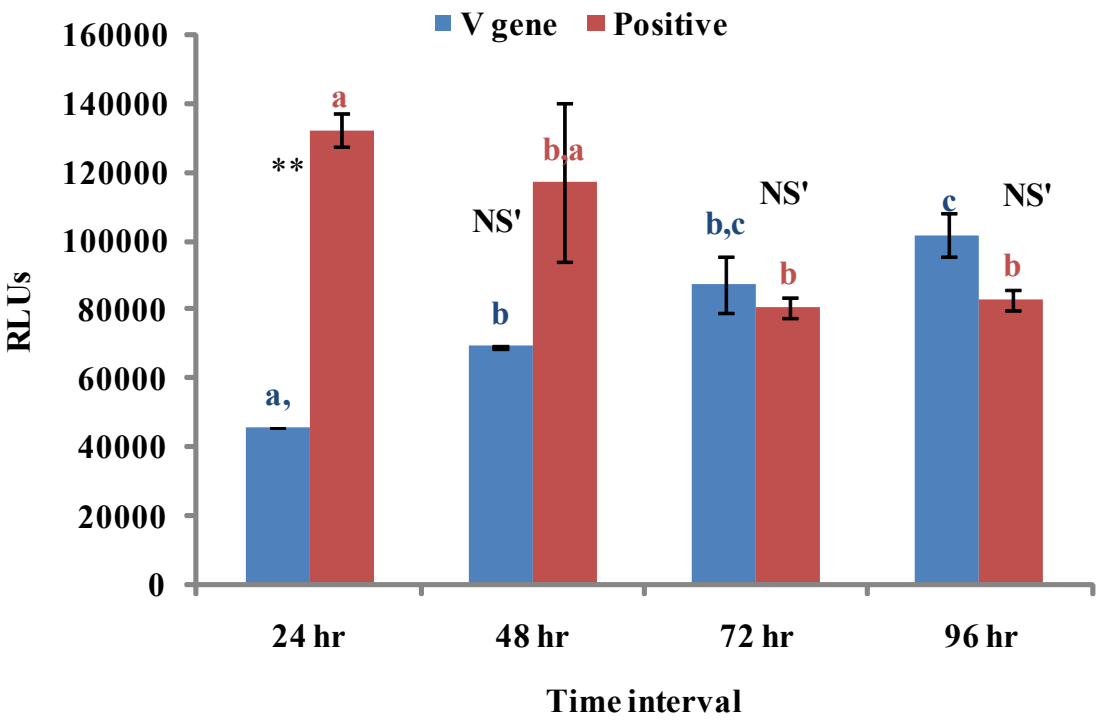

Fig. 4.44: Caspase-3 expression in B95a cells transfected with V gene construct and positive control.
The RLUs were recorded for different time intervals post treatment

Table 4.29: Caspase-Glo 3/7 assay analyses for caspase-3 expression in B95a cells transfected with V gene construct and negative control. The RLUs were recorded for different time intervals

Time Construct	24 hr	48 hr	72 hr	96 hr	F-value
V gene	45831.33[a] ±60.97	69300.54[b] ±136.04	87252.11[b,c] ±8116.08	101970.06[c] ±6090.45	22.73*
Negative	302.95[a] ±16.56	275.30[a] ±60.51	277.99[a] ±11.12	266.66[a] ±25.59	0.20[NS]
t- value	720.52**	463.57**	10.71**	16.69**	

a, b, c - within V gene and negative control, between different time periods means differ significantly ($p<0.05$)
*Overall significant difference within V gene ($p<0.01$)
NS- Overall non-significant difference within negative control
** Significant difference between the V genet and negative control at the same time period ($p<0.01$)

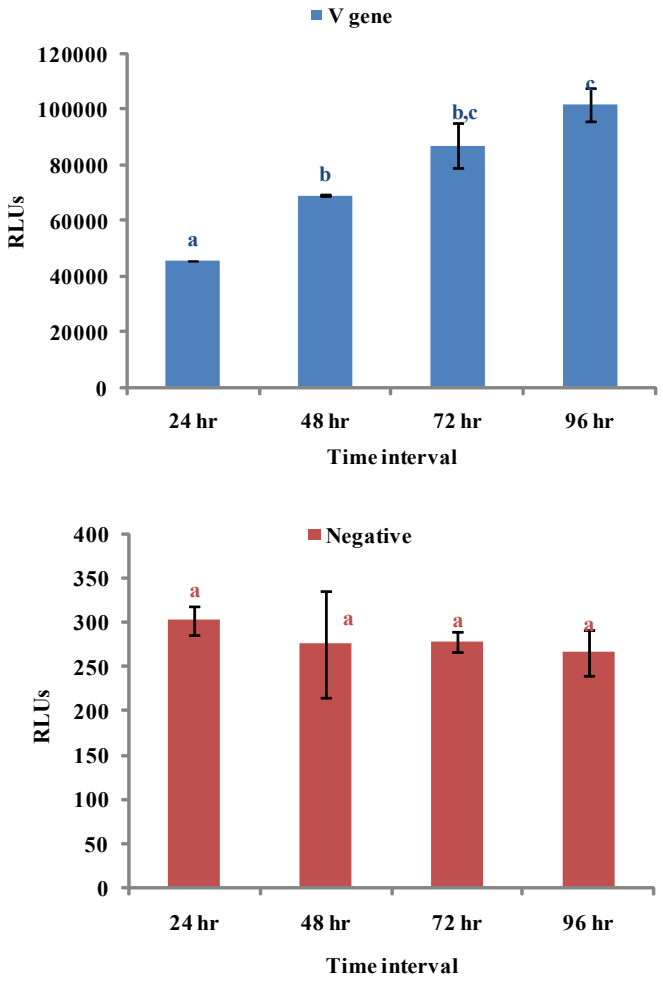

Fig. 4.45: Caspase-3 expression in B95a cells transfected with V gene construct and negative control.
The RLUs were recorded for different time intervals post treatment

Table 4.30: Caspase-Glo 3/7 assay analyses for caspase-3 expression in B95a cells transfected with V gene construct and B95a cells co-transfected with S2/V gene construct. The RLUs were recorded for different time intervals

Time / Construct	24 hr	48 hr	72 hr	96 hr	F-value
V gene	45831.33[a] ±60.97	69300.54[b] ±136.04	87252.11[b,c] ±8116.08	101970.06[c] ±6090.45	22.73*
S2/V gene	72975.07[a] ±95.29	133737.34[b] ±989.00	122017.99[b] ±17584.33	46386.29[a] ±1535.62	21.64*
t-value	-239.92***	-64.54***	-1.79[NS]	8.8**	

a, b, c - within V gene and S2/V gene, between different time periods means differ significantly ($p<0.05$)
*Overall significant difference within V gene and S2/V gene ($p<0.01$)
**Significant difference between the V genet and S2/V gene at the same time period ($p<0.05$)
***Significant difference between the V genet and S2/V gene at the same time period ($p<0.01$)
NS- No Significant difference between the V genet and S2/V gene at the same time period

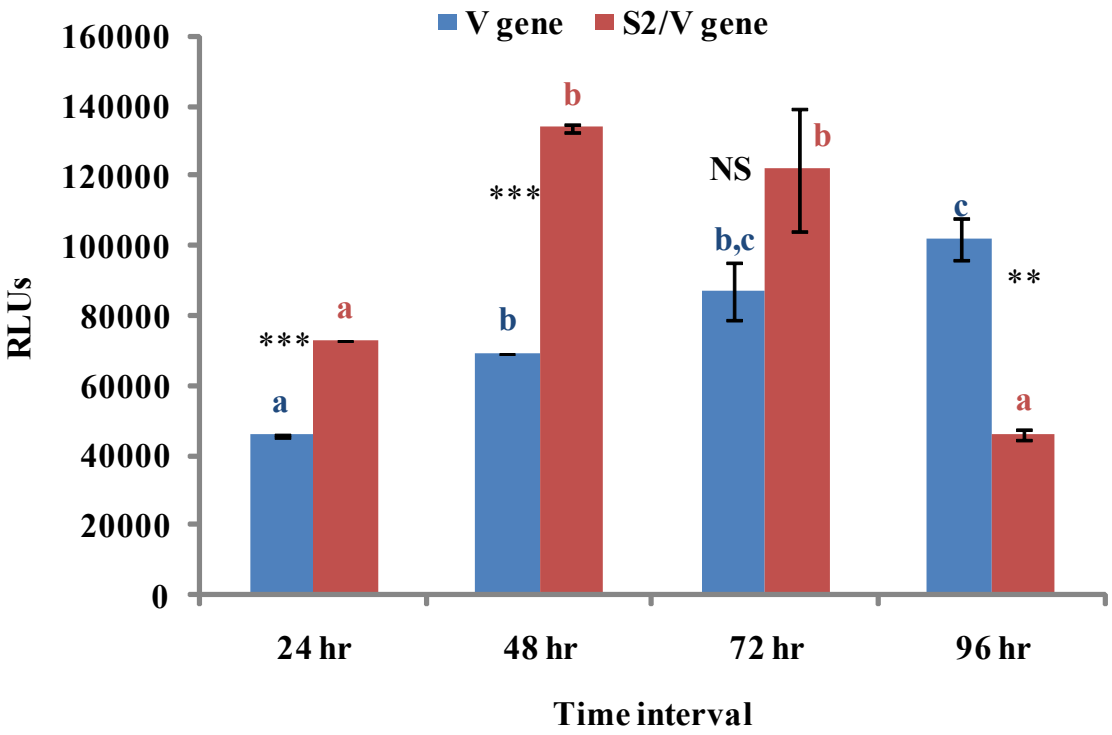

Fig. 4.46: Caspase-3 expression in B95a cells transfected with V gene construct and B95a cells co-transfected with S2/V gene construct.
The RLUs were recorded for different time intervals post treatment

Table 4.31: Caspase-Glo 3/7 assay analyses for caspase-3 expression in B95a cells transfected with V gene construct and B95a cells co-transfected with S2/ Virus construct. The RLUs were recorded for different time interval

Time / Construct	24 hr	48 hr	72 hr	96 hr	F- value
V gene	45831.33[a] ±60.97	69300.54[a] ±136.04	87252.11[b,c] ±8116.08	101970.06[c] ±6090.45	22.73*
S2/Virus	99593.82[a] ±493.03	123328.93[a] ±228.90	113753.33[a] ±18134.56	94167.35[a] ±4934.27	1.99[NS]
t- value	-108.22**	-202.90**	-1.33[NS']	0.99[NS']	

a, b, c - within V gene and S2/Virus, between different time periods means differ significantly ($p<0.05$)
*Overall significant difference within V gene ($p<0.01$)
NS- Overall non-significant difference within S2/Virus
**Significant difference between the V gene and S2/Virus at the same time period ($p<0.01$)
NS' No Significant difference between the V gene and S2/Virus at the same time period

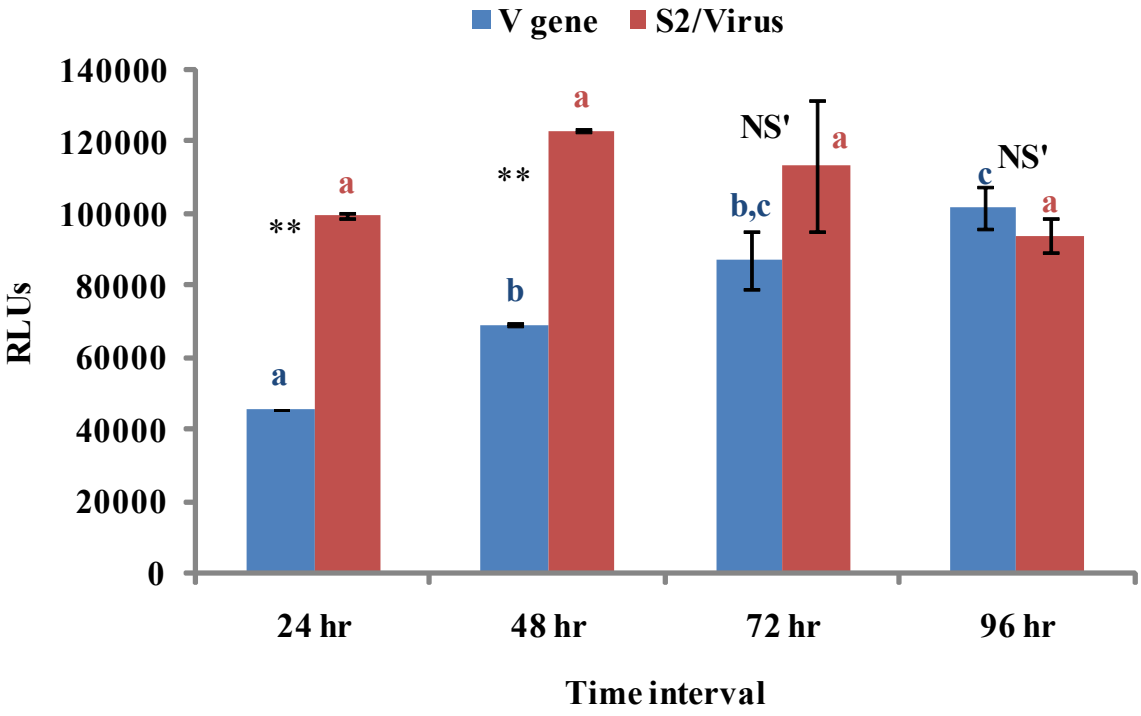

Fig. 4.47: Caspase-3 expression in B95a cells transfected with V gene construct and B95a cells co-transfected with S2/Virus construct.
The RLUs were recorded for different time intervals post treatment

Table 4.32: Caspase-Glo 3/7 assay analyses for caspase-3 expression in B95a cells transfected with V gene construct and B95a cells infected with virus. The RLUs were recorded for different time intervals

Time / Construct	24 hr	48 hr	72 hr	96 hr	F-value
V gene	45831.33^{a} ±60.97	69300.54^{b} ±136.04	$87252.11^{b,c}$ ±8116.08	101970.06^{c} ±6090.45	22.73*
Virus	72304.30^{a} ±374.81	59998.09^{a} ±533.078	73321.91^{a} ±3874.40	65402.92^{a} ±8717.57	1.71^{NS}
t-value	-69.71**	16.90**	$1.54^{NS'}$	$3.43^{NS'}$	

a, b, c - within V gene and S2/Virus, between different time periods means differ significantly ($p<0.05$)
*Overall significant difference within V gene ($p<0.01$)
NS- Overall non-significant difference within S2/Virus
**Significant difference between the V gene and S2/Virus at the same time period ($p<0.01$)
NS' No Significant difference between the V gene and S2/Virus at the same time period

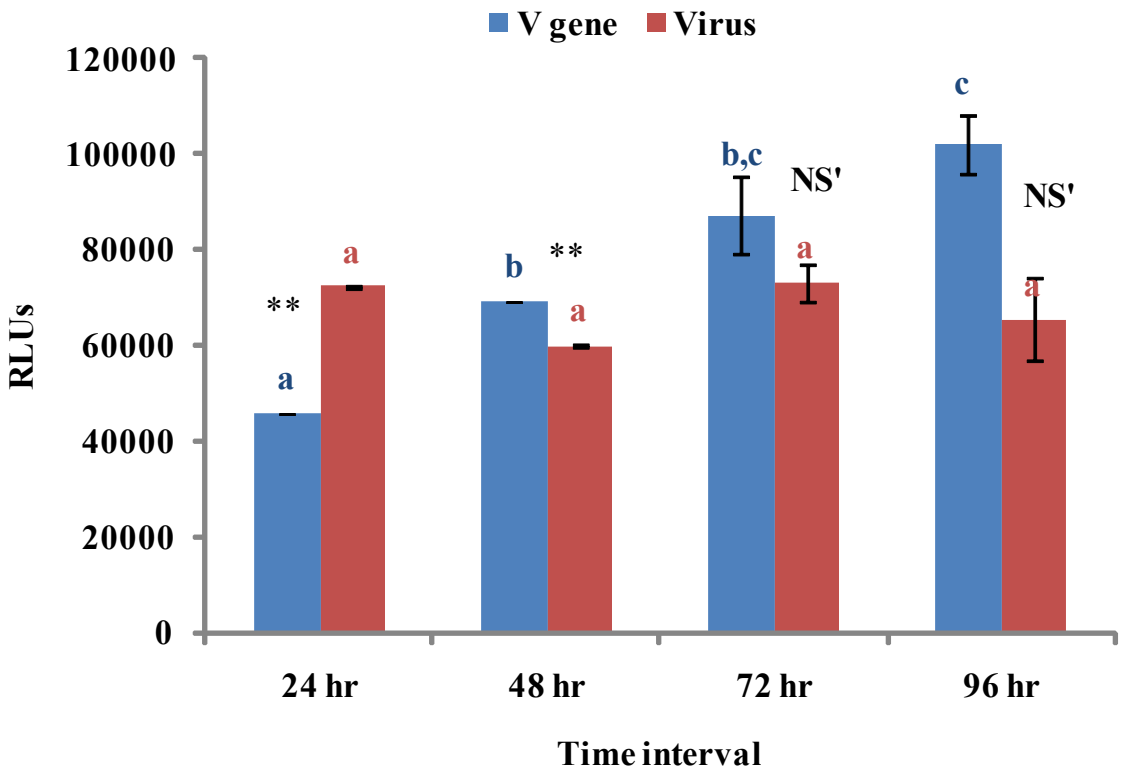

Fig. 4.48: Caspase-3 expression in B95a cells transfected with V gene construct and B95a cells infected with virus.
The RLUs were recorded for different time intervals post treatment

Table 4.33: Caspase-Glo 3/7assay analyses for caspase-3 expression in B95a cells co-transfected with S2/V gene construct and positive control. The RLUs were recorded for different time intervals

Time / Construct	24 hr	48 hr	72 hr	96 hr	F-value
S2/V gene	72975.07[a] ±95.29	133737.34[b] ±989.00	122017.99[b] ±17584.33	46386.29[b] ±1535.62	21.64*
Positive	132427.59[b] ±4733.76	117166.06[b,a] ±23282.15	80838.25[b] ±3225.45	83177.82[b] ±2951.32	4.45[NS]
t-value	-12.55**	0.71[NS']	2.30[NS']	-11.05**	

a, b - within S2/V gene and positive control, between different time periods means differ significantly ($p<0.05$)
*Overall significant difference within S2/V gene ($p<0.01$)
NS- Overall non-significant difference within positive control
**Significant difference between the S2/V gene and positive control at the same time period ($p<0.01$)
NS' No Significant difference between the S2/V gene and positive control at the same time period

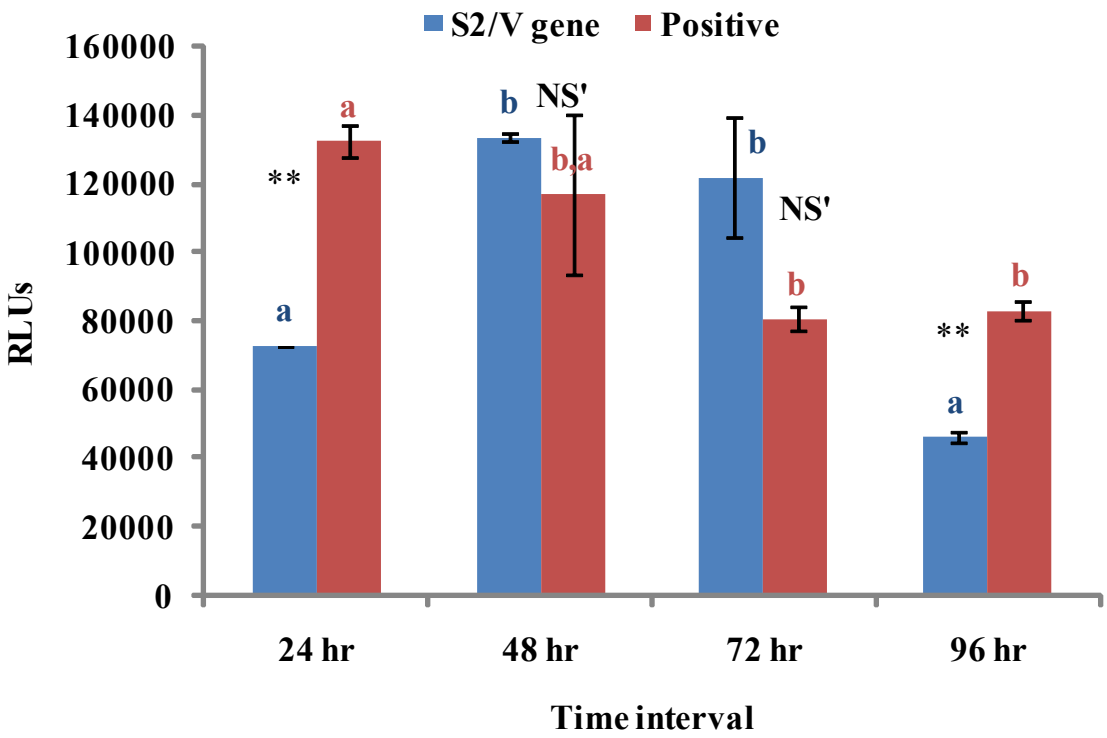

Fig. 4.49: Caspase-3 expression in B95a cells transfected with B95a cells co-transfected with S2/V gene construct and positive control.
The RLUs were recorded for different time intervals post treatment

Table 4.34: Caspase-Glo 3/7 assay analyses for caspase-3 expression in B95a cells co-transfected with S2/V gene construct and negative control. The RLUs were recorded for different time intervals

Time Construct	24 hr	48 hr	72 hr	96 hr	F-value
S2/V gene	72975.07[a] ±95.29	133737.34[b] ±989.00	122017.99[b] ±17584.33	46386.29[a] ±1535.62	21.64*
Negative	302.95[a] ±16.56	275.30[a] ±60.51	277.99[a] ±11.12	266.66[a] ±25.59	0.20[NS]
t-value	751.35***	134.69***	6.92**	30.02***	

a, b - within S2/V gene and negative control, between different time periods means differ significantly ($p<0.05$)
*Overall significant difference within S2/V gene ($p<0.01$)
NS- Overall non-significant difference within negative control
**Significant difference between the S2/V gene and negative control at the same time period ($p<0.05$)
*** Significant difference between the S2/V gene and negative control at the same time period ($p<0.01$)

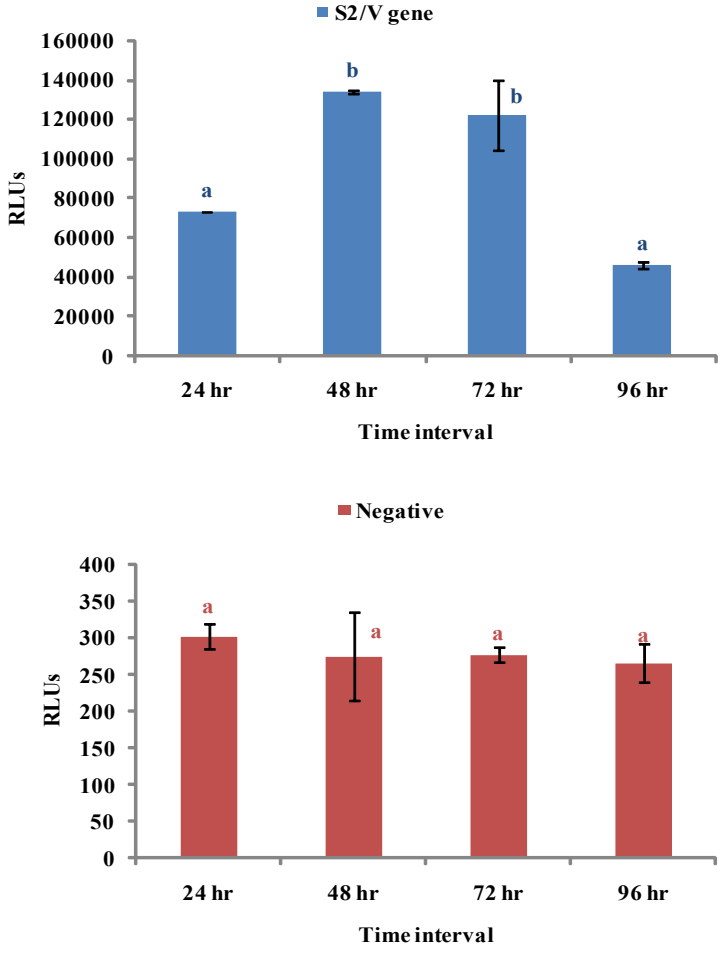

Fig. 4.50: Caspase-3 expression in B95a cells transfected with B95a cells co-transfected with S2/V gene construct and negative control.
The RLUs were recorded for different time intervals post treatment

Table 4.35: Caspase-Glo 3/7assay analyses for caspase-3 expression in B95a cells co-transfected with S2/V gene construct and B95a cells co-transfected with S2/Virus. The RLUs were recorded for different time intervals

Time Construct	24 hr	48 hr	72 hr	96 hr	F-value
S2/V gene	72975.07[a] ±95.29	133737.34[b] ±989.00	122017.99[b] ±17584.33	46386.29[a] ±1535.62	21.64*
S2/Virus	99593.82[a] ±493.03	123328.93[a] ±228.90	113753.33[a] ±18134.56	94167.35[a] ±4934.27	1.99[NS]
t-value	-53.00***	10.25***	0.32[NS']	-9.24**	

a, b - within S2/V gene and S2/Virus, between different time periods means differ significantly ($p<0.05$)
*Overall significant difference within S2/V gene ($p<0.01$)
NS- Overall non-significant difference within S2/Virus
**Significant difference between the S2/V gene and S2/Virus at the same time period ($p<0.05$)
*** Significant difference between the S2/V gene and S2/Virus at the same time period ($p<0.01$)
NS' No Significant difference between the S2/V gene and S2/Virus at the same time period

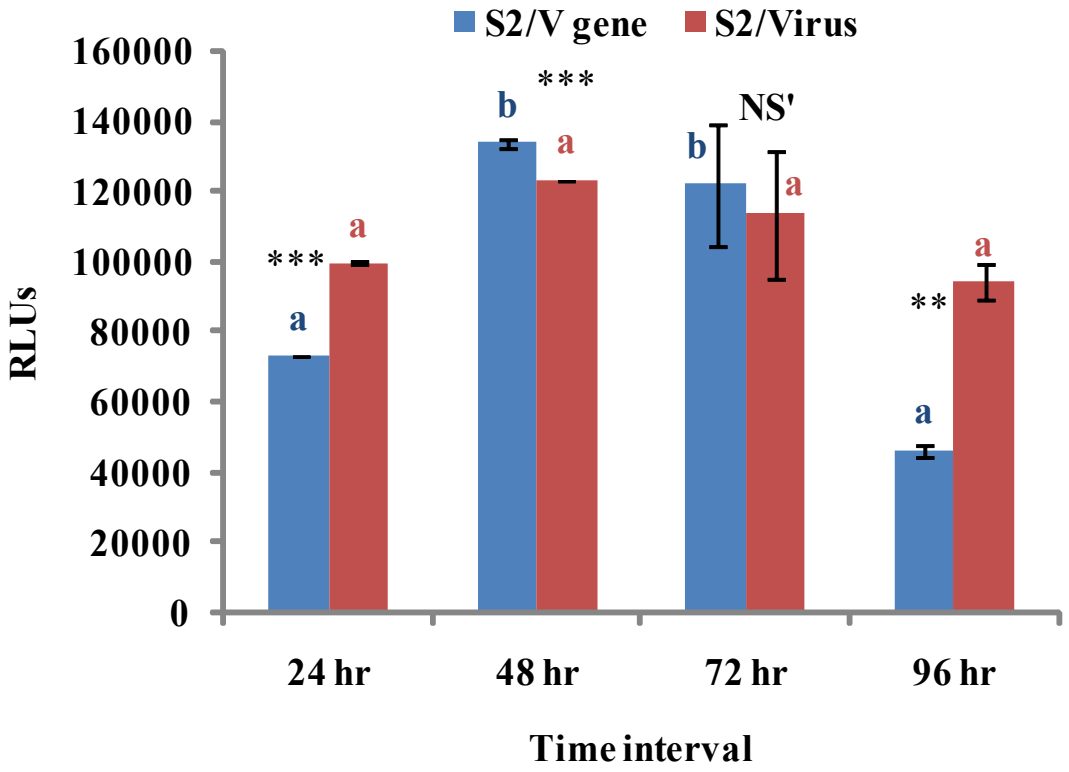

Fig. 4.51: Caspase-3 expression in B95a cells transfected with B95a cells co-transfected with S2/V gene construct and B95a cells co-transfected with S2/Virus.

The RLUs were recorded for different time intervals post treatment

Table 4.36: Caspase-Glo 3/7 assay analyses for caspase-3 expression in B95a cells co-transfected with S2/V gene construct and B95a cells infected with Virus. The RLUs were recorded for different time intervals

Time Construct	24 hr	48 hr	72 hr	96 hr	F-value
S2/V gene	72975.07[a] ±95.29	133737.34[b] ±989.00	122017.99[b] ±17584.33	46386.29[a] ±1535.62	21.64*
Virus	72304.30[a] ±374.81	59998.09[a] ±533.078	73321.91[a] ±3874.40	65402.92[a] ±8717.57	1.71[NS]
t-value	1.73[NS']	65.63**	2.70[NS']	-2.14[NS']	

a, b - within S2/V gene and Virus, between different time periods means differ significantly ($p<0.05$)
*Overall significant difference within S2/V gene ($p<0.01$)
NS- Overall non-significant difference within Virus
** Significant difference between the S2/V gene and Virus at the same time period ($p<0.01$)
NS' No Significant difference between the S2/V gene and Virus at the same time period

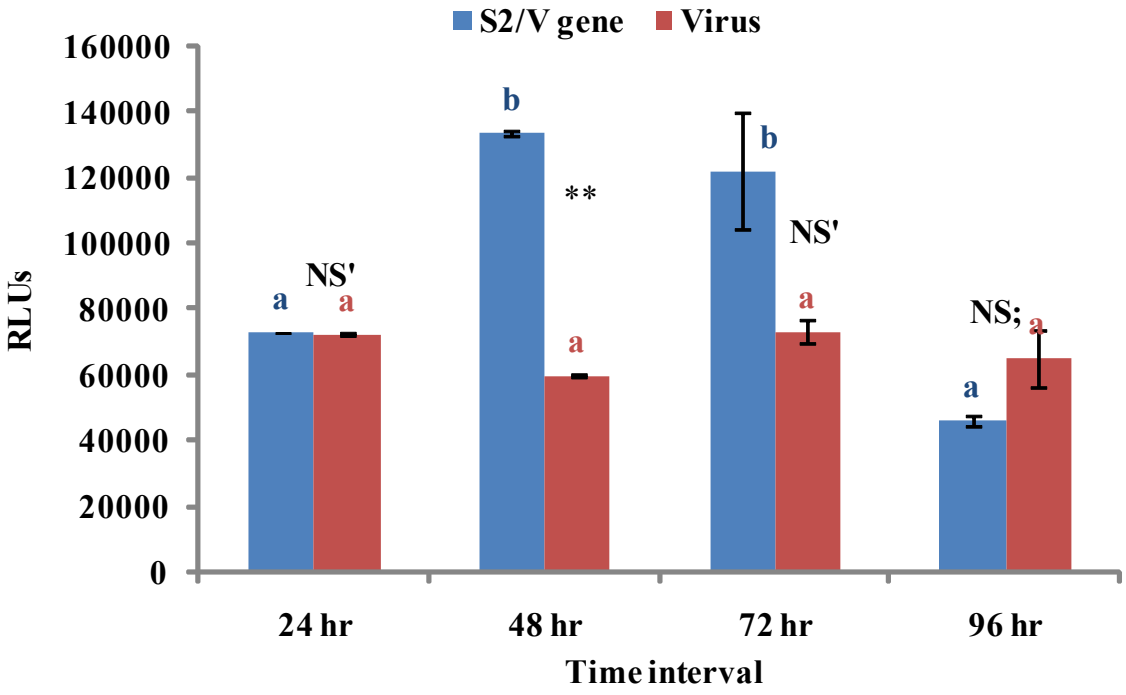

Fig. 4.52: Caspase-3 expression in B95a cells transfected with B95a cells co-transfected with S2/V gene construct and B95a cells infected with Virus. The RLUs were recorded for different time intervals post treatment

Table 4.37: Caspase-Glo 3/7 assay analyses for caspase-3 expression in B95a cells co-transfected with S2/Virus and Positive control. The RLUs were recorded for different time intervals

Time / Construct	24 hr	48 hr	72 hr	96 hr	F-value
S2/Virus	99593.82[a] ±493.03	123328.93[a] ±228.90	113753.33[a] ±18134.56	94167.35[a] ±4934.27	1.99[NS]
Positive	132427.59[a] ±4733.76	117166.06[b,a] ±23282.15	80838.25[b] ±3225.45	83177.82[a] ±2951.32	4.45[NS]
t-value	-6.89*	0.26[NS']	1.78[NS']	1.91[NS']	

a, b - within S2/V gene and Virus, between different time periods means differ significantly ($p<0.05$)
*Overall significant difference within S2/V gene ($p<0.01$)
NS- Overall non-significant difference within Virus
** Significant difference between the S2/V gene and Virus at the same time period ($p<0.01$)
NS' No Significant difference between the S2/V gene and Virus at the same time period

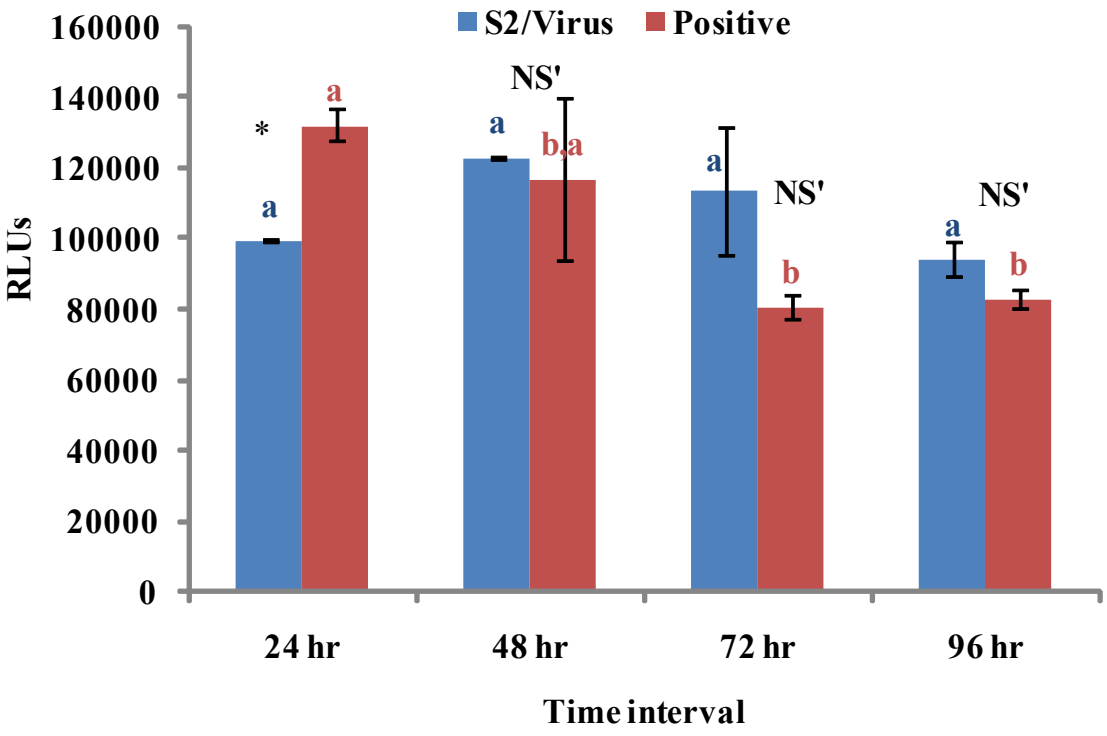

Fig. 4.53: Caspase-3 expression in B95a cells transfected with B95a cells co-transfected with S2/V gene construct and Positive control.
The RLUs were recorded for different time intervals post treatment

Table 4.38: Caspase-Glo 3/7 assay analyses for caspase-3 expression in B95a cells co-transfected with S2/Virus and negative control. The RLUs were recorded for different time intervals

Time / Construct	24 hr	48 hr	72 hr	96 hr	F-value
S2/Virus	99593.82[a] ±493.03	123328.93[a] ±228.90	113753.33[a] ±18134.56	94167.35[a] ±4934.27	1.99[NS]
Negative	302.95[a] ±16.56	275.30[a] ±60.51	277.99[a] ±11.12	266.66[a] ±25.59	0.20[NS]
t-value	201.27**	519.72**	6.25*	19.03**	

a - within S2/Virus and negative control, between different time periods means differ non-significantly ($p<0.05$)
NS- Overall non-significant difference within S2/Virus and negative control
* Significant difference between the S2/Virus and negative control at the same time period ($p<0.05$)
** Significant difference between the S2/Virus and negative control at the same time period ($p<0.01$)

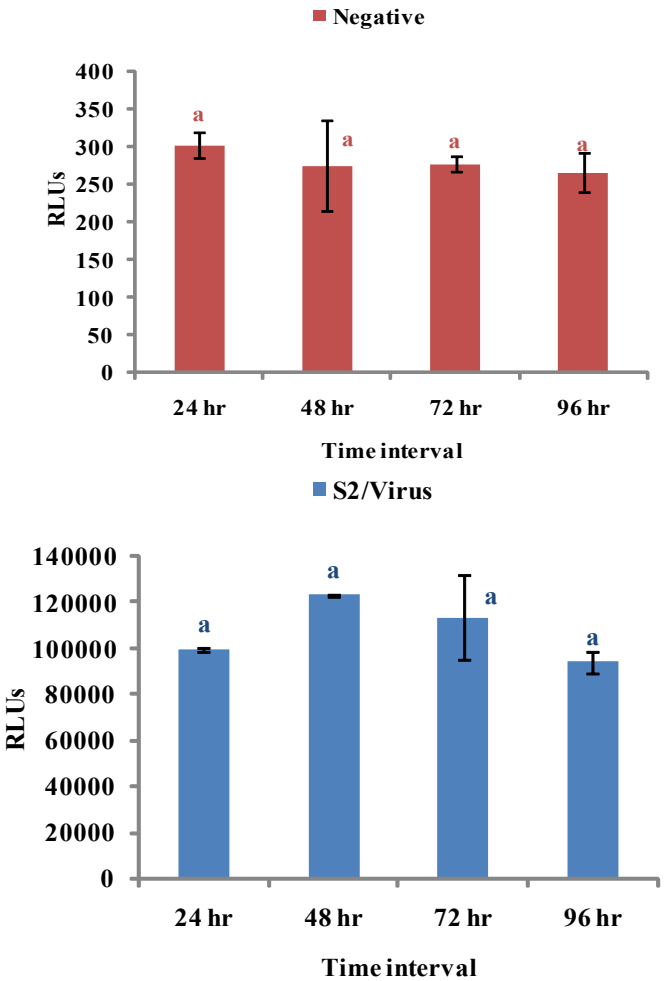

Fig. 4.54: Caspase-3 expression in B95a cells transfected with B95a cells co-transfected with S2/V gene construct and Negative control.
The RLUs were recorded for different time intervals post treatment

Table 4.39: Caspase-Glo 3/7 assay analyses for caspase-3 expression in B95a cells co-transfected with S2/Virus and B95a cells infected with Virus. The RLUs were recorded for different time intervals

Time / Construct	24 hr	48 hr	72 hr	96 hr	F-value
S2/Virus	99593.82[a] ±493.03	123328.93[a] ±228.90	113753.33[a] ±18134.56	94167.35[a] ±4934.27	1.99[NS]
Virus	72304.30[a] ±374.81	59998.09[a] ±533.078	73321.91[a] ±3874.40	65402.92[a] ±8717.57	1.71[NS]
t-value	44.06*	109.16*	2.18[NS']	2.87[NS']	

a - within S2/Virus and Virus, between different time periods means differ non-significantly ($p<0.05$)
NS- Overall non-significant difference within S2/Virus and Virus
* Significant difference between the S2/Virus and Virus at the same time period ($p<0.01$)
NS' No Significant difference between the S2/Virus and Virus at the same time period

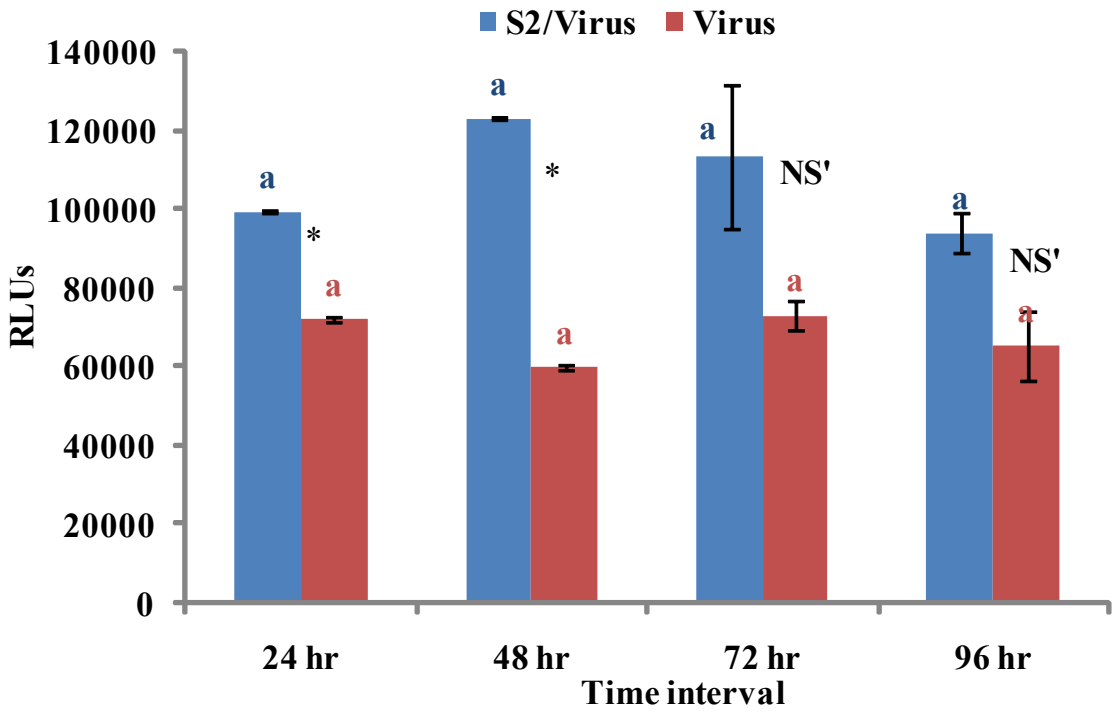

Fig. 4.55: Caspase-3 expression in B95a cells transfected with B95a cells co-transfected with S2/Virus and B95a cells infected with Virus.
The RLUs were recorded for different time intervals post treatment

Table 4.40: Caspase-Glo 3/7 assay analyses for caspase-3 expression in B95a cells infected with Virus and positive control. The RLUs were recorded for different time intervals

Time / Construct	24 hr	48 hr	72 hr	96 hr	F-value
Virus	72304.30[a] ±374.81	59998.09[a] ±533.078	73321.91[a] ±3874.40	65402.92[a] ±8717.57	1.71[NS]
Positive	132427.59[a] ±4733.76	117166.06[b,a] ±23282.15	80838.25[b] ±3225.45	83177.82[b] ±2951.32	4.45[NS]
t-value	-12.66[*]	-2.45[NS']	-1.49[NS']	-1.93[NS']	

a,b - within Virus and positive control, between different time periods means differ significantly ($p<0.05$)
NS- Overall non-significant difference within Virus and positive control
*Significant difference between the Virus and positive control at the same time period ($p<0.01$)
NS' No Significant difference between the Virus and positive control at the same time period

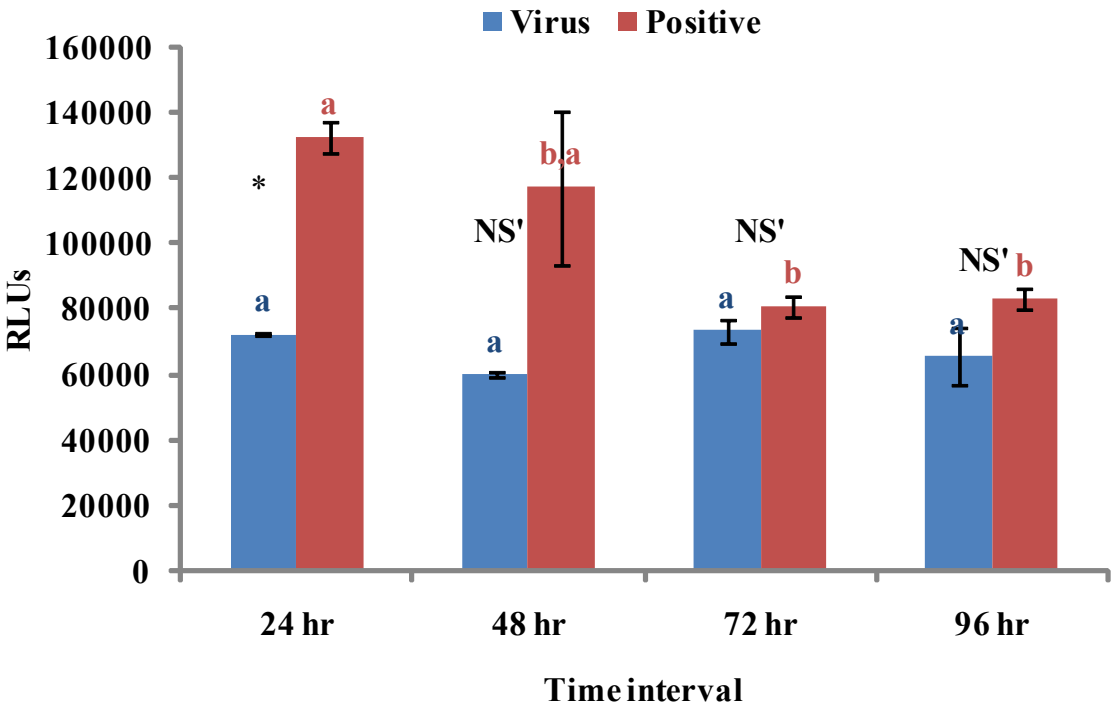

Fig. 4.56: Caspase-3 expression in B95a cells infected with virus and positive control. The RLUs were recorded for different time intervals post treatment

Table 4.41: Caspase-Glo 3/7 assay analyses for caspase-3 expression in B95a cells infected with Virus and negative control. The RLUs were recorded for different time intervals

Time Construct	24 hr	48 hr	72 hr	96 hr	F-value
Virus	72304.30[a] ±374.81	59998.09[a] ±533.078	73321.91[a] ±3874.40	65402.92[a] ±8717.57	1.71[NS]
Negative	302.95[a] ±16.56	275.30[a] ±60.51	277.99[a] ±11.12	266.66[a] ±25.59	0.20[NS]
t-value	191.91**	111.31**	18.85**	7.47*	

a, - within Virus and positive control, between different time periods means differ non-significantly ($p<0.05$)
NS- Overall non-significant difference within Virus & negative control
*Significant difference between the Virus and negative control at the same time period ($p<0.05$)
**Significant difference between the Virus and negative control at the same time period ($p<0.01$)
NS' No Significant difference between the Virus and negative control at the same time period

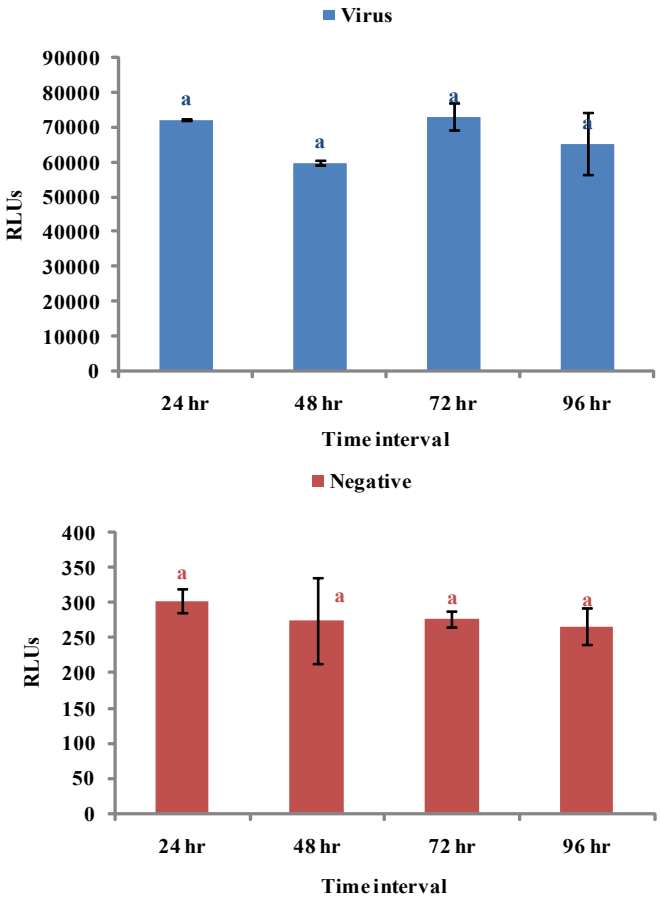

Fig. 4.57: Caspase-3 expression in B95a cells infected with Virus and negative control. The RLUs were recorded for different time intervals post treatment

Table 4.42: Caspase-Glo 8 assay analyses for caspase-8 expression in positive and negative controls. The RLUs were recorded for different time intervals post treatment

Time Construct	24 hr	48 hr	72 hr	96 hr	F-value
Positive	15569.40[a] ±4807.52	16705.35[a] ±4161.58	18716.68[a] ±2060.24	21163.03[a] ±186.10	0.54[NS]
Negative	165.77[a,b] ±4.76	121.31[a] ±1.16	176.99[a] ±19.19	161.82[a] ±17.55	3.37[NS]
t-value	3.20NS'	3.95NS'	8.99*	112.34**	

a, b - within positive and negative controls, between different time periods means differ significantly ($p<0.05$)
NS- Overall non-significant difference within positive and negative controls
*Significant difference between the positive and negative controls at the same time period ($p<0.05$)
**Significant difference between the positive and negative controls at the same time period ($p<0.01$)
NS' No Significant difference between the positive and negative controls at the same time period

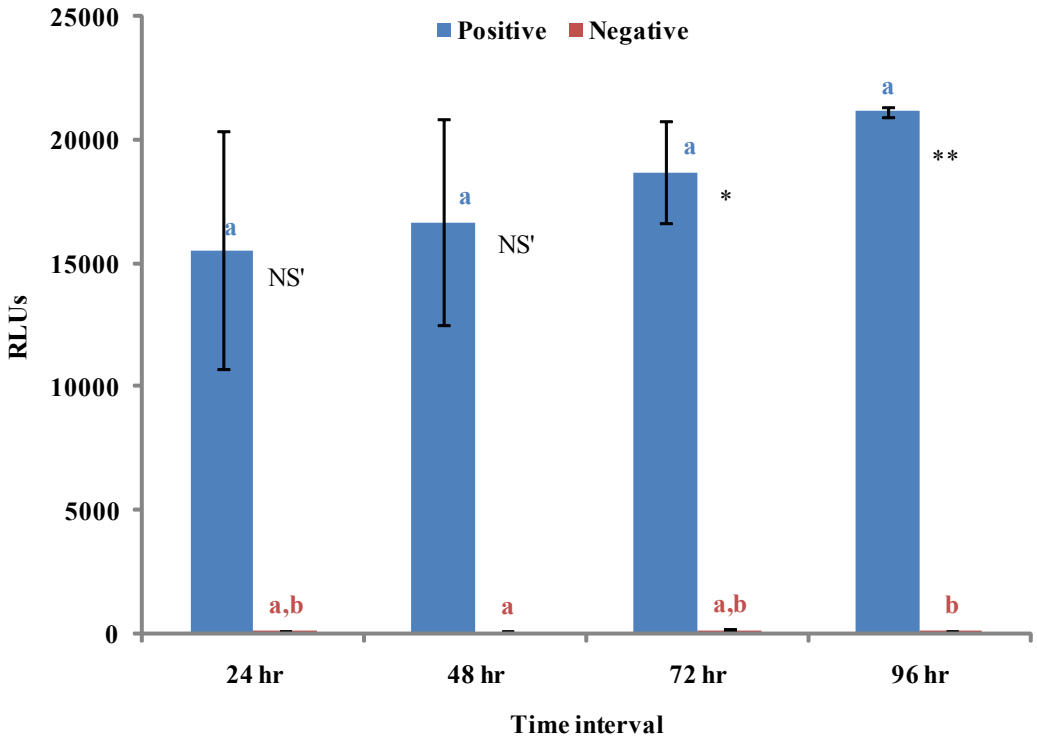

Fig. 4.58: Caspase-8 expression in B95a cells positive and negative control.
The RLUs were recorded for different time intervals post treatment

Table 4.43: Caspase-Glo 8 assay analyses for caspase-8 expression in B95a cells transfected with S2 construct and positive control. The RLUs were recorded for different time intervals

Time / Construct	24 hr	48 hr	72 hr	96 hr	F-value
S2	4036.53[a] ±29.14	6629.15[b] ±52.93	7906.15[c] ±154.67	12887.40[d] ±57.410	1788.43*
Positive	15569.40[a] ±4807.52	16705.35[a] ±4161.58	18716.68[a] ±2060.24	21163.03[a] ±186.10	0.54[NS]
t- value	-2.39[NS']	-2.42[NS']	-5.23**	-42.49***	

a,b,c,d - within S2 construct and positive control, between different time periods means differ significantly ($p<0.05$)
*Overall significant difference within S2 construct ($p<0.01$)
NS- Overall non-significant difference within positive control
** Significant difference between the S2 construct and positive control at the same time period ($p<0.05$)
***Significant difference between the S2 construct and positive control at the same time period ($p<0.01$)
NS' No Significant difference between the S2 construct and positive control at the same time period

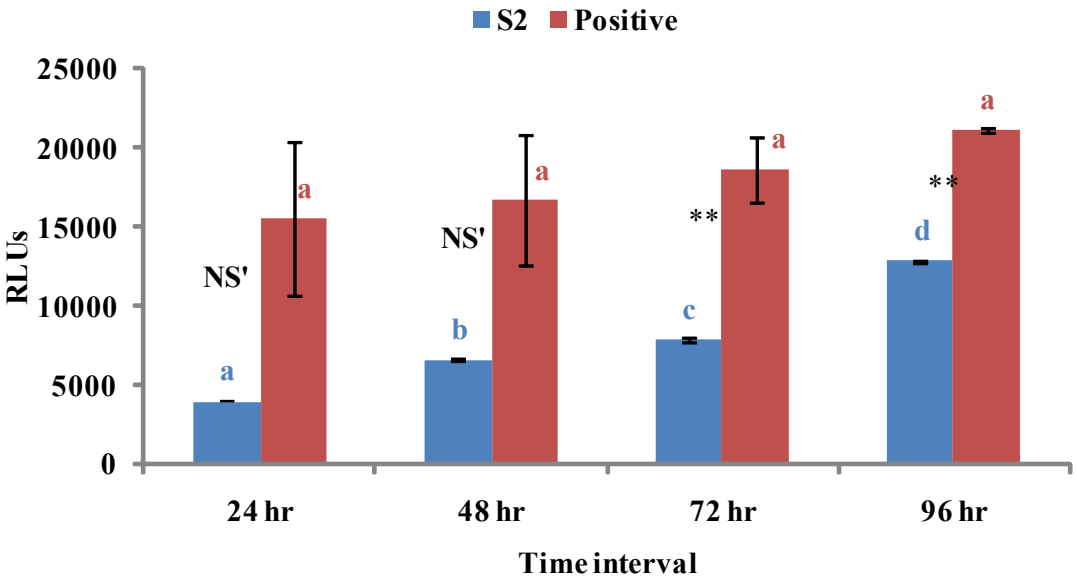

Fig. 4.59: Caspase-8 expression in B95a cells transfected with B95a cells transfected with S2 construct and positive control.
The RLUs were recorded for different time intervals post treatment

Table 4.44: Caspase-Glo 8 assay analyses for caspase-8 expression in B95a cells transfected with S2 construct and negative control. The RLUs were recorded for different time intervals

Time / Construct	24 hr	48 hr	72 hr	96 hr	F-value
S2	4036.53[a] ±29.14	6629.15[b] ±52.93	7906.15[c] ±154.67	12887.40[d] ±57.410	1788.43*
Negative	165.77[a,b] ±4.76	121.31[a] ±1.16	176.99[a,b] ±19.19	161.82[b] ±17.55	3.37[NS]
t-value	131.05**	122.92**	49.58**	211.97**	

a, b,c,d - within S2 construct and negative control, between different time periods means differ significantly ($p<0.05$)
*Overall significant difference within S2 construct ($p<0.01$)
**Significant difference between the S2 construct and negative control at the same time period ($p<0.01$)
NS- Overall non-significant difference within negative control

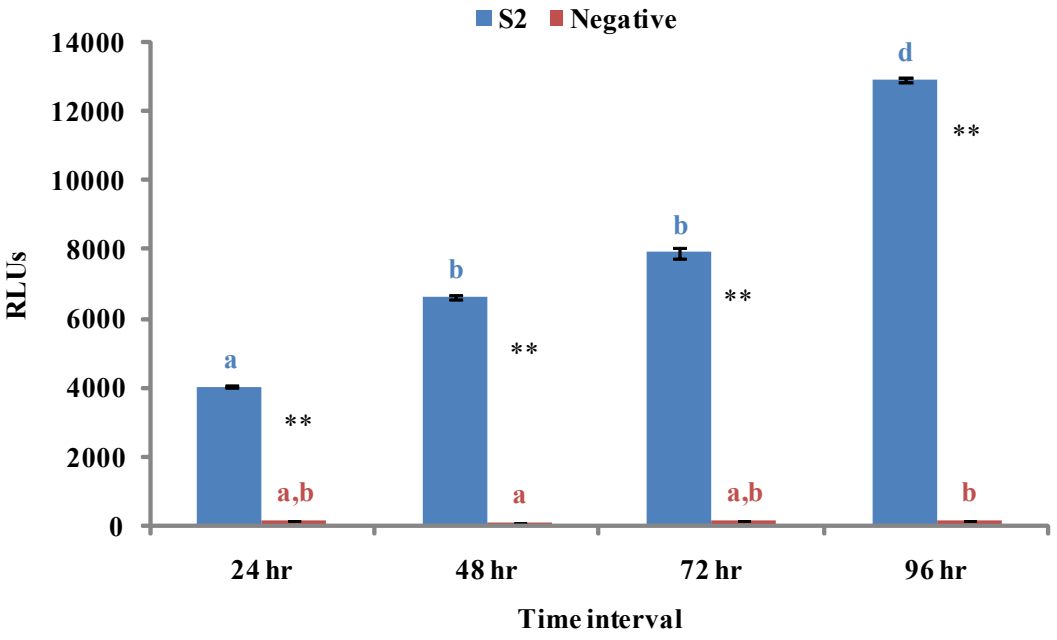

Fig. 4.60: Caspase-8 expression in B95a cells transfected with S2 construct and negative control.
The RLUs were recorded for different time intervals post treatment

Table 4.45: Caspase-Glo 8 assay analyses for caspase-8 expression in B95a cells transfected with S2 construct and B95a cells transfected with V gene construct. The RLUs were recorded for different time intervals

Time / Construct	24 hr	48 hr	72 hr	96 hr	F-value
S2	4036.53[a] ±29.14	6629.15[b] ±52.93	7906.15[c] ±154.67	12887.40[d] ±57.410	1788.43*
V gene	8539.89[a] ±117.31	12465.96[b] ±166.30	12762.68[c] ±46.19	19403.18[d] ±86.75	1788.43*
t-value	-37.25**	-33.44**	-30.08**	-62.63**	

a,b,c,d - within S2 construct and V gene, between different time periods means differ significantly ($p<0.05$)
*Overall significant difference within S2 construct and V gene ($p<0.01$)
**Significant difference between the S2 construct and V gene at the same time period ($p<0.01$)

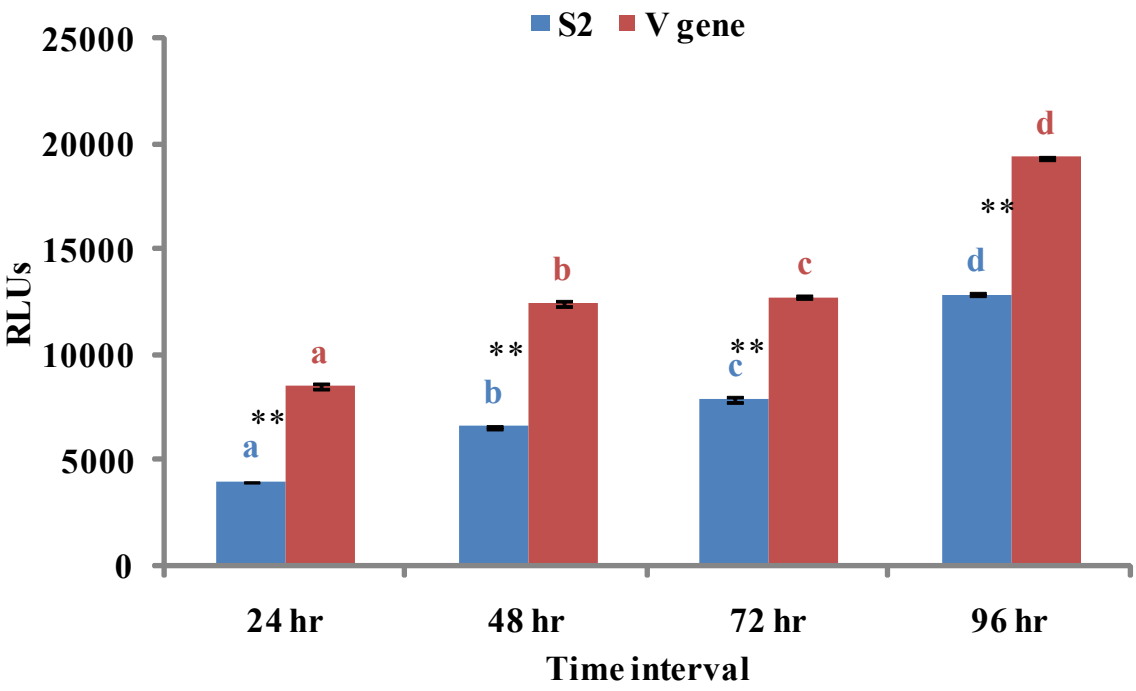

Fig. 4.61: Caspase-8 expression in B95a cells transfected with S2 construct and B95a cells transfected with V gene construct.
The RLUs were recorded for different time intervals post treatment

Table 4.46: Caspase-Glo 8 assay analyses for caspase-8 expression in B95a cells transfected with S2 construct and B95a cells co-transfected with S2/V gene construct. The RLUs were recorded for different time intervals

Time Construct	24 hr	48 hr	72 hr	96 hr	F-value
S2	4036.53[a] ±29.14	6629.15[b] ±52.93	7906.15[c] ±154.67	12887.40[d] ±57.410	1788.43*
S2/V gene	6906.84[a] ±128.56	21856.21[b] ±110.56	12491.44[c] ±90.37	21037.24[d] ±269.88	1869.94*
t-value	-21.77**	-124.21**	-25.59**	-29.53**	

a,b,c,d - within S2 construct and S2/V gene, between different time periods means differ significantly ($p<0.05$)
*Overall significant difference within S2 construct and S2/V gene ($p<0.01$)
**Significant difference between the S2 construct and S2/V gene at the same time period ($p<0.01$)

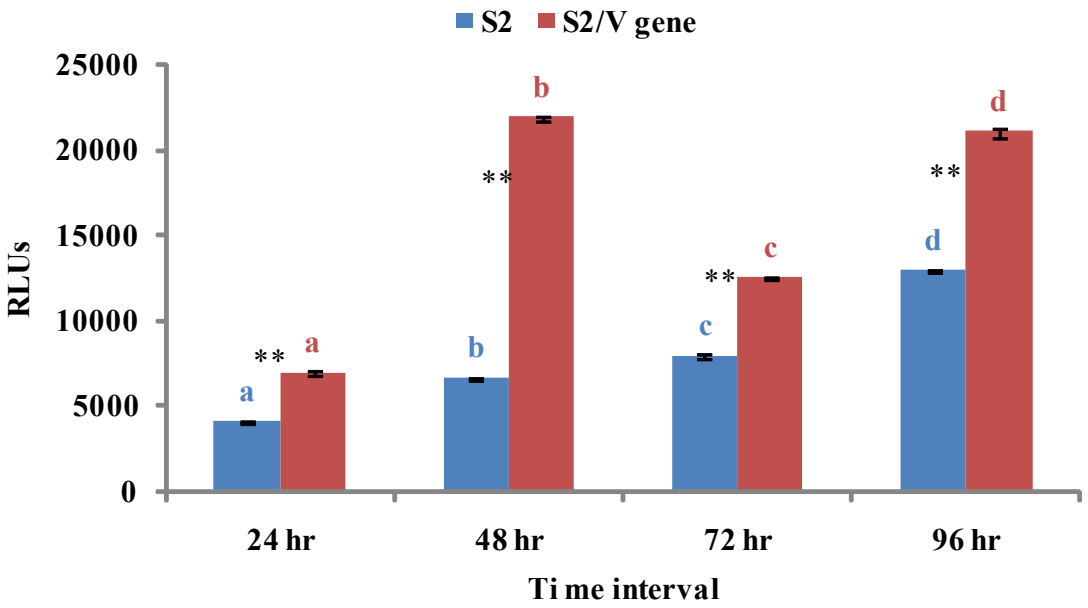

Fig. 4.62: Caspase-8 expression in B95a cells transfected with S2 construct and B95a cells co-transfected with S2/V gene construct.
The RLUs were recorded for different time intervals post treatment

Table 4.47: Caspase-Glo 8 assay analyses for caspase-8 expression in B95a cells transfected with S2 construct and B95a cells co-transfected with S2/Virus construct. The RLUs were recorded for different time intervals

Time / Construct	24 hr	48 hr	72 hr	96 hr	F-value
S2	4036.53[a] ±29.14	6629.15[b] ±52.93	7906.15[c] ±154.67	12887.40[d] ±57.410	1788.43*
S2/Virus	9701.43[a] ±148.55	12178.70[b] ±58.60	12942.40[c] ±97.66	14047.11[d] ±23.33	382.36*
t-value	-37.41**	-70.27**	-27.53**	-18.71**	

a,b,c,d - within S2 construct and S2/Virus, between different time periods means differ significantly ($p<0.05$)
*Overall significant difference within S2 construct and S2/Virus ($p<0.01$)
**Significant difference between the S2 construct and S2/Virus at the same time period ($p<0.01$)

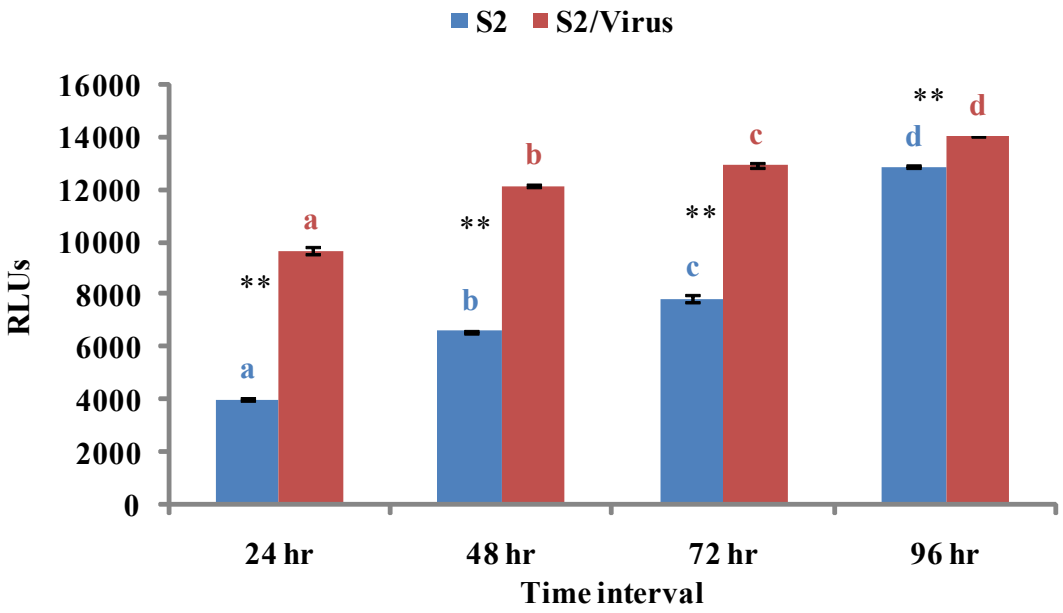

Fig. 4.63: Caspase-8 expression in B95a cells transfected with S2 construct and B95a cells co-transfected with S2/Virus construct.
The RLUs were recorded for different time intervals post treatment

Table 4.48: Caspase-Glo 8 assay analyses for caspase-8 expression in B95a cells transfected with S2 construct and B95a cells infected with virus. The RLUs were recorded for different time intervals

Time / Construct	24 hr	48 hr	72 hr	96 hr	F-value
S2	4036.53[a] ±29.14	6629.15[b] ±52.93	7906.15[c] ±154.67	12887.40[d] ±57.410	1788.43*
Virus	2700.13[a] ±6.77	6571.43[b] ±8.05	11132.87[c] ±340.20	16932.31[d] ±148.95	1087.72*
t-value	44.65***	1.07[NS]	-8.63**	-25.33***	

a,b,c,d - within S2 construct and Virus, between different time periods means differ significantly ($p<0.05$)
*Overall significant difference within S2 construct and Virus ($p<0.01$)
**Significant difference between the S2 construct and Virus at the same time period ($p<0.05$)
***Significant difference between the S2 construct and Virus at the same time period ($p<0.01$)
NS No Significant difference between the S2 construct and Virus at the same time period

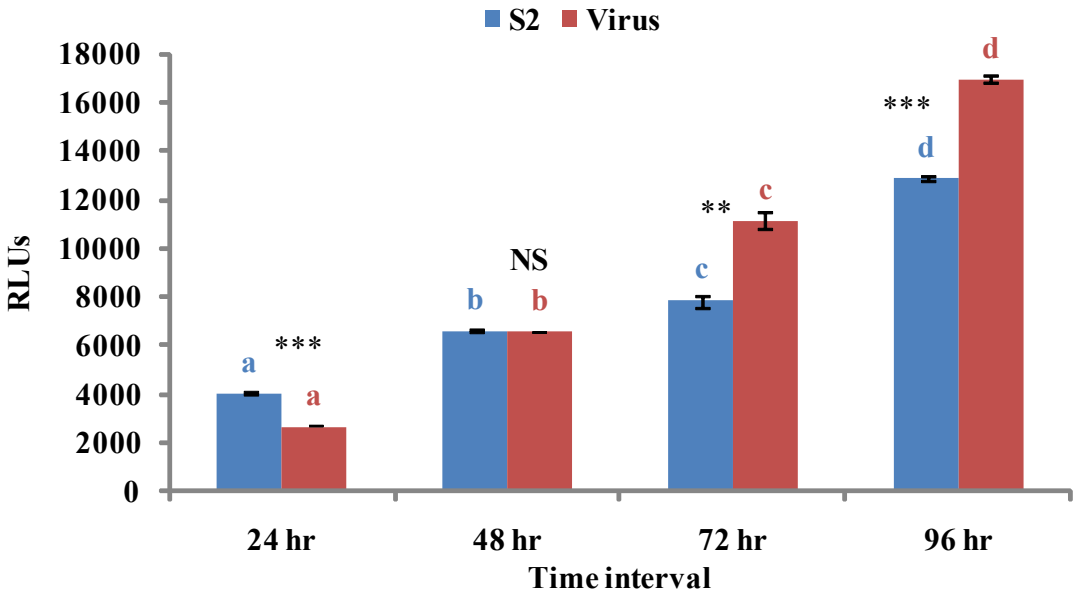

Fig. 4.64: Caspase-8 expression in B95a cells transfected with S2 construct and B95a cells infected with Virus.
The RLUs were recorded for different time intervals post treatment

Table 4.49: Caspase-Glo 8 assay analyses for caspase-8 expression in B95a cells transfected with V gene construct and positive control. The RLUs were recorded for different time intervals

Time Construct	24 hr	48 hr	72 hr	96 hr	F-value
V gene	8539.89^{a} ±117.31	12465.96^{b} ±166.30	12762.68^{c} ±46.19	19403.18^{d} ±86.75	1788.43*
Positive	15569.40^{a} ±4807.52	16705.35^{a} ±4161.58	18716.68^{a} ±2060.24	21163.03^{a} ±186.10	0.54^{NS}
t- value	-1.46$^{NS'}$	-1.01$^{NS'}$	-2.88$^{NS'}$	-8.57**	

a,b,c,d - within V gene and positive control, between different time periods means differ significantly ($p<0.05$)
*Overall significant difference within V gene ($p<0.01$)
NS- Overall non-significant difference within positive control
** Significant difference between the V gene and positive control at the same time period ($p<0.05$)
NS' No Significant difference between the V gene and positive control at the same time period

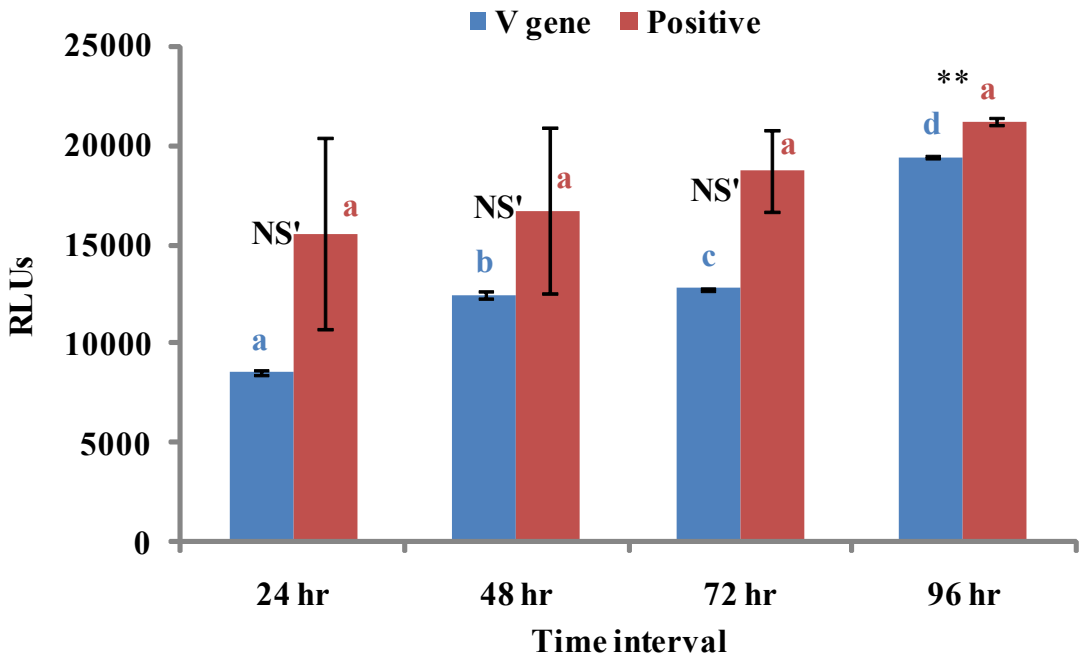

Fig. 4.65: Caspase-8 expression in B95a cells transfected with V gene and positive control.
The RLUs were recorded for different time intervals post treatment

Table 4.50: Caspase-Glo 8 assay analyses for caspase-8 expression in B95a cells transfected with V gene construct and negative control. The RLUs were recorded for different time intervals

Time Construct	24 hr	48 hr	72 hr	96 hr	F-value
V gene	8539.89^{a} ±117.31	12465.96^{b} ±166.30	12762.68^{c} ±46.19	19403.18^{d} ±86.75	1788.43*
Negative	165.77^{a,b} ±4.76	121.31^{a} ±1.16	176.99^{a,b} ±19.19	161.82^{b} ±17.55	3.37^{NS}
t-value	71.32**	74.22**	251.60**	217.37**	

a,b,c,d - within V gene and negative control, between different time periods means differ significantly ($p<0.05$)
*Overall significant difference within V gene ($p<0.01$)
NS- Overall non-significant difference within negative control
** Significant difference between the V gene and negative control at the same time period ($p<0.01$)

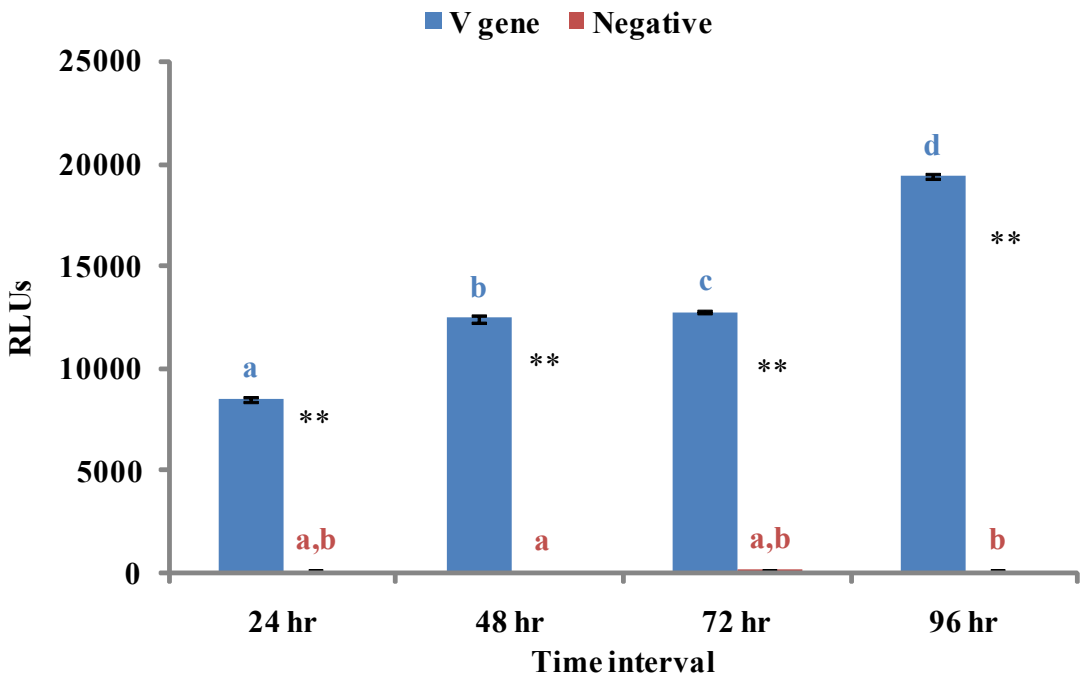

Fig. 4.66: Caspase-8 expression in B95a cells transfected with V gene and negative control.
The RLUs were recorded for different time intervals post treatment

Table 4.51: Caspase-Glo 8 assay analyses for caspase-8 expression in B95a cells transfected with V gene construct and B95a cells co-transfected with S2/V gene construct. The RLUs were recorded for different time intervals

Time / Construct	24 hr	48 hr	72 hr	96 hr	F-value
V gene	8539.89^{a} ±117.31	12465.96^{b} ±166.30	12762.68^{c} ±46.19	19403.18^{d} ±86.75	1788.43*
S2/V gene	6906.84^{a} ±128.56	21856.21^{b} ±110.56	12491.44^{c} ±90.37	21037.24^{d} ±269.88	1869.94*
t-value	9.38**	-47.02***	2.67^{NS}	-5.76**	

a,b,c,d - within V gene and S2/V gene, between different time periods means differ significantly ($p<0.05$)
*Overall significant difference within V gene and S2/V gene ($p<0.01$)
**Significant difference between the V gene and S2/V gene at the same time period ($p<0.05$)
***Significant difference between the V gene and S2/V gene at the same time period ($p<0.01$)
NS- No Significant difference between the V gene and S2/V gene at the same time period

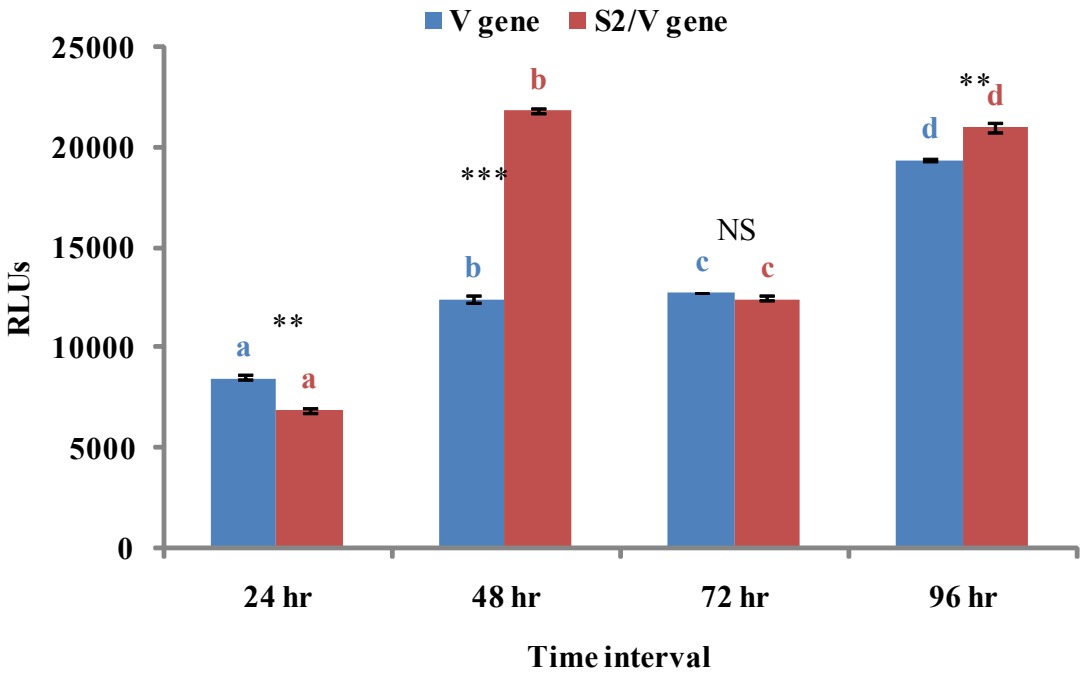

Fig. 4.67: Caspase-8 expression in B95a cells transfected with V gene construct and B95a cells co-transfected with S2/V gene construct. The RLUs were recorded for different time intervals post treatment

Table 4.52: Caspase-Glo 8 assay analyses for caspase-8 expression in B95a cells transfected with V gene construct and B95a cells co-transfected with S2/ Virus construct. The RLUs were recorded for different time interval

Time / Construct	24 hr	48 hr	72 hr	96 hr	F- value
V gene	8539.89[a] ±117.31	12465.96[b] ±166.30	12762.68[c] ±46.19	19403.18[d] ±86.75	1788.43*
S2/Virus	9701.43[a] ±148.55	12178.70[b] ±58.60	12942.40[c] ±97.66	14047.11[d] ±23.33	382.36*
t- value	6.13**	1.62[NS]	-1.66[NS]	59.61***	

a,b,c,d - within V gene and S2/Virus, between different time periods means differ significantly ($p<0.05$)
*Overall significant difference within V gene and S2/Virus ($p<0.01$)
**Significant difference between the V gene and S2/Virus at the same time period ($p<0.05$)
***Significant difference between the V gene and S2/Virus at the same time period ($p<0.01$)
NS No Significant difference between the V gene and S2/Virus at the same time period

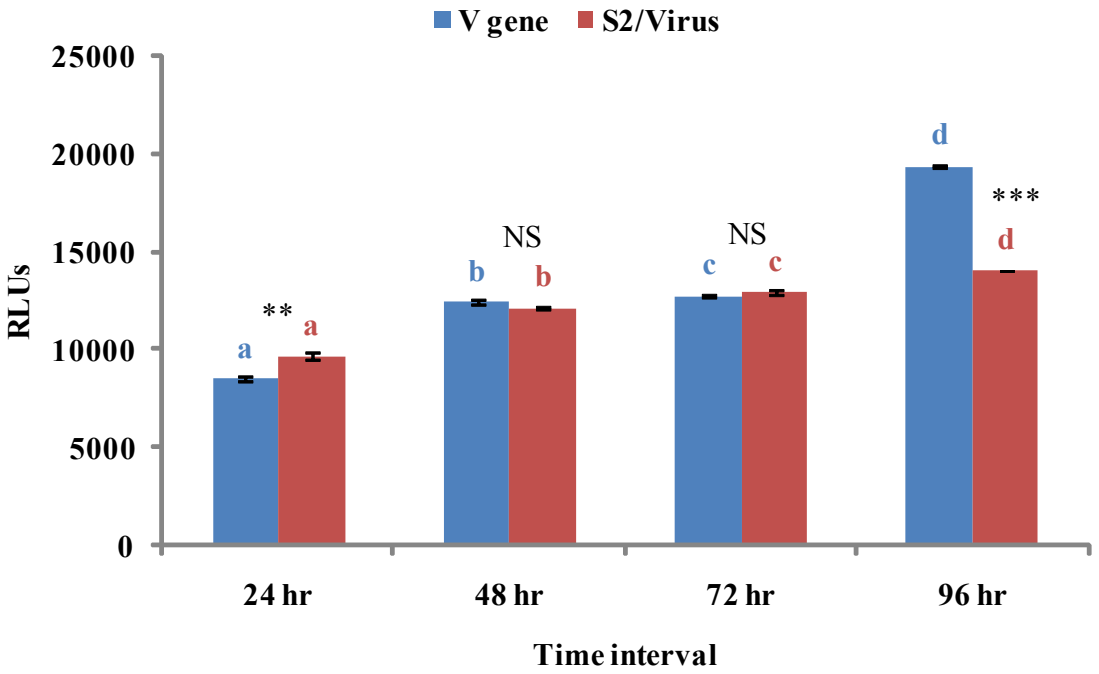

Fig. 4.68: Caspase-8 expression in B95a cells transfected with V gene construct and B95a cells co-transfected with S2/Virus construct. The RLUs were recorded for different time intervals post treatment

Table 4.53: Caspase-Glo 8 assay analyses for caspase-8 expression in B95a cells transfected with V gene construct and B95a cells infected with virus. The RLUs were recorded for different time intervals

Time / Construct	24 hr	48 hr	72 hr	96 hr	F-value
V gene	8539.89[a] ±117.31	12465.96[b] ±166.30	12762.68[c] ±46.19	19403.18[d] ±86.75	1788.43*
Virus	2700.13[a] ±6.77	6571.43[b] ±8.05	11132.87[c] ±340.20	16932.31[d] ±148.95	1087.72*
t-value	49.69***	35.40***	4.74**	14.33***	

a,b,c,d - within V gene and Virus, between different time periods means differ significantly ($p<0.05$)
*Overall significant difference within V gene and Virus ($p<0.01$)
**Significant difference between the V gene and Virus at the same time period ($p<0.05$)
***Significant difference between the V gene and Virus at the same time period ($p<0.01$)

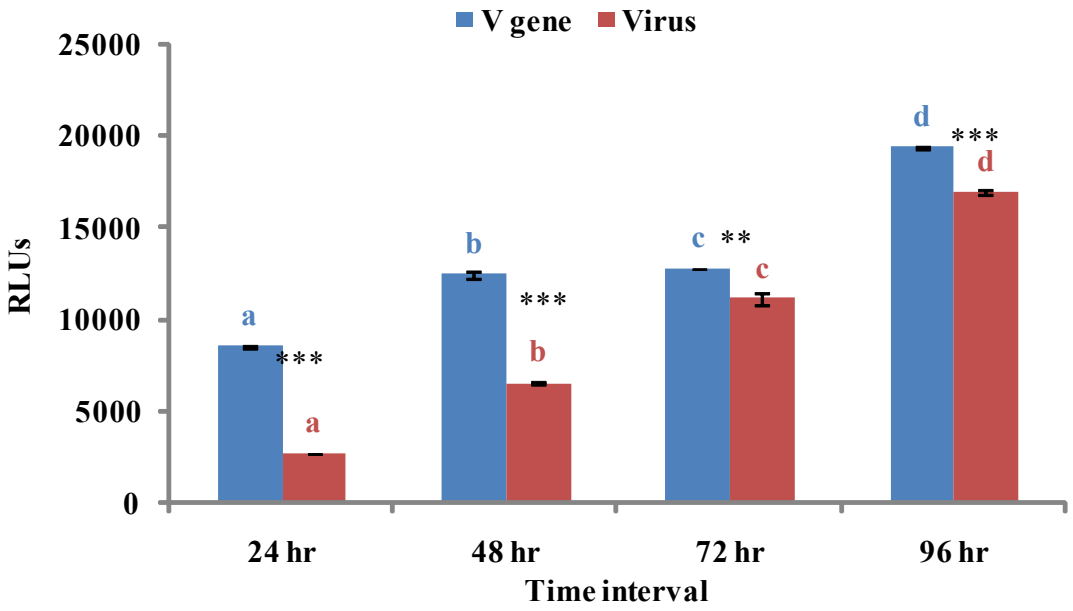

Fig. 4.69: Caspase-8 expression in B95a cells transfected with V gene construct and B95a cells infected with virus.
The RLUs were recorded for different time intervals post treatment

Table 4.54: Caspase-Glo 8 assay analyses for caspase-8 expression in B95a cells co-transfected with S2/V gene construct and positive control. The RLUs were recorded for different time intervals

Time / Construct	24 hr	48 hr	72 hr	96 hr	F-value
S2/V gene	6906.84[a] ±128.56	21856.21[b] ±110.56	12491.44[c] ±90.37	21037.24[d] ±269.88	1869.94*
Positive	15569.40[a] ±4807.52	16705.35[a] ±4161.58	18716.68[a] ±2060.24	21163.03[a] ±186.10	0.54[NS]
t-value	-1.80[NS']	1.23[NS']	-3.01[NS']	-0.38[NS']	

a,b,c,d - within V gene and Virus, between different time periods means differ significantly ($p<0.05$)
*Overall significant difference within V gene and Virus ($p<0.01$)
**Significant difference between the V gene and Virus at the same time period ($p<0.05$)
***Significant difference between the V gene and Virus at the same time period ($p<0.01$)

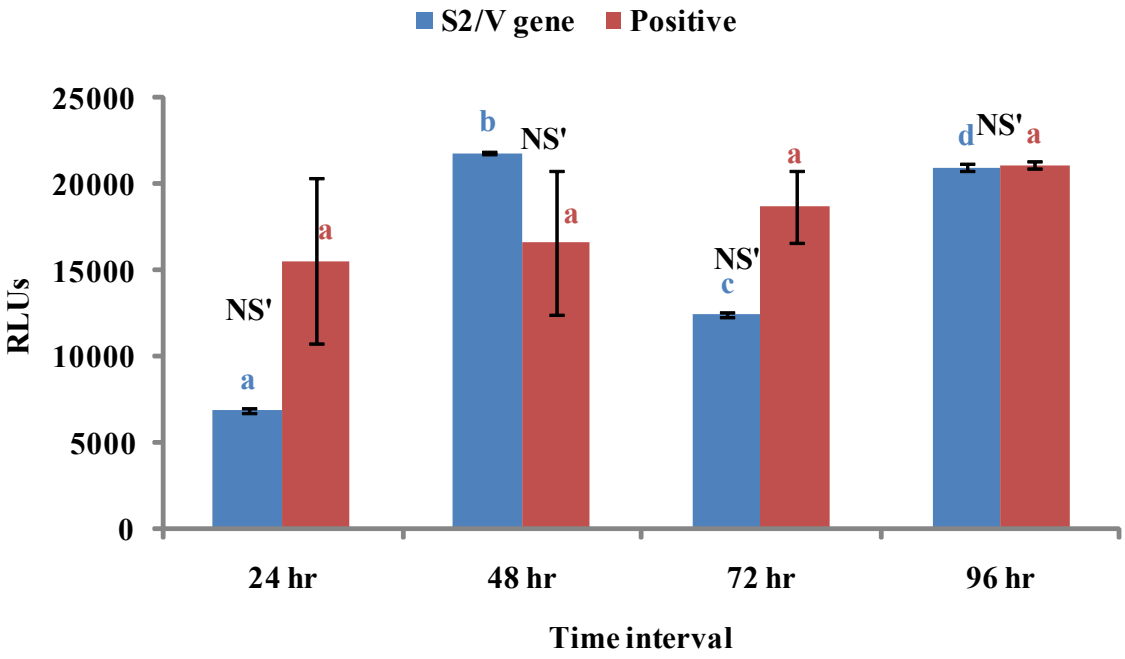

Fig. 4.70: Caspase-8 expression in B95a cells transfected with B95a cells co-transfected with S2/V gene construct and positive control.
The RLUs were recorded for different time intervals post treatment

Table 4.55: Caspase-Glo 8 assay analyses for caspase-8 expression in B95a cells co-transfected with S2/V gene construct and negative control. The RLUs were recorded for different time intervals

Time Construct	24 hr	48 hr	72 hr	96 hr	F- value
S2/V gene	6906.84^{a} ±128.56	21856.21^{b} ±110.56	12491.44^{c} ±90.37	21037.24^{d} ±269.88	1869.94*
Negative	$165.77^{a,b}$ ±4.76	121.31^{a} ±1.16	$176.99^{a,b}$ ±19.19	161.82^{b} ±17.55	3.37^{NS}
t- value	52.39**	196.56**	133.28**	77.18**	

a,b,c.d - within S2/V gene and negative control, between different time periods means differ significantly ($p<0.05$)
*Overall significant difference within S2/V gene ($p<0.01$)
NS- Overall non-significant difference within negative control
** Significant difference between the S2/V gene and negative control at the same time period ($p<0.01$)

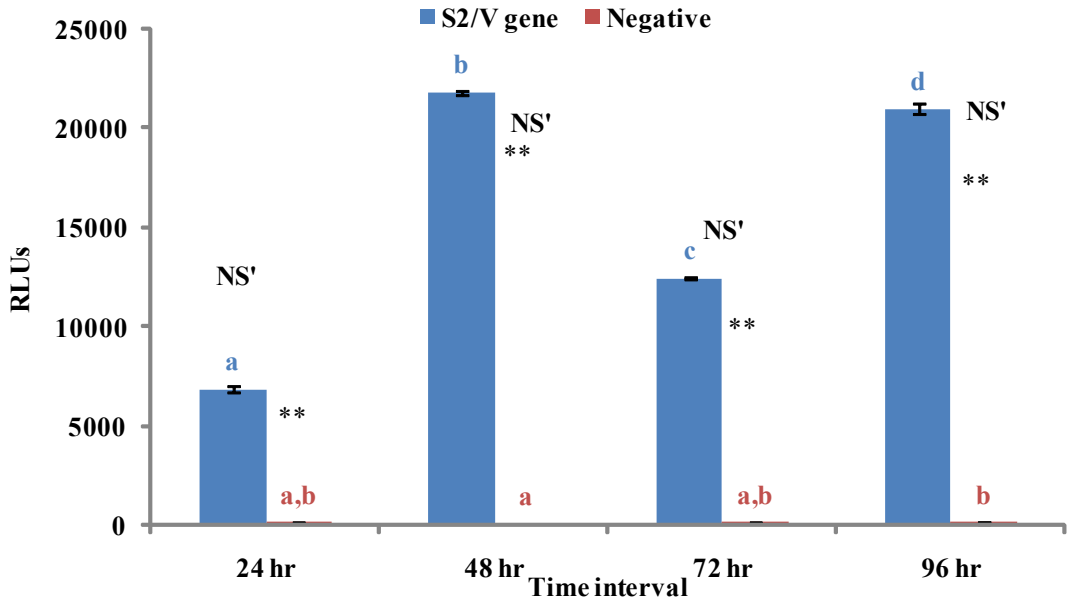

Fig. 4.71: Caspase-8 expression in B95a cells transfected with B95a cells co-transfected with S2/V gene construct and negative control.
The RLUs were recorded for different time intervals post treatment

Table 4.56: Caspase-Glo 8 assay analyses for caspase-8 expression in B95a cells co-transfected with S2/V gene construct and B95a cells co-transfected with S2/Virus. The RLUs were recorded for different time intervals

Time Construct	24 hr	48 hr	72 hr	96 hr	F-value
S2/V gene	6906.84[a] ±128.56	1856.21[b] 2±110.56	12491.44[c] ±90.37	21037.24[d] ±269.88	1869.94*
S2/Virus	9701.43[a] ±148.55	12178.70[b] ±58.60	12942.40[c] ±97.66	14047.11[d] ±23.33	382.36*
t-value	-14.22**	77.33**	-3.38[NS]	25.80**	

a,bc,d - within S2/V gene and S2/Virus, between different time periods means differ significantly ($p<0.05$)
*Overall significant difference within S2/V gene and S2/Virus ($p<0.01$)
** Significant difference between the S2/V gene and S2/Virus at the same time period ($p<0.01$)
NS No Significant difference between the S2/V gene and S2/Virus at the same time period

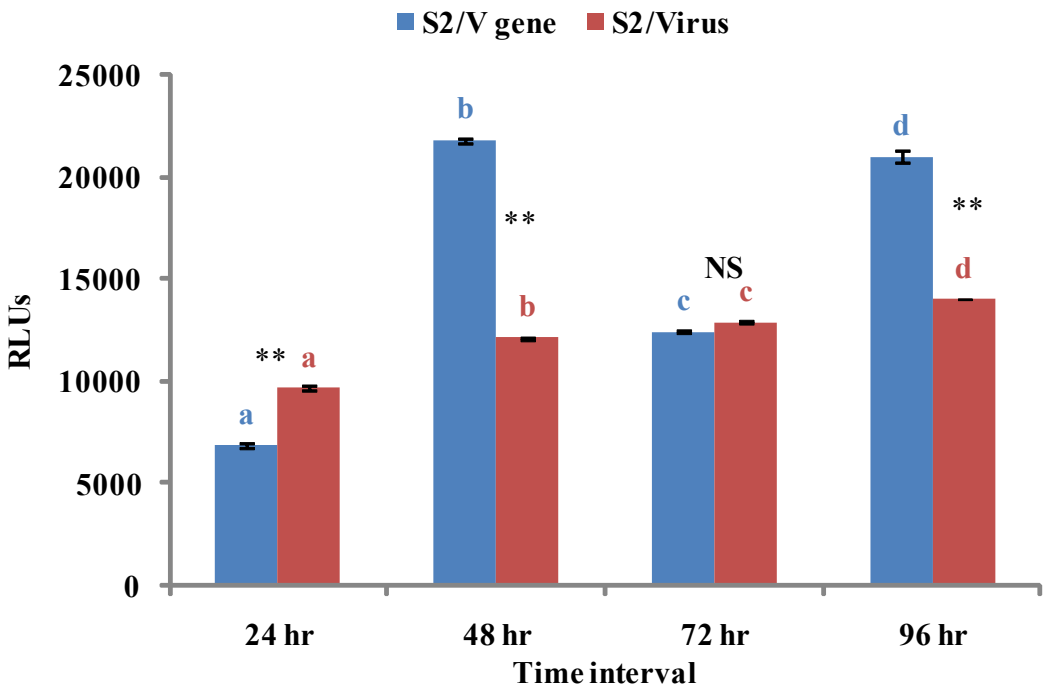

Fig. 4.72: Caspase-8 expression in B95a cells transfected with B95a cells co-transfected with S2/V gene construct and B95a cells co-transfected with S2/Virus.

The RLUs were recorded for different time intervals post treatment

Table 4.57: Caspase-Glo 8 assay analyses for caspase-8 expression in B95a cells co-transfected with S2/V gene construct and B95a cells infected with Virus. The RLUs were recorded for different time intervals

Time Construct	24 hr	48 hr	72 hr	96 hr	F-value
S2/V gene	6906.84[a] ±128.56	21856.21[b] ±110.56	12491.44[c] ±90.37	21037.24[d] ±269.88	1869.94*
Virus	2700.13[a] ±6.77	6571.43[b] ±8.05	11132.87[c] ±340.20	16932.31[d] ±148.95	1087.72*
t-value	32.67**	137.87**	3.86[NS]	13.31**	

a,b,c,d - within S2/V gene and Virus, between different time periods means differ significantly ($p<0.05$)
*Overall significant difference within S2/V gene and Virus ($p<0.01$)
** Significant difference between the S2/V gene and Virus at the same time period ($p<0.01$)
NS No Significant difference between the S2/V gene and Virus at the same time period

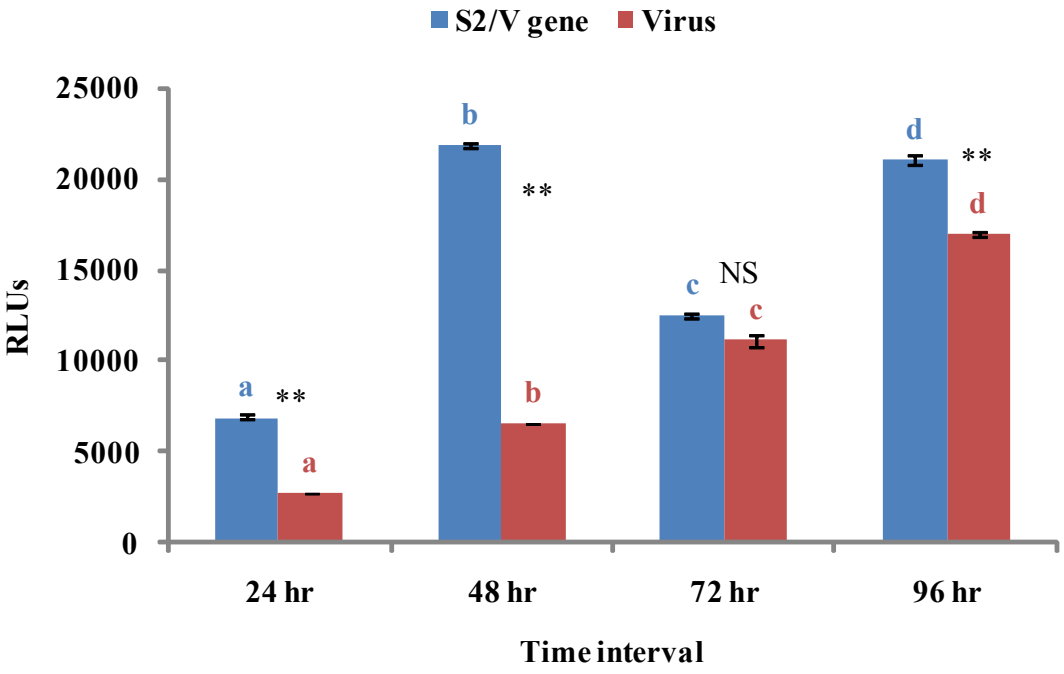

Fig. 4.73: Caspase-8 expression in B95a cells transfected with B95a cells co-transfected with S2/V gene construct and B95a cells infected with Virus. The RLUs were recorded for different time intervals post treatment

Table 4.58: Caspase-Glo 8 assay analyses for caspase-8 expression in B95a cells co-transfected with S2/Virus and Positive. The RLUs were recorded for different time intervals

Time Construct	24 hr	48 hr	72 hr	96 hr	F-value
S2/Virus	9701.43[a] ±148.55	12178.70[b] ±58.60	12942.40[c] ±97.66	14047.11[d] ±23.33	382.36*
Positive	15569.40[a] ±4807.52	16705.35[a] ±4161.58	18716.68[a] ±2060.24	21163.03[a] ±186.10	0.54[NS]
t- value	-1.22[NS']	-1.08[NS']	-2.80[NS']	-37.93**	

a,b,c,d - within S2/Virus and positive control, between different time periods means differ significantly ($p<0.05$)
*Overall significant difference within S2/Virus ($p<0.01$)
NS- Overall non-significant difference within positive control
** Significant difference between the S2/Virus and positive control at the same time period ($p<0.01$)
NS' No Significant difference between the S2/Virus and positive control at the same time period

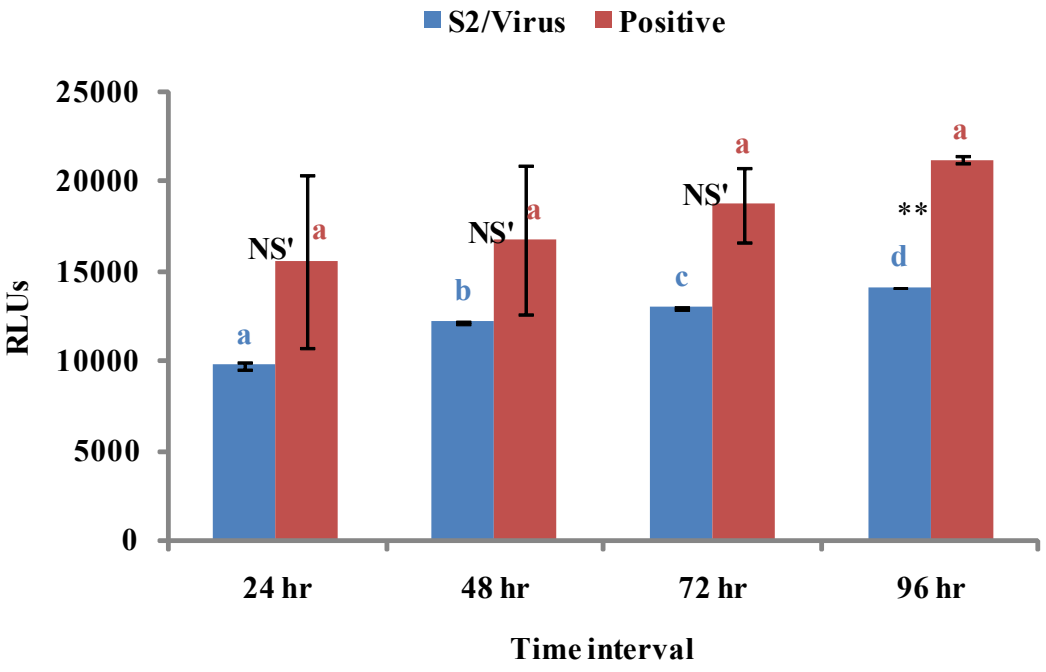

Fig. 4.74: Caspase-8 expression in B95a cells transfected with B95a cells co-transfected with S2/Virus construct and positive control.
The RLUs were recorded for different time intervals post treatment

Table 4.59: Caspase-Glo 8 assay analyses for caspase-8 expression in B95a cells co-transfected with S2/Virus and negative control. The RLUs were recorded for different time intervals

Time Construct	24 hr	48 hr	72 hr	96 hr	F-value
S2/Virus	9701.43[a] ±148.55	12178.70[b] ±58.60	12942.40[c] ±97.66	14047.11[b] ±23.33	382.36*
Negative	165.77[a,b] ±4.76	121.31[a] ±1.16	176.99[a,b] ±19.19	161.82[b] ±17.55	3.37[NS]
t-value	64.15**	205.71**	128.25**	475.50**	

a,b,c,d - within S2/Virus and negative control, between different time periods means differ non-significantly ($p<0.05$)
*Overall significant difference within S2/Virus ($p<0.01$)
NS- Overall non-significant difference within negative control
** Significant difference between the S2/Virus and negative control at the same time period ($p<0.01$)

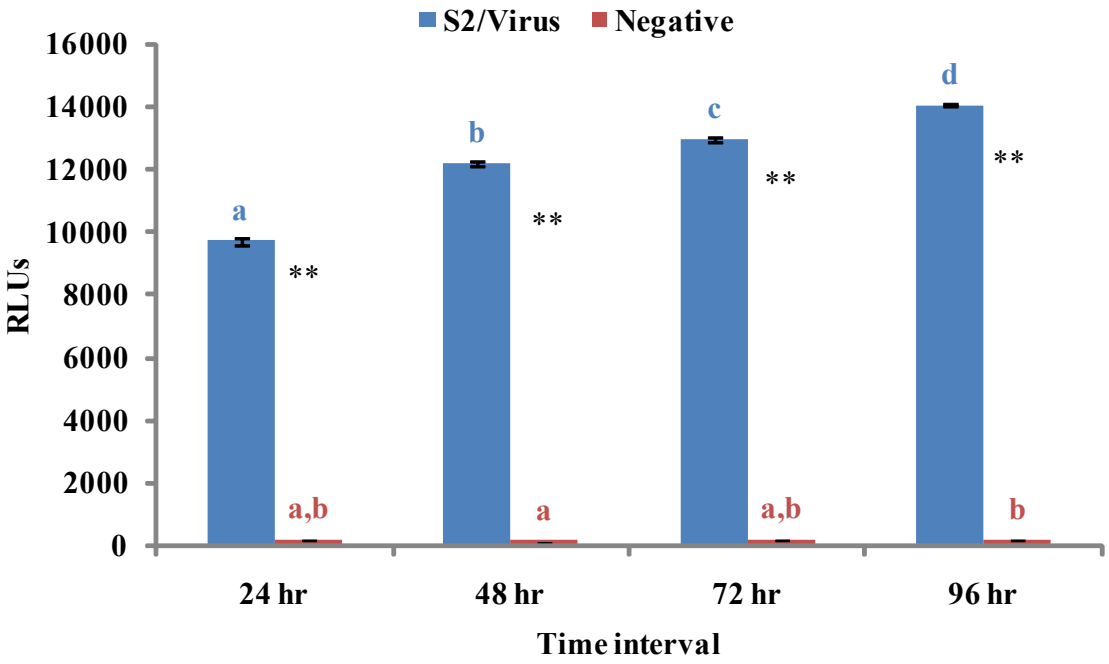

Fig. 4.75: Caspase-8 expression in B95a cells transfected with B95a cells co-transfected with S2/Virus construct and negative control.
The RLUs were recorded for different time intervals post treatment

Table 4.60: Caspase-Glo 8 assay analyses for caspase-8 expression in B95a cells co-transfected with S2/Virus and B95a cells infected with Virus. The RLUs were recorded for different time intervals

Time Construct	24 hr	48 hr	72 hr	96 hr	F-value
S2/Virus	9701.43[a] ±148.55	12178.70[b] ±58.60	12942.40[c] ±97.66	14047.11[d] ±23.33	382.36*
Virus	2700.13[a] ±6.77	6571.43[b] ±8.05	11132.87[c] ±340.20	16932.31[d] ±148.95	1087.72*
t-value	47.07***	94.79***	5.11**	-19.13***	

a,b,c,d - within S2/Virus and Virus, between different time periods means differ non-significantly ($p<0.05$)
* Overall significant difference within S2/Virus and Virus ($p<0.01$)
** Significant difference between the S2/Virus and Virus at the same time period ($p<0.05$)
*** Significant difference between the S2/Virus and Virus at the same time period ($p<0.01$)

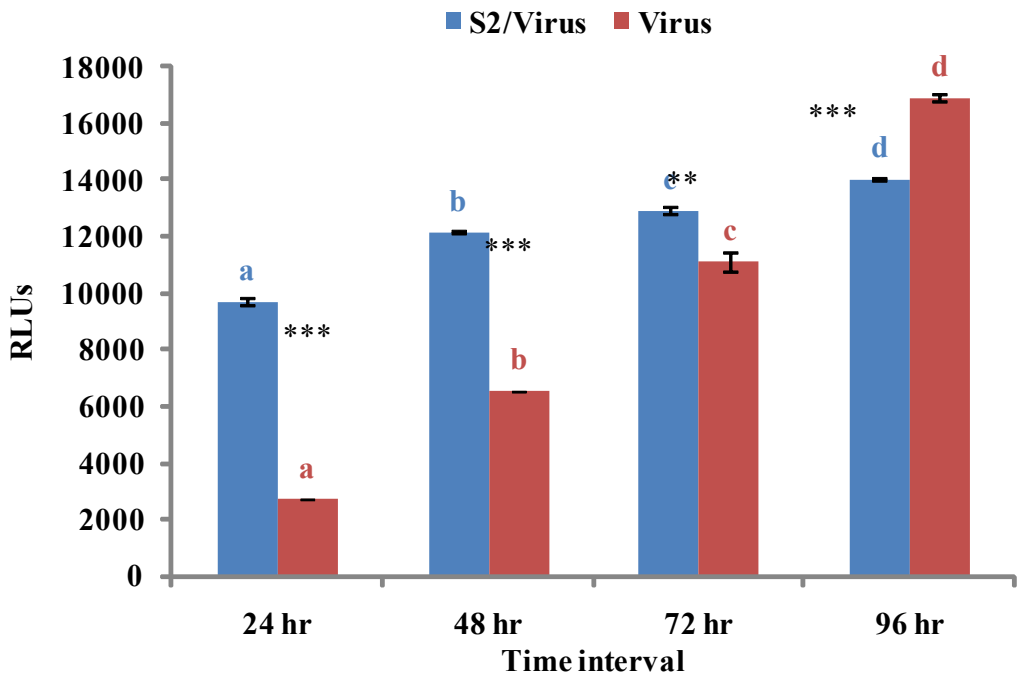

Fig. 4.76: Caspase-8 expression in B95a cells transfected with B95a cells co-transfected with S2/Virus construct and B95a cells infected with Virus.
The RLUs were recorded for different time intervals post treatment

Table 4.61: Caspase-Glo 8 assay analyses for caspase-8 expression in B95a cells infected with Virus and positive control. The RLUs were recorded for different time intervals

Time Construct	24 hr	48 hr	72 hr	96 hr	F-value
Virus	2700.13^{a} ±6.77	6571.43^{b} ±8.05	11132.87^{c} ±340.20	16932.31^{d} ±148.95	1087.72*
Positive	15569.40^{a} ±4807.52	16705.35^{a} ±4161.58	18716.68^{a} ±2060.24	21163.03^{a} ±186.10	0.54^{NS}
t-value	$-2.67^{NS'}$	$-2.43^{NS'}$	$-3.62^{NS'}$	-17.74**	

a,b,c,d - within Virus and positive control, between different time periods means differ significantly ($p<0.05$)
* Overall significant difference within Virus ($p<0.01$)
NS- Overall non-significant difference within positive control
** Significant difference between the Virus and positive control at the same time period ($p<0.01$)
NS' No Significant difference between the Virus and positive control at the same time period

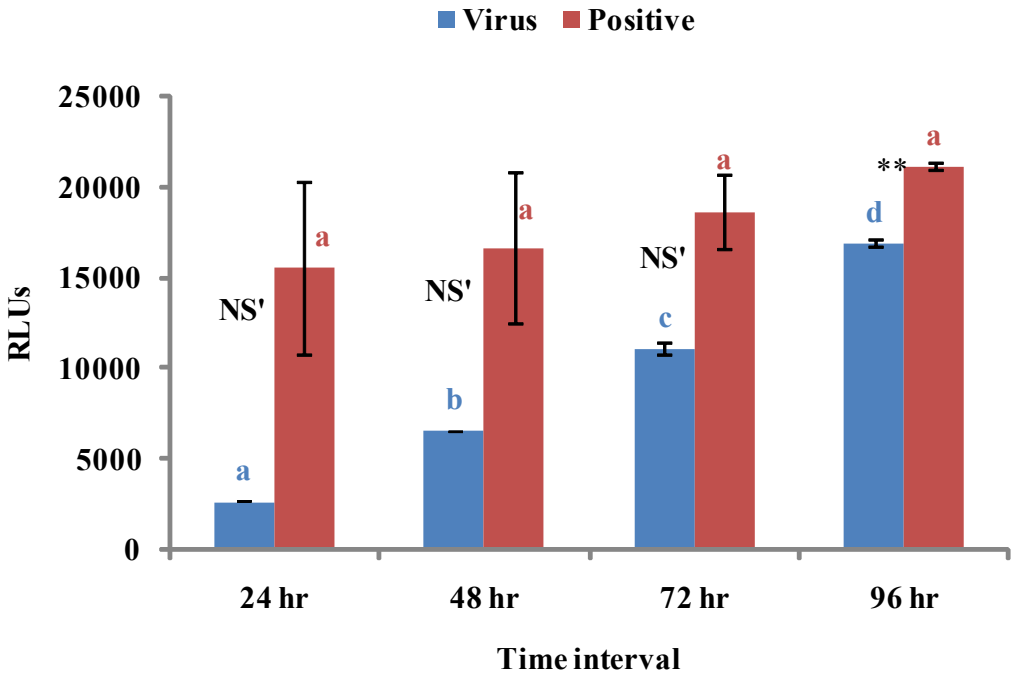

Fig. 4.77: Caspase-8 expression in B95a cells transfected with B95a cells infected with virus and positive control.
The RLUs were recorded for different time intervals post treatment

Table 4.62: Caspase-Glo 8 assay analyses for caspase-8 expression in B95a cells infected with Virus and negative control. The RLUs were recorded for different time intervals

Time Construct	24 hr	48 hr	72 hr	96 hr	F-value
Virus	2700.13^{a} ±6.77	6571.43^{b} ±8.05	11132.87^{c} ±340.20	16932.31^{d} ±148.95	1087.72*
Negative	165.77^{a,b} ±4.76	121.31^{a} ±1.16	176.99^{a,b} ±19.19	161.82^{b} ±17.55	3.37^{NS}
t-value	305.85$^{NS'}$	792.98$^{NS'}$	32.15$^{NS'}$	111.81**	

a,b,c,d - within Virus and positive control, between different time periods means differ non-significantly ($p<0.05$)
*Overall non-significant difference within Virus ($p<0.01$)
NS- Overall non-significant difference within negative control
**Significant difference between the Virus and negative control at the same time period ($p<0.01$)
NS' No Significant difference between the Virus and negative control at the same time period

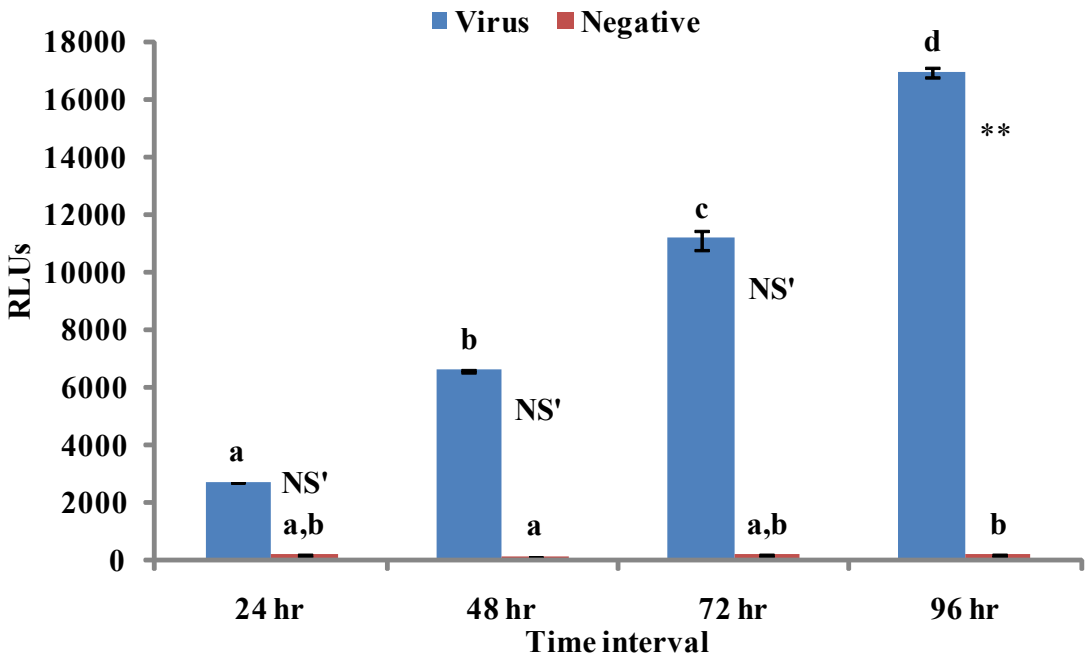

Fig. 4.78: Caspase-8 expression in B95a cells infected with Virus and negative control. The RLUs were recorded for different time intervals post treatment

Table 4.63: Caspase-Glo 9 assay analyses for caspase-9 expression in positive and negative controls. The RLUs were recorded for different time intervals post treatment

Time Construct	24 hr	48 hr	72 hr	96 hr	F-value
Positive	81209.54[a] ±4315.95	125037.38[c] ±5678.23	91351.32[a,b] ±4691.70	106012.63[b,c] ±6241.10	12.96**
Negative	308.83[a] ±55.72	344.30[a] ±23.29	312.11[a] ±28.14	344.44[a] ±4.92	0.34[NS]
t- value	18.74*	21.96*	19.40*	16.93*	

a, b, c - within positive and negative control, between different time periods means differ significantly ($p<0.05$)
**Overall significant difference within positive control ($p<0.05$)
* Significant difference between positive and negative control at the same time period ($p<0.05$)
NS- Overall non-significant difference within negative control

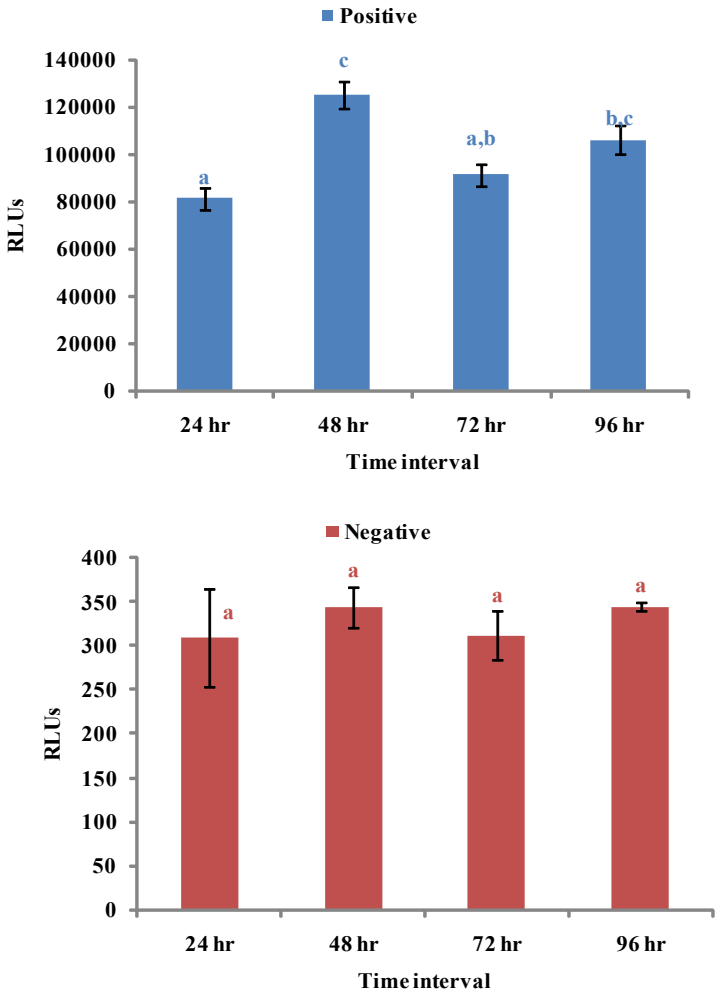

Fig. 4.79: Caspase-9 expression in B95a cells positive and negative control.
The RLUs were recorded for different time intervals post treatment

Table 4.64: Caspase-Glo 9 assay analyses for caspase-9 expression in B95a cells transfected with S2 construct and positive control. The RLUs were recorded for different time intervals

Time Construct	24 hr	48 hr	72 hr	96 hr	F-value
S2	111734.25[a] ±6425.33	131400.08[a] ±8614.80	199973.60[b] ± 13542.44	214525.46[b] ±13834.18	20.77***
Positive	81209.54[a] ±4315.95	125037.38[c] ±5678.23	91351.32[a,b] ±4691.70	106012.63[b,c] ±6241.10	12.96**
t- value	3.94NS	0.61NS	7.57*	7.15*	

a, b, c- within S2 construct and positive control, between different time periods means differ significantly ($p<0.05$)
***Overall significant difference within S2 construct ($p<0.01$)
** Overall significant difference within positive control ($p<0.05$)
* Significant difference between the S2 construct and positive control at the same time period ($p<0.05$)
NS- No Significant difference between the S2 construct and positive control at the same time period

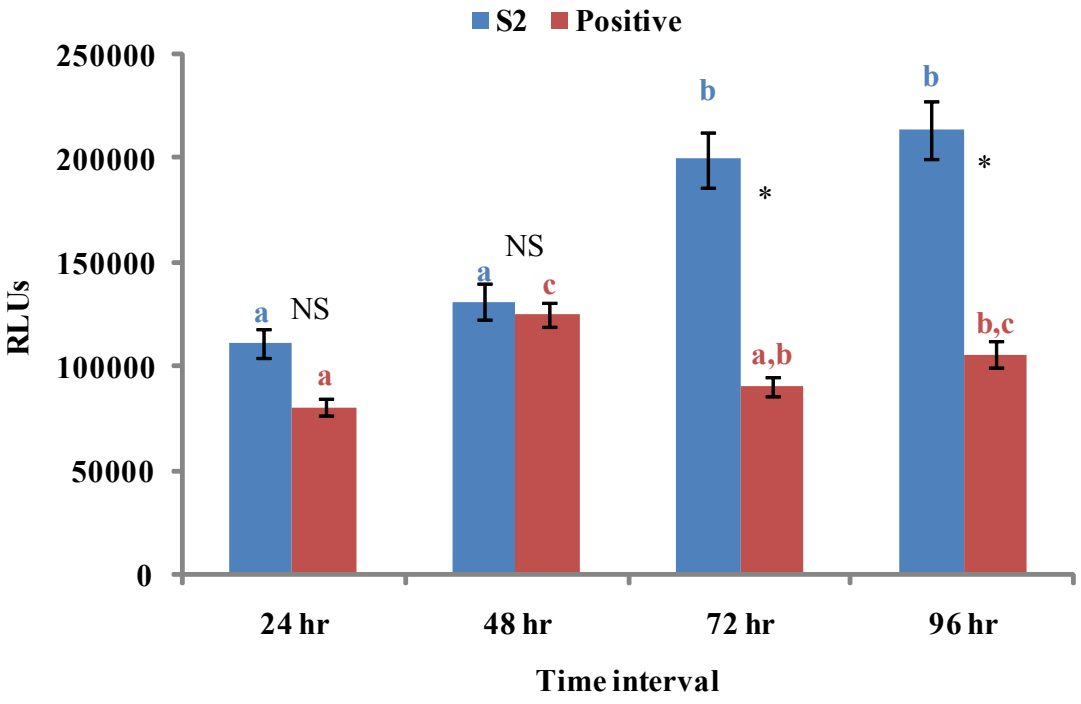

Fig. 4.80: Caspase-9 expression in B95a cells transfected with S2 construct and positive control.
The RLUs were recorded for different time intervals post treatment

Table 4.65: Caspase-Glo 9 assay analyses for caspase-9 expression in B95a cells transfected with S2 construct and negative control. The RLUs were recorded for different time intervals

Time / Construct	24 hr	48 hr	72 hr	96 hr	F-value
S2	111734.25[a] ±6425.33	131400.08[a] ±8614.80	199973.60[b] ± 13542.44	214525.46[b] ±13834.18	20.77**
Negative	308.83[a] ±55.72	344.30[a] ±23.29	312.11[a] ±28.14	344.44[a] ±4.92	0.34[NS]
t- value	17.34*	15.21*	14.74*	15.48*	

a, b - within S2 construct and negative control, between different time periods means differ significantly ($p<0.05$)
**Overall significant difference within S2 construct ($p<0.01$)
* Significant difference between the S2 construct and negative control at the same time period ($p<0.05$)
NS- Overall non-significant difference within negative control

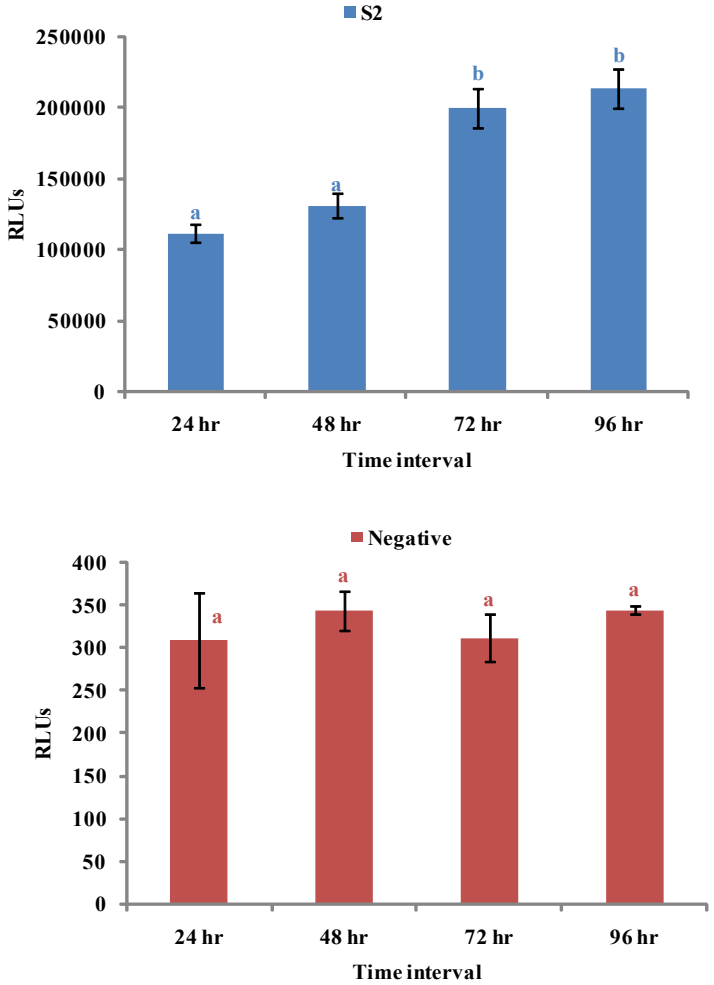

Fig. 4.81: Caspase-9 expression in B95a cells transfected with S2 construct and negative control.

The RLUs were recorded for different time intervals post treatment

Table 4.66: Caspase-Glo 9 assay analyses for caspase-9 expression in B95a cells transfected with S2 construct and B95a cells transfected with V gene construct. The RLUs were recorded for different time intervals

Time Construct	24 hr	48 hr	72 hr	96 hr	F-value
S2	111734.25[a] ±6425.33	131400.08[a] ±8614.80	199973.60[b] ± 13542.44	214525.46[a] ±13834.18	20.77*
V Gene	133177.80[a] ±9559.13	126817.90[a] ±7038.98	155695.75[a] ± 11779.54	233802.51[b] ±13696.46	20.72*
t- value	-1.86[NS]	0.41[NS]	2.46[NS]	-0.99[NS]	

a, b - within S2 and V gene, between different time periods means differ significantly ($p<0.05$)
*Overall significant difference within S2 and V gene ($p<0.01$)
NS- No Significant difference between the S2 and V gene at the same time period

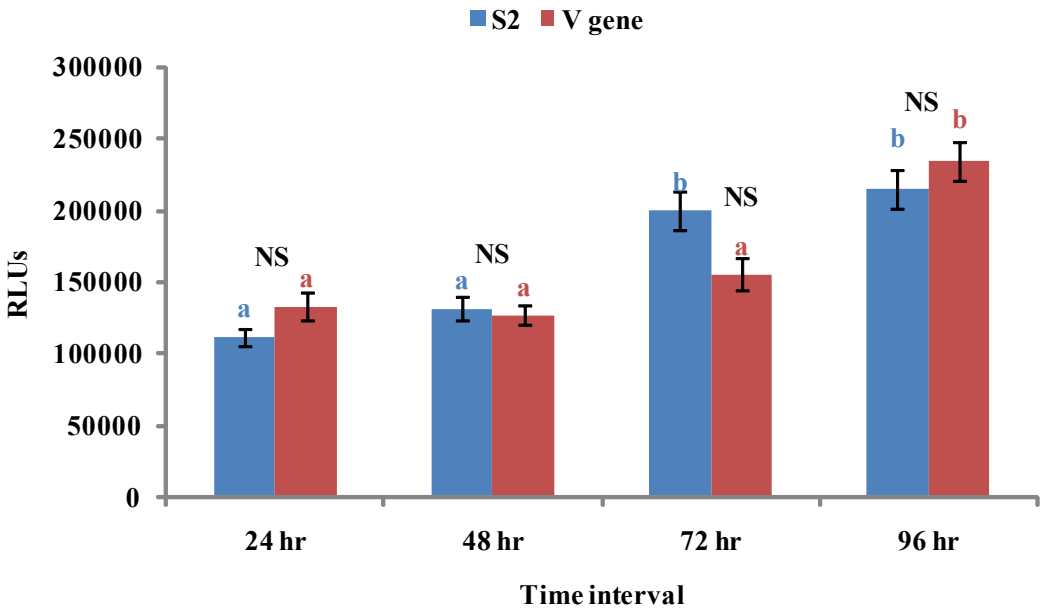

Fig. 4.82: Caspase-9 expression in B95a cells transfected with S2 construct and B95a cells transfected with V gene construct.
The RLUs were recorded for different time intervals post treatment

Table 4.67: Caspase-Glo 9 assay analyses for caspase-9 expression in B95a cells transfected with S2 construct and B95a cells co-transfected with S2/V gene construct. The RLUs were recorded for different time intervals

Time Construct	24 hr	48 hr	72 hr	96 hr	F- value
S2	111734.25[a] ±6425.33	131400.08[a] ±8614.80	199973.60[b] ± 13542.44	214525.46[b] ±13834.18	20.77**
S2/V gene	85692.36[a] ±5101.019	214027.16[b] ±12959.32	237148.30[b] ± 14029.71	217835.65[b] ±12477.42	35.21**
t- value	3.17[NS]	-5.31*	-1.9[NS]	-0.17[NS]	

a, b - within S2 and S2/V gene, between different time periods means differ significantly ($p<0.05$)
**Overall significant difference within S2 and S2/V gene ($p<0.01$)
*Significant difference between the S2 and S2/V gene at the same time period ($p<0.05$)
NS- No Significant difference between the S2 and S2/V gene at the same time period

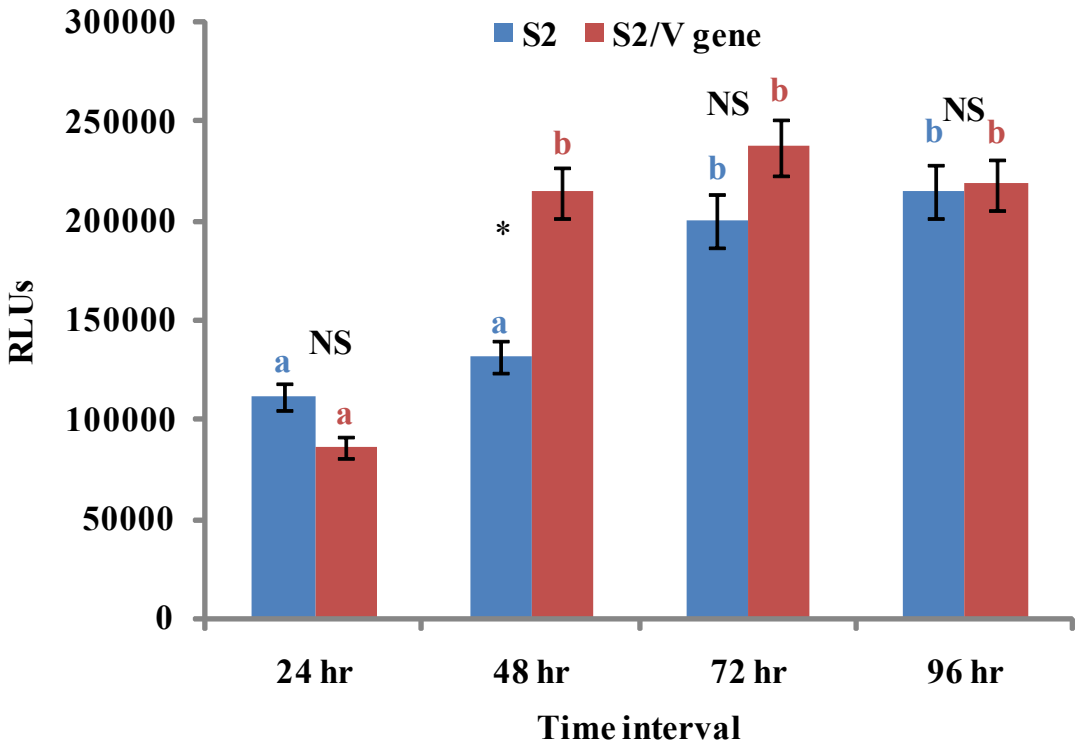

Fig. 4.83: Caspase-9 expression in B95a cells transfected with S2 construct and B95a cells co-transfected with S2/V gene construct.
The RLUs were recorded for different time intervals post treatment

Table 4.68: Caspase-Glo 9 assay analyses for caspase-9 expression in B95a cells transfected with S2 construct and B95a cells co-transfected with S2/Virus construct. The RLUs were recorded for different time intervals

Time Construct	24 hr	48 hr	72 hr	96 hr	F-value
S2	111734.25[a] ±6425.33	131400.08[a] ±8614.80	199973.60[b] ±13542.44	214525.46[b] ±13834.18	20.77*
S2/Virus	116281.31[a] ±4904.12	122674.39[a] ±7099.42	165500.94[b] ±9423.50	195023.21[b] ±12252.78	17.66*
t-value	-0.56[NS]	0.78[NS]	2.08[NS]	1.05[NS]	

a, b - within S2 and S2/Virus, between different time periods means differ significantly ($p<0.05$)
*Overall significant difference within S2 and S2/Virus ($p<0.01$)
NS- No Significant difference between the S2 and S2/Virus at the same time period

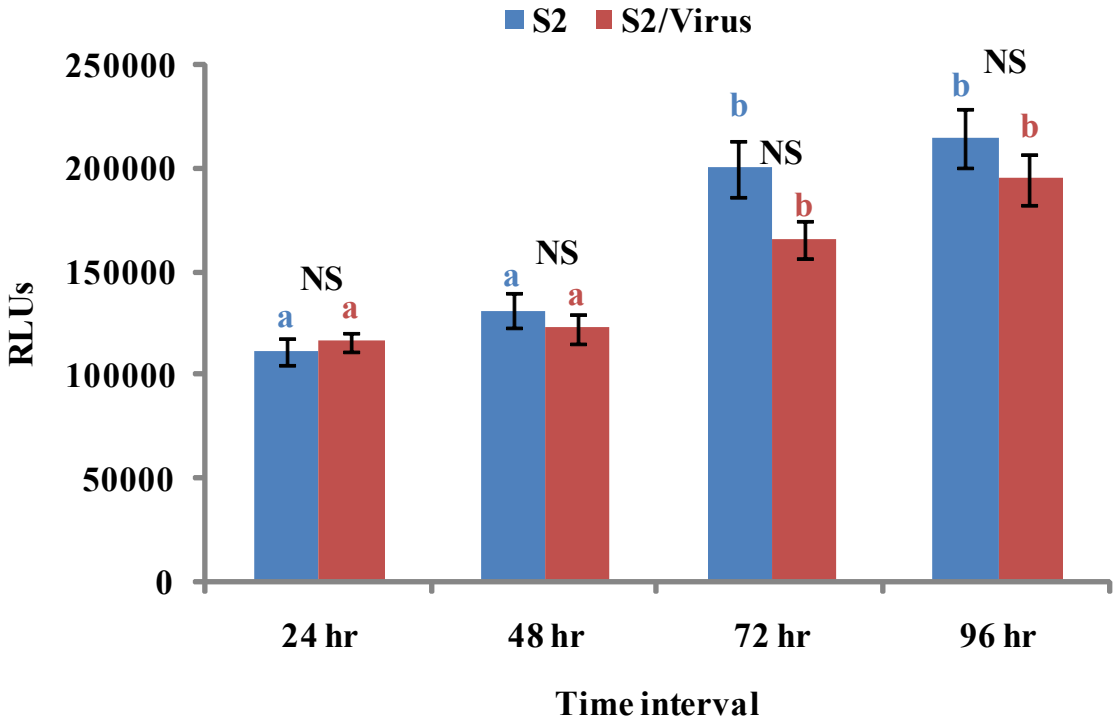

Fig. 4.84: Caspase-9 expression in B95a cells transfected with S2 construct and B95a cells co-transfected with S2/Virus construct.
The RLUs were recorded for different time intervals post treatment

Table 4.69: Caspase-Glo 9 assay analyses for caspase-9 expression in B95a cells transfected with S2 construct and B95a cells infected with virus. The RLUs were recorded for different time intervals

Time Construct	24 hr	48 hr	72 hr	96 hr	F-value
S2	111734.25[a] ±6425.33	131400.08[a] ±8614.80	199973.60[b] ±13542.44	214525.46[b] ±13834.18	20.77**
Virus	100855.10[a,b] ±4238.08	72709.93[a] ±4600.83	110537.07[b] ±6604.79	219195.75[c] ±11639.86	75.73**
t-value	1.41[NS]	6.00*	5.93*	-0.25[NS]	

a, b,c - within S2 and Virus, between different time periods means differ significantly ($p<0.05$)
**Overall significant difference within S2 and Virus ($p<0.01$)
*Significant difference between the S2 and Virus at the same time period ($p<0.05$)
NS- No Significant difference between the S2 and Virus at the same time period

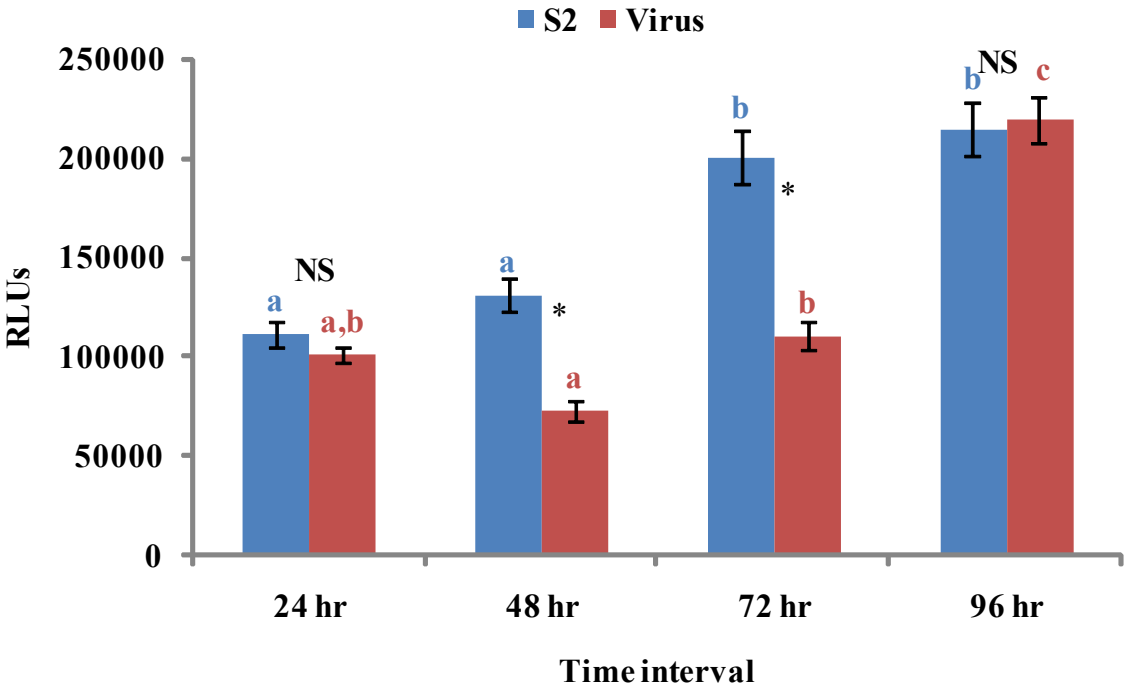

Fig. 4.85: Caspase-9 expression in B95a cells transfected with S2 construct and B95a cells infected with virus.
The RLUs were recorded for different time intervals post treatment

Table 4.70: Caspase-Glo 9 assay analyses for caspase-9 expression in B95a cells transfected with V gene construct and positive control. The RLUs were recorded for different time intervals

Time Construct	24 hr	48 hr	72 hr	96 hr	F-value
V Gene	133177.80[a] ±9559.13	126817.90[a] ±7038.98	155695.75[a] ± 11779.54	233802.51[b] ±13696.46	20.72***
Positive	81209.54[a] ±4315.95	125037.38[a] ±5678.23	91351.32[a,b] ±4691.70	106012.63[b,c] ±6241.10	12.96**
t- value	4.95*	0.19NS	5.07*	8.49*	

a, b, c- within V gene and positive control, between different time periods means differ significantly ($p<0.05$)
***Overall significant difference within V gene ($p<0.01$)
** Overall significant difference within positive control ($p<0.05$)
* Significant difference between the V gene and positive control at the same time period ($p<0.05$)
NS- No Significant difference between the V gene and positive control at the same time period

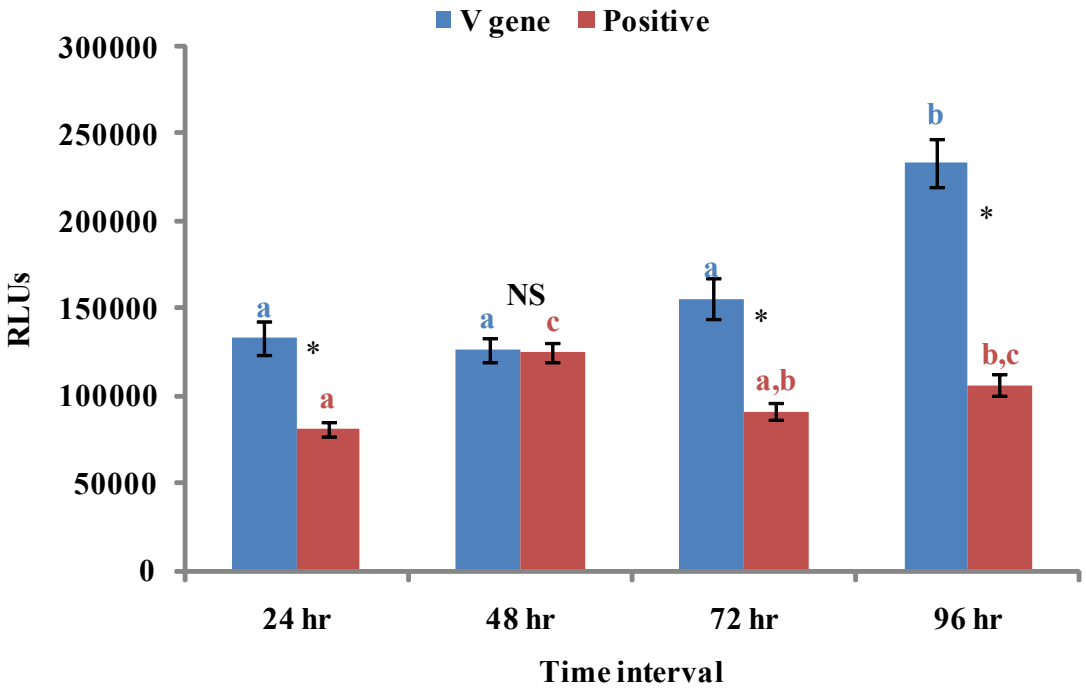

Fig. 4.86: Caspase-9 expression in B95a cells transfected with V gene construct and positive control.
The RLUs were recorded for different time intervals post treatment

Table 4.71: Caspase-Glo 9 assay analyses for caspase-9 expression in B95a cells transfected with V gene construct and negative control. The RLUs were recorded for different time intervals

Time Construct	24 hr	48 hr	72 hr	96 hr	F-value
V Gene	133177.80^{a} ±9559.13	126817.90^{a} ±7038.98	155695.75^{a} ± 11779.54	233802.51^{B} ±13696.46	20.72**
Negative	308.83^{a} ±55.72	344.30^{a} ±23.29	312.11^{a} ±28.14	344.44^{a} ±4.92	0.34^{NS}
t-value	13.89*	17.96*	13.19*	17.04*	

a, b - within V gene and negative control, between different time periods means differ significantly ($p<0.05$)
**Overall significant difference within V gene ($p<0.01$)
*Significant difference between the V gene and negative control at the same time period ($p<0.01$)
NS- Overall non-significant difference within negative control

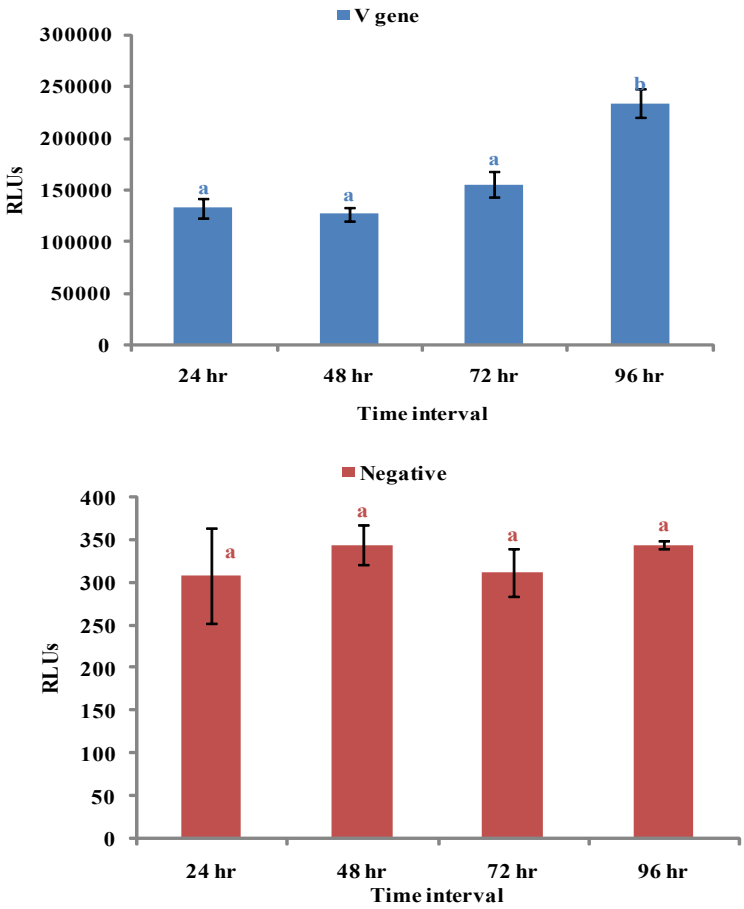

Fig. 4.87: Caspase-9 expression in B95a cells transfected with V gene construct and negative control.

The RLUs were recorded for different time intervals post treatment

Table 4.72: Caspase-Glo 9 assay analyses for caspase-9 expression in B95a cells transfected with V gene construct and B95a cells co-transfected with S2/V gene construct. The RLUs were recorded for different time intervals

Time / Construct	24 hr	48 hr	72 hr	96 hr	F- value
V Gene	133177.80[a] ±9559.13	126817.90[a] ±7038.98	155695.75[a] ± 11779.54	233802.51[b] ±13696.46	20.72**
S2/V Gene	85692.36[a] ±5101.019	214027.16[b] ±12959.32	237148.30[b] ± 14029.71	217835.65[b] ±12477.42	35.21**
t- value	4.38*	-5.91*	-4.44*	0.86[NS]	

a, b - within V gene and S2/V gene, between different time periods means differ significantly ($p<0.05$)
**Overall significant difference within V gene and S2/V gene ($p<0.01$)
*Significant difference between the V gene and S2/V gene at the same time period ($p<0.05$)
NS- No Significant difference between the V gene and S2/V gene at the same time period

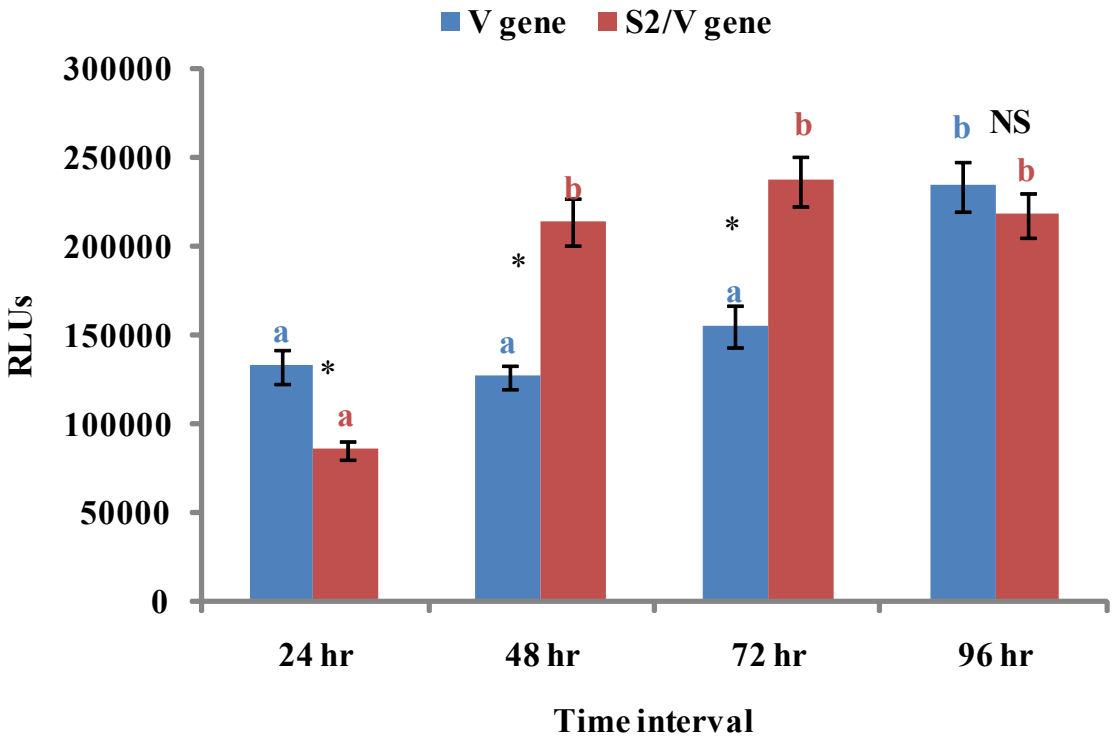

Fig. 4.88: Caspase-9 expression in B95a cells transfected with V gene construct and B95a cells co-transfected with S2/V gene construct.
The RLUs were recorded for different time intervals post treatment

Table 4.73: Caspase-Glo 9 assay analyses for caspase-9 expression in B95a cells transfected with V gene construct and B95a cells co-transfected with S2/ Virus construct. The RLUs were recorded for different time interval

Time / Construct	24 hr	48 hr	72 hr	96 hr	F- value
V Gene	133177.80[a] ±9559.13	126817.90[a] ±7038.98	155695.75[a] ± 11779.54	233802.51[b] ±13696.46	20.72*
S2/Virus	116281.31[a] ±4904.12	122674.39[a] ±7099.42	165500.94[b] ± 9423.50	195023.21[b] ±12252.78	17.66*
t- value	1.57[NS]	0.41[NS]	-0.65[NS]	2.11[NS]	

a, b - within V gene and S2/Virus, between different time periods means differ significantly ($p<0.05$)
*Overall significant difference within V gene and S2/Virus ($p<0.01$)
NS- No Significant difference between the V gene and S2/Virus at the same time period

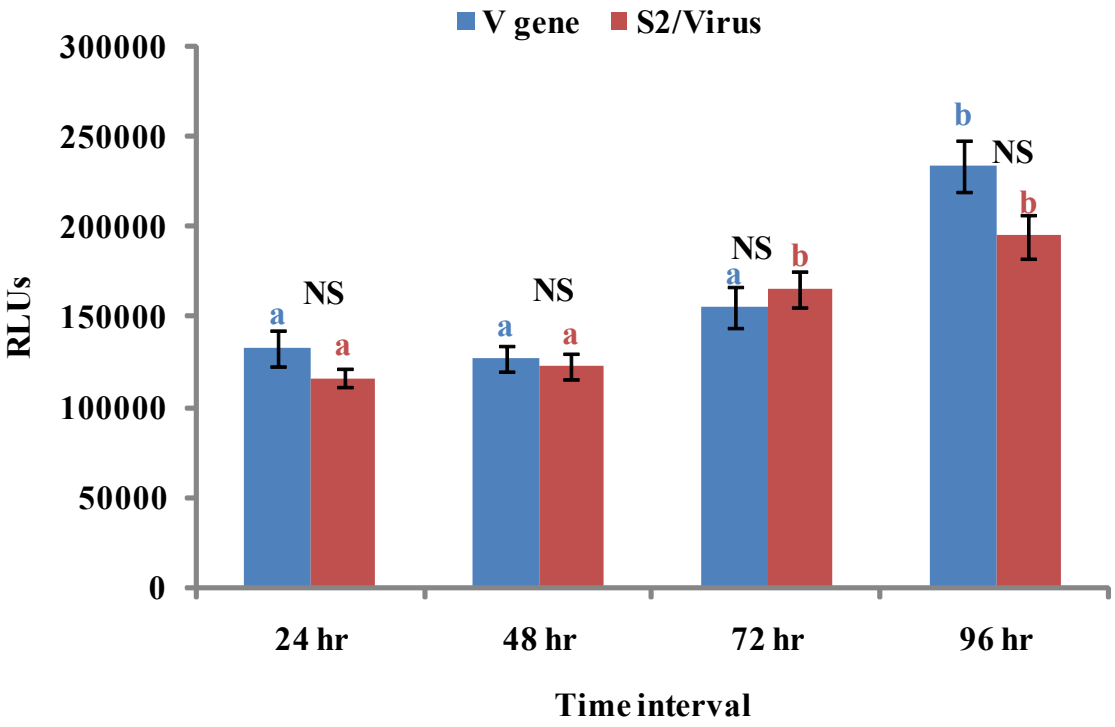

Fig. 4.89: Caspase-9 expression in B95a cells transfected with V gene construct and B95a cells co-transfected with S2/Virus construct.
The RLUs were recorded for different time intervals post treatment

Table 4.74: Caspase-Glo 9 assay analyses for caspase-9 expression in B95a cells transfected with V gene construct and B95a cells infected with virus. The RLUs were recorded for different time intervals

Time Construct	24 hr	48 hr	72 hr	96 hr	F-value
V Gene	133177.80[a] ±9559.13	126817.90[a] ±7038.98	155695.75[a] ± 11779.54	233802.51[b] ±13696.46	20.72**
Virus	100855.10[a,b] ±4238.08	72709.93[a] ±4600.83	110537.07[b] ± 6604.79	219195.75[c] ±11639.86	75.73**
t- value	3.09[NS]	6.43*	3.34[NS]	0.81[NS]	

a, b,c- within V gene and Virus, between different time periods means differ significantly ($p<0.05$)
**Overall significant difference within V gene and Virus ($p<0.01$)
*Significant difference between the V gene and Virus at the same time period ($p<0.05$)
NS- No Significant difference between the V gene and Virus at the same time period

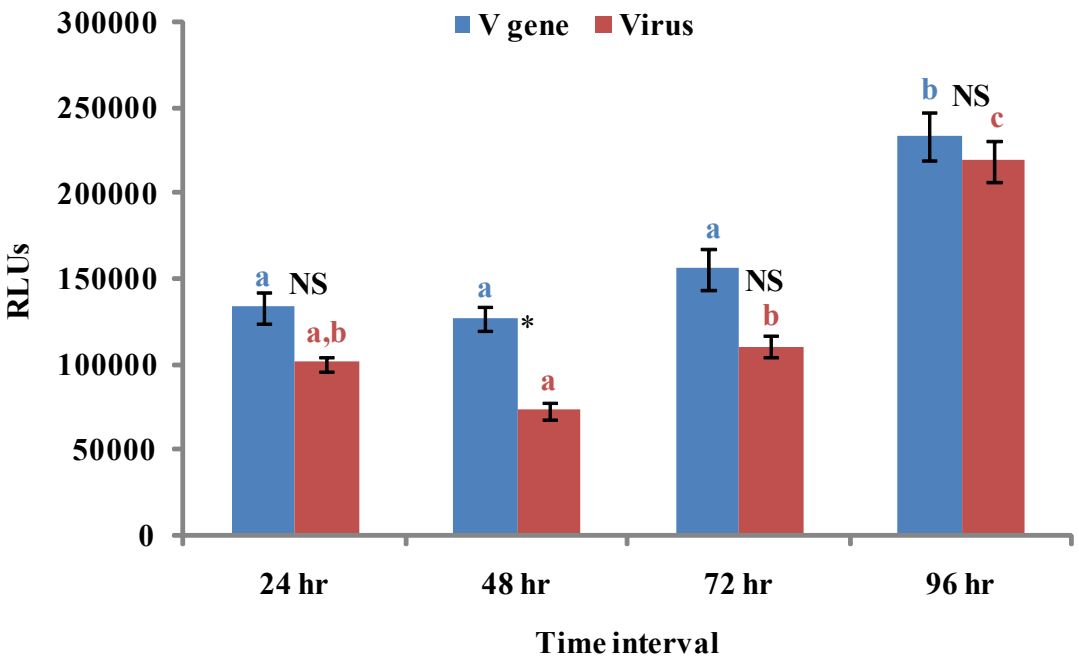

Fig. 4.90: Caspase-9 expression in B95a cells transfected with V gene construct and B95a cells infected with Virus.
The RLUs were recorded for different time intervals post treatment

Table 4.75: Caspase-Glo 9 assay analyses for caspase-9 expression in B95a cells co-transfected with S2/V gene construct and positive control. The RLUs were recorded for different time intervals

Time Construct	24 hr	48 hr	72 hr	96 hr	F-value
S2/V Gene	85692.36[a] ±5101.019	214027.16[b] ±12959.32	237148.30[b] ± 14029.71	217835.65[b] ±12477.42	35.21***
Positive	81209.54[a] ±4315.95	125037.38[c] ±5678.23	91351.32[a,b] ±4691.70	106012.63[b,c] ±6241.10	12.96**
t- value	0.67[NS]	6.29*	9.85*	8.01*	

a, b, c- within S2/V gene and positive control, between different time periods means differ significantly ($p<0.05$)
***Overall significant difference within S2/V gene ($p<0.01$)
** Overall significant difference within positive control ($p<0.05$)
* Significant difference between the S2/V gene and positive control at the same time period ($p<0.05$)
NS- No Significant difference between the S2/V gene and positive control at the same time period

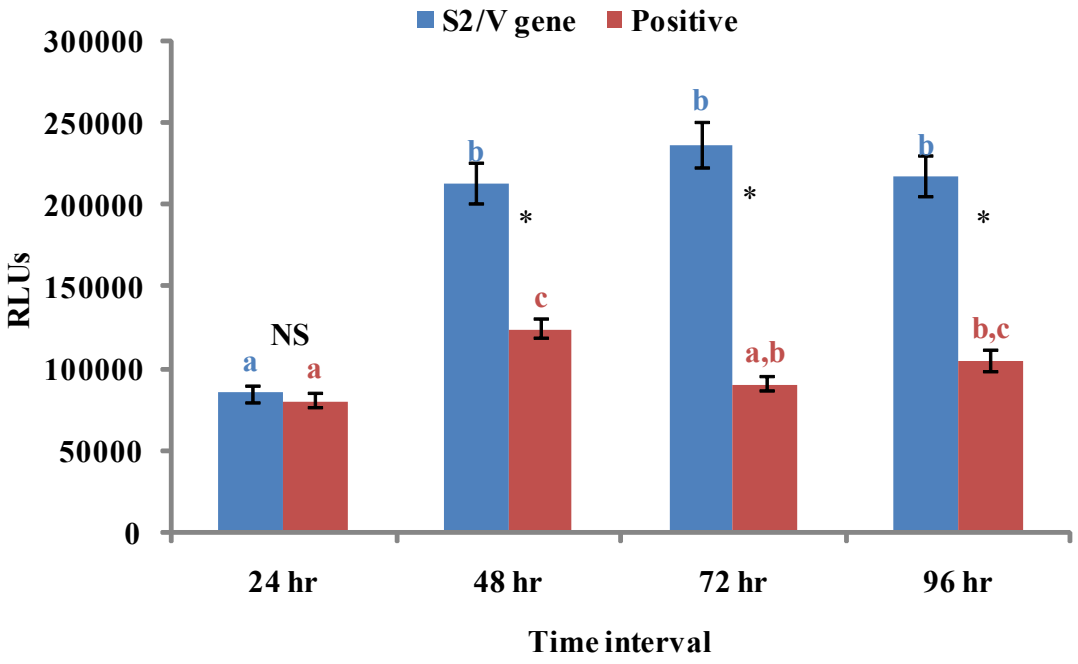

Fig. 4.91: Caspase-9 expression in B95a cells co-transfected with S2/V gene construct and positive control.
The RLUs were recorded for different time intervals post treatment

Table 4.76: Caspase-Glo 9 assay analyses for caspase-9 expression in B95a cells co-transfected with S2/V gene construct and negative control. The RLUs were recorded for different time intervals

Time Construct	24 hr	48 hr	72 hr	96 hr	F-value
S2/V Gene	85692.36[a] ±5101.019	214027.16[b] ±12959.32	237148.30[b] ± 14029.71	217835.65[b] ±12477.42	35.21**
Negative	308.83[a] ±55.72	344.30[a] ±23.29	312.11[a] ±28.14	344.44[a] ±4.92	0.34[NS]
t- value	16.73*	16.48*	16.88*	17.43*	

a, b - within S2/V gene and negative control, between different time periods means differ significantly ($p<0.05$)
**Overall significant difference within S2/V gene ($p<0.01$)
*Significant difference between the S2/V gene and negative control at the same time period ($p<0.01$)
NS- Overall non-significant difference within negative control

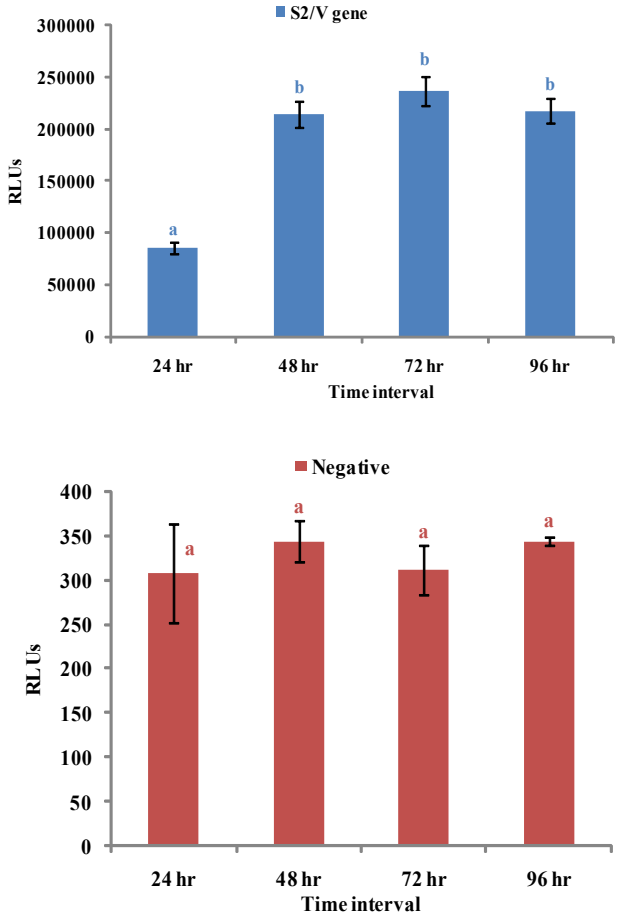

Fig. 4.92: Caspase-9 expression in B95a cells co-transfected with S2/V gene construct and negative control.

The RLUs were recorded for different time intervals post treatment

Table 4.77: Caspase-Glo 9 assay analyses for caspase-9 expression in B95a cells co-transfected with S2/V gene construct and B95a cells co-transfected with S2/Virus. The RLUs were recorded for different time intervals

Time Construct	24 hr	48 hr	72 hr	96 hr	F-value
S2/V Gene	85692.36^{a} ±5101.019	214027.16^{b} ±12959.32	237148.30^{b} ± 14029.71	217835.65^{b} ±12477.42	35.21**
S2/Virus	116281.31^{a} ±4904.12	122674.39^{a} ±7099.42	165500.94^{b} ± 9423.50	195023.21^{b} ±12252.78	17.66**
t-value	-4.32^{NS}	6.18*	4.23^{NS}	1.30^{NS}	

a, b,- within S2/V gene and S2/Virus, between different time periods means differ significantly ($p<0.05$)
**Overall significant difference within S2/V gene and S2/Virus ($p<0.01$)
*Significant difference between the S2/V gene and S2/Virus at the same time period ($p<0.05$)
NS- No Significant difference between the S2/V gene and S2/Virus at the same time period

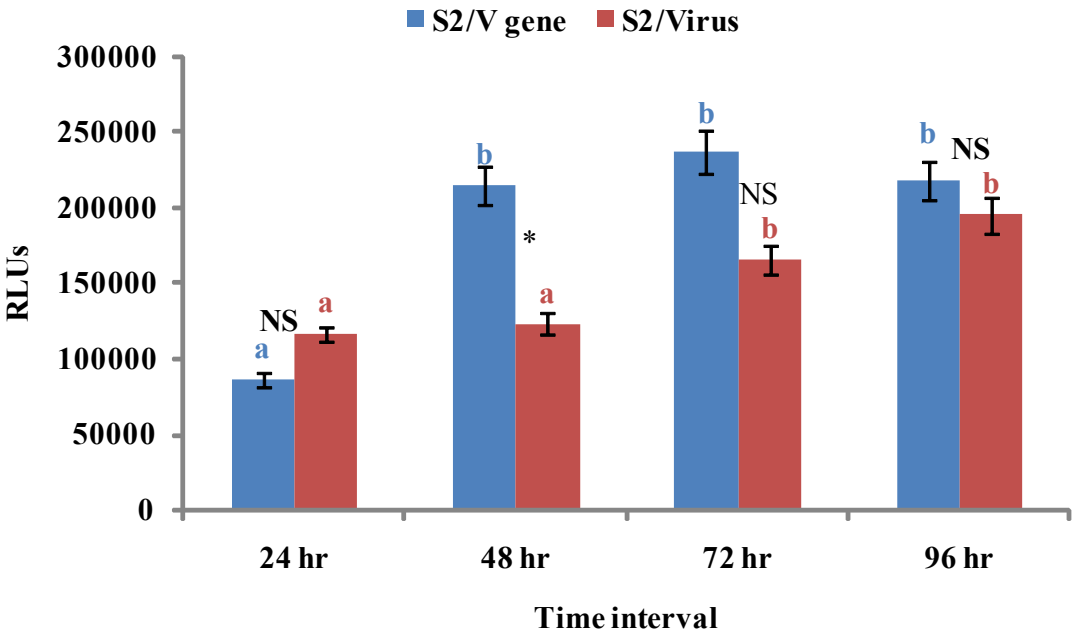

Fig. 4.93: Caspase-9 expression in B95a cells co-transfected with S2/V gene construct and B95a cells co-transfected with S2/Virus.
The RLUs were recorded for different time intervals post treatment

Table 4.78: Caspase-Glo 9 assay analyses for caspase-9 expression in B95a cells co-transfected with S2/V gene construct and B95a cells infected with Virus. The RLUs were recorded for different time intervals

Time Construct	24 hr	48 hr	72 hr	96 hr	F-value
S2/V Gene	85692.36^{a} ±5101.019	214027.16^{b} ±12959.32	237148.30^{b} ± 14029.71	217835.65^{b} ±12477.42	35.21**
Virus	100855.10^{a,b} ±4238.08	72709.93^{a} ±4600.83	110537.07^{b} ± 6604.79	219195.75^{c} ±11639.86	75.73**
t- value	-2.28^{NS}	10.27*	8.16*	0.08^{NS}	

a, b, c- within S2/V gene and Virus, between different time periods means differ significantly ($p<0.05$)
**Overall significant difference within S2/V gene and Virus ($p<0.01$)
*Significant difference between the S2/V gene and Virus at the same time period ($p<0.05$)
NS- No Significant difference between the S2/V gene and Virus at the same time period

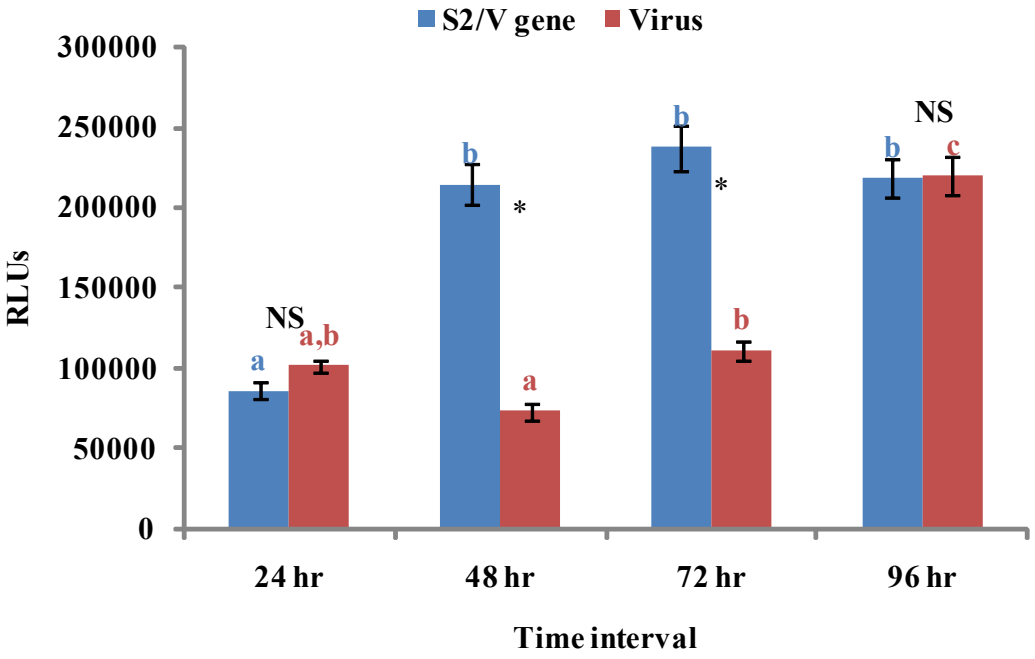

Fig. 4.94: Caspase-9 expression in B95a cells co-transfected with S2/V gene construct and B95a cells infected with Virus.
The RLUs were recorded for different time intervals post treatment

Table 4.79: Caspase-Glo 9 assay analyses for caspase-9 expression in B95a cells co-transfected with S2/Virus and Positive. The RLUs were recorded for different time intervals

Time / Construct	24 hr	48 hr	72 hr	96 hr	F-value
S2/Virus	116281.31[a] ±4904.12	122674.39[a] ±7099.42	165500.94[b] ±9423.50	195023.21[b] ±12252.78	17.66***
Positive	81209.54[a] ±4315.95	125037.38[c] ±5678.23	91351.32[a,b] ±4691.70	106012.63[b,c] ±6241.10	12.96**
t-value	5.36*	-0.26[NS]	7.04*	6.47*	

a, b, c- within S2/Virus and positive control, between different time periods means differ significantly ($p<0.05$)
***Overall significant difference within S2/Virus ($p<0.01$)
** Overall significant difference within positive control ($p<0.05$)
* Significant difference between the S2/Virus and positive control at the same time period ($p<0.05$)

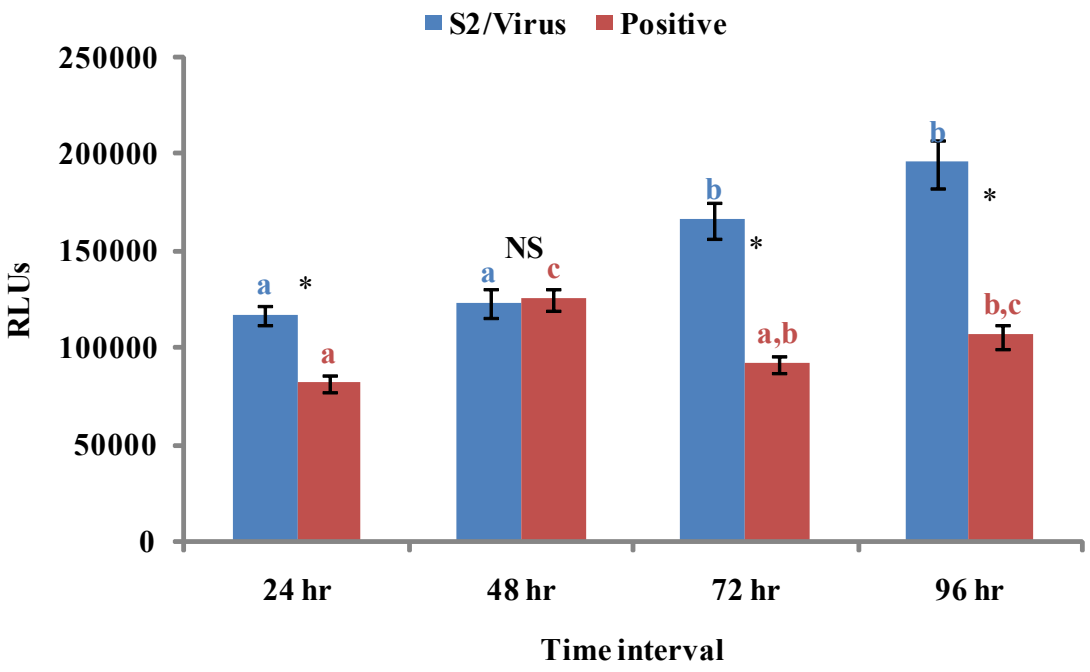

Fig. 4.95: Caspase-9 expression in B95a cells co-transfected with S2/Virus and Positive control.
The RLUs were recorded for different time intervals post treatment

Table 4.80: Caspase-Glo 9 assay analyses for caspase-9 expression in B95a cells co-transfected with S2/Virus and negative control. The RLUs were recorded for different time intervals

Time / Construct	24 hr	48 hr	72 hr	96 hr	F-value
S2/Virus	116281.31[a] ±4904.12	122674.39[a] ±7099.42	165500.94[b] ±9423.50	195023.21[b] ±12252.78	17.66**
Negative	308.83[a] ±55.72	344.30[a] ±23.29	312.11[a] ±28.14	344.44[a] ±4.92	0.34[NS]
t-value	23.64*	17.23*	17.52*	15.88*	

a, b - within S2/Virus and negative control, between different time periods means differ significantly ($p<0.05$)
**Overall significant difference within S2/Virus ($p<0.01$)
*Significant difference between the S2/Virus and negative control at the same time period ($p<0.01$)
NS- Overall non-significant difference within negative control

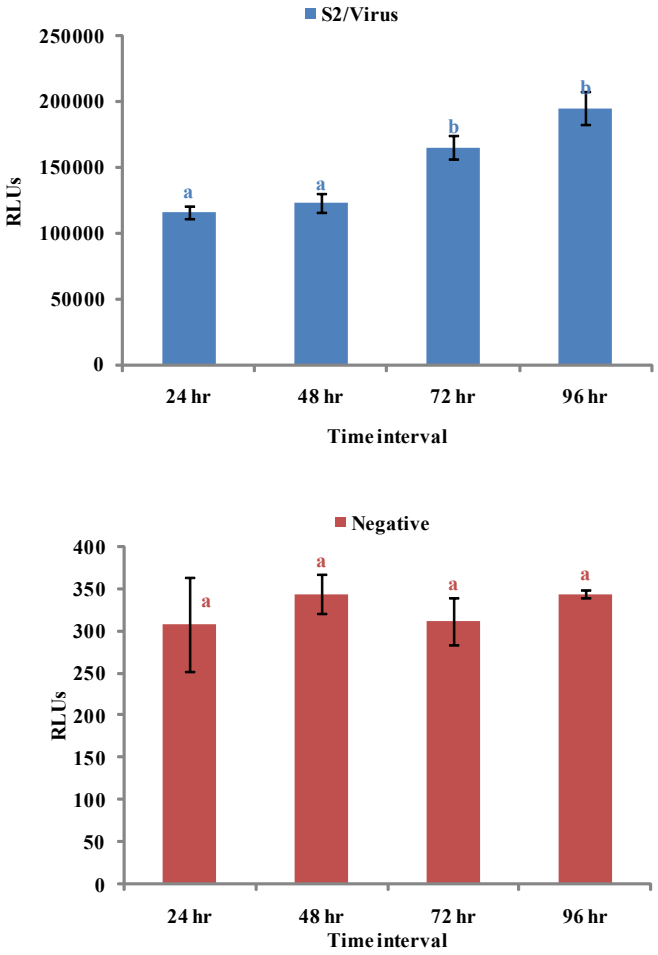

Fig. 4.96: Caspase-9 expression in B95a cells co-transfected with S2/Virus and negative control.

The RLUs were recorded for different time intervals post treatment

Table 4.81: Caspase-Glo 9 assay analyses for caspase-9 expression in B95a cells co-transfected with S2/Virus and B95a cells infected with Virus. The RLUs were recorded for different time intervals

Time Construct	24 hr	48 hr	72 hr	96 hr	F-value
S2/Virus	116281.31[a] ±4904.12	122674.39[a] ±7099.42	165500.94[b] ±9423.50	195023.21[b] ±12252.78	17.66**
Virus	100855.10[a,b] ±4238.08	72709.93[a] ±4600.83	110537.07[b] ±6604.79	219195.75[c] ±11639.86	75.73**
t-value	2.38[NS]	5.90*	4.77*	-1.43[NS]	

a, b, c - within S2/Virus and Virus, between different time periods means differ significantly ($p<0.05$)
**Overall significant difference within S2/Virus and Virus ($p<0.01$)
*Significant difference between the S2/Virus and Virus at the same time period ($p<0.05$)
NS- No Significant difference between the S2/Virus and Virus at the same time period

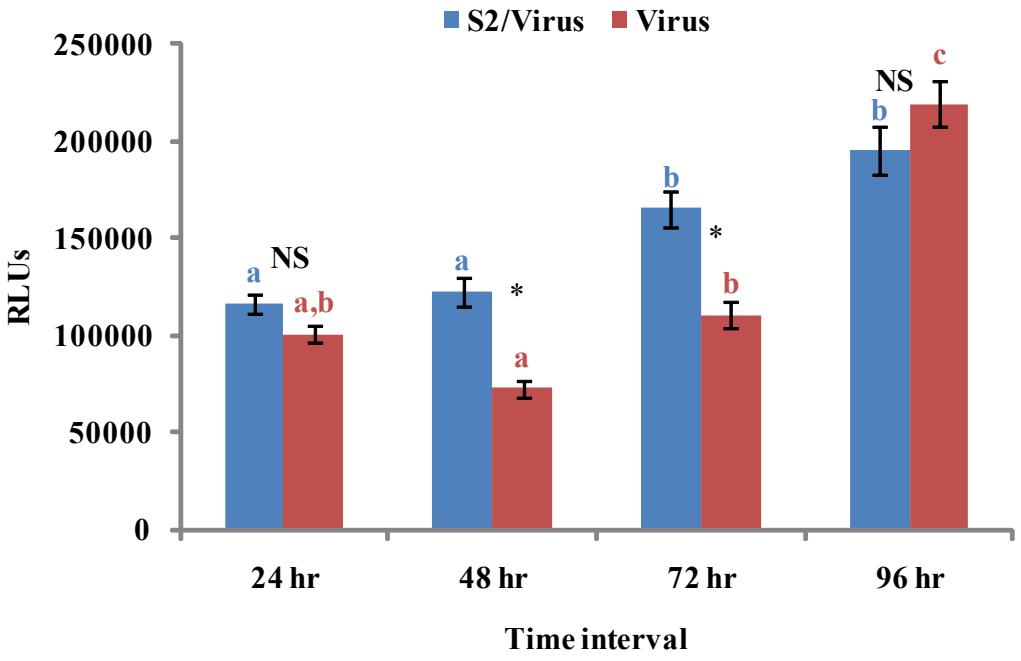

Fig. 4.97: Caspase-9 expression in B95a cells co-transfected with S2/Virus and B95a cells infected with Virus.
The RLUs were recorded for different time intervals post treatment

Table 4.82: Caspase-Glo 9 assay analyses for caspase-9 expression in B95a cells infected with Virus and positive control. The RLUs were recorded for different time intervals

Time Construct	24 hr	48 hr	72 hr	96 hr	F-value
Virus	$100855.10^{a,b}$ ±4238.08	72709.93^{a} ±4600.83	110537.07^{b} ±6604.79	219195.75^{c} ±11639.86	75.73***
Positive	81209.54^{a} ±4315.95	125037.38^{c} ±5678.23	$91351.32^{a,b}$ ±4691.70	$106012.63^{b,c}$ ±6241.10	12.96**
t-value	3.24^{NS}	-7.16*	2.36^{NS}	8.57*	

a, b, c- within Virus and positive control, between different time periods means differ significantly ($p<0.05$)
***Overall significant difference within Virus ($p<0.01$)
**Overall significant difference within positive control ($p<0.05$)
*Significant difference between the Virus and positive control at the same time period ($p<0.05$)
NS- No Significant difference between the Virus and positive control at the same time period

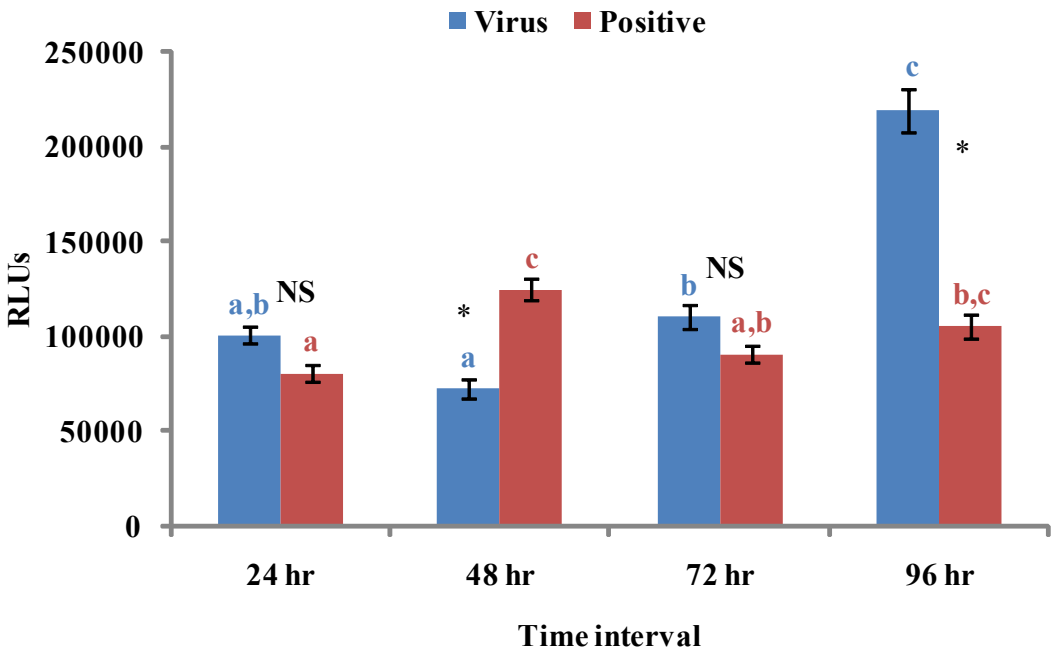

Fig. 4.98: Caspase-9 expression in B95a cells infected with Virus and positive control. The RLUs were recorded for different time intervals post treatment

Table 4.83: Caspase-Glo 9 assay analyses for caspase-9 expression in B95a cells infected with Virus and negative control. The RLUs were recorded for different time intervals

Time Construct	24 hr	48 hr	72 hr	96 hr	F-value
Virus	$100855.10^{a,b}$ ±4238.08	72709.93^{a} ±4600.83	110537.07^{b} ±6604.79	219195.75^{c} ±11639.86	75.73**
Negative	308.83^{a} ±55.72	344.30^{a} ±23.29	312.11^{a} ±28.14	344.44^{a} ±4.92	0.34^{NS}
t-value	23.72*	15.72*	16.68*	18.80*	

a, b, c - within Virus and negative control, between different time periods means differ significantly ($p<0.05$)
**Overall significant difference within Virus ($p<0.01$)
*Significant difference between the Virus and negative control at the same time period ($p<0.01$)
NS- Overall non-significant difference within negative control

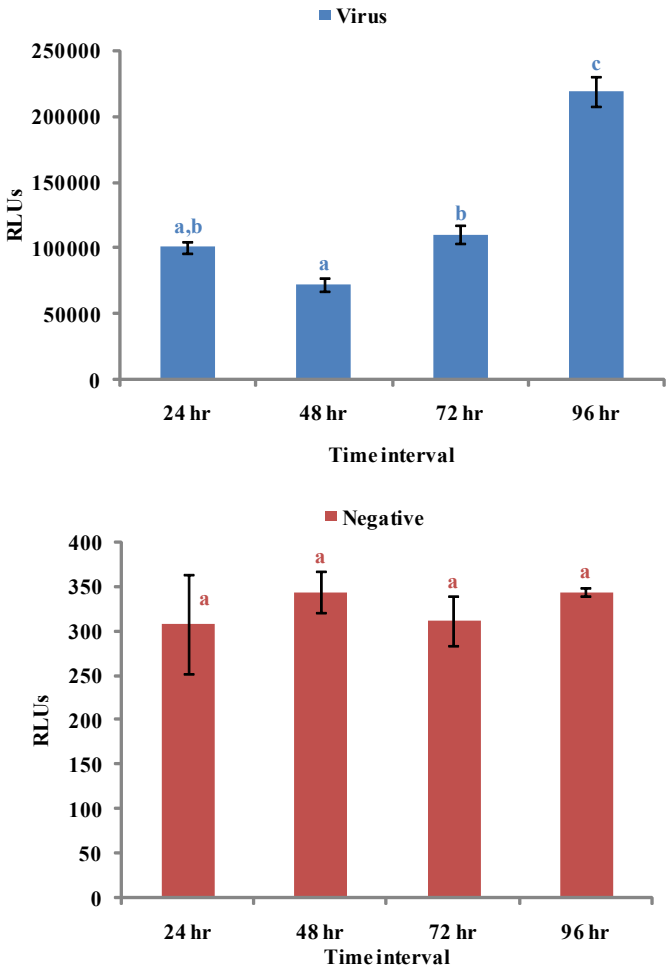

Fig. 4.99: Caspase-9 expression in B95a cells infected with Virus and negative control. The RLUs were recorded for different time intervals post treatment

Discussion

5 DISCUSSION

Peste des petits ruminants (PPR), also known as 'goat plague', is a trans-boundary and enzootic viral disease characterized by fever, sores in the mouth, diarrhea, pneumonia, and sometimes death. Cattle and several wild ruminants have been infected most often experimentally, but goats and sheep are the usual targets. This disease is prevalent throughout the developing world particularly Asia, the Middle East, and Africa (Parida *et al*., 2016). Drawing cues from the successful eradication of the related disease, rinderpest in cattle the Food and Agriculture Organization of the United Nations (FAO) and the OIE has targeted the eradication of PPR by the year 2030 (Baazizi *et al.*, 2017).

PPR was first reported in the Ivory Coast (Western Africa) in 1942, and was called 'Kata' and has since extended its range in Asia, the Middle East, and Africa posing an immediate threat of incursion into Europe, South East Asia and South Africa. After being misdiagnosed for a long time it's presence was confirmed in India in1987 from Arasur village of Villupuram district of Tamil Nadu (Shaila *et al*., 1996). Currently, PPR outbreaks are being reported regularly from different parts of the country. Despite, the availability of robust vaccines their use in a systematic and rational manner is not widespread, resulting in this devastating disease becoming one of the important tropical diseases to be neglected in the developing world including India.

The PPR Virus is a member of the *Morbillivirus* in the family of paramyxoviruses that is related to rinderpest, measles and canine distemper. Negative-stranded PPRV genome (RNA) is made up of 15,948 nucleotides and six genes that encode eight proteins. At the 3'

and 5' ends there are untranslated regions (UTRs) of 52 nt and 37 nt, respectively. The terminator region of each gene is followed by a three nucleotide-long conserved (GAA) region called intergenic region (IG). IG region is also found at the junction of leader sequences and the N gene (first gene) and between the L gene (last gene) and the trailer region. Each transcription unit (to produce individual viral protein) is composed of the coding sequence(s), IG region and the conserved start and stop signals that flank the coding sequence(s). Nucleocapsid (N) protein, Phosphoprotein (P), Matrix (M) protein, Fusion (F) protein, Haemagglutinin-neuraminidase (HN) protein and Large (L) protein make up the structural protein component of the virion. Apart from the full length P protein, the open reading frame (ORF) of the P gene also produces two non structural proteins, namely C and V by alternative reading frame and RNA editing (Munir, 2012; Kumar *et al*., 2014). In the last half a decade viral proteins have become the target for anti-viral therapeutic and vaccine development. Subunit vaccines prepared by expressing the PPRV F and/or H gene in pox and adeno viral vectors have been found to be experimentally protective (Chandran *et al*., 2010; Caufour *et al.*, 2014). A successful attempt has been made to develop a subunit vaccine by expressing the H protein of PPRV in peanut plants (*Arachis hypogea*) that elicits virus- neutralizing antibody responses in sheep (Khandelwal *et al*., 2011).

Another sphere that has been grabbing attention is the viral nonstructural proteins that have emerged as potential targets for development of novel antiviral agents (Bhakat *et al*., 2014). By definition viral non structural proteins are proteins coded for by the genome of the virus and are expressed in infected cells. However, these proteins are not assembled in the virion. These proteins are synthesized in minute amounts in infected cells or during a short period of time making their detection an uphill task. The viruses for which the viral genome sequence is known, the expected protein sequences of these non structural proteins can be deduced from the genome sequence and research be carried out. This is evident in researches carried out in Respiratory syncytial virus nonstructural proteins 1 and 2 (Yang *et al*., 2015), Influenza virus NS1 protein (Engel, 2013), Hepatitis C Virus Non-structural Protein 3(Lahm *et al*., 2002) to name a few. In all these studies the non-structural proteins were considered as targets for drug development.

Keeping in mind the economic whiplash, being just a decade away from 2030 and cues from the pre-existing literature on the PPRV non-structural proteins, we investigated the role of V protein in eliciting the immune response and apoptosis. V protein is synthesized in the infected cells by a co-transcriptional process that causes the RNA polymerase to stutter on the nascent mRNA of the P gene (Bailey *et al*., 2005). The impact/importance of V protein encoding region of P gene expression in viral expression was studied using double-stranded RNA-mediated interference (RNAi). The silencing of a gene is a consequence of degradation of RNA into short RNAs that activate ribonucleases to target homologous mRNA. The study was carried out *in vitro* in B95a cell line.

To carry out RNAi experiments in mammalian cells, it requires (1) a double-stranded siRNA that specifically targets the RNA transcript of interest/ Selecting the siRNA sequence in the target gene, (2) an effective siRNA delivery system/ synthesis of siRNAs or construction of plasmids bearing DNA sequence encoding for siRNAs, (3) controls to ensure the specificity of the siRNA treatment, (4) optimizing transfection of the siRNAs or the plasmids expressing siRNAs in the target cells and (5) a biological assay to detect the effect of knocking down the target RNA/ monitoring the efficacy of gene silencing. The amount of siRNA needed and the length of time required for destruction of the target RNA must be determined empirically and may vary with different cell lines and the confluency of the cells (Harborth *et al*., 2001; Curtis and Nardulli, 2009).

With the help of computer programs developed by Lin (Jack Lin's siRNA sequence finder; www.Ic.sunysb.edu/stu/shiklin/rnai.html), Ambion (www.ambion.com) and Invivogen siRNA Wizard (www.sirnawizard.com) potential siRNA sequences were obtained. Following a general rule that the sequence of one strand be AA (N19) TT, where N is any nucleotide, *i.e*., these siRNAs must have a 2-nucleotide 32 overhang of uridine residues a number of siRNAs were synthesized. All were 21 nucleotides long with a 52 -phosphate and 32 -hydroxyl group for efficiency. Then they were cross checked whether these selected sequences match mRNA sequences other than those of intended target (Agrawal *et al*., 2003). Among several siRNAs synthesized against different regions of the same target mRNA three of them targeting positions 167-192(S1); 560-585 (S2) and 727-752(S3) were used in the study and their silencing efficiencies were determined.

The gene knockdown effect using exogenous siRNA isn't always upto the mark. To overcome this lacuna the siRNA is modified in such a way as to allow it to be expressed by an appropriate vector, *e.g.* a plasmid (Abbott, 2006). The vectors that express siRNAs within mammalian cells typically use an RNA polymerase III promoter (e.g. U6 or H1; U6 is involved in gene splicing; H1 is the RNase component of human RNase P) to drive expression of a short hairpin RNA that mimics the structure of a siRNA. The insert that encodes this hairpin is designed to have two inverted repeats separated by a short spacer sequence .One inverted repeat is complementary to the mRNA to which the siRNA is targeted. A string of thymidines added to the 3' end serves as a pol III transcription termination site. Once inside the cell, the vector constitutively expresses the hairpin RNA, which induces silencing of the target gene. It is assumed (although not known for certain) that the resulting siRNA transcript is then processed by Dicer (Elbashir *et al*., 2001, Pushparaj *et al*., 2008). In the study psiRNA RNA-h7SKGFPzeo an enhanced green fluorescent protein (eGFP)-encoding plasmid was used. The siRNA inserts were cloned downstream of a RNA polymerase III promoter, the human 7SK or H1 promoter. These siRNA inserts were then transcribed into a short dsRNA with a hairpin structure (shRNAs) consisting of a 21 bp double stranded region corresponding to the target sequence and a small loop formed by the spacer region. With the help of white-blue selection system, positive clones were selected. These recombinant plasmid(s) containing siRNA insert(s) were used to transfect the B95a cell lines using lipofectamine 2000. The efficiency of transfection was determined using fluorescent microscopy. The microscopic images were manually analyzed to assess both the transfection efficiency and the cell viability. The ratio of the number of transfected (green) cells to the total number of cells gave the transfection efficiency. As the images always showed the same part of the cell culture, we were able to assess the cell viability by counting the total number of cells in the images. As absolute cell numbers were counted, this gave a better indication of the cell viability than relative assays like the MTT test. As control, B95a cells were cultivated under the same conditions, but without transfection agent.

The expression of eGFP seemed to have started after ~24 hr with a steep increase, reaching almost 100% after 48 hr. The number of cells first increased but then dropped to ~

50% of the initial value continued to remain so. In the control, the number of cells steadily increased to more than 300% of the initial value. In total, after transfection with Lipofectamine for 72 h, 50% of the original cell number was still there, and all of them are transfected. A closer evaluation of the images indicated that the transfection was associated with the cell division. During transfection the biosynthesis of a specific protein (here eGFP) is turned on.

The siRNA-induced silencing of V protein encoding region of P gene was determined using Fluorscent microscopy and quantitative real-time PCR (qRT-PCR). The ability of the siRNA constructs to silence the V protein encoding region of the P gene was studied by co-transecting the B95a cell with plasmids containing the whole V protein encoding region of the P gene along with plasmids containing these siRNA constructs. Gene silencing by siRNA occurs in the cytoplasm, in contrast to transfection with DNA that has to enter the cell nucleus. Consequently, gene silencing is typically easier than transfection. We have compared the gene silencing efficiency of three different siRNA constructs of B95a-eGFP cells with Lipofectamine. In this case, the intracellular biosynthesis of eGFP is blocked and the green fluorescence started vanishing gradually. Staying true to the fact that siRNAs synthesized against different regions of the same target mRNA show different silencing efficiencies these constructs showed a varied degree of silencing. S1 and S2 were seen to down regulate the gene expression whereas the S3 construct abrogates silencing. Sequence fidelity between these small RNA species and the RNA transcript is thought to be the critical parameter determining whether RNA cleavage or post-transcriptional blockade is induced. RNA cleavage can occur when an exact sequence match between the antisense siRNA strand and the cognate target transcript is present, and translational repression occurs when there is less homology between the two species (Doench *et al*., 2003). The gene silencing efficiency probes the intracellular degradation of the corresponding protein because it essentially prevents the biosynthesis of the protein. This is a completely different mechanism than transfection where the biosynthesis of a specific protein is turned on. It is therefore not surprising that it is slower than the transfection. Both transfection and gene silencing will be transient, that is, after DNA or siRNA are consumed. To evaluate gene silencing, measuring gene expression is critical, as it validates decreased expression of the target gene. RNAi results in a sequence specific knockdown of gene expression at the

post-transcriptional level, as introduced siRNA causes the degradation of identical mRNAs. The presence of exogenous siRNA may induce changes in V protein encoding region of the P gene expression and validation of target-gene silencing can be evaluated through qRT-PCR.In our study the S1 and S2 constructs were seen to repress the V protein encoding region of the P gene expression wherein the relative fold change was less than 1.This silencing efficiency was evident both in cells cotransfected with plasmid containing the whole gene of interest as well as cells infected with the whole virus. On the other S3 construct happened to stir an up regulation of the gene by fold changes up to 22 times.

A hallmark of a viral infection is an acute reaction by the infected cell. This includes activation of pre-existing antiviral defense machinery, commitment to apoptosis, and production of specific cytokines. These events contribute to the reduction of viral replication and to the limitation of viral spread. Immediately following a viral infection, a strong host response is initiated. For a range of viruses it has now been clarified that the mere interaction of viral surface proteins with cellular surface proteins starts a cellular reaction that in many cases leads to the first wave of cytokine production after infection. In addition, many viral proteins not present in the infectious particle but produced during the course of the viral life cycle are able to affect cellular signaling in a manner leading to cytokine production. Moreover, accumulation of viral RNA and overload of the cellular protein synthesis machinery induces signals that are able to trigger an early host response to the infection. A study in influenza virus which is the causative agent of influenza has shown the ability of the virus to trigger secretion of a whole range of cytokines and chemokines are induced in different cell types. These include IL-1, IL-2, IL-6, IL-8, IL-10, IL-15, IL-18, transforming growth factor β (TGF-β), TNF-α, IFN-α/β, IFN-γ, GM-CSF, MIP-1α/β, and RANTES (Ramshaw *et al.,* 1997).

Studies in the past decade have shown that cytokines have a major impact in immune responses to persistent viral infections. At early time points following a viral infection, these soluble mediators, in particular IL-10 and type I IFNs dispense direct and indirect suppressive signals, essential for the persistence of the virus in the host. Even more, cytokines contribute to the continuous silencing of immune functions, which can be reversed by antibody blocking approaches (Brooks *et al*., 2006).

The exposure of B95a cells to components of viruses results in the release of cytokines and chemokines from the affected cell. These mediators play a critical role in the initiation of immune responses (Ohno *et al*., 2004). Thus, the immunostimulatory effects of PPRV infection in B95a cells were assessed by testing culture supernatants from infected and uninfected B95a cells for various cytokines. Despite viral replication in cultured cells, and of PPRV infections in B95a cells did not secrete detectable concentrations of proinflammatory or immunoregulatory cytokines. The cells transfected and co-transfected with plasmids also failed to trigger the secretion of cytokines. Culture supernatants were assayed for IFN-γ, IFN-1α, IL-2, IL-4 and IL-10. Our results were compatible with that of Manjunath *et al*.,(2017) who reported that expression of IFNs – α and β was found to be non –significant in cultured PBMCs at different time points and suggested that the stimulation of ISGs(Interferon stimulation genes) could be IFN independent. The works of Boxer *et al*. (2009) in rinderpest virus echoed the same results wherein the non-structural protein blocked the induction of interferon I pathway. The inability of the cultured cells to secrete IFN-γ (Type-II) is an important observation yet to be reported in PPRV infections. This observation has been previously reported in rinderpest virus. Nanda and Baron (2006) demonstrated that the non-structural proteins (C, V and W proteins) of rinderpest virus blocks Type I and Type II interferon action. The inability of the cell cultures co-transfected with siRNA constructs to secrete cytokines provides the possibility that the production of these immune components is independent of the non-structural protein synthesis. Ma *et al*. (2015) identified the amino-acid residues in the V protein of peste des petits ruminants essential for interference and suppression of STAT-mediated interferon signaling. It was demonstrated that only PPRV V protein interferes with the production of IFN-β. PPRV N, P, V proteins can restrict the ISRE and GAS promoter expression to limit the IFN signaling transduction, but in comparison with N, P proteins, V protein has the strongest ability to block the IFN signaling, especially, type I IFN-dependent pathway. The results also showed that N and P proteins were able to inhibit ISRE more effectively than GAS promoter, maybe due to the fact that STAT2 protein is the primary target for N and P proteins-mediated type I IFN signaling inhibition (Ma *et al*., 2015). Further studies are a must to confirm and clearly understand about the IFN blockade. Previous reports demonstrated that both the C- and N-

terminal domains of Morbillivirus V protein contribute to inhibition of the IFN signaling (Ramachandran *et al*., 2008). Mutations such as deletion or substation at position 110 (Tyrosine) in the V protein seem to impair its ability to bind with STAT1 and decreased the inhibition of the IFN signaling; this was recorded both in MV and PPRV (Ramachandran *et al*., 2008; Devaux *et al*., 2007; Matsuura and Stewart, 2005; Nishio *et al*., 2002; Nishio *et al*., 2001, Ma *et al*., 2015).

Several stimuli, such as viral infection induce energy dependent cell death referred to as apoptosis. Certain morphological and biochemical processes are involved in induction of apoptosis including cell shrinkage, partial detachment from the substratum, plasma membrane blebbing, chromatin condensation and intra-nucleosomal cleavage which leads to fragmentation of cells into apoptotic bodies that are phagocytosed without eliciting an inflammatory response (Hardwick, 2001). Induction and inhibition of apoptosis has been seen as an advantage for the viruses. It is suggested that viral prevention of apoptosis helps to prevent the premature death of the host cells, and therefore maximizes the chances for viral persistence or increase the viral progeny from infected cells. On the other hand, viruses also induce apoptosis to facilitate the release of progeny viruses and for dissemination to neighboring cells. Additionally, induction of apoptosis helps to establish cytotoxicity that facilitates viral pathogenesis (Roulston *et al*., 1999).

Although the mechanism for the inhibition of apoptosis in PPRV is yet to be defined, it has been comprehensively studied in other members of the family Paramyxoviridae and in viruses belonging to other families. It indicates a universal viral mechanism of self-defense (Laine *et al*., 2005). Previously, PPRV-induced apoptosis has been described which suggests the essential role of this mechanism in viral replication and invasion of host defense mechanisms that limit replication by killing infected cells (Mondal *et al*., 2001). The researchers elucidated when goat PBMCs were infected with PPRV,the induction of apoptosis was directly proportional to that of replication of PPRV. The researchers further strengthened their results with DNA fragmentation assay and electron microscopy. Although the ability of PPRV to induce apoptosis was elucidated, but the mechanism that caused this still remains to be studied. The capability of PPRV infection to trigger autophagy and enhances autophagic flux in cell lines was reported less than five years ago (Zhang *et al*., 2013).

Investigation regarding the role of viral protein in the induction and the pathway involved in the activation of apoptosis remains scarce till day. The nucleoprotein of MV, a close relative of PPRV, has been identified as an apoptotic inducer. Due to high similarity of the N protein between MV and PPRV, it is likely that *Morbilliviruses* share this character in their N protein. We assessed the effect of V protein encoding region of the P gene on the activities of the main caspases (caspase 3/7, 8 and 9) in B95a cells, we carried out viral infection, transfection and co-transfection in the cell line. As the S2 construct have shown to have a better silencing efficiency it was used to study the caspases activities. The cellular caspase 3/7 activities increased in all the various conditions in a time dependent manner. It has been recognized that caspase 3/ 7 is activated by caspases 8 or 9; therefore these two caspases activity was also measured using the same methods under the same conditions. Caspase 8 activation is the step immediately following death-inducing signalling complex (DISC) formation. The latter is the part of the extrinsic apoptosis pathway which involves death ligands bound to cell surface death receptors. Caspase 9 activation is a part of the intrinsic apoptosis pathway, which involves cytochrome C release from the mitochondria. Although it is widely assumed that the apoptotic death of mammalian cells is closely associated with activation of caspases, there is evidence indicating that caspase activation is also involved with processes that are not necessarily related to apoptosis. For examples, caspase 3 activity is involved with skeletal muscle differentiation (Fernando *et al.,* 2002). It has been reported that caspase activation may contribute to subtle signalling pathways, some of which may enhance cell survival and proliferation (Cai *et al*., 2004). As we did not further examine the cell line for cell death it is safe to say that caspase activation is not synonymous with apoptotic death; therefore increased caspase activities cannot be regarded as a sole indicator of cell death.

It has been suggested that PPRV- induced apoptosis can be associated with viral implication in the immune system. Although the mechanism of immunosuppression in PPRV has to be further studied and elucidated properly, a character that is believed to be common in all paramyxoviruses, the induction of apoptosis might be associated with immune suppression as is seen in MV (Schnorr *et al*., 1997)

In a nutshell, two out of three siRNAs targeting V protein encoding region of the P mRNA have a potent ability to inhibit the mRNA transcription. The ability of the gene to inhibit

cytokine secretion was well documented whereas the inability of the siRNA transfected cells to secret cytokines needs to be further investigated. The caspases have demonstrated that the irrespective of the gene silencing there was no significant change in their activity. For better understanding of role of V protein encoding region of the P gene in caspase activities and cytokine production further experiments using reverse genetics like gene knockout are mandatory.

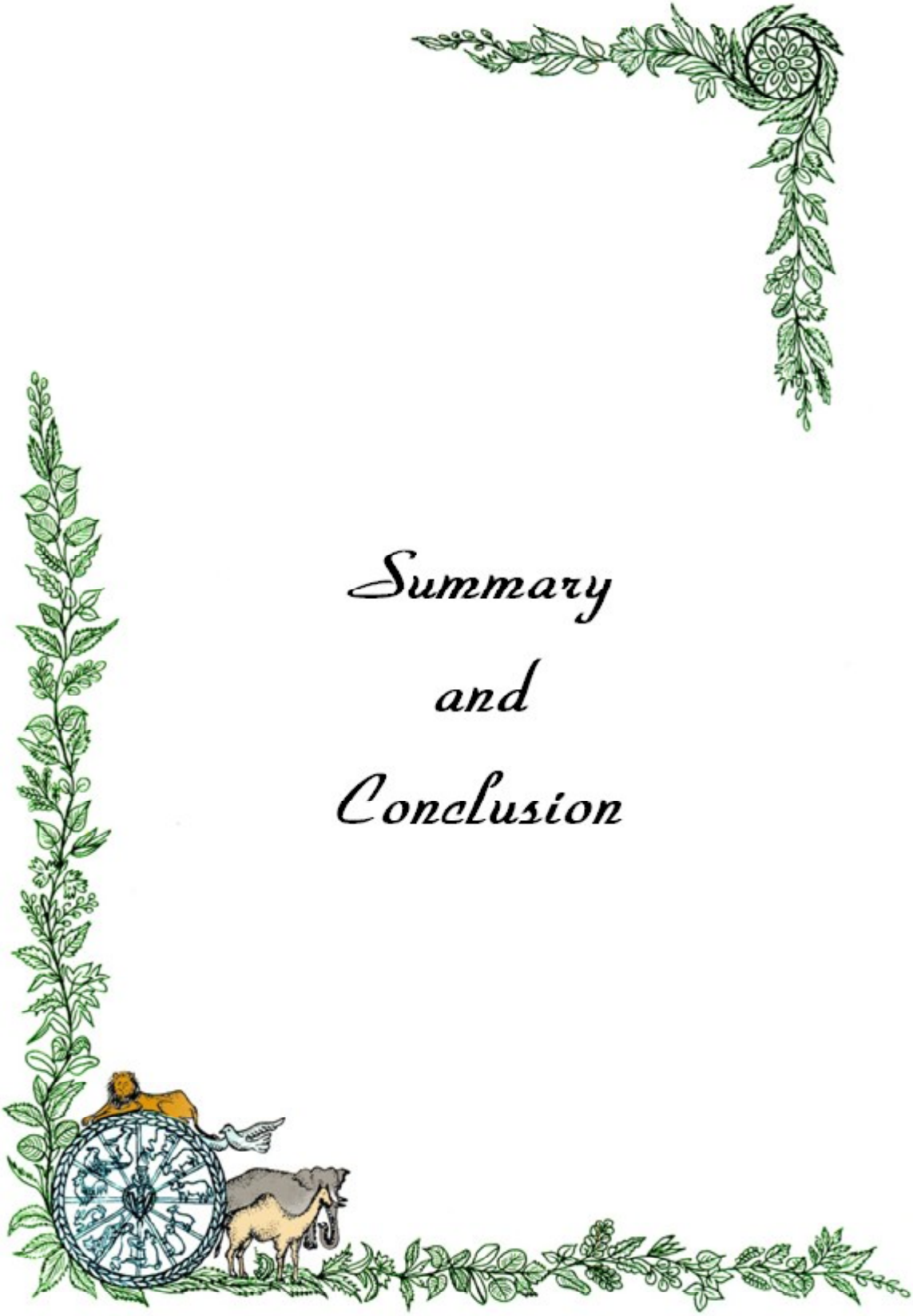

Summary and Conclusion

6 SUMMARY AND CONCLUSIONS

India is home to about 200.23 million small ruminants (135.17 million goats and 65.06 million sheep). They play an important role in the food and nutritional security of millions of rural people especially the landless, marginal and small farmers. The socio-economic value of small ruminant rearing as compared to other livestock species, for poor farmers is immense. Goat and sheep are also among the main meat-producing animals in India, whose meat (chevon/ mutton) is readily preferred irrespective of caste, creed and religion. They produce a variety of products, mainly meat, milk, skin, wool and manure and are especially useful in the semi-arid and arid regions, where they can sustain on sparse vegetation and extreme climatic conditions. There is an array of diseases that affect small animals one of them is PPR. This viral disease is more common in goats than sheep. Being acute in nature and notifiable by OIE, India alone incurs a loss of upto $2569.00 million/year due to PPR outbreaks. One of the recent therapeutic strategies involves targeting the non-structural proteins of the virus. In order to devise an effective agent the gene encoding nonstructural protein need to be studied thoroughly as well as their role in physio-pathology of the disease. RNAi is considered one the yard stick/industry standard for investigating role of a gene in a cell culture system as well as *in vivo* models. In the present study, attempts were made to assess the efficiency of transfection and efficiency of gene expression using qRT-PCR and fluorescent microscopy. The role of the gene is eliciting an immune response and ability to provoke caspase cascade were also studied. The summary of the results are as follows:

- The V protein (one of the non-structural protein) encoding region of the P gene was considered for the study.

- Three different siRNA inserts namely siRNA, S1 (167-192); S2 (560-585) and S3 (727-752) targeting different regions of the gene were designed and used.
- During transfection the biosynthesis of a specific protein (here eGFP) is turned on and the expression of eGFP seemed to have started after ~24 hr with a steep increase, reaching almost 100% after 48 hr.
- On the contrary the intracellular biosynthesis of eGFP is blocked and the green fluorescence started vanishing gradually during gene silencing by siRNA.
- S1 and S2 were seen to down regulate the gene expression whereas the S3 construct repels silencing.
- S3 showed an up regulation of the gene by fold changes up to 22 times.
- The ability of V protein encoding region of the P gene to produce cytokines in B95a cells was assessed using viral infection, transfection and co-transfection in the cell line.
- Culture supernatants were assayed for IFN-γ, IFN-1α, IL-2, IL-4 and IL-10.
- The exposure of B95a cells to plasmid(s) containing the siRNA constructs and the virus failed to trigger the release of cytokines.
- The inability of the cell cultures co-transfected with siRNA constructs to secrete cytokines provides the possibility that the production of these immune components is independent of the non-structural protein synthesis.
- The V protein encoding region of the P gene seems to impair its ability to bind with STAT1 and decreased the inhibition of the IFN signaling.
- The study the effect of V protein encoding region of the P gene on the activities of the main caspases (caspase 3/7, 8 and 9) in B95a cells, we carried out viral infection, transfection and co-transfection in the cell line.
- It has been recognized that caspase 3/7 is activated by caspases 8 or 9; therefore these two caspases activity was also measured using the same methods under the same conditions.

- Although, the mechanism of immunosuppression in PPRV has to be further studied and elucidated properly, a character that is believed to be common in all paramyxoviruses, the induction of apoptosis might be associated with immune suppression as is seen in MV.

Mini Abstract

7 MINI ABSTRACT

The viral non structural proteins are proteins coded for by the genome of the virus and are expressed only in infected cells. However, these proteins are not assembled in the virion. These proteins are synthesized in minute amounts in infected cells or during a short period of time making their detection difficult. In the recent years viral nonstructural proteins have emerged as potential targets for development of novel antiviral agents. Peste des petits ruminants (PPR) is an acute and devastating disease of small ruminants caused by the PPR virus (PPRV). It's 16 Kb genome encodes for two non-structural proteins along with the six structural ones. Here, the role one of the non-structural protein encoding regions (V protein) in cytokine secretion and caspase cascade was studied using gene silencing. *siRNA* constructs targeting three different regions of the gene 167-192(S1); 560-585(S2) and 727-752(S3) were designed. Then they were annealed into a vector (psiRNA RNA-h7SKGFPzeo) that was transfected into the B95a cells using Lipofectamine. The efficiency of transfection was determined using fluorescent microscopy. The microscopic images were manually analyzed to quantify both the transfection efficiency and the cell viability. The expression of eGFP seemed to have started after ~24 hr with a steep increase, reaching almost 100% after 48 hr. The number of cells first increased but then dropped to ~ 50% of the initial value where it remained. The siRNA-induced silencing of V protein encoding region of P gene was determined using Fluorscent microscopy and quantitative real-time PCR (qRT-PCR). The ability of the siRNA constructs to silence the V protein encoding region of the P gene was studied by co-transecting the B95a cell with plasmids containing the whole V protein encoding region of the P gene along with plasmids containing these siRNA constructs. the S1 and S2 constructs were seen to repress the V protein encoding region of the P gene expression wherein the relative fold change was less than 1.This silencing efficiency was evident both in cells cotransfected with plasmid containing the whole gene of interest as well as cells infected with the whole virus. On the other S3 construct happened to stir an up regulation of the gene by fold changes up to 22 times. A hallmark of a viral infection is an acute reaction by the infected cell. This includes activation of pre-existing antiviral defense machinery, commitment to apoptosis, and production of specific cytokines. Despite viral replication in cultured cells, and of PPRV infections in B95a cells did not secrete detectable concentrations of proinflammatory or immunoregulatory cytokines. The cells transfected and co-transfected with plasmids also failed to trigger the secretion of cytokines. The amino-acid residues in the V protein of peste des petits ruminants seem essential for interference and suppression of STAT-mediated interferon signaling. Investigation regarding the role of V protein encoding region of P gene in the induction and the pathway involved in the activation of apoptosis revealed an increase in the activity of Caspases 3/7, 8 and 9 which were recorded in RLUs. As caspase activation is not synonymous with apoptotic death; therefore increased caspase activities cannot be regarded as a sole indicator of cell death. It has been suggested that PPRV- induced apoptosis can be associated with viral implication in the immune system. Although, the mechanism of immunosuppression in PPRV has to be further studied and elucidated properly, a character that is believed to be common in all paramyxoviruses, the induction of apoptosis might be associated with immune suppression.

लघु सारांश

8 लघु सारांश

वायरल गैर स्ट्रक्चरल प्रोटीन वायरस के जीनोम द्वारा कोडित प्रोटीन होते हैं और केवल संक्रमित कोशिकाओं में ही व्यक्त किये जाते हैं। हालांकि, ये प्रोटीन विरियन में इकट्ठा नहीं होते है तथा ये प्रोटीन संक्रमित कोशिकाओं में सूक्ष्म मात्रा में तथा थोड़े समय के लिए संश्लेषित होते हैं एवं उस दौरान उनका पता लगाना मुश्किल होता है। हाल के वर्षों में वायरल नॉनस्ट्रक्चरल प्रोटीन नवीन एंटीवायरल एजेटों के विकास के लिए संभावित लक्ष्य के रूप में उभरे हैं। पीपीआर वायरस (पीपीआरवी) की वजह से पेस्टे डेस पेटीट रूमिनेन्ट्स (पीपीआर) छोटे रोमनकों की एक विकट और विनाशकारी बीमारी है। इस वायरस का 16 केवी का जीनोम छः संरचनात्मक और दो गैर–संरचनात्मक प्रोटीनों को एनकोड करता है। यहा साइटोकिनी स्राव और कस्पेस कैसकेड में एक गैर–स्ट्रक्चरल प्रोटीन एन्कोडिंग क्षेत्र (वी प्रोटीन) की भूमिका का अध्ययन जीन साइलंसिंग का उपयोग करके लिया गया। तीन अलग–अलग क्षेत्र 167–192 (एस1), 560–585 (एस2) और 727–752 (एस3) को लक्षित करते हुए एसआई आरएनए डिजाइन किए गए। इन एसआई आरएनए को वेक्टर (psiRNA RNA-h7SKGFPzeo) में एनील करने के उपरांत लिफाफेक्टमिन का उपयोग कर बी95 कोशिकाओं में ट्रांसफेक्ट किया गया। अभिकर्मक की दक्षता फ्लोरोसेंट माइक्रोस्कोपी का उपयोग करके निर्धारित की गई। सूक्ष्म छवियों का विश्लेषण मैन्युअल रूप से अभिकर्मक दक्षता और सेल व्यवहार्यता दोनों को मापने के लिए किया गया। ईजीएफपी की अभिव्यक्ति 24 घण्टों के बाद तीव्र वृद्धि के साथ शुरू हुई तथा 48 घण्टें बाद लगभग 100 प्रतिशत तक पहुंच गई। कोशिकाओं की संख्या पहले बढ़ी लेकिन बाद में प्रारंभिक मान के 50 प्रतिशत तक गिर गई एवं इस स्तर पर बनी रही। पी जीन के वी प्रोटीन एन्कोडिंग क्षेत्र की एसआई आरएनए से प्रेरित चुप्पी को फ्लोरोसेंट माइक्रोस्कोपी और मात्रात्मक रीयल–टाइम पीसीआर (क्यूआरटी–पीसीआर) का उपयोग करके निर्धारित किया गया। पी जीन के वी प्रोटीन एन्कोडिंग क्षेत्र को चुप्पी करने की एसआई आरएनए की क्षमता को बी95 कोशिका को पी जीन के पूरे वी प्रोटीन एन्कोडिंग क्षेत्र युक्त प्लास्मिड तथा इनके एसआई आरएनए युक्त प्लाज्मिड को सह–ट्रांस्फेक्ट करवाया गया। पी जीन के वी प्रोटीन एन्कोडिंग क्षेत्र की अभिव्यक्ति को दबाने के लिए एस1 और एस2 कंस्ट्रक्ट का प्रभाव देखा जिसमें तुलनात्मक रूप से 1 गुना से कम परिवर्तन था। पूरे वायरस से संक्रमित कोशिकाओं के साथ साथ वे कोशिकाए जो की हित वाले जीन से को–ट्रांस्फेक्ट की गई। उन कोशिकाओं में इस चुप्पी की दक्षता स्पष्ट हुई। वही दूसरी तरफ एस3 कस्ट्रक्ट ने जीन के अप विनियमन को 22 गुना तक बढाया। वायरल संक्रमण की एक पहचान संक्रमित सेल द्वारा एक तीव्र प्रतिक्रिया है। इसमें पूर्व–मौजूदा एंटीवायरल रक्षा मशीनरी, एपप्टोसिस के प्रति प्रतिबद्धता और विशिष्ट साइटोकिन्स का उत्पादन शामिल है। पालित कोशिकाओं में वायरल प्रतिकृति होने के बावजूद, बी95 कोशिकाओं में पीपीआरवी संक्रमण की वजह से प्रोइन्फ्लमेटरी या इम्योरोरेगुलेटरी साइटोकिन्स के पता लगाने योग्य सांद्रता को प्रदर्शित नहीं गया। ट्रांस्फेक्टेड तथा प्लास्मिड के साथ सह–ट्रांसफेक्ट कोशिकाएं भी साइटोकिन्स सिग्नलिंग के हस्तक्षेप और दमन के लिए पेस्टे डेस पेटीट रूमिनेन्ट्स के वी प्रोटीन के एमिनो एसिड आवश्यक लगते हैं। कास्पप्स 3/7, 8 और 9 की गतिविधि में वृद्धि जोकि आरएलयू में दर्ज की गई से पता चला की पी जीन के वी प्रोटीन एन्कोडिंग क्षेत्र की अपोप्टोसिस के सक्रियण में शामिल मार्ग और उत्पादन में भूमिका है। कस्पेस सक्रियण एपोपोटिक मृत्यु का पर्याप नहीं है, इसलिए बढ़ी हुई कस्पासे गतिविधियों को सेल मृत्यु के एक मात्र संकेतक के रूप में नहीं माना जा सकता है। अतः पीपीआरवी–प्रेरित अपोप्टोसिस प्रतिरक्षा प्रणाली में वायरल प्रभाव के साथ जुड़ा हो सकता है। अपोप्टोसिस का अनुगम प्रतिरक्षा दमन के साथ जुड़ा हो सकता है। अतः पीपीआरवी में प्रतिरक्षा विज्ञान की व्यवस्था को और अधिक व्याख्या की आवश्यकता है जोकि सभी पैरामीक्सोवायरस में सामान्य माना जाता है।

References

9 REFERENCES

Abbott, A. 2006. Youthful duo snags a swift Nobel for RNA control of genes.Nature, **443:**488.

Abubakar, M., Jamal, S. M., Arshed, M. J., Hussain, M. and Ali, Q. 2009. Peste des petits ruminants virus (PPRV) infection; its association with species, seasonal variations and geography. Tropical animal health and production, **41(7)**, 1197.

Adams, M.J., Carstens, E.B. and Lefkowitz, E.J. 2012. Virus taxonomy: classification and nomenclature of viruses: Ninth Report of the International Committee on Taxonomy of Viruses. Ed: King, AMQ, San Diego, Elsevier.

Adombi, C.M., Lelenta, M., Lamien, C.E., Shamaki, D., Koffi, Y.M., Traoré, A., Silber, R., Couacy-Hymann, E., Bodjo, S.C., Djaman, J.A., Luckins, A.G. and Diallo, A. 2011. Monkey CV1 cell line expressing the sheep-goat SLAM protein: a highly sensitive cell line for the isolation of peste des petits ruminants virus from pathological specimens. J Virol Methods. **173(2)**:306-313.

Agrawal, N., Dasaradhi, P. V. N., Mohmmed, A., Malhotra, P., Bhatnagar, R. K. and Mukherjee, S. K. 2003. RNA interference: biology, mechanism, and applications. Microbiology and Molecular Biology Reviews, **67**(4): 657-685.

Altschul, S. F., Madden, T. L., Schäffer, A. A., Zhang, J., Zhang, Z., Miller, W. and Lipman, D. J. 1997. Gapped BLAST and PSI-BLAST: a new generation of protein database search programs. Nucleic acids research, **25(17)**: 3389-3402.

Amarasinghe, G. K., Bào, Y., Basler, C. F., Bavari, S., Beer, M., Bejerman, N. and Calisher, C. H. 2017. Taxonomy of the order Mononegavirales: Update 2017. Archives of Virology, 1-12.

Andzhaparidze, O. G., Chaplygina, N. M., Bogomolova, N. N., Lotte, V. D. and Koptiaeva, I. B. 1986. Characteristics of the ribonucleoprotein of the measles virus persisting in a human cell culture. Voprosy virusologii, **31(5)**, 567-572.

Ashkenazi, A. and Dixit, V. M. 1998. Death receptors: signaling and modulation. Science, **281(5381):** 1305-1308.

Axe, E. L., Walker, S. A., Manifava, M., Chandra, P., Roderick, H. L., Habermann, A and Ktistakis, N. T. 2008. Autophagosome formation from membrane compartments enriched in phosphatidylinositol 3-phosphate and dynamically connected to the endoplasmic reticulum. The Journal of cell biology, **182(4):** 685-701.

Baazizi, R., Mahapatra, M., Clarke, B. D., Ait-Oudhia, K., Khelef, D. and Parida, S. 2017. Peste des petits ruminants (PPR): A neglected tropical disease in Maghreb region of North Africa and its threat to Europe. PloS one, **12(4):** e0175461.

Bailey, D., Banyard, A., Dash, P., Ozkul, A. and Barrett, T. 2005. Full genome sequence of peste des petits ruminants virus, a member of the Morbillivirus genus. Virus research, **110(1):** 119-124.

Balamurugan, V., Hemadri, D., Gajendragad, M. R., Singh, R. K. and Rahman, H. 2014. Diagnosis and control of peste des petits ruminants: a comprehensive review. Virus Disease, **25(1)**, 39-56.

Balamurugan, V., Sen, A., Venkatesan, G., Bhanot, V., Yadav, V., Bhanuprakash, V. and Singh, R. K. 2012. Peste des petits ruminants virus detected in tissues from an Asiatic lion (Panthera leo persica) belongs to Asian lineage IV. Journal of Veterinary Science, **13**(2): 203-206.

Baltimore, D. 1971. Expression of animal virus genomes. Bacteriol Rev **35 (3)** :235–241.

Bankamp, B., Horikami, S.M., Thompson, P.D., Huber, M., Billeter, M. and Moyer, S.A. 1996. Domains of the Measles virus N protein required for binding to P protein and self-assembly. Virology. **216**:272–277.

Banyard, A.C., Parida, S., Batten, C., Oura, C., Kwiatek, O. and Libeau, G. 2010. Global distribution of peste des petits ruminants virus and prospects for improved diagnosis and control. J Gen Virol.; **91(12)**: 2885–97.

Baron, M.D., Parida, S. and Oura, C.A. 2011. Peste des petits ruminants: a suitable candidate for eradication. Veterinary Record **169**: 16–21.

Barrett, T., Banyard, A.C. and Diallo, A. 2006. Molecular biology of the Morbilliviruses. In Rinderpest and Peste Des Petits Ruminants Virus: Plague of Large and Small Ruminants; Biology of Animal Infections; Academic Press: London, UK, 31–67.

Barrett, T., Banyard, A.C. and Diallo, A. 2006. Molecular biology of the Morbilliviruses. In Rinderpest and Peste Des Petits Ruminants Virus: Plague of Large and Small Ruminants; Biology of Animal Infections; Academic Press: London, UK; 31–67.

Barrett, T., Visser, I.K.G., Mamaev, L., Goatley, L., Bressem, M.F. and Van Osterhaus, A.D.M. 1993. Dolphin and porpoise morbilliviruses are genetically distinct from phocine distemper virus. Virology, **193** 1010-1012

Bazarsky, E., Wolfson, M., Galron, D., Granot, Y., Argov, S., Isakov, N. and Rager-Zisman, B. 1997. Persistent measles virus infection of murine neuroblastoma cells differentially affects the expression of PKC individual isoenzymes. Virus Genes, **15(3):** 227-234.

Beaton, A. R., Rodriguez, J., Reddy, Y. K. and Roy, P. 2002. The membrane trafficking protein calpactin forms a complex with bluetongue virus protein NS3 and mediates virus release. Proceedings of the National Academy of Sciences, **99(20):** 13154-13159.

Bellini, W.J., Englund, G., Rozenblatt, S., Arnheiter, H. and Richardson, C.D. 1985. Measles virus P gene codes for two proteins. Journal of Virology. 908–919.

Benne, R., Van Den Burg, J., Brakenhoff, J. P., Sloof, P., Van Boom, J. H. and Tromp, M. C. (1986). Major transcript of the frameshifted coxll gene from trypanosome mitochondria contains four nucleotides that are not encoded in the DNA. Cell, **46(6):** 819-826.

Bhakat, S., Karubiu, W., Jayaprakash, V. and Soliman, M. E. 2014. A perspective on targeting non-structural proteins to combat neglected tropical diseases: Dengue, West Nile and Chikungunya viruses. European Journal of Medicinal Chemistry, **87**:677-702.

Bieback, K., Lien, E., Klagge, I. M., Avota, E., Schneider-Schaulies, J., Duprex, W. P. and Schneider-Schaulies, S. 2002. Hemagglutinin protein of wild-type measles virus activates toll-like receptor 2 signaling. Journal of Virology, **76(17):** 8729-8736.

Boxer, E. L., Nanda, S. K. and Baron, M. D. 2009. The rinderpest virus non-structural C protein blocks the induction of type 1 interferon. Virology, **385**(1): 134-142.

Brander, C. and Walker, B.D. 2000. Modulation of host immune responses by clinically relevant human DNA and RNA viruses. Curr. Opin. Microbiol. **3:** 379–386.

Brindley, M.A., Takeda, M., Plattet, P. and Plemper, R.K 2012. Triggering the measles virus membrane fusion machinery. Proc. Natl. Acad. Sci.**109**:3018–3027.

Brooks, D. G., Trifilo, M. J., Edelmann, K. H., Teyton, L., McGavern, D. B. and Oldstone, M. B. 2006. Interleukin-10 determines viral clearance or persistence in vivo. Nature Medicine, **12(11):** 1301-1309.

Cai, J., Chen, Y., Murphy, T. J., Jones, D. P. and Sartorelli, A. C. 2004. Role of caspase activation in butyrate-induced terminal differentiation of HT29 colon carcinoma cells. Archives of Biochemistry and Biophysics, **424**(2): 119-127.

Calain, P. and Roux, L. 1993. The rule of six, a basic feature for efficient replication of Sendai virus defective interfering RNA. Journal of Virology, **67(8):** 4822-4830.

Cattaneo, R. 1991. Different types of messenger RNA editing. Annu Rev Genet.**25**:71-88.

Cattaneo, R., Kaelin, K., Baczko, K. and Billeter, M. A. 1989. Measles virus editing provides an additional cysteine-rich protein. Cell, **56(5):** 759-764.

Caufour, P., Rufael, T., Lamien, C. E., Lancelot, R., Kidane, M., Awel, D. and Diallo, A. 2014. Protective efficacy of a single immunization with capripoxvirus-vectored recombinant peste des petits ruminants vaccines in presence of pre-existing immunity. Vaccine, **32**(30): 3772-3779.

Chandran, D., Reddy, K. B., Vijayan, S. P., Sugumar, P., Rani, G. S., Kumar, P. S., Srinivasan, V. A. 2010. MVA recombinants expressing the fusion and hemagglutinin genes of PPRV protects goats against virulent challenge. Indian Journal of Microbiology, **50**(3): 266-274.

Chard, L.S., Bailey, D.S., Dash, P., Banyard, A. and Barrett, T. 2008. Full genome sequences of two virulent strains of peste-des-petits ruminants virus, the Cote d'Ivoire 1989 and Nigeria 1976 strains. Virus Research. **136**:192–197.

Ciancanelli, M.J. and Basler, C.F. 2006. Mutation of YMYL in the Nipah virus matrix protein abrogates .budding and alters subcellular localization. Journal of Virology. **80(12):**70–78.

Cohen, G. M. 1997. Caspases: the executioners of apoptosis. Biochemical Journal, **326(1):** 1-16.

Colf, L.A., Juo, Z.S. and Garcia, K.C. 2007. Structure of the measles virus hemagglutinin. Nat Struct Mol Biol **14**: 1227–1228.

Couacy-Hymann, E., Bodjo, S. C., Danho, T., Koffi, M. Y., Libeau, G. and Diallo, A. 2007. Early detection of viral excretion from experimentally infected goats with peste-des-petits ruminants virus. Preventive veterinary medicine, **78(1):** 85-88.

Cullen, B. R. 2014. Viruses and RNA interference: issues and controversies. Journal of Virology, **88(22):** 12934-12936.

Curtis, C. D. and Nardulli, A. M. 2009. Using RNA interference to study protein function. The Nuclear Receptor Superfamily: Methods and Protocols, 187-204.

Dampier, W. and Tozeren, A. 2007. Signaling perturbations induced by invading H. pylori proteins in the host epithelial cells: a mathematical modeling approach. J. Theor. Biol. **248:** 130–144.

Das, S.C., Baron, M.D. and Barrett, T. 2000. Recovery and characterization of a chimeric rinderpest virus with the glycoproteins of peste-des-petits-ruminants virus: homologous F and H proteins are required for virus viability. Journal of Virology. **74**: 9039–9047.

de Almeida, R. S., Keita, D., Libeau, G. and Albina, E. 2007. Control of ruminant morbillivirus replication by small interfering RNA. Journal of General Virology, **88(8):** 2307-2311.

Devaux, P., von Messling, V., Songsungthong, W., Springfeld, C. and Cattaneo, R. 2007. Tyrosine 110 in the measles virus phosphoprotein is required to block STAT1 phosphorylation. Virology, **360(1):** 72-83.

Dhar, P., Sreenivasa, B.P., Barrett, T., Corteyn, M., Singh, R.P. and Bandyopadhyay, S.K. 2002. Recent epidemiology of peste des petits ruminants virus (PPRV). Vet Microbiol.; **88**:153–159.

Diallo, A. 1990. Morbillivirus group: genome organization and proteins. Vet Microbiol. **23**:155–163.

Diallo, A., Barrett, T., Lefevre, P.C. and Taylor, W.P. 1987. Comparison of proteins induced in cells infected with rinderpest and peste des petits ruminants viruses. Journal of General Virology **68**:2033–2038.

Díaz-Troya, S., Pérez-Pérez, M. E., Florencio, F. J. and Crespo, J. L. 2008. The role of TOR in autophagy regulation from yeast to plants and mammals. Autophagy, **4(7):** 851-865.

Didcock, L., Young, D. F., Goodbourn, S. and Randall, R. E. 1999. The V protein of simian virus 5 inhibits interferon signalling by targeting STAT1 for proteasome-mediated degradation. Journal of virology, **73(12):** 9928-9933.

Doench, J. G., Petersen, C. P. and Sharp, P. A. 2003. siRNAs can function as miRNAs. Genes and Development, **17**(4): 438-442.

Dykxhoorn, D. M. and Lieberman, J. 2006. Silencing viral infection. PLoS medicine, **3(7):** e242.

Egelman, E. H., Wu, S. S., Amrein, M., Portner, A. and Murti, G. 1989. The Sendai virus nucleocapsid exists in at least four different helical states. Journal of Virology, **63(5):** 2233-2243.

El Najjar, F., Schmitt, A.P. and Dutch, R.E. 2014. Paramyxovirus glycoprotein incorporation, assembly and budding:A three way dance for infectious particle production. Viruses.**6**: 3019–3054.

Elbashir, S. M., Harborth, J., Lendeckel, W., Yalcin, A., Weber, K. and Tuschl, T. 2001. Duplexes of 21-nucleotide RNAs mediate RNA interference in cultured mammalian cells. Nature, **411**(6836): 494-498.

Enari, M., Sakahira, H., Yokoyama, H., Okawa, K., Iwamatsu, A. and Nagata, S. 1998. A caspase-activated DNase that degrades DNA during apoptosis, and its inhibitor ICAD. Nature, **391**(6662), 43-50.

Engel, D. A. 2013. The influenza virus NS1 protein as a therapeutic target. Antiviral research, **99**(3) : 409-416.

Fan, R., Dong, Y., Huang, G. and Takeuchi, Y. 2014. Apoptosis in virus infection dynamics models. Journal of Biological Dynamics, **8(1):** 20-41.

Fernando, P., Kelly, J. F., Balazsi, K., Slack, R. S. and Megeney, L. A. 2002. Caspase 3 activity is required for skeletal muscle differentiation. Proceedings of the National Academy of Sciences, **99**(17): 11025-11030.

Fire, A., Xu, S., Montgomery, M. K., Kostas, S. A., Driver, S. E. and Mello, C. C. 1998. Potent and specific genetic interference by double-stranded RNA in Caenorhabditis elegans. Nature, **391**(6669), 806-811.

Flanagan, E.B., Ball, L.A.and Wertz, G.W. 2000. Moving the glycoprotein gene of vesicular stomatitis virus to promoter-proximal positions accelerates and enhances the protective immune response. Journal of Virology.**74**:7895–7902.

Galbraith, S.E., Tiwari, A., Baron, M.D., Lund, B.T., Barrett, T. and Cosby, S.L. 1998. Morbillivirus downregulation of CD46. Journal of Virology .**72**:10292–10297.

Galinski, M. S., Troy, R. M. and Banerjee, A. K. 1992. RNA editing in the phosphoprotein gene of the human parainfluenza virus type 3. Virology, **186(2):** 543-550.

Gargadennec, L. and Lalanne, A. 1942. La peste des petits ruminants. Bull Serv Zootech Epizoot Afr Occid Fr. **5**: 15–21.

Geiss, G. K., Salvatore, M., Tumpey, T. M., Carter, V. S., Wang, X., Basler, C. F. and García-Sastre, A. 2002. Cellular transcriptional profiling in influenza A virus-infected lung epithelial cells: the role of the nonstructural NS1 protein in the evasion of the host innate defense and its potential contribution to pandemic influenza. Proceedings of the National Academy of Sciences, **99(16):** 10736-10741.

Gibbs, E.P., Taylor, W.P., Lawman, M.J. and Bryant, J. 1979. Classification of peste des petits ruminants virus as the fourth member of the genus Morbillivirus. Intervirology **11**: 268–274.

Glick, D., Barth, S. and Macleod, K. F. 2010. Autophagy: cellular and molecular mechanisms. The Journal of Pathology, **221(1):** 3-12.

Gotoh, B., Takeuchi, K., Komatsu, T., Yokoo, J., Kimura, Y., Kurotani, A. and Nagai, Y. (1999). Knockout of the Sendai virus C gene eliminates the viral ability to prevent the interferon α/β mediated responses. FEBS letters, **459(2):** 205-210.

Gray, M. 2003. Diversity and evolution of mitochondrial RNA editing systems. IUBMB life, **55(45):** 227-233.

Green, D. R. 2000. Apoptotic pathways: paper wraps stone blunts scissors. Cell, **102(1):** 1-4.

Green, D. R. and Reed, J. C. 1998. Mitochondria and apoptosis. Science-AAAS-Weekly Paper Edition, **281**(5381): 1309-1311.

Harborth, J., Elbashir, S. M., Bechert, K., Tuschl, T. and Weber, K. 2001. Identification of essential genes in cultured mammalian cells using small interfering RNAs. Journal of cell science, **114**(24): 4557-4565.

Hardwick, J. M. 2001. Apoptosis in viral pathogenesis. Cell death and differentiation, **8(2):** 109-110.

Hashiguchi, T., Ose, T., Kubota, M., Maita, N., Kamishikiryo, J., Maenaka, K. and Yanagi Y. 2011. Structure of the measles virus hemagglutinin bound to its cellular receptor SLAM. Nat Struct Mol Biol **18:** 135–141.

Hashiguchi, T., Kajikawa, M., Maita, N., Takeda, M., Kuroki, K., Sasaki, K., Kohda, D., Yanagi, Y. and Maenaka, K. 2007. Crystal structure of measles virus hemagglutinin provides insight into effective vaccines. P Natl Acad Sci USA **104**: 19535–19540.

Hausmann, S., Garcin, D., Delenda, C. and Kolakofsky, D. 1999. The versatility of paramyxovirus RNA polymerase stuttering. Journal of Virology, **73(7):** 5568-5576.

Hu, S., Snipas, S. J., Vincenz, C., Salvesen, G. and Dixit, V. M. 1998. Caspase-14 is a novel developmentally regulated protease. Journal of Biological Chemistry, **273(45):** 29648-29653.

Huang, Z., Krishnamurthy, S., Panda, A. and Samal, S. K. 2003. Newcastle disease virus V protein is associated with viral pathogenesis and functions as an alpha interferon antagonist. Journal of Virology, **77(16):** 8676-8685.

Ichim, G. and Tait, S. W. 2016. A fate worse than death: apoptosis as an oncogenic process. Nature Reviews Cancer. infected with rinderpest and peste des petits ruminants viruses. J. Gen. Virol. **68**: 2033–2038.

Ismail, T.M., Yamanaka, M.K., Saliki, J.T., el-Kholy, A., Mebus, C. and Yilma, T. 1995. Cloning and expression of the nucleoprotein of Peste des petits ruminants virus in baculovirus for use in serological diagnosis. Virology, **208**, 776–778.

Jacks, T. and Varmus, H. E. 1985. Expression of the Rous sarcoma virus pol gene by ribosomal frameshifting. Science, **230:** 1237-1243.

Jacques, J.P. and Kolakofsky, D. 1991. Pseudo-templated transcription in prokaryotic and eukaryotic organisms. Gene Dev. **5**:707–713.

Johansson, K., Bourhis, J.M., Campanacci, V., Cambillau, C., Canard, B. and Longhi, S. 2003. Crystal structure of the measles virus phosphoprotein domain responsible for the induced folding of the C-terminal domain of the nucleoprotein. Journal of Biological Chemistry .**278(44)**:567-573.

Kato, A., Kiyotani, K., Sakai, Y., Yoshida, T. and Nagai, Y. 1997. The paramyxovirus, Sendai virus, V protein encodes a luxury function required for viral pathogenesis. The EMBO journal, **16(3):** 578-587.

Keita D,Servan de Almeida R,Libeau G,Albina E(2008) Identification and mapping of a region on the mRNA of Morbillivirus nucleoprotein susceptible to RNA interference. Antiviral Research. **80**:158–167.

Kerr, J. F., Wyllie, A. H. and Currie, A. R. 1972. Apoptosis: a basic biological phenomenon with wide-ranging implications in tissue kinetics. British journal of cancer, **26(4):** 239.

Khandelwal, A., Renukaradhya, G. J., Rajasekhar, M., Sita, G. L. and Shaila, M. S. 2011. Immune responses to hemagglutinin-neuraminidase protein of peste des petits ruminants virus expressed in transgenic peanut plants in sheep. Veterinary immunology and immunopathology, **140**(3): 291-296.

Kolakofsky, D., Curran, J. , Pelet, T. and Jacques, J. P. 1993, Paramyxovirus P gene mRNA editing. RNA editing. Ellis Horwood, Chichester, England. 105-123.

Kolakofsky, D., Pelet, T., Garcin, D., Hausmann, S., Curran, J. and Roux, L. 1998. Paramyxovirus RNA synthesis and the requirement for hexamer genome length: the rule of six revisited. Journal of Virology, **72(2):** 891-899.

Komatsu, T., Takeuchi, K., Yokoo, J. and Gotoh, B. 2004. C and V proteins of Sendai virus target signaling pathways leading to IRF-3 activation for the negative regulation of interferon-β production. Virology, **325(1):** 137-148.

Kondo, H., Chiba, S., Toyoda, K. and Suzuki, N. 2012. Evidence for negative-strand RNA virus infection in fungi. Virology. **435 (2)**: 201–9.

Koonin, E.V. 1991. The phylogeny of RNA-dependent RNA polymerases of positive-strand RNA viruses. J. Gen. Virol. **72 (9)**: 2197–206.

Kroemer, G. and Reed, J. C. 2000. Mitochondrial control of cell death. Nature medicine, **6(5):** 513-520.

Kubota, T., Yokosawa, N., Yokota, S. I. and Fujii, N. 2001. C terminal CYS-RICH region of mumps virus structural V protein correlates with block of interferon α and γ signal transduction pathway through decrease of STAT 1-α. Biochemical and biophysical research communications, **283(1):** 255-259.

Kumar, N., Chaubey, K.K., Chaudhary, K., Singh, S.V., Sharma, D.K., Gupta, V.K., Mishra, A.K. and Sharma, S. 2013. Isolation, identification and characterization of a Peste des Petits Ruminants virus from an outbreak in Nanakpur, India. J Virol Methods.**189(2)**:388-392.

Kumar, N., Maherchandani, S., Kashyap, S. K., Singh, S. V., Sharma, S., Chaubey, K. K., and Ly, H. 2014. Peste des petits ruminants virus infection of small ruminants: a comprehensive review. Viruses, **6(6):** 2287-2327.

Kurotani, A., Kiyotani, K., Kato, A., Shioda, T., Sakai, Y., Mizumoto, K., Yoshida, T., Nagai Y. 1998. Sendai virus C proteins are categorically nonessential gene products but silencing their expression severly impairs viral replication and pathogenesis. Genes to Cells. **3**:111–124.

Kwiatek, O., Ali, Y.H., Saeed, I.K., Khalafalla, A.I., Mohamed, O.I. and Obeida, A.A. 2011. Asian lineage of peste des petits ruminants virus, Africa. Emerg Infect Dis. ; 17: 1223–31.

Lahm, A., Yagnik, A., Tramontano, A. and Koch, U. 2002. Hepatitis C virus proteins as targets for drug development: the role of bioinformatics and modelling. Current drug targets, **3**(4) :281-296.

Laine, D., Bourhis, J. M., Longhi, S., Flacher, M., Cassard, L., Canard, B. and Valentin, H. (2005). Measles virus nucleoprotein induces cell-proliferation arrest and apoptosis through NTAIL–NR and NCORE–FcγRIIB1 interactions, respectively. Journal of General Virology, **86(6):** 1771-1784.

Langedijk, J.P., Daus, F.J. and van Oirschot, J.T. 1997. Sequence and structure alignment of Paramyxoviridae attachment proteins and discovery of enzymatic activity for a Morbillivirus hemagglutinin. Journal of Virology. **71**:6155–6167.

Li, H., Zhu, H., Xu, C. J. and Yuan, J. 1998. Cleavage of BID by caspase 8 mediates the mitochondrial damage in the Fas pathway of apoptosis. Cell, **94(4):** 491-501.

Liszewski, M.K., Post, T.W. and Atkinson, J.P. 1991. Membrane cofactor protein (MCP or CD46): newest member of the regulators of complement activation gene cluster. Annu Rev Immunol. **9**:431–455.

Livak, K. J. and Schmittgen, T. D. 2001. Analysis of relative gene expression data using real-time quantitative PCR and the 2" ΔΔCT method. Methods, **25(4):** 402-408.

Ma, X., Yang, X., Nian, X., Zhang, Z., Dou, Y., Zhang, X. and Cai, X. 2015. Identification of amino-acid residues in the V protein of peste des petits ruminants essential for interference and suppression of STAT-mediated interferon signaling. Virology, **483:** 54-63.

Maas, S. and Rich, A. 2000. Changing genetic information through RNA editing. Bioessays, **22(9):** 790-802.

Mahapatra, M., Parida, S., Baron, M.D. and Barrett, T. 2006. Matrix protein and glycoproteins F and H of Peste-des-petits-ruminants virus function better as a homologous complex. Journal of General Virology. **87**:2021–2029.

Mahapatra, M., Parida, Egziabher, B.G., Diallo, A. and Barrett, T. 2003 Sequence analysis of the phosphoprotein gene of peste des petits ruminants (PPR) virus: editing of the gene transcript. Virus Research .**96**:85–98.

Maiuri, M. C., Zalckvar, E., Kimchi, A. and Kroemer, G. 2007. Self-eating and self-killing: crosstalk between autophagy and apoptosis. Nature reviews Molecular cell biology, **8(9):** 741-752.

Manjunath, S., Kumar, G. R., Mishra, B. P., Mishra, B., Sahoo, A. P., Joshi, C. G. and Janga, S. C. 2015. Genomic analysis of host–Peste des petits ruminants vaccine viral transcriptome uncovers transcription factors modulating immune regulatory pathways. Veterinary Research, **46(1):** 15.

Manjunath, S., Mishra, B. P., Mishra, B., Sahoo, A. P., Tiwari, A. K., Rajak, K. K. and Wani, S. A. 2017. Comparative and temporal transcriptome analysis of peste des petits ruminants virus infected goat peripheral blood mononuclear cells. Virus Research, **229**: 28-40.

Manktelow, E., Shigemoto, K. and Brierley, I. 2005. Characterization of the frameshift signal of Edr, a mammalian example of programmed" 1 ribosomal frameshifting. Nucleic Acids Research, **33(5):** 1553-1563.

Mariner, J. C., House, J. A., Sollod, A. E., Stem, C., Van den Ende, M. and Mebus, C. A. 1990. Comparison of the effect of various chemical stabilizers and lyophilization cycles on the thermostability of a Vero cell-adapted rinderpest vaccine. Veterinary Microbiology, **21(3):** 195-209.

Masse, N., Ainouze, M., Neel, B., Wild, T.F., Buckland, R. and Langedijk, J.P. 2004. Measles virus (MV) hemagglutinin: evidence that attachment sites for MV receptors SLAM and CD46 overlap on the globular head. J Virol **78**: 9051–9063.

Matsuura, Y. and Stewart, M. 2005. Nup50/Npap60 function in nuclear protein import complex disassembly and importin recycling. The EMBO Journal, **24(21):** 3681-3689.

Mizushima, N. 2007. Autophagy: process and function. Genes and Development, **21(22):** 2861-2873.

Mondal, B., Sreenivasa, B. P., Dhar, P., Singh, R. P. and Bandyopadhyay, S. K. 2001. Apoptosis induced by peste des petits ruminants virus in goat peripheral blood mononuclear cells. Virus Research, **73(2):** 113-119.

Munir, M., Zohari, S., Berg, M. 2013. Current advances in molecular diagnosis and vaccines for peste de petits ruminants. In: Munir, M., Zohari, S. and Berg, M. (eds) Molecular Biology and Pathogenesis of Peste des Petits Ruminants Virus. *Springe*r, Berlin, Germany, 105–133.

Munir, M., Zohari, S., & Berg, M. 2012. *Molecular biology and pathogenesis of peste des petits ruminants virus*. Springer Science & Business Media.

Muthuchelvan, D., Sanyal, A., Sarkar, J., Sreenivasa, B.P. and Bandyopadhyay, S.K. 2006a. Comparative nucleotide sequence analysis of the phosphoprotein gene of peste des petits ruminants vaccine virus of Indian origin. Res.Vet. Sci. **81(1)**: 158–164.

Muthuchelvan, D., Sanyal, A., Singh, R.P., Hemadri, D., Sen, A., Sreenivasa, B.P., Singh, R.K. and Bandyopadhyay, S.K. 2005. Comparative sequence analysis of the large polymerase protein (L) gene of peste-des-petits ruminants (PPR) vaccine virus of Indian origin. Archive of Virology **150**: 2467–2481.

Muthuchelvan, D., Sanyal, A., Sreenivasa, B. P., Saravanan, P., Dhar, P., Singh, R. P. and Bandyopadhyay, S. K. 2006b. Analysis of the matrix protein gene sequence of the Asian lineage of peste-des-petits ruminants vaccine virus. Veterinary Microbiology, **113(1):** 83-87.

Nanda, S. K. and Baron, M. D. 2006. Rinderpest virus blocks type I and type II interferon action: role of structural and nonstructural proteins. Journal of Virology, **80**(15) :7555-7568.

Navratil, V., de Chassey, B., Meyniel, L., Pradezynski, F., André, P., Rabourdin-Combe, C., and Lotteau, V. 2010. System-level comparison of protein-protein interactions between viruses and the human type I interferon system network. J. Proteome Res. **9:** 3527–3536.

Nishio, M., Garcin, D., Simonet, V., & Kolakofsky, D. 2002. The carboxyl segment of the mumps virus V protein associates with Stat proteins in vitro via a tryptophan-rich motif. Virology, **300**(1): 92-99.

Nishio, M., Tsurudome, M., Ito, M., Kawano, M., Komada, H. and Ito, Y. 2001. High resistance of human parainfluenza type 2 virus protein-expressing cells to the antiviral and anti-cell proliferative activities of alpha/beta interferons: cysteine-rich V-specific domain is required for high resistance to the interferons. Journal of virology, **75(19):** 9165-9176.

Noyce, R.S., Bondre, D.G., Ha, M.N., Lin, L.T., Sisson, G., Tsao, M.S. and Richardson, C.D. 2011.Tumor cell marker PVRL4 (nectin 4) is an epithelial cell receptor for measles virus. PLoS Pathog. **7(8)**:e1002240.

Noyce, R.S. and Richardson, C.D. 2012. Nectin 4 is the epithelial cell receptor for measles virus. Trends in Microbiology.**20(9)**: 429–439.

Ohno, S., Seki, F., Ono, N. and Yanagi, Y. 2003. Histidine at position 61 and its adjacent amino acid residues are critical for the ability of SLAM (CD150) to act as a cellular receptor for measles virus. J Gen Virol .**84**: 2381–2388.

Ohno, S., Ono, N., Takeda, M., Takeuchi, K. and Yanagi, Y. 2004. Dissection of measles virus V protein in relation to its ability to block alpha/beta interferon signal transduction. Journal of general virology, **85**(10): 2991-2999.

Owens, R. J., Limn, C. and Roy, P. 2004. Role of an arbovirus nonstructural protein in cellular pathogenesis and virus release. Journal of virology, **78(12):** 6649-6656.

Parida, S., Muniraju, M., Altan, E., Baazizi, R., Raj, G. D. and Mahapatra, M. 2016. Emergence of PPR and its threat to Europe. Small Ruminant Research, **142**:16-21.

Parisien, J. P., Lau, J. F., Rodriguez, J. J., Sullivan, B. M., Moscona, A., Parks, G. D. and Horvath, C. M. 2001. The V protein of human parainfluenza virus 2 antagonizes type I interferon responses by destabilizing signal transducer and activator of transcription 2. Virology, **283(2):** 230-239.

Park, K.H. and Krystal, M. 1992. *In vivo* model for pseudo-templated transcription in Sendai virus. Journal of Virology. **66**:7033–7039.

Paterson, R. G. and Lamb, R. A. 1990. RNA editing by G-nucleotide insertion in mumps virus P-gene mRNA transcripts. Journal of virology, **64(9):** 4137-4145.

Pawar, R. M., Dhinakar, G. R. and Balachandran, C. 2008. Relationship between the level of signaling lymphocyte activation molecule mRNA and replication of Peste-des-petits-ruminants virus in peripheral blood mononuclear cells of host animals. Acta Virologica, **52(4):** 231-236.

Plemper, R.K., Hammond, A.L. and Cattaneo, R. 2001. Measles virus envelope glycoproteins heterooligomerize in the endoplasmic reticulum. Journal of Biological Chemistry. **276(44)**:239-246.

Poole, Emma, Biao He, Robert A. Lamb, Richard E. Randall, and Stephen Goodbourn. 2002. The V proteins of simian virus 5 and other paramyxoviruses inhibit induction of interferon-β." Virology **303(1):** 33-46.

Pushparaj, P. N., Aarthi, J. J., Manikandan, J. and Kumar, S. D. 2008. siRNA, miRNA, and shRNA: in vivo applications. Journal of Dental Research, **87**(11): 992-1003.

Radecke, F. and Billeter, M.A. 1996. The nonstructural C protein is not essential for multiplication of edmonston B strain measles virus in cultured cells. Virology **217**: 418–421.

Ramachandran, A., Parisien, J. P. and Horvath, C. M. 2008. STAT2 is a primary target for measles virus V protein-mediated alpha/beta interferon signaling inhibition. Journal of Virology, **82(17)**: 8330-8338.

Ramshaw, I. A., Ramsay, A. J., Karupiah, G., Rolph, M. S., Mahalingam, S. and Ruby, J. C. 1997. Cytokines and immunity to viral infections. Immunological reviews, **159(1):** 119-135.

Reed, L. J. and Muench, H. 1938. A simple method of estimating fifty percent endpoint 1 2. American journal of epidemiology, **27(3):** 493-497.

Renukaradhya, G.J., Sinnathamby, G., Seth, S., Rajasekhar, M. and Shaila, M.S. 2002. Mapping of B-cell epitopic sites and delineation of functional domains on the hemagglutinin-neuraminidase protein of peste des petits ruminants virus. Virus Research. **90**:171–185.

Rodriguez, J. J., Parisien, J. P. and Horvath, C. M. 2002. Nipah virus V protein evades alpha and gamma interferons by preventing STAT1 and STAT2 activation and nuclear accumulation. Journal of virology, **76(22):** 11476-11483.

Roulston, A., Marcellus, R. C. and Branton, P. E. 1999. Viruses and apoptosis. Annual Reviews in Microbiology, **53(1):** 577-628.

Sabatini, D. M. 2006. mTOR and cancer: insights into a complex relationship. Nature Reviews Cancer, **6(9):** 729-734.

Santiago, C., Bjorling, E., Stehle, T. and Casasnovas, J.M. 2002. Distinct kinetics for binding of the CD46 and SLAM receptors to overlapping sites in the measles virus hemagglutinin protein. J. Biol. Chem. **277**: 32294–32301.

Santiago, C., Celma, M.L., Stehle, T. and Casasnovas, J.M. 2010. Structure of the measles virus hemagglutinin bound to the CD46 receptor. Nat Struct Mol Biol**. 17**: 124–129.

Schnorr, J. J., Seufert, M., Schlender, J., Borst, J., Johnston, I. C., Ter Meulen, V. and Schneider-Schaulies, S. 1997. Cell cycle arrest rather than apoptosis is associated with measles virus contact-mediated immunosuppression in vitro. Journal of general virology, **78(12):** 3217-3226.

Servan, De Almeida, R., Keita, D., Libeau, G. and Albina, E. 2007. Control of ruminant Morbillivirus replication by small interfering RNA. Journal of General Virology **88**: 2307–2311.

Seth, S. and Shaila, M.S. 2001. The hemagglutinin-neuraminidase protein of peste des petits ruminants virus is biologically active when transiently expressed in mammalian cells. Virus Research. 7**5**:169–177.

Shaila, M.S., Purashothaman, V., Bhavsar, D., Venugopal, K. and Venkatesan, R.A. 1989. Peste des petits ruminants of sheep in India. Vet. Rec., **125**: 602.

Shaila, M.S., Shamaki, D., Forsyth, M.A., Diallo, A., Goatley, L., Kitching, R.P. and Barrett, T. 1996. Geographic distribution and epidemiology of peste des petits ruminants virus. Virus Research **43**:149–153.

Shatkin, A.J. 1974. Animal RNA viruses: Genome structure and function. Annu. Rev. Biochemistry **43**:643-665.

Singh, R.K., Balamurugan V., Bhanuprakash V., Sen A., Saravanan P., Pal Yadav, M. 2009. Possible control and eradication of peste des petits ruminants from India: Technical aspects. Vet. Ital. **45**:449–462.

Singh, R.P., Saravanan, P., Sreenivasa, B.P., Singh, R.K. and Bandyopadhyay,S.K. 2002. Prevalence and distribution of peste des petits ruminants virus infection in small ruminants in India. Rev. Sci. Tech. **23:** 807–819.

Singh, R. P., Sreenivasa, B. P., Dhar, P., Shah, L. C. and Bandyopadhyay, S. K. 2004. Development of a monoclonal antibody based competitive-ELISA for detection and titration of antibodies to peste des petits ruminants (PPR) virus. Veterinary microbiology, **98(1):** 3-15.

Sreenivasa, B. P., Singh, R. P., Mondal, B., Dhar, P. and Bandyopadhyay, S. K. 2006. Marmoset B95a cells: a sensitive system for cultivation of peste des petits ruminants (PPR) virus. Veterinary research communications, **30(1):** 103-108.

Srinivas, R.P. and Gopal, T. 1996. Peste des petits ruminants (PPR): a new menace to sheep and goats.Livestock Advisor **21**: 22–26.

Steinhauer, D.A. and Holland, J.J. 1987. Rapid evolution of RNA viruses. Annu. Rev. Microbiol. **41**: 409–33.

Steward, M., Samson, A. C. R., Errington, W. and Emmerson, P. T. 1995. The Newcastle disease virus V protein binds zinc. Archives of Virology, **140(7):** 1321-1328.

Steward, M., Vipond, I. B., Millar, N. S. and Emmerson, P. T. 1993. RNA editing in Newcastle disease virus. Journal of General Virology, **74(12):** 2539-2547.

Sweetman, D.A., Miskin, J. and Baron. M.D. 2001. Rinderpest virus C and V proteins interact with the major (L) component of the viral polymerase. Virology. **281(2)**:193-204.

Tapparel, C., Hausmann, S., Pelet, S., Curran, J., Kolakofsky, D. and Roux, L. 1997. Inhibition of sendai virus genome replication due to promoter-increased selectivity: A possible role of the accessory proteins. Journal of Virology. **71**:9588–9599.

Taylor, W.P. and Abegunde, A. 1979.The isolation of peste des petits ruminants virus from Nigerian sheep and goats. Research in Veterinary Science. **26**:94–96.

Taylor, W.P., Al Busaidy, S. and Barrett, T. 1990. The epidemiology of peste des petits ruminants in the Sultanate of Oman. Veterinary Microbiology **22**: 341–352.

Thomas, S. M., Lamb, R. A. and Paterson, R.G. 1988. Two mRNAs that differ by two nontemplated nucleotides encode the amino coterminal proteins P and V of the paramyxovirus SV5. Cell, **54(6):** 891-902.

Thomson, B. J. 2001. Viruses and apoptosis. International Journal of Experimental Pathology, **82(2):** 65-76.

Vidal, S., Curran, J. and Kolakofsky, D. 1990. A stuttering model for paramyxovirus P mRNA editing. The EMBO Journal, **9(6):** 2017.

Visomirski-Robic, L. M. and Gott, J. M. 1997. Insertional editing of nascent mitochondrial RNAs in Physarum. Proceedings of the National Academy of Sciences, **94(9):** 4324-4329.

Von Hippel, P. H. and Yager, T. D. 1992. The elongation-termination decision in transcription. Science, **255**(5046): 809-812.

Vongpunsawad, S., Oezgun, N., Braun, W. and Cattaneo, R. 2004. Selectively receptor-blind measles viruses: identification of residues necessary for SLAM or CD46-induced fusion and their localization on a new hemagglutinin structural model. J Virol **78**: 302–313.

Wansley, E. K. and Parks, G. D. 2002. Naturally occurring substitutions in the P/V gene convert the noncytopathic paramyxovirus simian virus 5 into a virus that induces alpha/beta interferon synthesis and cell death. Journal of Virology, **76(20):** 10109-10121.

Wardrop, E. A. and Briedis, D. J. 1991. Characterization of V protein in measles virus-infected cells. Journal of Virology, **65(7):** 3421-3428.

Wei, Y., Pattingre, S., Sinha, S., Bassik, M. and Levine, B. 2008. JNK1-mediated phosphorylation of Bcl-2 regulates starvation-induced autophagy. Molecular cell. **30(6):** 678-688.

Xie, Z. and Klionsky, D. J. 2007. Autophagosome formation: core machinery and adaptations. Nature cell biology, **9(10):** 1102-1109.

Yanagi, Y., Ono, N., Tatsuo, H., Hashimoto, K. and Minagawa, H. 2002. Measles virus receptor SLAM (CD150). Virology.**299**: 155–161.

Yang, P., Zheng, J., Wang, S., Liu, P., Xie, M. and Zhao, D. 2015. Respiratory syncytial virus nonstructural proteins 1 and 2 are crucial pathogenic factors that modulate interferon signaling and Treg cell distribution in mice. Virology, **485**: 223-232.

Yoneda, M., Bandyopadhyay, S.K., Shiotani, M., Fujita, K., Nuntaprasert, A., Miura, R., Baron, M.D. Barrett, T. and Kai, C. 2002. Rinderpest virus H protein: role in determining host range in rabbits. Journal of General Virology **83**:1457–1463.

Yoneda, M.,Miura, R., Barrett, T., Tsukiyama-Kohara, K. and Kai, C. 2004. Rinderpest virus phosphoprotein gene is a major determinant of species-specific pathogenicity. Journal of Virology.**78**:6676–6681.

Young, D. F., Chatziandreou, N., He, B., Goodbourn, S., Lamb, R. A. and Randall, R. E. 2001. Single amino acid substitution in the V protein of simian virus 5 differentiates its ability to block interferon signaling in human and murine cells. Journal of virology, **75(7):** 3363-3370.

Yunus, M. and Shaila, M.S. 2012. Establishment of an in vitro transcription system for peste des petits ruminant virus. Virology Journal .**9**:302.

Zhang, Y., Wu, S., Lv, J., Feng, C., Deng, J., Wang, C. and Lin, X. 2013. Peste des petits ruminants virus exploits cellular autophagy machinery for replication. Virology, **437**(1): 28-38.

Appendix

APPENDIX

A) 1X Phosphate Buffer Saline (pH 7.4)

NaCl	4.0 gm
KCL	100 mg
Na_2HPO_4	710 mg
KH_2PO_4	100 mg
Distilled water	up to 500 ml

B) DEPC Treated Water

To ensure free from RNase contamination, water used to dissolve RNA (or prepare buffers required for RNA works) was treated with 0.1% Diethyl pyrocarbonate (DEPC).

DEPC (M/s Sigma)	1.00 ml
Distilled water	1000 ml

The DEPC was mixed vigorously and left overnight at 37°C. To remove DEPC, the water was autoclaved at 120ºC at 15lb pressure for 10 minutes before use.

C) Reagents used in agarose gel electrophoresis

1. Tris-acetate-EDTA (TAE) buffer 50X

Tris base	242 g
Glacial acetic acid	57.1 ml
0.5 M EDTA (pH 8.0)	100 ml

Distilled water was added to make up to a final volume of 1000 ml. A working solution of 1X was used.

2. Ethidium bromide stock solution (10 mg/ml)

Ethidium bromide	100 mg
Distilled water	10 ml

The solution was mixed and stored at 4°C. A final concentration of 0.5µg/ml was used in preparing agarose gel.

3. Loading dye (6x)

Bromophenol blue	0.25% (w/v)
Xylene cyanol FF	0.25% (w/v)
Sucrose	40% (w/v)

Store at -20°C.

D) Reagents used for bacteriological work

1. LB (Luria-Bertani) broth

Tryptone	10 g
Yeast extract	5 g
NaCl	10 g
Deionized water	950 ml

Adjust the pH to 7.0 with 5N NaOH. Volume was made up to 1L and sterilized by autoclaving at 121° C and 15 lb pressure for 20 minutes and the solution was stored at 4°C.

2. LB agar

3.5% (w/v) LB agar (Himedia, Mumbai, India) in deionized water
Sterilized by autoclaving at 121° C and 15 lb pressure for 20 minutes and the solution was stored at 4°C

3. IPTG (1M)

IPTG	248 mg
Distilled water	1 ml

Sterilized by filtration and stored at -20°C

4. Kanamycin stock (100 mg/ml)

Kanamycin	500 mg
Distilled water	5 ml

Sterilized by filtration through 0.22 µ filter and stored at -20°C.

5. Zeocin stock (100 mg/ml)

Zeocin	500 mg
Distilled water	5 ml

Sterilized by filtration through 0.22 µ filter and stored at -20°C.

6. 100mM $CaCl_2.2H_2O$ (100 mL)

$CaCl_2.2H_2O$	1.47 gm
Milli Q water upto	100 mL

Mix the contents properly and filter sterilized by 0.22 µM membrane filter and store at 4°C.

E. Reagents used in cell culture

1. RPMI-1640 (1 Liter)

10 ml of Glutamine (3%), 15 ml of $NaHCO_3$ (7.5%) and 1 ml of antibiotic and antimycotic solutions (100X) were added per liter of media and incubated at 37°C overnight before use.

2. Growth media (10% serum)

RPMI-1640	90 ml
Foetal calf serum	10 ml

3. Maintenance media (2% serum)

RPMI-1640	98 ml
Foetal calf serum	2 ml

4. Trypsin Versene solution (0.25%)

NaCl	10 gm
KCl	0.250 gm
Na_2HPO_4	1.9 gm
KH_2PO_4	0.250 gm
Trypsin	2.5 gm
Versene (EDTA)	1.4 gm
0.4% Phenol red	1.0 µl

Distilled water was added to make the volume up to 1000 ml.

5. Sodium bicarbonate stock

7.5% (w/v) solution was prepared in distilled water and sterilized by filtration through 0.2 μm membrane filter. Kept at 4°C for a period not more than one month. One litre of media requires up to 15 ml of this solution.

6. L-Glutamine stock

3% (w/v) solution was prepared in distilled water and sterilized by filtration through 0.2 μm membrane filter. Aliquots were made and stored at –20°C. Just before use it was warmed it 37°C for few minutes only till a clear solution is visible. Keeping glutamine at 37°C for longer time reduces its activity. One litre of media requires 10 ml of glutamine.

This document was created with Win2PDF available at http://www.win2pdf.com.
The unregistered version of Win2PDF is for evaluation or non-commercial use only.
This page will not be added after purchasing Win2PDF.